

# Group Contribution sPC-SAFT Equation of State

**Tihic, Amra**

*Publication date:*
2008

*Document Version*
Publisher's PDF, also known as Version of record

Technical University of Denmark

# Group Contribution sPC-SAFT Equation of State

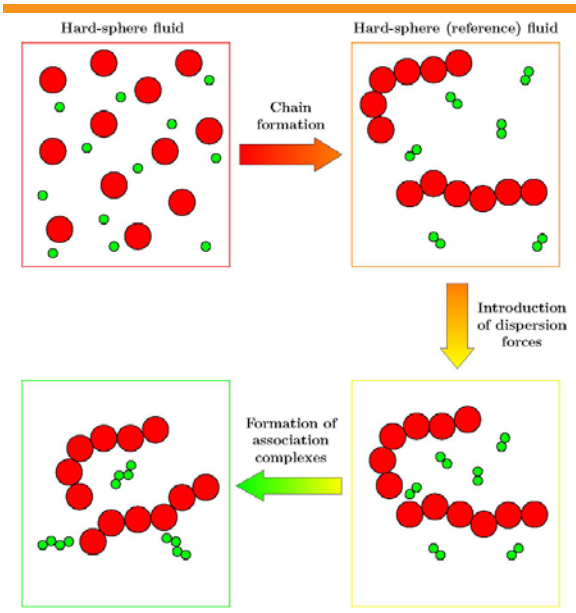


Amra Tihić

2008

DTU Chemical Engineering
Department of Chemical and Biochemical Engineering

# Group Contribution sPC-SAFT Equation of State

Ph.D. Thesis

Amra Tihić

May 13, 2008

Supervisors: Georgios M. Kontogeorgis
Michael L. Michelsen
Nicolas von Solms
Leonidas Constantinou

IVC-SEP
Department of Chemical and Biochemical Engineering
Technical University of Denmark

## Summary

Modelling of thermodynamic properties and phase equilibria with equations of state (EoS) remains an important issue in chemical and related industries. The simplified Perturbed Chain-Statistical Associating Fluid Theory (sPC-SAFT) EoS is widely used for various industrial applications. The model requires three parameters: the segment number ($m$), the hard-core segment diameter ($\sigma$), and the segment-segment interaction energy parameter ($\epsilon/k$) for each pure non-associating fluid. They are typically fitted to experimental vapour pressure and liquid density data. Since high-molecular-weight compounds, like polymers, do not have a detectable vapour pressure, there is a need for a predictive calculation method for parameters of polymers and other complex compounds. This thesis suggests a solution to this problem.

The main objective of this project is to develop a group-contribution (GC) version of the sPC-SAFT EoS where the parameters of the model are calculated from a predefined GC scheme. In this way, the PC-SAFT parameters for complex compounds can still be estimated when experimental data are unavailable. The applied GC methodology includes two levels of contributions; both first-order groups (FOG) and second-order groups (SOG). The latter can, to some extent, capture proximity effects and distinguish among structural isomers.

Initially, the PC-SAFT parameter table is extended with over 500 newly estimated parameter sets for pure non-associating compounds from different chemical families using mainly experimental data from the DIPPR database. The chemical families include alkanes, branched alkanes, alkenes, alkynes, benzene derivatives, gases, ethers, esters, ketones, cyclo- and fluorinated hydrocarbons, polynuclear aromatics, nitroalkanes, sulphides, and plasticizers. Several important types of experimental thermodynamic data, such as vapour-liquid and liquid-liquid equilibria, are collected from the literature and used to systematically evaluate the performance of the sPC-SAFT model when using these new PC-SAFT parameters.

The experimentally derived PC-SAFT parameters display clear linear trends, which are utilized to fit parameter sets ($m$, $\sigma$, and $\epsilon/k$) for distinct chemical groups contained in the compounds from this database using an optimization routine. At present, the table includes 45 FOG and 26 SOG, but can be further extended using the outlined methodology. The parameters of new compounds can now be calculated by summing up the contributions of these well-defined groups of atoms after being multiplied by their number of occurrences within the molecule.

The fluid phase equilibria of some larger and complex compounds not included in the optimisation database are examined to confirm the predictive capability of the proposed GC sPC-SAFT EoS. Good agreement between predictions and experimental data is demonstrated. For many binary mixtures investigated, a small binary interaction parameter, $k_{ij}$, is needed before the model accurately correlates the experimental data. As a possibility, a more predictive way to calculate the required $k_{ij}$ values has been investigated using an additional physical parameter (the ionization energy of involved compounds), and it shows some promising initial results.

Further testing, on e.g. multicomponent and solid-liquid equilibria modelling, is needed to establish the real potential of the GC sPC-SAFT EoS. It is expected that optimization and extension of the proposed GC scheme can lead to further improvements within the general limitations of the PC-SAFT and sPC-SAFT models. However, the current work has already shown that with the newly developed GC scheme in hand to calculate parameters for complex compounds, the sPC-SAFT model has become a relevant and useful engineering tool for the design and development of complex products. These include e.g. detergents or food ingredients, pharmaceuticals, and specialty chemicals, where predictions of thermodynamic and phase equilibria properties are required, but for which required vapour pressure and/or liquid density data may not be available.

**Resumé (Summary in Danish)**

Modellering af termodynamiske egenskaber og faseligevægte er en udfordring for den kemiske industri. Forenklet *Perturbed Chains-Statistical Associating Fluid Theory* (sPC-SAFT) er en tilstandsligning med udbredt anvendelse i en række industrielle sammenhænge. Modellen benytter tre parametre: segment antal ($m$), hård-kugle segment diameter ($\sigma$) og segment-segment interaktionsenergi ($\epsilon/k$) for hver enkelt ikke-associerende stof som indgår i beregningen. Disse parametre kan typisk fittes til eksperimentelle værdier for damptryk og væskefasedensitet. Stoffer med meget høj molekylevægt, som fx. polymere, har så lave damptryk, at det i praksis er umuligt at måle. Dermed opstår et behov for en beregningsmetode til at forudsige modelparametre for polymere og andre komplekse stoffer. Denne afhandling præsenterer en løsning på dette problem.

Formålet med dette projekt er at udvikle en gruppebidragsbaseret (GC) udgave af sPC-SAFT tilstandsligningen, hvor modelparametrene beregnes udfra veldefinerede funktionelle grupper og deres individuelle bidrag, uden at der gøres brug af eksperimentelle data. Gruppebidragsmetoden inkluderer bidrag fra både første ordens (FOG) og anden ordens funktionelle grupper (SOG), hvor tilstedeværelsen af sidstnævnte gør det muligt at korrigere for gensidige påvirkninger mellem nærliggende grupper samt skelne mellem isomere strukturer.

Som udgangspunkt for projektet er den eksisterende tabel med PC-SAFT parametre udvidet med parametersæt for over 500 nye ikke-associerende stoffer. Hertil er anvendt eksperimentelle data fra DIPPR databasen. De kemiske stofgrupper som er repræsenteret i denne database omfatter alkaner, forgrenede alkaner, alkener, alkyner, benzenderivater, gasser, ethere, estere, ketoner, cyklo- and fluorerede kulbrinter, polyaromatiske kulbrinter, nitroalkaner, sulfider og blødgørere. En række vigtige eksperimentelle datatyper er desuden indsamlet fra litteraturen; heriblandt gas-væske (VLE) og væske-væske (LLE) ligevægtsdata, som er anvendt til systematisk evaluering af sPC-SAFT modellens funktionalitet ved brug af disse nye parametersæt.

De eksperimentelt baserede PC-SAFT parametre udviser tydelig lineær opførsel. Dette er udnyttet ved den efterfølgende optimering og udledning af parametersæt ($m$, $\sigma$ og $\epsilon/k$) for specifikke funktionelle gruppe, der optræder i stoffer inkluderet i databasen. Den fremkomne gruppebidragstabel indeholder 45 FOG og 26 SOG. Tabellen kan yderligere udvides ved at følge den beskrevne fremgangsmåde. Udfra denne tabel kan modelparametre beregnes for nye stoffer ved at summere bidrag fra de enkelte funktionelle grupper multipliceret med antallet af deres forekomster i molekylstrukturen.

For at bekræfte GC sPC-SAFT tilstandsligningens forudsigende evner er faseligevægtsdata modelleret for en række komplekse stoffer, som ikke er inkluderet i optimeringsdatabasen. Der er opnået god overensstemmelse mellem modelforudsigelser og eksperimentelle data. For flere binære systemer er det nødvendigt at anvende en binær interaktionsparameter ($k_{ij}$) med lav numerisk værdi for at opnå nøjagtig korrelation med de eksperimentelle data. I den forbindelse er en teoretisk fremgangsmåde til beregning af $k_{ij}$ blevet undersøgt. Metoden gør brug af ioniseringsenergien for individuelle stoffer som en ekstra parameter og har vist lovende resultater.

Yderligere karakterisering af modellens evner til at forudsige fx. multikomponent-blandinger og faststof-væske ligevægte er nødvendig for at bestemme det reelle potential af GC sPC-SAFT tilstandsligningen. Det forventes, at videre optimering og udvidelse af gruppebidragsskemaet kan forbedre modellens nøjagtighed og anvendelsesområde indenfor de generelle begrænsninger i PC-SAFT og sPC-SAFT modellerne.

Med den anvendte gruppebidragsmetode til beregning af parametersæt for komplekse stoffer er sPC-SAFT tilstandsligningen blevet et attraktivt ingeniørværktøj til brug ifm. design og udvikling af komplicerede produkter, som fx. ingredienser til vaskemidler og fødevarer, farmaceutiske stoffer og specialkemikalier, hvor det er vigtigt at kunne forudsige termodynamiske egenskaber og faseligevægte, og hvor mulighederne tidligere har været begrænset af mangel på relevante eksperimentelle data.

# Preface

This thesis is submitted in partial fulfillment of the requirements to obtain the Doctor of Philosophy degree at the Technical University of Denmark (DTU). The work has been carried out at the IVC-SEP (Centre of Phase Equlibria and Separation Processes) at the Department of Chemical and Biochemical Engineering, DTU, under the supervision of Professors Georgios M. Kontogeorgis and Michael L. Michelsen, Asc. Prof. Nicolas von Solms and Dr. Leonidas Constantinou.

The project was financially supported by the Danish Technical Research Council (Statens Forskningsråd for Teknologi og Produktion, FTP) in the framework of a grant entitled Computer-Aided Product Design Using the PC-SAFT Equation of State. The author gratefully acknowledges their support.

I would like to express my gratitude to my adviser Prof. Georgios M. Kontogeorgis for his support over the last many years since my graduate student studies. An extra thanks for his endless passion and enthusiasm for this work from the beginning.

I am very thankful to Professor Michael L. Michelsen and Asc. Prof. Nicolas von Solms for their help. Your ideas and comments through this work have always been highly appreciated.

Also, I would like to thank Prof. Leonidas Constantinou for giving me the opportunity to visit the Research Center of Cyprus and always being ready to answer any questions I might have.

To the colleagues that I have worked with in the past three years at KT: I have enjoyed being a part of the IVC-SEP research group benefiting from the expertise available within the group. Thanks to you all.

At last but no least to my dear families, Tihić and Segal, for supporting me in all the decisions I have made and always been by my side. Vaša ljubav i podrška su uvijek bili i ostali za mene svjetlost u mračnim tunelima.

Finally to Christian... You mean everything to me. Without your understanding and support the accomplishment of this work would not have been possible.

Amra Tihić
Kgs. Lyngby, Denmark
May 13, 2008

# Table of Contents

# List of Figures

# List of Tables

# List of Symbols

**Abbreviations**

$AAD$ Average Absolute Deviation

$AAE$ Average Absolute Error

$ABC$ Atoms and Bonds in the properties of Conjugate forms

$BR$ Butadiene rubber (polybutadiene)

$CPA$ Cubic Plus Association EoS

$DIPPR$ Design Institute for Physical Properties

$EoS$ Equation of State

$ESD$ Elliott-Suresh-Donohue

$FAME$ Fatty Acid Methyl Ester

$FC$ Fluorocarbons

$FOG$ First-Order Groups

$FV$ Free-Volume

$GC$ Group Contribution

$GC\ EoS$ Group Contribution EoS

$GCLF$ Group Contribution Lattice-Fluid

$HC$ Hydrocarbons

$IGC$ Inverse Gas Chromatography

$iPP$ *iso*-Polypropylene

$LBY\text{-}UNI$ Lyngby modified group interaction parameters

$LCST$ Lower Critical Solution Temperature

$LCVM$ Linear Combination of Vidal and Michelsen mixing rule

$LLE$ Liquid-liquid equilibrium

$MD$ Molecular Dynamics

$MEK$ Methyl Ethyl Ketone

$MHV2$ Modified Huron-Vidal second order

$NRHB$ Non-Random Hydrogen Bonding

$NRTL$ Non-Random Two-Liquid

$P\text{-}\alpha MS$ Poly($\alpha$-methyl styrene)

$PAH$ Polynuclear Aromatic Hydrocarbons

$PBD$ Poly(butylene)

$PBMA$ Poly(butyl methacrylate)

$PC\text{-}SAFT$ Perturbed Chain Statistical Associating Fluid Theory

$PDMS$ Poly(dimethyl siloxane)

$PDMSM$ Poly(dimethyl silamethylene)

$PE$ Polyethylene

$PHSC$ Perturbed Hard Sphere Chain

$PIB$ Polyisobutylene

$PIPMA$ Poly(isopropyl methylacrylate)

$PMA$ Poly(methyl acrylate)

$PMMA$ Poly(methyl methacrylate)

$PP$ Polypropylene

$PRISM$ Polymer Reference Interaction Site Model

$PS$ Polystyrene

$PVAc$ Poly(vinyl acetate)

$PVAc$ Poly(vinyl chloride)

$PVT$ Pressure, Volume, Temperature

$sPC\text{-}SAFT$ Simplified PC-SAFT

$PSRK$ Predictive Soave-Redlich-Kwong

$SAFT$ Statistical Associating Fluid Theory

$SAFT\text{-}HR$ Statistical Associating Fluid Theory - Hard Sphere

$SAFT\text{-}LJ$ Statistical Associating Fluid Theory - Lennard Jones

$SAFT\text{-}VR$ Statistical Associating Fluid Theory - Varial Range

$SL$ Sanchez-Lacombe

$SLE$ Solid-Liquid Equilibria

$SOG$ Second-Order Groups

$SRK$ Soave-Redlich-Kwong EoS

$SSAFT$ Simplified Statistical Associating Fluid Theory

$STP$ Standard Temperature Pressure

$THF$ Tetrahydrofuran

$TPT$ Thermodynamic Perturbation Theory

$UCST$ Upper Critical Solution Temperature

$UNIFAC$ Universal Functional Group Activity Coefficients

$UNIQUAC$ Universal Quasichemical Group Activity Coefficients

$VF$ Volume Fraction

$VLE$ Vapour-Liquid Equilibrium

$VOC$ Volatile Organic Compounds

**Symbols**

$\tilde{a}$ Reduced Helmholtz energy

$A$ Helmholtz energy [J]

$a$ Parameter in the energy term $[\text{bar L}^2/\text{mol}^2]$

$a_{A/B}$ Permselectivity

$aw$ Activity-Weight

$B$ Second virial coefficient $[\text{cm}^3\,\text{mol}/\text{g}^2]$

$b$ Co-volume parameter $[\text{L}/\text{mol}]$

| | |
|---|---|
| $D$ | Diffusion coefficient [$^{cm^2}/_{s}$ or $^{m^2}/_{s}$] |
| $d$ | Temperature-dependent segment diameter [Å] |
| $D_{ij}$ | Universal constants |
| $g$ | Radial distribution function |
| $G^E$ | Excess Gibbs energy |
| $H$ | Henry's constant [$^{L\ atm}/_{mol}$ or $^{Pa\ m^3}/_{mol}$] |
| $I$ | Ionisation potential [eV] |
| $k$ | Boltzmann's constant [$1.38066 \times 10^{-23}\ ^{J}/_{K}$] |
| $k_{ij}$ | Binary interaction parameter |
| $\overline{m}$ | Mean segment number per molecule |
| $M$ | Number of association sites per molecule |
| $m$ | Segment number per molecule |
| $M_n$ | Number average polymer molecular weight |
| $M_w$ | Molecular weight [$^{g}/_{mol}$] |
| $N$ | Number of molecules |
| $n$ | Number of moles |
| $N_A$ | Avogadros' constant [$6.022 \times 10^{23}\ ^{1}/_{mol}$] |
| $N_c$ | Number of carbon atoms |
| $N_{DP}$ | Number of data points |
| $n_i$ | Occurence of the type $i$ first-order group in a compound |
| $n_j$ | Occurence of the type $j$ second-order group in a compound |
| $NC$ | Number of compounds |
| $P$ | Permeability coefficient [$^{cm^3(STP)\ cm}/_{cm^2\ s\ Pa}$] |
| $P$ | Pressure [Pa or atm] |
| $P^{exp}$ | Experimental vapour pressure [Pa or atm] |
| $P^{sat}$ | Saturated vapour pressure [Pa or atm] |
| $Q$ | Quadrupolar moment term |

| | |
|---|---|
| $R$ | Ideal gas constant [$8.3145\,{}^{\mathrm{J}}/_{\mathrm{mol\,K}}$] |
| $R^2$ | Coefficient of determination of a linear regression |
| $S$ | Shape factor |
| $S$ | Sorption coefficient [${}^{\mathrm{cm^3(STP)}}/_{\mathrm{cm^3\,Pa}}$] |
| $T$ | Temperature [K or °C] |
| $T_b$ | Boiling point temperature [K or °C] |
| $T_r$ | Reduced temperature |
| $u$ | Intermolecular potential |
| $V$ | Total volume [$\mathrm{cm^3}$ or L] |
| $V_L$ | Liquid volume [${}^{\mathrm{cm^3}}/_{\mathrm{mol}}$] |
| $w$ | Weight fraction |
| $x, y$ | Mole fraction |
| $X^A$ | Mole fraction of molecules NOT bonded at site A |
| $Z$ | Compressibility factor ($= {}^{PV}/_{nRT}$) |

**Greek letters**

| | |
|---|---|
| $\chi$ | Flory-Huggins interaction parameter |
| $\Delta^{AB}$ | Association strength |
| $\epsilon$ | (Energy parameter) depth of the dispersion potential [J] |
| $\eta$ | Packing fraction, reduced segment density |
| $\gamma^{\infty}$ | Mole fraction activity coefficient at infinite dilution |
| $\kappa^{AB}$ | Volume of association |
| $\mu$ | Dipole moment [D] |
| $\nu^0$ | Closed packed hard-core volume |
| $\nu^{00}$ | Segment volume |
| $\Omega^{\infty}$ | Weight fraction activity coefficient at infinite dilution |
| $\rho$ | Total number density of molecules [$\mathrm{\AA}^{-3}$] |
| $\Sigma$ | Summation |

| | |
|---|---|
| $\sigma$ | Segment diameter $\left[\text{Å}\right]$ (temperature-independent) |
| $\zeta$ | Partial volume fraction |

**Superscripts**

| | |
|---|---|
| $assoc$ | Association |
| $calc$ | Calculated |
| $chain$ | Chain |
| $disp$ | Dispersion |
| $est$ | Estimated |
| $exp$ | Experimental |
| $hc$ | Hard chain |
| $hs$ | Hard sphere |
| $id$ | Ideal |
| $\propto$ | Infinite dilution |
| $sat$ | Saturated |
| $seg$ | Segment |

**Subscripts**

| | |
|---|---|
| 1 | Component index for the solvent/short chain alkane |
| 2 | Component index for the polymer/long chain alkane |
| $AB$ | Alkyl benzene |
| $BR$ | Benzene ring |
| $i, j$ | Component $i$, $j$ |
| $PA$ | Polyaromatic |

# Chapter 1

# Introduction

*"Applied thermodynamics today is 'primarily a tool for stretching' experimental data: given some data for limited conditions, thermodynamics provides procedures for generating data at other conditions."* by Prof. J.M. Prausnitz

## 1.1 Introduction

The chemical industry is involved in the development of high-value products, e.g. in the areas of specialty chemicals, functional materials, paints, detergents, pharmaceuticals, and food ingredients. Development of these complex "soft" products requires the ability to find molecular structures with the required functionality and without undesirable side effects for health or the environment. Such characteristics are related to the physical properties (thermodynamics) of the molecules and the mixtures involved. Predicting the product properties based on molecular structure is often referred to as *Computer-Aided Product Design*. This type of modelling requires special considerations due to

- the complexity of molecules which are normally composed of several interlinked aromatic cores and multiple substituents containing heteroatoms [N, P, O, X (= F, Cl, etc.)]
- the presence of various types of intermolecular forces (polarity, hydrogen bonding, etc.) where some of them are due to the aromatic delocalized $\pi$-electrons and the electronegative heteroatoms, and
- the frequent coexistence of many phases at equilibrium e.g. vapour-liquid-liquid or solid-liquid-liquid.

In order to facilitate modelling of chemical systems of various complexities, it is beneficial to have predictive thermodynamic models.

## 1.2 Industrial Applications of Polymers

By definition, polymers (or synonymous "macromolecules") are very large molecules that contain more than 100 atoms (up to millions). The production, modification, and processing of polymers are very important to world industry. The world production of polymers has now by far exceeded the production of steel (by weight) and is close to 250 million tons in the year 2007. The initial problem of plastics waste disposal seems to be solved by a combination of legal actions and economically viable collection and redistribution systems.

Most polymers produced as structural materials, "standard plastics", are based on polyolefins such as PE, PP, and similar hydrocarbon polymers and copolymers. The application of plastics to substitute more conventional materials, e.g. metals, glass, ceramics, in the packaging industry, or to develop new technologies, e.g. optical devices, is innovative and a constant source of industrial evolution. More expensive "specialty" polymers, those made from different, complicated starting monomers or from complex mixtures, are increasingly substituted by new generations of inexpensive "commodity" polymers; those produced from a few simple starting compounds. This relates to the constant improvement of the processing properties and physical characteristics of polyolefins by invention and adaptation of novel catalysts in the polymerization processes. The new structural variations at the level of the molecular architecture lead to a constant evolution of the properties in application [1].

Polymers produced as functional materials serve in a multitude of applications; as additives, processing aids, adhesives, coatings, viscosity regulators, lubricants, and many more. They are found in cosmetics and pharmaceuticals, semi-prepared foods, in printing inks and paints; they are used as super absorbers in hygienic products and in the processing of ceramics and concrete, as flocculants in waste-water treatments, and as adhesive in the hardware production of various electro-optical equipments. This is just to mention a few. Recent developments of functional polymers have had revolutionary effects on the industry in which they found applications. The widespread use of polymers in biomedical applications plays an increasing role as implants, in dentistry, in the surgery of connective tissue and arteries, artificial lenses, as well as general medical technology [1, 2].

The truth is that plastics and other polymers, e.g. elastomers and fibers, have taken over many roles in the world we live in today, to a point where it is impossible to escape them; from the containers of the food we eat to the trash we produce. Plastics are unavoidable! That is why various challenges of establishing a model-based understanding of chemical products and processes inspire thermodynamic researchers. Solutions to these challenges may arrive from the developments and further improvements in statistical theories, molecular simulations, and other similar computational tools. Moreover, advanced equipment and extended experimental databases are needed to assist in the assessment of these challenges without which no models can ever be developed and tested.

### 1.2.1 High-Priority Research Topics

A brief Internet survey among the largest leading industries in polymer production, such as DuPont, BASF, DSM, etc., gave the following high-priority targets for research devoted to polymers:

- *"Solvent free" polymerization* processes to reduce environmental hazards and reduce the costs of polymer production.
- A development of *analytical and quantitative predictive methods* of characterization of structure and performance of polymers. Among these, the analytical characterization of particulate systems and of dispersions needs to be improved.
- *Polymerization in aqueous media.* Water born polymers and water based coatings will reduce environmental hazards of present technologies. To achieve this it is important to develop fast and precise methods to determine phase equilibrium of aqueous polymer mixtures.
- Enhanced efforts in the finding and evolution of *better catalysts for olefins polymerization*, with emphasis on metallocene based catalysts, to improve already existing large-scale polymer productions.
- Understanding and improving the *mechanisms of adhesion* and failure of adhesives, being possibly prevented by various surface modifications, adhesion between living systems (cells) and polymers, the co-called bioadhesives.
- Improved availability of *computational techniques* to understand the behaviour of polymer materials and phase equilibrium in order to relate details of the molecular structure and changes during processing and applications. Recent modified computational techniques used by academia need to be transferred to industries, and, at the same time improving the methods of simulations with regards to the broad spectrum of applications and properties of polymers in practice.
- Understanding how and why *weak- and long-range interactions* among the molecular constituents in various polymeric materials lead to hierarchical structures and in most cases time-dependent physical and engineering properties.

## 1.3 The Role of Thermodynamics

During industrial applications, polymers are usually subjected to various conditions of temperatures and pressures. Furthermore, they are also very often in contact with gasses and fluids, either as on-duty materials (as containers, pipes) or as process intermediates (in foaming, moulding). Therefore, careful characterization and investigation must be done not only at the early stages of their development, but also throughout their life cycle. Their properties as function of temperature and pressure must be well established, including phase transitions, phase diagrams, and chemical reactivity. Knowledge of gas solubility and gas diffusion in polymers, as well as swelling capacity is quite essential in many areas and requires information on the type and extent of the interactions between the polymer and the gas.

When engineers first attempted to model polymerization chemistries, they either had to limit their efforts to modelling single-phase properties or use polymer thermodynamic models with composition-dependent interaction parameters that offered little extrapolation capability [3]. The lack of experimental data and engineering models for polymer thermodynamics further limited the value of these polymer modelling efforts. The progress within computer-based simulation and modelling of various properties of polymers of interest have speeded up the process of research and development in polymer science. Theoretical treatment of polymer solutions was initiated independently and simultaneously by Flory [4] and Huggins [5] in 1942. The *Flory-Huggins theory* is based on the lattice model. The limitations of the Flory-Huggins theory have been recognized for a long time and there has been considerable subsequent work done to correct the deficiencies and extend lattice-type theory [3]. Today, proven polymer thermodynamic models, such as the polymer NRTL activity coefficient models of Chen from 1993 [6], and the Perturbed-Chain Statistical Associating Fluid Theory (PC-SAFT) Equation of State (EoS) of Gross and Sadowski from 2002 [7], with composition-independent model parameters, are available to allow interpolation and extrapolation of phase behaviours. For example, an engineer can ask how the phase behaviour of a mixture changes when the number of carbons in a solvent molecule is increased or decreased or when a hydrogen bonding group is added to one of the components [8].

Nevertheless, existing relevant software is often unable to serve the purpose adequately and needs further improvements. As an example, let us take the computation of phase equilibrium for polymer systems where no distribution of polymer molecular weight and chemical compositions of various phases are taken into account. Industrial polymer(s) is(are) polydisperse. After the feed polymer phase separates, the molecular weight distribution of polymers in the light phase is different from that in the heavy phase. Research is still on-going to enhance robustness of the existing algorithms for solving this kind of problem. Recently, Jog and Chapman [9] and Gosh *et al.* [10] have developed and implemented robust algorithms for polydisperse polymers. Further discussion on calcu-

lation methods for polydisperse polymer solutions can be found in the work of Hu and others [11–13].

Another example to be mentioned is the pharmaceutical process design where the choice of solvents and solvent mixtures, from among hundreds of common candidates, for reaction, separation, and purification is very important. Phase behaviour, such as solubility, of the new molecules in solvents depends on the choice of solvents in the initial recipe developments [14]. Often little or no experimental data are available for the new molecules. Predictive models that allow for computation of phase behaviour are needed. Existing solubility parameter models, such as that of Hansen [15], offer limited predictive power, and group contribution models, such as UNIFAC by Fredenslund *et al.* [16], may possibly fail due to inadequacy of functional group additivity rule with large, complex molecules and various limitations for complex types of phase equilibria and mixtures.

Indeed many articles have been written on the development of applied thermodynamics in the chemical industry and the practical challenges that remain. For example, Prausnitz [17–20] has reviewed many years of progress in developing and applying phase equilibria models to various processes and presented how molecular thermodynamics and chemical engineering with a variety of novel, powerful concepts, and experimental tools are making a liberating impact on the subject concerned in this thesis. Additionally, Abildskov and Kontogeorgis [21] discussed the challenges of applied thermodynamics. Several other relevant investigations have been published, such as by Zeck [22], Villadsen [23], Arlt *et al.* [24], Mathias [25], etc.

## 1.4 Project Objectives

The prediction or correlation of the thermodynamic properties and phase equilibria with equations of state remains an important goal in chemical and related industries. Since the early 1980's, when the theory of Wertheim [26–29] emerged from statistical thermodynamics, the method has been implemented into a new generation of engineering equations of state called Statistical Associating Fluid Theory (SAFT). Numerous modifications and improvements of different versions of SAFT have been proposed and applied to various mixtures over the last years, such as SAFT hard-sphere (SAFT-HS) [30–32], simplified SAFT [33], SAFT Lennard-Jones (SAFT-LJ) [34,35], perturbed-chain SAFT (PC-SAFT) [7], simplified PC-SAFT (sPC-SAFT) [36], polar SAFT [37], soft-SAFT [38, 39], SAFT variable range (SAFT-VR) [40, 41] to mention only a few. Two reviews [42, 43] provide more detailed discussions of recent developments and applications of the various types of SAFT.

Both versions of the PC-SAFT model, the original and simplified, are able to predict the effects of molecular weight, copolymerization, and hydrogen bonding on the thermodynamic properties and phase behaviour of complex fluids including solvents, monomers, and polymer solutions and blends. Complete description of these systems requires three

physically meaningful temperature-independent parameters: the segment number ($m$), the hard-core segment diameter ($\sigma$), and the segment-segment interaction energy parameter ($\epsilon/k$) for each pure non-associating fluid. They are typically fitted to vapour pressure and liquid density data. Associating fluids require two additional compound parameters, the association energy ($\epsilon^{AB}$), and the association volume ($\kappa^{AB}$).

Since high-molecular-weight compounds, like polymers, do not have a detectable vapour pressure and commonly undergo thermal degradation before exhibiting a critical point, determination of EoS parameters is sometimes based solely on experimental density data [44]. Unfortunately, derivation of polymer parameters based only on density data usually results in poor prediction of phase equilibria with the SAFT EoS. Alternatively, density data for the pure polymer together with mixture phase equilibria data can be used. This method is not practical and moreover the parameters may depend on the type of mixture data used. Hence, there is a need for a predictive calculation method for polymers and complex compounds EoS parameters.

One suggested solution to this problem is to develop a group contribution scheme for estimating the parameters of these EoS based on low molecular weight compounds, for which data is available, and then extrapolate to complex molecules.

The main objective of this project is to develop a theoretically based engineering tool that can be used for complex mixtures of importance to polymer and pharmaceutical industries. The thermodynamic model to be developed is a group-contribution (GC) version of the sPC-SAFT [36] EoS where the parameters of the model are estimated via the group contribution method developed by Constantinou and Gani in 1994 [45].

Several practically important types of experimental thermodynamic data, such as VLE and LLE, will be collected from the literature and used to evaluate the performance of the predictive GC sPC-SAFT model. The only data required for calculating these properties are the molecular structure of the compounds of interest in terms of functional groups, and a single binary interaction parameter for accurate mixture calculations.

The thesis is, accordingly, divided into the following chapters. Details regarding chemical structures of complex compounds investigated in this work and supplementary materials are provided in the appendices.

Chap. 1: **Introduction**
Current chapter. Provides an introduction to the subject of the thesis and problem objectives.

Chap. 2: **The SAFT Model**
Provides a brief description of the models that are used throughout this thesis.

Chap. 3: **Group Contribution Approach**
Gives a short overview of the use of the group contribution formalism within the SAFT formalism, and explains the group-contribution concept based on the so-called *"conjugation principle"* applied in this work.

Chap. 4: **Extension of the PC-SAFT Parameter Table**
Presents applications of the sPC-SAFT model using an extended parameter table for predicting VLE and LLE for non-associating systems. Parts of this work are published in Ref. [46]. A more predictive way to calculate the required $k_{ij}$ values is investigated using an additional physical parameter (ionization energy of involved compounds).

Chap. 5: **Validation of sPC-SAFT in Novel Polymer Applications**
The sPC-SAFT description of the phase equilibria of binary mixtures of polymers with non-associating and associating solvents, as well as some polymer blends with available polymer parameters is presented. Ability of the model to correlate the solubility of plasticizers in poly(vinyl chloride) (PVC) is investigated, and the results are compared with free-volume activity coefficient models, such as UNIFAC, ENTROPIC-FV, etc. Prediction of the infinite dilution activity coefficients in athermal and nearly athermal systems is tested as well. Parts of this work are published in Ref. [47].

Chap. 6: **The GC sPC-SAFT Model**
Outlines the important steps in the development of the model including a GC scheme for first-order and second-order groups, as well as various approaches considered during the work.

Chap. 7: **Analysis and Application of GC sPC-SAFT**
The predictive capability of the GC approach is tested. Additionally, VLE and LLE modeling of mixtures of some industrially important polymers are investigated. Numerous other chemical systems, e.g. biofuels, phytochemicals, alkyl and aryl sulfides, thiols and aromatic compounds including various benzene derivatives, etc, are investigated with the proposed approach. A part of this work considering polymer systems is published in Ref. [48].

Chap. 8: **Conclusion and Future Work**
Summarizing important conclusions and rounding off the thesis with proposals of subjects for future work.

## References


[1] N. J. Mills, *Plastics: Microstructure and Engineering Applications*. Arnold, London, UK, 1993.

[2] S. L. Rose, *Fundamental Principles of Polymeric Materials*. John Wiley and Sons, USA, 1993.

[3] J. M. Prausnitz, R. N. Lichtenthaler, and E. Gomes de Azevedo, *Molecular Thermodynamics of Fluid Phase Equilibria*. Prantice-Hall, Englewood Cliffs, NJ, 1999.

[4] P. J. Flory, "Thermodynamics of High Polymer Solutions," *J. Chem. Phys.*, vol. 10, pp. 51–61, 1942.

[5] M. L. Huggins, "Some Properties of Solutions of Long-Chain Compounds," *J. Phys. Chem.*, vol. 46, pp. 151–158, 1942.

[6] C.-C. Chen, "A Segment-Based Local Composition Model for the Gibbs Energy of Polymer Solutions," *Fluid Phase Equilibria*, vol. 83, pp. 301–312, 1993.

[7] J. Gross and G. Sadowski, "Modeling Polymer Systems Using the Perturbed-Chain Statistical Associating Fluid Theory Equation of State," *Ind. Eng. Chem. Res.*, vol. 41, pp. 1084–1093, 2002.

[8] D. Ghonasgi and W. G. Chapman, "Prediction of the Properties of Model Polymer Solutions and Blends," *AIChE J.*, vol. 40, pp. 878–887, 1994.

[9] P. K. Jog and W. G. Chapman, "An Algorithm for Calculation of Phase Equilibria in Polydisperse Polymer Solutions Using the SAFT Equation of State," *Macromolecules*, vol. 35, pp. 1002–1011, 2002.

[10] A. Ghosh, P. D. Ting, and W. G. Chapman, "Thermodynamic Stability Analysis and Pressure-Temperature Flash for Polydisperse Polymer Solutions," *Ind. Eng. Chem. Res.*, vol. 43, pp. 6222–6230, 2004.

[11] J. Cai, H. Liu, and J. M. Prausnitz, "Critical Properties of Polydisperse Fluid Mixtures from an Equation of State," *Fluid Phase Equlibria*, vol. 168, pp. 91–106, 2000.

[12] Y. Hu, X. Ying, D. T. Wu, and J. M. Prausnitz, "Liquid-Liquid Equilibria for Solutions of Polydisperse Polymers. Continuous Thermodynamics for the Close-Packed Lattice Model," *Macromolecules*, vol. 26, pp. 6817–6823, 1993.

[13] Y. Hu and J. M. Prausnitz, "Stability Theory for Polydisperse Fluid Mixtures," *Fluid Phase Equlibria*, vol. 130, pp. 1–18, 1997.

[14] K. A. Connors, *Thermodynamics of Pharmaceutical Systems: An Introduction for Students of Pharmacy*. John Wiley and Sons, USA, 2002.

[15] C. M. Hansen, *Hansens Solubility Parameters: A User's Handbook*. CRC Press LLC, Boca Raton, Florida, 1999.

[16] A. Fredenslund, R. L. Jones, and J. M. Prauznitz, "Group-Contribution Estimation of Activity Coefficients in Nonideal Liquid Mixtures," *AIChE J.*, vol. 21, pp. 1086–1099, 1975.

[17] J. M. Prausnitz, "Biotechnology: A New Frontier for Molecular Thermodynamics," *Fluid Phase Equilibria*, vol. 53, pp. 439–451, 1989.

[18] J. M. Prausnitz, "Some New Frontiers in Chemical Engineering Thermodynamics," *Fluid Phase Equilibria*, vol. 104, pp. 1–20, 1995.

[19] J. M. Prausnitz, "Thermodynamics and the Other Chemical Engineering Sciences: Old Models for New Chemical Products and Processes," *Fluid Phase Equilibria*, vol. 158–160, pp. 95–111, 1999.

[20] J. M. Prausnitz, "Chemical Engineering and the Post-Modern World," *Chem. Eng. Sci.*, vol. 56, pp. 3627–3639, 2001.

[21] J. Abildskov and G. Kontogeorgis, "Chemical Product Design: A New Challenge of Applied Thermodynamics," *Chem. Eng. Res. Dev.*, vol. 82, pp. 1505–1510, 2004.

[22] S. Zeck, "Thermodynamics in Process Development in the Chemical Industry - Importance, Benefits, Current State and Future Development," *Fluid Phase Equilibria*, vol. 70, pp. 125–140, 1991.

[23] J. Villadsen, "Putting Structure into Chemical Engineering: Proceedings of an Industry/University Conference," *Chem. Eng. Sci.*, vol. 52, pp. 2857–2864, 1997.

[24] W. Arlt, O. Spuhl, and A. Klamt, "Challenges in Thermodynamics," *Chem. Eng. Process*, vol. 43, pp. 221–238, 2004.

[25] P. M. Mathias, "Applied Thermodynamics in Chemical Technology: Current Practice and Future Challenges," *Fluid Phase Equilibria*, vol. 228–229, pp. 49–57, 2002.

[26] M. S. Wertheim, "Fluid with Highly Directional Attractive Forces. I. Statistical Thermodynamics," *J. Stat. Phys.*, vol. 35, pp. 19–34, 1984.

[27] M. S. Wertheim, "Fluid with Highly Directional Attractive Forces. II. Thermodynamic Perturbation Theory and Integral Equations," *J. Stat. Phys.*, vol. 35, pp. 35–47, 1984.

[28] M. S. Wertheim, "Fluid with Highly Directional Attractive Forces. III. Multiple Attraction Sites," *J. Stat. Phys.*, vol. 42, pp. 459–476, 1986.

[29] M. S. Wertheim, "Fluid with Highly Directional Attractive Forces. IV. Equilibrium Polymerization," *J. Stat. Phys.*, vol. 42, pp. 477–492, 1986.

[30] W. G. Chapman, K. E. Gubbins, G. Jackson, and M. Radosz, "New Reference Equation of State for Associating Liquids," *Ind. Eng. Chem. Res.*, vol. 29, pp. 1709–1721, 1990.

[31] A. Galindo, P. J. Whitehead, and G. Jackson, "Predicting the High-Pressure Phase Equilibria of Water+$n$-Alkanes Using a Simplified SAFT Theory with Transferable Intermolecular Interaction Parameters," *J. Phys. Chem.*, vol. 100, pp. 6781–6792, 1996.

[32] A. Galindo, P. J. Whitehead, G. Jackson, and A. N. Burgess, "Predicting the Phase Equilibria of Mixtures of Hydrogen Fluoride with Water, Difluromethane (HFC-32), and 1,1,1,2-Tetrafluoroethane (HFC-134a) Using a Simplified SAFT Approach," *J. Phys. Chem. B.*, vol. 101, pp. 2082–2091, 1997.

[33] Y. H. Fu and S. I. Sandler, "A Simplified SAFT Equation of State for Associating Compounds and Mixtures," *Ind. Eng. Chem. Res.*, vol. 34, pp. 1897–1909, 1995.

[34] T. Kraska and K. E. Gubbins, "Phase Equilibria Calculations with a Modified SAFT Equation of State, Fluid Phase Equilibria," *Ind. Eng. Chem. Res.*, vol. 35, pp. 4727–4737, 1996.

[35] T. Kraska and K. E. Gubbins, "Phase Equilibria Calculations with a Modified SAFT Equation of State. 1. Pure Alkanes, Alkanols, and Water," *Ind. Eng. Chem. Res.*, vol. 35, pp. 4738–4746, 1996.

[36] N. von Solms, M. L. Michelsen, and G. M. Kontogeorgis, "Computational and Physical Performance of a Modified PC-SAFT Equation of State for Highly Asymmetric and Associating Mixtures," *Ind. Eng. Chem. Res.*, vol. 42, pp. 1098–1105, 2003.

[37] E. K. Karakatsani, T. Spyriouni, and I. G. Economou, "Extended SAFT Equations of State for Dipolar Fluids," *AIChE. J.*, vol. 51, pp. 2328–2342, 2005.

[38] F. J. Blas and L. F. Vega, "Thermodynamic Behaviour of Homonuclear and Heteronuclear Lennard-Jones Chains with Association Sites from Simulation and Theory," *Mol. Phys.*, vol. 92, pp. 135–150, 1997.

[39] F. J. Blas and L. F. Vega, "Prediction of Binary and Ternary Diagrams Using the Statistical Associating Fluid Theory (SAFT) Equation of State," *Ind. Eng. Chem. Res.*, vol. 37, pp. 660–674, 1998.

[40] A. Gil-Villegas, A. Galindo, P. J. Whitehead, S. J. Mills, G. Jackson, and A. N. Burgess, "Statistical Associating Fluid Theory for Chain Molecules with Attractive Potentials of Variable Range," *J. Chem. Phys.*, vol. 106, pp. 4168–4186, 1997.

[41] A. Galindo, L. A. Davies, A. Gil-Villegas, and G. Jackson, "The Thermodynamics of Mixtures and the Corresponding Mixing Rules in the SAFT-VR Approach for Potentials of Variable Range," *Mol. Phys.*, vol. 93, pp. 241–252, 1998.

[42] E. A. Müller and K. E. Gubbins, "Molecular-Based Equations of State for Associating Fluids: A Review of SAFT and Related Approaches," *Ind. Eng. Chem. Res.*, vol. 40, pp. 2193–2211, 2001.

[43] I. G. Economou, "Statistical Associating Fluid Theory: A Successful Model for Calculation of Thermodynamic and Phase Equilibrium Properties of Complex Fluid Mixtures," *Ind. Eng. Chem. Res.*, vol. 41, pp. 953–962, 2002.

[44] O. Pfohl, C. Riebesell, and R. Z. Dohrn, "Measurement and Calculation of Phase Equilibria in the System *n*-Pentane + Poly(dimethylsiloxane) at 308.15–423.15 K," *Fluid Phase Equilibria*, vol. 202, pp. 289–306, 2002.

[45] L. Constantinou and R. Gani, "New Group Contribution Method for Estimating Properties of Pure Compounds," *AIChE J.*, vol. 40, pp. 1697–1710, 1994.

[46] A. Tihic, G. M. Kontogeorgis, N. von Solms, and M. L. Michelsen, "Application of the Simplified Perturbed-Chain SAFT Equation of State Using an Extended Parameter Table," *Fluid Phase Equilibria*, vol. 248, pp. 29–43, 2007.

[47] I. G. Economou, Z. A. Makrodimitri, G. M. Kontogeorgis, and A. Tihic, "Solubility of Gases and Solvents in Silicon Polymers: Molecular Simulation and Equation of State Modeling," *Molecular Simulation*, vol. 33, pp. 851–860, 2007.

[48] A. Tihic, G. M. Kontogeorgis, N. von Solms, M. L. Michelsen, and L. Constantinou, "A Predictive Group-Contribution Simplified PC-SAFT Equation of State: Application to Polymer Systems," *Ind. Eng. Chem. Res.*, vol. 47, pp. 5092–5101, 2008.

# Chapter 2

# The SAFT Model

*"A theory is the more impressive the greater the simplicity of its premises, the more different kinds of things it relates, and the more extended its area of applicability. Therefore, the deep impression which thermodynamics made upon me. It is the only physical theory of universal content which I am convinced will never be overthrown, within the framework of applicability of its basic concepts."* by Albert Einstein

## 2.1 Introduction

Accurate and, preferably, simple equations of state (EoS) are needed for the study of small-molecules/solvent or macromolecules/solvent mixtures and simulation of different process scenarios. Models should be able to predict the changes in phase behaviour as a function of solvent quality or as a function of the solute nature, e.g. polymer, with a minimum number of fitted parameters [1]. Most conventional engineering EoS are variations of the van der Waals equations. These equations are based on the idea of a hard-sphere reference term to represent the repulsive interactions, and a mean-field term to account for the dispersion and other long-range forces. Some commonly used EoS, such as cubic, involve improvements to either the treatment of the hard-sphere contribution or the mean-field terms. Such models are found to be very flexible in fitting phase equilibrium data for simple, nearly spherical molecules such as low molecular mass hydrocarbons, and simple inorganic compounds, e.g. nitrogen or carbon monoxide.

During the last decade cubic EoS have been employed in the oil and chemical industry with extensions to polymer applications [2, 3]. The extensions of these equations to polymers possess some theoretical limitations and weaknesses and are, therefore, mainly accomplished in an empirical way. Chain formation, which is of utmost importance in polymer solutions, is not explicitly taken into account. The $a$ and $b$ parameters, which in the case of low molecular compounds are obtained via the critical pressure and temperature, now have to be calculated either through empirical correlations or from some fixed values of "critical" polymer properties that are the same for all polymers. As a result,

extra parameters are usually needed in the correlation equations, which are adjusted to a specific set of experimental data depending on the desired application of the EoS and, thus, cannot be considered universal. Additionally, cubic EoS with conventional mixing rules are not adequate for systems with polar or associating compounds (e.g. water) that present high deviations from ideality in the liquid phase. This is because in the cubic EoS only the dispersive interactions are explicitly taken into account.

A better predictive capability can generally be expected with an equation such as the Statistical Associating Fluid Theory (SAFT) [4, 5] or the Sanchez-Lacombe (SL) [6] EoS. Both of these non-cubic EoS are derived from statistical mechanics. The SL equation is a lattice-gas expression that accounts for dispersion and repulsive interactions. Chain formation for short chains can be considered but association is not accounted for. The SAFT EoS has been developed by Chapman et al. [7] and is based on the perturbation theory of Wertheim [8–11]. Perturbation theories divide the interactions of molecules into a repulsive part and a contribution due to the attractive part of the potential. To calculate the repulsive contribution, a reference fluid is defined in which no attractions are present. Each perturbation is a correction that results in the model resembling more closely the actual mixture.

The development of segment-based non-cubic EoS obtained from statistical mechanics is performed in a quite rigorous and systematic way. As one of the few approaches that has, in practice, been able to migrate from "small molecules" to macromolecules, the ability of the SAFT approach to perform calculations of the phase equilibria of mixtures of compounds with wide disparities in molecular size, such a polymer/solvent mixtures, is very successful.

It is worth mentioning that in the various SAFT modifications, different attractive terms are proposed, i.e. different terms for the dispersion term of the EoS, while the chain and association terms remain essentially unchanged. Several reviews of EoS that include comparisons of some of the SAFT models are available [12, 13]. In the past 18 years (since SAFT appeared), more than 450 published articles dealing directly with the SAFT approach and its application, and more than 5400 cross-references have proved that the SAFT framework indeed provides a state-of-art thermodynamic description of multi-compound mixtures of varying complexity. (Based on ISI Web of Science survey [14].)

## 2.2 The SAFT Equation of State

In SAFT, molecules are modelled as chains of covalently bounded spheres. Homologous series, such as *n*-alkanes and polymers, can be modelled as chains of identical spheres where the number of spheres in the chain is proportional to the molecular weight. In SAFT, the reduced residual Helmholtz energy is of the form:

$$\tilde{a} \equiv \frac{A}{NkT} = \tilde{a}^{seg} + \tilde{a}^{chain} + \tilde{a}^{assoc} \tag{2.1}$$

where $\tilde{a}^{seg}$ is the part of the Helmholtz energy due to segment-segment interactions, $\tilde{a}^{chain}$ is the term due to chain formation, and $\tilde{a}^{assoc}$ represents the contribution due to association between different molecules, e.g. hydrogen bonding.

A detailed discussion of the mathematical form of the SAFT equations can be found elsewhere [12, 13] and is not provided here. However, in the following subsections, a brief description is given of the SAFT model used in this work.

### 2.2.1 Original SAFT Equation of State

As mentioned before, Wertheim [8–11] developed a statistical thermodynamic theory for fluids with a repulsive core and one or more highly directional short-range attractive sites. Wertheim [15] extended his theory to non-associating chain fluids and developed the first- and second-order thermodynamic perturbation theories (TPT1 and TPT2) for a polydisperse mixture of chains of varying lengths with mean length $\overline{m}$. Following the work of Wertheim [15], Chapman and co-workers [4, 7, 16] developed an EoS for spherical and chain molecules of fixed length $m$ with one or more hydrogen-bonded sites. Their model led to an EoS for associating chain molecules called the Statistical Associating Fluid Theory (SAFT) and therefore it is often referred to as *original* SAFT in the literature. In fact, there are relatively small differences between the SAFT model of Chapman *et al.* [4] and the SAFT model of Huang and Radosz [5], which has also gained considerable popularity maybe due to the numerous parameters available for real fluids. In the implementation of Chapman *et al.*, for the hard-sphere term, the Carnahan-Starling equation [17] is used, while the dispersion term is expressed by Cotterman *et al.* [18]. Huang and Radosz [5] applied a different dispersion term proposed by Chen and Kreglewski [19] in their SAFT framework. The difference will be shown later on. In this study, when referred to the *original* SAFT, the Chapman model is implied.

As with any theory, SAFT is based on the following assumptions [20]:

1. Only one bond can form at any associating site [10].
2. Only single bonds are formed between molecules.
3. The property of the fluid is independent of the angles between association sites on the molecule [21].
4. When solved by thermodynamic perturbation theory, the theory includes the effect of chain-like and three-like associated clusters, but not ring clusters.

One of the possible ways of writing the original SAFT EoS for pure fluids [4] is in terms of the compressibility factors:

$$Z = 1 - Z^{hs} + Z^{chain} + Z^{assoc} + Z^{disp} \tag{2.2}$$

where

$$Z^{hs} = \frac{4\eta - 3\eta^2}{(1-\eta)^2} \tag{2.3}$$

$$Z^{chain} = (1-m)\ln\left[\frac{1-\frac{1}{2}\eta}{(1-\eta)^3}\right] \tag{2.4}$$

$$Z^{assoc} = \sum_{A=1}^{M}\left[\ln X^A - \frac{X^A}{2}\right] + \frac{1}{2}M \tag{2.5}$$

$$Z^{disp} = m\frac{u^0}{kT}\left(a_1^{disp} + \frac{u^0}{kT}a_2^{disp}\right) \qquad \text{(Chapman } et\ al.\text{ [4])} \tag{2.6}$$

$$\text{where } a_1^{disp} = -11.604\eta - 6.132\eta^2 - 2.871\eta^3 + 13.885\eta^4$$
$$\text{where } a_2^{disp} = -2.575\eta + 13.463\eta^2 - 29.992\eta^3 + 21.470\eta^4$$

$$Z^{disp} = m\sum_{i=1}^{4}\sum_{j=1}^{9} D_{ij}\left(\frac{u}{kT}\right)^i\left(\frac{\eta}{0.74048}\right)^j \text{ (Huang \& Radosz [5])} \tag{2.7}$$

$$\text{where } \frac{u}{k} = \left(\frac{u^0}{k}\right)\left(1 + \frac{\epsilon}{kT}\right) \quad \text{and} \quad \epsilon/k = 10\,\text{K}$$
$$\text{except for a few small molecules (for details, see [5])}$$

with the auxiliary definitions

$$\eta = 0.74048\rho m\nu^0 \tag{2.8}$$

$$\nu^0 = \nu^{00}\left[1 + 0.2977\left(\frac{u^0}{kT}\right)^{-1}\right] \Bigg/ \left[1 + 0.33163\left(\frac{u^0}{kT}\right)^{-1}\right] + \left[0.00140477 + 0.025337\frac{m-1}{m}\right] \Bigg/ \left[\frac{u^0}{kT}\right]^2 \tag{2.9}$$

(Chapman *et al.* [4])

$$\nu^0 = \nu^{00}\left[1 + \mathcal{C}\exp\left(-3\frac{u^0}{kT}\right)\right]^3 \qquad \text{(Huang \& Radosz [5])} \tag{2.10}$$

$$\text{where } \mathcal{C} = 0.12 \text{ (except for hydrogen, which is 0.241)}$$

$$X^A = \left(1 + \sum_{B=1}^{M} \rho X^B \Delta^{AB}\right)^{-1} \tag{2.11}$$

$$\Delta^{AB} = \sqrt{2}\nu^0 \frac{1 - \frac{1}{2}\eta}{(1-\eta)^3} \left[\exp\left(\frac{\epsilon^{AB}}{kT}\right) - 1\right] \kappa^{AB} \tag{2.12}$$

(Chapman *et al.* [4])

$$\Delta^{AB} = \sqrt{2}\nu^{00} \frac{1 - \frac{1}{2}\eta}{(1-\eta)^3} \left[\exp\left(\frac{\epsilon^{AB}}{kT}\right) - 1\right] \kappa^{AB} \tag{2.13}$$

(Huang & Radosz [5])

Chapman *et al.* [4] reported that the agreement with molecular simulation data was good at all stages of the model development, for associating spheres, mixtures of associating spheres, and non-associating chains up to $m = 8$.

#### 2.2.1.1 Pure Component Parameters

The first step in the application of the SAFT EoS to multicompound mixtures, or generally in any EoS, is to determine the pure compound parameters. There are five pure compound parameters in the equation. The first parameter is the number of hard spheres, $m$, that form a molecule. The second parameter is the volume of a mole of these spheres when they are closely packed, $\nu^{00}$ (in $^{\mathrm{cm}^3}/_{\mathrm{mol}}$); this variable sets their size. The third pure compound parameter is the segment energy, $u^0$ (in K), which determines segment-segment interactions. In addition to these three parameters for non-associating compounds, the equation has two associating parameters, $\epsilon^{AA}$ and $\kappa^{AA}$. The parameter $\epsilon^{AA}$ characterizes the association energy and the parameter $\kappa^{AA}$ characterizes the associating volume for the associating site A.

These parameters are normally determined by fitting experimental vapor pressure and liquid density data. The fitted parameters were found to be well-behaved and physically reasonable, following a simple relationship with molar mass within a given homologous series, so that extrapolation could be made to fluids not included in the fit.

It is known that the resulting predictions around the critical point are not good unless an additional term is explicitly considered taking into account the density (and composition) fluctuations appearing in this region. This approach has been considered by some research groups [22–27]. In order to provide a better description of the critical region, the crossover formalism has been applied within the SAFT approach. Unfortunately, this formalism cannot be applied to mixtures in a straightforward way. Its application to even pure fluids is complex enough to avoid its use for practical applications. As an alternative

solution, the pure compound parameters of the SAFT equation can be rescaled to the critical point of each pure fluid and then used to predict the mixture behaviour [28–30]. This approach leads to two different sets of molecular parameters; those used for subcritical calculations and those rescaled to the critical point for near-critical calculations. It is worth mentioning that although the critical region is more accurately represented with the scaled parameters, the problems affect the accuracy at lower temperatures. In particular, the saturated liquid densities are under predicted with these parameters. However, all mixtures modeled in this work have been far away from the critical region, and therefore there has been no need to consider these improvements.

#### 2.2.1.2 Polymer Parameters

Since high molecular weight polymers have no detectible vapour pressure and thermally degrade before reaching the critical point, EoS parameters for polymers are generally determined using measured data for pure liquid molar volumes. Unfortunately, with original SAFT, it is seen that a regression over polymer parameters from this type of data generally leads to incorrect phase equilibrium calculations.

For example, in their original work, Huang and Radosz [5] proposed $\nu^{00} = 12\,\mathrm{mL/mol}$ and $u^0/k = 210\,\mathrm{K}$ for polymers, and to estimate segment number parameters from the $n$-alkanes corollary: $m = 0.05096 M_n$, where $M_n$ stands for the number average polymer molecular weight, which is the sum of the molecular weights of the individual molecules present in a sample divided by their total number; that is $M_n = \frac{\sum N_i M_i}{\sum N_i}$. An alternative approach to obtain the polymer parameters is to regress a pure compound parameter from the polymer binary phase equilibrium data. A third alternative based on a combination of these two approaches was proposed by Lora *et al.* [31]. They extended the group contribution approach of Huang and Radosz for calculating $m$ and $\nu^{00}$ to acrylate polymers as a function of the value for a repeating unit, with $m$ being corrected for the size of the polymer according to $M_n$.

The polymers are polydisperse in all of these approaches, but the calculations are performed by taking a monodisperse molecular weight equal to $M_n$, because of the otherwise large amount of work required to model and characterize polydisperse polymers. However, it has been possible to model the polymers as a mixture of pseudo-compounds, as the data for the molecular weight fractions of the polymers are available [5].

#### 2.2.1.3 Binary Mixtures and Mixing Rules

The great utility of EoS is for phase equilibrium calculations involving mixtures. The assumption in such calculations is that the same EoS used for pure fluids can be used for mixtures. This is commonly achieved by using mixing rules and combining rules, which relate the properties of the pure compounds to that of the mixtures. Mixing rules are

commonly used in various mixture models ranging from cubic EoS to theoretically-based molecular models.

The mixing rule based on the van der Waals one-fluid theory, referred to as the *vdW1* mixing rule, is applied in the original SAFT EoS. Mixing rules are only required for the dispersion term in the SAFT EoS, in fact only for two parameters, $u/k$ and $m$.

A mixing rule is needed for the average segment number, $m$, which is given from the expression:

$$m = \sum_i \sum_j x_i x_j m_{ij} \tag{2.14}$$

where $m_{ij} = \frac{1}{2}(m_i + m_j)$.

A second mixing rule is needed for the energy of attraction between segments, $u/k$. Chapman *et al.* [4] used:

$$\nu^0 = \frac{\sum_i \sum_j x_i x_j m_i m_j \left(\nu^0\right)_{ij}}{\left(\sum_i \sum_j x_i x_j m_{ij}\right)^2} \tag{2.15}$$

$$\frac{u^0}{k}\nu^0 = \frac{\sum_i \sum_j x_i x_j m_i m_j \frac{u^0_{ij}}{k} \left(\nu^0\right)_{ij}}{\left(\sum_i \sum_j x_i x_j m_{ij}\right)^2} \tag{2.16}$$

where $u^0_{ij} = \left(u^0_{ii} u^0_{jj}\right)^{1/2}(1 - k_{ij})$ and $\left(\nu^0\right)_{ij} = \left(\frac{1}{2}\left[\left(\nu^0\right)_i^{1/3} + \left(\nu^0\right)_j^{1/3}\right]\right)^3$.

Huang and Radosz [5] used:

$$\frac{u}{k} = \frac{\sum_i \sum_j x_i x_j m_i m_j \frac{u_{ij}}{k} \left(\nu^0\right)_{ij}}{\sum_i \sum_j x_i x_j m_{ij} \left(\nu^0\right)_{ij}} \tag{2.17}$$

where $u_{ij} = \left(u_{ii} u_{jj}\right)^{1/2}(1 - k_{ij})$ and $\left(\nu^0\right)_{ij} = \left(\frac{1}{2}\left[\left(\nu^0\right)_i^{1/3} + \left(\nu^0\right)_j^{1/3}\right]\right)^3$. In addition, they proposed an alternative mixing rule based on volume fraction ($VF$) expressed with:

$$\frac{u}{k} = \frac{\sum_i \sum_j x_i x_j m_i m_j \frac{u_{ij}}{k} \left(\nu^0\right)_{ii} \left(\nu^0\right)_{jj}}{\sum_i \sum_j x_i x_j m_{ij} \left(\nu^0\right)_{ii} \left(\nu^0\right)_{jj}} \tag{2.18}$$

Both mixing rules assume that the local composition of the fluid is similar to the bulk composition (one-fluid theory) and therefore the parameters of the mixture fluid can be calculated as an average of the parameters of pure compounds using a weighting factor (mole fraction of volume fraction). Huang and Radosz [5] concluded that the two mixing rules provide similar results for VLE calculations except when close to the critical region where the VF mixing rule is more accurate, and so it is to be preferred if the investigated system contains a compound near its critical point.

#### 2.2.1.4 Binary Interaction Parameter

The binary interaction parameter $k_{ij}$ is a fitted, binary mixture parameter that corrects the mean-field energy contribution of SAFT. This parameter is determined by fitting to experimental mixture phase equilibrium data.

It is essential to keep in mind that binary interaction parameters are used to "correct" a theory, in a way that real systems can be represented with higher accuracy. Larger values of the binary interaction parameter would indicate that the applied model (or combining rule) is not the most adequate to represent the system of interest and that modifications or different models should be utilized instead.

### 2.2.2 PC-SAFT Equation of State

One of the successful SAFT modifications is the PC-SAFT EoS [32]. The main difference between SAFT and PC-SAFT is the perturbation sequence: PC-SAFT takes the reference system to be the mixture of hard-sphere chains and then introduces the dispersive attractions. In Figure 2.1, the physical basis underlying PC-SAFT is shown schematically.

The PC-SAFT equation of state is an attempt to model asymmetric and highly non-ideal systems. PC-SAFT has previously been applied to high-pressure liquid-liquid equilibria of mixtures of polymers and polymer blends with various hydrocarbon solvents [32,34,35], where it has shown improved performance over the original SAFT [4,5]. It has also recently been applied to associating mixtures of alcohols in short-chain hydrocarbons [36], where both vapour-liquid and liquid-liquid equilibrium were simultaneously described with a single binary interaction parameter. Most recently it has been extended to copolymer systems [37], systems with polar and quadrupolar components [38–42], etc.

#### 2.2.2.1 Model Description

In the framework of PC-SAFT, molecules are assumed to be chains of freely jointed spherical segments and can be expressed in terms of the reduced residual Helmholtz energy, which is made up of the following contributions:

$$\tilde{a} \equiv \frac{A}{NkT} = \tilde{a}^{id} + \tilde{a}^{hc} + \tilde{a}^{disp} + \tilde{a}^{assoc} \tag{2.19}$$

The hard-sphere chain contribution accounting for the repulsion of the chain-like molecules is made up by the hard-sphere and the chain formation contributions:

$$\tilde{a}^{hc} = \overline{m}\tilde{a}^{hs} + \tilde{a}^{chain} = \overline{m}\tilde{a}^{hs} - \sum_i x_i(m_i - 1)\rho\frac{\partial \ln g_{ii}^{hs}}{\partial \rho} \tag{2.20}$$

where $\overline{m}$ is the average number of segments per chain:

$$\overline{m} = \sum_{i=1}^{NC} x_i m_i \tag{2.21}$$

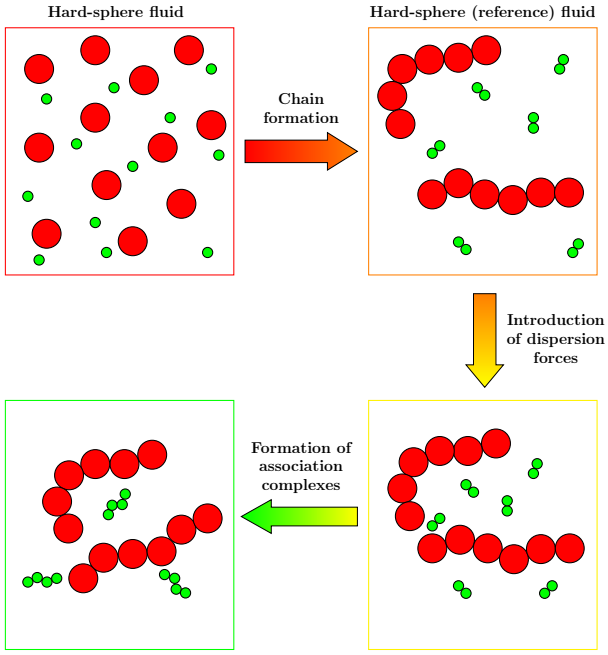


Figure 2.1: Schematic illustration of the physical basis of the PC-SAFT model. The illustration is freely adopted from [33].

The hard-sphere term is given by the mixture version of the Carnahan-Starling [17] EoS for hard-spheres.

$$\tilde{a}^{hs} = \frac{1}{\zeta_0}\left[\frac{3\zeta_1\zeta_2}{1-\zeta_3} + \frac{\zeta_2^3}{\zeta_3\left(1-\zeta_3\right)^2} + \left(\frac{\zeta_2^3}{\zeta_3^2}-\zeta_0\right)\ln\left(1-\zeta_3\right)\right] \tag{2.22}$$

where $\zeta_n$ are the partial volume fractions defined by:

$$\zeta_n = \frac{\pi\rho}{6}\sum_i x_i m_i d_i^n, \qquad n \in \{0,1,2,3\} \tag{2.23}$$

and $d_i$ is the Chen and Kreglewski [19] temperature-dependent segment diameter of component $i$:

$$d_i = \sigma_i\left[1 - 0.12\exp\left(-\frac{3\epsilon_i}{kT}\right)\right] \tag{2.24}$$

The temperature-dependent segment diameter of component $i$ is the outcome of the integration of the equation for the effective hard-collision diameter of the chain segments:

$$d(T) = \int_0^\sigma \left[1 - \exp\left(-\frac{u(r)}{kT}\right)\right] \mathrm{d}r \tag{2.25}$$

which is based on the modified square well potential for segment-segment interactions. The chain term in Equation (2.20) depends also on the radial distribution function at contact, which is given by:

$$g_{ij}^{hs}(d_{ij}) = \frac{1}{1-\zeta_3} + \left(\frac{d_i d_j}{d_i + d_j}\right) \frac{3\zeta_2}{(1-\zeta_3)^2} + \left(\frac{d_i d_j}{d_i + d_j}\right)^2 \frac{2\zeta_2^2}{(1-\zeta_3)^2} \tag{2.26}$$

The radial distribution function denotes the probability density for finding a hard-sphere belonging to a $j$-molecule at a distance $d$ from a hard sphere belonging to an $i$-molecule.

In most versions of the SAFT equation the dispersion term contribution to the molecular Helmholtz energy is proportional to the number of segments. However, in PC-SAFT, the dispersion term is written for chains of segments based on second order perturbation theory, i.e. the attractive part of the chain interactions is calculated from a first and a second order perturbation, according to Barker and Henderson [43]. Basically, these are calculated by integrating the intermolecular interactions over the entire mixture volume, which leads to:

$$\tilde{a}^{disp} = -2\pi\rho I_1 m^2 \epsilon \sigma^3 - \pi\rho\overline{m}\left(1 + \tilde{a}^{hc} + \rho\frac{\partial\tilde{a}^{hc}}{\partial\rho}\right)^{-1} I_2 m^2 \epsilon^2 \sigma^3 \tag{2.27}$$

The required integrals are approximated by power-series in density, where the coefficients of the power series are functions of the chain length:

$$I_1 = \sum_{i=0}^{6} a_i\left(\overline{m}\right)\eta^i \tag{2.28}$$

$$I_2 = \sum_{i=0}^{6} b_i\left(\overline{m}\right)\eta^i \tag{2.29}$$

The dependency of the coefficients $a_i(\overline{m})$ and $b_i(\overline{m})$ upon segment number is described by the equations:

$$a_i(\overline{m}) = a_{01} + \frac{\overline{m}-1}{\overline{m}}a_{1i} + \frac{\overline{m}-1}{\overline{m}}\frac{\overline{m}-2}{\overline{m}}a_{2i} \tag{2.30}$$

$$b_i(\overline{m}) = b_{01} + \frac{\overline{m}-1}{\overline{m}}b_{1i} + \frac{\overline{m}-1}{\overline{m}}\frac{\overline{m}-2}{\overline{m}}b_{2i} \tag{2.31}$$

and

$$m^2\epsilon^y\sigma^3 = \sum_{i=1}^{NC}\sum_{i=j}^{NC} x_i x_j m_i m_j \left(\frac{\epsilon_{ij}}{kT}\right)^y \sigma_{ij}^3, \qquad y \in \{1,2\} \tag{2.32}$$

The cross-parameters are obtained from the combining rules:

$$\sigma_{ij} = \frac{\sigma_i + \sigma_j}{2} \tag{2.33}$$

$$\epsilon_{ij} = \sqrt{\epsilon_{ii}\epsilon_{jj}}\,(1 - k_{ij}) \tag{2.34}$$

The constants in Equations (2.30) and (2.31) are considered to be universal, and are obtained by an indirect regression to experimental pure compound vapour pressures for a series of $n$-alkanes. The fitting procedure and the values of fitting constants can be found in Ref. [32] based on results of Chiew [44].

The association contribution is only included for systems containing components capable of self-associating and cross-associating (e.g. alcohols and acids). The association contribution is:

$$\tilde{a}^{assoc} = \sum_i x_i \sum_{A_i} \left(\ln X^{A_i} - \frac{1}{2}X^{A_i} + \frac{1}{2}\right) \tag{2.35}$$

where $X^{A_i}$ is the fraction of A-sites on molecule $i$ that does not form associating bonds with other active sites. This number is found through the solution of the non-linear system of equations:

$$X^{A_i} = \left(1 + N_A \sum_j \rho_j \sum_{B_j} X^{B_j}\Delta^{A_iB_j}\right)^{-1} \tag{2.36}$$

where $\rho_j$ is the molar density of component $j$, and $\Delta^{A_iB_j}$ is a measure of the association strength between site A on molecule $i$ and site B on molecule $j$. This parameter in turn is a function of the association volume $\kappa^{A_iB_j}$, the association energy $\epsilon^{A_iB_j}$, and the radial distribution function as follows:

$$\Delta^{A_iB_j} = \sigma_{ij}^3 g^{hs}(d^+)\kappa^{A_iB_j}\left[\exp\left(\frac{\epsilon^{A_iB_j}}{kT}\right) - 1\right] \tag{2.37}$$

where $\Delta^{A_iB_j}$ is the so-called association strength. Note that the temperature independent diameter $\sigma$ is used in Equation (2.37).

### 2.2.3 Simplified PC-SAFT Equation of State

In the simplified PC-SAFT (sPC-SAFT) EoS [45], the expression for the contributions from dispersion ($\tilde{a}^{disp}$) is identical to Equations (2.27)–(2.34) of the original PC-SAFT presented in the previous paragraph.

The targets of the modification are Equations (2.22) and (2.26) and the motivation is that since the segment diameters of the species in the mixture are frequently very similar to each other, Equations (2.22) and (2.26) will reduce to the much simpler pure component versions. This, in turn, makes the computation of the derivatives in phase equilibrium calculations simpler and less computational intensive, both for the hard-sphere chain term, Equation (2.20), and for the association term, Equation (2.35).

Therefore, by assuming that all the segments in the mixture have the same mean diameter $d$, that gives a mixture volume fraction identical to that of the actual mixture, the volume fraction $\zeta_3 = \frac{\pi\rho}{6}\sum_i x_i m_i d_i^3$ is now based on the diameter of a one-component mixture having a volume corresponding to the fraction $\zeta_3$:

$$\zeta_3 \equiv \eta = \frac{\pi\rho}{6} d^3 \sum_i x_i m_i \tag{2.38}$$

This average diameter is then given by the following expression:

$$d = \left( \frac{\sum_i x_i m_i d_i^3}{\sum_i x_i m_i} \right)^{1/3} \tag{2.39}$$

When this modification is applied to Equations (2.22) and (2.26), they are reduced to:

$$\tilde{a}^{hs} = \frac{4\zeta - 3\zeta^2}{(1-\zeta)^2} \tag{2.40}$$

$$g^{hs} = \frac{1 - \frac{1}{2}\zeta}{(1-\zeta)^3} \tag{2.41}$$

Modifications of the sPC-SAFT EoS compared to the original PC-SAFT are given in Table 2.1.

Table 2.1: Modifications of the sPC-SAFT EoS compared to the original PC-SAFT.

| PC-SAFT [32] | sPC-SAFT [45] |
|---|---|
| $g_{ij}^{hs} = \frac{1}{1-\zeta_3} + \left(\frac{d_i d_j}{d_i+d_j}\right)^2 \frac{3\zeta_2}{(1-\zeta_3)^2} + \left(\frac{d_i d_j}{d_i+d_j}\right)^2 \frac{2\zeta_2^2}{(1-\zeta_3)^3}$ | $g^{hs}(\eta) = \frac{1-\eta/2}{(1-\eta)^3}$ |
| $\tilde{a}^{hs} = \frac{1}{\zeta_0}\left[\frac{3\zeta_1\zeta_2}{1-\zeta_3} + \frac{\zeta_2^3}{\zeta_3(1-\zeta_3)^2} + \left(\frac{\zeta_2^3}{\zeta_3^2} - \zeta_0\right)\ln(1-\zeta_3)\right]$ | $\tilde{a}^{hs} = \frac{4\eta-3\eta^2}{(1-\eta)^2}$ |

When it comes to the association term, the modification yields a composition-independent expression for the radial distribution function used in Equation (2.37), which means that this complex contribution to $\Delta^{A_i B_j}$ is factored out of the component summation of Equation (2.36).

#### 2.2.3.1 Pure Component Parameters

The sPC-SAFT requires, like the original PC-SAFT, three pure component parameters for a non-associating compound: the segment number, $m$, the interaction energy, $\epsilon/k$, expressed in K, and the hard core segment radius, $\sigma$, expressed in Å. For associating compounds, sPC-SAFT needs two additional parameters: the association energy (well-depth) $\epsilon^{AB}$ and the dimensionless association co-volume (well-width) $\kappa^{AB}$. For volatile substances, the values for these parameters can be obtained by fitting experimental data, e.g. vapour pressures and liquid densities.

#### 2.2.3.2 Polymer Parameters

For polymers, the current practice is to estimate the pure component parameters from volumetric (PVT) data and experimental binary data. Alternatively, for polyolefins, the parameters can be estimated by extrapolating the $n$-alkane parameters. As a result, the effect of chemical structure, chain architecture, branching, and morphology of the polymer on the phase behaviour of a mixture is calculated implicitly through the binary interaction parameter(s).

von Solms *et al.* [45] have observed that for $n$-alkanes (from ethane to eicosane), the following equations show linearity of pure component parameters as a function of $M_w$:

$$m = 0.02537 M_w + 0.9081 \tag{2.42}$$

$$m\epsilon/k = 6.918 M_w + 127.3 \tag{2.43}$$

Inspired by similar linear trends, an alternative approach to estimate polymer parameters has been proposed by Kouskoumvekaki *et al.* [46] based on analysis from $n$-alkane series. By assuming that the functional form of Equations (2.42) and (2.43) holds for all polymers, these two equations can be rewritten in a more generalized form:

$$m = A_m M_w + B_m \tag{2.44}$$

$$m\epsilon/k = A_\epsilon M_w + B_\epsilon \tag{2.45}$$

In order to find the four constants in Equations (2.44) and (2.45), Kouskoumvekaki *et al.* made the assumption that polymers become indistinguishable in the limit of zero $M_w$; hence $B_m = 0.9081$ and $B_\epsilon = 127.3$. The two remaining constants $A_m$ and $A_\epsilon$ can be obtained by using Equations (2.44) and (2.45), and the values of the parameters $m$ and $\epsilon/k$ for the monomer unit of the polymer under study. Meaning that by dividing Equations (2.44) and (2.45) by $M_w$ and considering the limit of high $M_w$, Equations (2.46) and (2.47) are obtained:

$$m/M_w = A_m \tag{2.46}$$

$$\epsilon/k = A_\epsilon/A_m \tag{2.47}$$

The parameters $m$ and $\epsilon/k$ of the polymer are afterwards calculated with Equations (2.46) and (2.47). The value of the last missing parameter $\sigma$ is obtained by fitting the value to the pure polymer PVT data over a wide range of temperatures and pressures. Following this procedure, Kouskoumvekaki *et al.* [46] obtained results including values of the constants $A_m$ and $A_\epsilon$ for investigated monomers, and PC-SAFT parameters for a number of polymers.

However, it has been observed earlier [46] that pure component polymer parameters for PC-SAFT obtained by methods, which use binary phase equilibrium, are not unique for each polymer, but rather dependent on the binary system chosen for the regression. This is demonstrated by results in Table 2.2 when comparing the pure component parameters of PVC regressed from pure polymer PVT data and binary phase equilibrium data in five different ways. The PVC parameter estimation methods are listed as following:

Case 1: The method developed by Kouskoumvekaki *et al.* [46].

Case 2: Using PVT and a single binary VLE data set for the system PVC–1,4-dioxane.

Case 3: Using PVT and the same binary VLE data sets as Case 2, excluding the binary interaction parameter.

Case 4: Using PVT and six binary VLE data sets for PVC with di(1-butyl)ether, 1,4-dioxane, tetrachloromethane, toluene, tetrahydrofuran (THF), and vinyl chloride.

Case 5: Using PVT and the same number of binary VLE data sets as Case 4, excluding the binary interaction parameter.

Table 2.2: Values of PC-SAFT parameters and average deviations between calculated and experimental liquid densities of poly(vinyl chloride) (PVC) using different methods.

| Case | Data set | $m/M_w$ [mol/g] | $\sigma$ [Å] | $\epsilon/k$ [K] | $T$ range [K] | $P$ range [bar] | AAD $\rho$ [%] |
|---|---|---|---|---|---|---|---|
| 1. | Kouskoumvekaki *et al.* [46] approach | 0.0210 | 3.724 | 315.93 | 373–423 | 1–1000 | 0.5 |
| 2. | PVT + single binary VLE incl. $k_{ij}$ | 0.0121 | 4.726 | 541.56 | 373–423 | 1–1000 | 1.6 |
| 3. | PVT + single binary VLE excl. $k_{ij}$ | 0.0298 | 3.213 | 221.19 | 373–423 | 1–1000 | 1.2 |
| 4. | PVT + all binary VLE incl. $k_{ij}$ | 0.0097 | 5.030 | 495.86 | 373–423 | 1–1000 | 1.4 |
| 5. | PVT + all binary VLE excl. $k_{ij}$ | 0.0142 | 4.298 | 360.92 | 373–423 | 1–1000 | 0.8 |

The results summarized in Table 2.2 show that the values of all parameters depend to a great extent on the number of the binary data sets used in combination with the

pure polymer PVT data, as well as the presence of a binary interaction parameter. How these different parameter sets effect phase equilibria calculations for PVC will be further analysed in Chapters 5 and 7.

Good initial values are important in the optimization of the parameters based on experimental data, because the dispersive and associating forces are intercorrelated. For example, the estimated value of the liquid density can be increased by increasing the association energy, but also by decreasing the hard-core radius. Thus, the five parameters are largely intercorrelated and multiple solutions can be obtained [47].

## 2.3 Final Comments

Past efforts have mainly concentrated on developing SAFT equations suitable for phase equilibrium calculations. Numerous published works have demonstrated that the SAFT equations are particularly useful for complex phase equilibrium problems, including polymers and their mixtures, surfactants and micellar systems, water and electrolytes, and fluids with strong intermolecular bonding. Even though SAFT-based models have received an acceptance in academia and in industry, more work remains before these models can become standard tools for process simulations. In terms of polymer applications, one of the most important limitations of SAFT models is the currently used methods to estimate polymer model parameters. For example, derivation of polymer parameters based only on density data usually results in poor predictions of phase equilibria with the SAFT EoS. Recent publications have demonstrated that this shortcoming remains even in the newest versions of the SAFT EoS, such as PC-SAFT and sPC-SAFT. Hence, there is a need for a predictive calculation method for polymer EoS parameters.

The study of strength and limitations of sPC-SAFT model to present mixtures with small molecules and those with small molecules and macromolecules will be carried out in the following chapters. Most of the work is performed using sPC-SAFT version of EoS, while some comparisons are performed with the original PC-SAFT model.

## References

[1] C. F. Kirkby and M. A. McHugh, "Phase Behaviour of Polymers in Supercritical Fluid Solvents," *Chem. Rev.*, vol. 99, pp. 565–602, 1999.

[2] G. M. Kontogeorgis, V. I. Harismiadis, A. Fredenslund, and D. P. Tassios, "Application of the van der Waals Equation of State to Polymers. I. Correlation," *Fluid Phase Equilibria*, vol. 96, pp. 65–92, 1994.

[3] T. Sako, A. H. Wu, and J. M. Prausnitz, "A Cubic Equation of State for High-Pressure Phase Equilibria of Mixtures Containing Polymers and Volatile Fluids," *J. Appl. Chem. Sci.*, vol. 38, pp. 1839–1858, 1989.

[4] W. G. Chapman, K. E. Gubbins, G. Jackson, and M. Radosz, "New Reference Equation of State for Associating Liquids," *Ind. Eng. Chem. Res.*, vol. 29, pp. 1709–1721, 1990.

[5] S. H. Huang and M. Radosz, "Equation of State for Small, Large, Polydisperse, and Associating Molecules," *Ind. Eng. Chem. Res.*, vol. 29, pp. 2284–2294, 1990.

[6] I. C. Sanchez and R. H. Lacombe, "Statistical Thermodynamics of Polymer Solutions," *Macromolecules*, vol. 11, pp. 1145–1156, 1978.

[7] W. G. Chapman, G. Jackson, and K. E. Gubbins, "Phase Equilibria of Associating Fluids: Chain Molecules with Multiple Bonding Sites," *Mol. Phys.*, vol. 65, pp. 1057–1079, 1988.

[8] M. S. Wertheim, "Fluid with Highly Directional Attractive Forces. I. Statistical Thermodynamics," *J. Stat. Phys.*, vol. 35, pp. 19–34, 1984.

[9] M. S. Wertheim, "Fluid with Highly Directional Attractive Forces. II. Thermodynamic Perturbation Theory and Integral Equations," *J. Stat. Phys.*, vol. 35, pp. 35–47, 1984.

[10] M. S. Wertheim, "Fluid with Highly Directional Attractive Forces. III. Multiple Attraction Sites," *J. Stat. Phys.*, vol. 42, pp. 459–476, 1986.

[11] M. S. Wertheim, "Fluid with Highly Directional Attractive Forces. IV. Equilibrium Polymerization," *J. Stat. Phys.*, vol. 42, pp. 477–492, 1986.

[12] E. A. Müller and K. E. Gubbins, "Molecular-Based Equations of State for Associating Fluids: A Review of SAFT and Related Approaches," *Ind. Eng. Chem. Res.*, vol. 40, pp. 2193–2211, 2001.

[13] I. G. Economou, "Statistical Associating Fluid Theory: A Successful Model for Calculation of Thermodynamic and Phase Equilibrium Properties of Complex Fluid Mixtures," *Ind. Eng. Chem. Res.*, vol. 41, pp. 953–962, 2002.

[14] "ISI Web of Science." `http://isiwebofknowledge.com`. ISI Web of Knowledge, Thomson Scientific, January 2008.

[15] M. S. Wertheim, "Thermodynamic Perturbation Theory of Polymerisation," *J. Chem. Phys.*, vol. 87, pp. 7323–7330, 1987.

[16] G. Jackson, W. G. Chapman, and K. E. Gubbins, "Phase Equilibria of Associating Fluids Spherical Molecules with Multiple Bonding Sites," *Mol. Phys.*, vol. 65, pp. 1–31, 1988.

[17] N. F. Charnahan and K. E. Starling, "Equation of State for Nonattracting Rigid Spheres," *J. Chem. Phys.*, vol. 51, pp. 635–636, 1969.

[18] R. L. Cotterman, B. J. Schwarz, and J. M. Prausnitz, "Molecular Thermodynamics for Fluid at Low and High Densities. Part 1: Pure Fluid Containing Small and Large Molecules," *AIChE J.*, vol. 32, pp. 1787–1798, 1986.

[19] S. S. Chen and A. Kreglewski, "Applications of Augmented van der Waals Theory of Fluids. I. Pure Fluids," *Ber. Bunsen. Phys. Chem.*, vol. 81, pp. 1048–1052, 1977.

[20] D. Ghonasgi and W. G. Chapman, "Prediction of the Properties of Model Polymer Solutions and Blends," *AIChE J.*, vol. 40, pp. 878–887, 1994.

[21] D. Ghonasgi and W. G. Chapman, "Theory and Simulation for Associating Chain Fluids," *Molec. Phys.*, vol. 80, pp. 161–175, 1993.

[22] A. K. Wyscalkowska, J. V. Senger, and M. A. Anisimov, "Critical Fluctuations and the Equation of State of van der Waals," *Physica A*, vol. 334, pp. 482–512, 2004.

[23] S. B. Kiselev, "Cubic Crossover Equation of State," *Fluid Phase Equilibria*, vol. 147, pp. 7–23, 1998.

[24] S. B. Kiselev and D. Friend, "Cubic Crossover Equation of State for Mixtures," *Fluid Phase Equilibria*, vol. 162, pp. 51–82, 1999.

[25] L. Lue and J. M. Prausnitz, "Renormalization Group Corrections to an Approximate Free-Energy Model for Simple Fluids Near to and Far From the Critical Region," *J. Chem. Phys.*, vol. 108, pp. 5529–5536, 1998.

[26] J. Jiang and J. M. Prausnitz, "Equation of State for Thermodynamic Properties of Chain Fluids Near-To and Far-From the Vapour-Liquid Critical Region," *J. Chem. Phys.*, vol. 111, pp. 5964–5974, 1999.

[27] J. Cai and J. M. Prausnitz, "Thermodynamics for Fluid Mixtures near to and far from the Vapour-Liquid Critical Region," *Fluid Phase Equlibria*, vol. 219, pp. 205–217, 2004.

[28] F. Llovell, J. C. Pàmies, and L. F. Vega, "Thermodynamic Properties of Lennard-Jones Chain Molecules: Renormalization-Group Corrections to a Modified Statistical Associating Fluid Theory," *J. Chem. Phys.*, vol. 121, pp. 10715–10724, 2004.

[29] F. J. Blas and L. F. Vega, "Critical Behaviour and Partial Miscibility Phenomena in Binary Mixtures of Hydrocarbons by the Statistical Associating Fluid Theory," *J. Chem. Phys.*, vol. 109, pp. 7405–7413, 1998.

[30] C. McCabe, A. Gil-Villegas, and G. Jackson, "Predicting the High Pressure Phase Equilibria of Methane+$n$-Hexane Using the SAFT-VR Approach," *J. Phys. Chem. B*, vol. 102, pp. 4183–4188, 1998.

[31] M. Lora, F. Rindfleisch, and M. A. McHugh, "Influence of the Alkyl Tail on the Solubility of Poly(alkyl acrylates) in Ethylene and $CO_2$ at High Pressures: Experiments and Modeling," *J. Appl. Poly. Sci.*, vol. 73, pp. 1979–1991, 1999.

[32] J. Gross and G. Sadowski, "Perturbed-Chain SAFT: An Equation of State Based on Perturbation Theory for Chain Molecules," *Ind. Eng. Chem. Res.*, vol. 40, pp. 1244–1260, 2001.

[33] J. M. Prausnitz, R. N. Lichtenthaler, and E. Gomes de Azevedo, *Molecular Thermodynamics of Fluid Phase Equilibria*. Prantice-Hall, Englewood Cliffs, NJ, 1999.

[34] J. Gross and G. Sadowski, "Modeling Polymer Systems Using the Perturbed-Chain Statistical Associating Fluid Theory Equation of State," *Ind. Eng. Chem. Res.*, vol. 41, pp. 1084–1093, 2002.

[35] F. Tumakaka, J. Gross, and G. Sadowski, "Modeling of Polymer Phase Equilibria using Perturbed-Chain SAFT," *Fluid Phase Equilibria*, vol. 194, pp. 541–551, 2002.

[36] J. Gross and G. Sadowski, "Application of the Perturbed-Chain SAFT Equation of State to Associating Systems," *Ind. Eng. Chem. Res.*, vol. 41, pp. 5510–5515, 2002.

[37] J. Gross, O. Spuhl, F. Tumakaka, and G. Sadowski, "Modeling Copolymer Systems Using the Perturbed-Chain SAFT Equation of State," *Ind. Eng. Chem. Res.*, vol. 42, pp. 1266–1274, 2003.

[38] E. K. Karakatsani, T. Spyriouni, and I. G. Economou, "Extended SAFT Equations of State for Dipolar Fluids," *AIChE. J.*, vol. 51, pp. 2328–2342, 2005.

[39] E. K. Karakatsani and I. G. Economou, "Perturbed Chain-Statistical Associating Fluid Theory Extended to Dipolar and Quadrupolar Molecular Fluids," *J. Phys. Chem. B*, vol. 110, pp. 9252–9261, 2006.

[40] M. Kleiner and J. Gross, "An Equation of State Contribution for Polar Components: Polarizable Dipoles," *AIChE J.*, vol. 52, pp. 1951–1961, 2006.

[41] J. Gross and J. Vrabec, "An Equation of State Contribution for Polar Components: Dipolar Molecules," *AIChE J.*, vol. 52, pp. 1194–1204, 2006.

[42] J. Gross, "An Equation of State Contribution for Polar Components: Quadrupolar Molecules," *AIChE J.*, vol. 51, pp. 2556–2568, 2005.

[43] J. A. Barker and D. Henderson, "Perturbation Theory and Equation of State for fluids. II. A Successful Theory of Liquids," *J. Chem. Phys.*, vol. 47, pp. 4714–4721, 1967.

[44] Y. Chiew, "Percus-Yevich Integral Equation Theory for Athermal Hard-Sphere Chains: II. Average Intermolecular Correlation Function," *Mol. Phys.*, vol. 73, pp. 359–373, 1991.

[45] N. von Solms, M. L. Michelsen, and G. M. Kontogeorgis, "Computational and Physical Performance of a Modified PC-SAFT Equation of State for Highly Asymmetric and Associating Mixtures," *Ind. Eng. Chem. Res.*, vol. 42, pp. 1098–1105, 2003.

[46] I. A. Kouskoumvekaki, N. von Solms, T. Lindvig, M. L. Michelsen, and G. M. Kontogeorgis, "Novel Method for Estimating Pure-Component Parameters for Polymers: Application to the PC-SAFT Equation of State," *Ind. Chem. Eng. Res.*, vol. 43, pp. 2830–2838, 2004.

[47] I. A. Kouskoumvekaki, N. von Solms, M. L. Michelsen, and G. M. Kontogeorgis, "Application of a Simplified Perturbed Chain SAFT Equation of State to Complex Polymer Systems Using Simplified Mixing Rules," *Fluid Phase Equilibria*, vol. 215, pp. 71–78, 2004.

# Chapter 3

# Group Contribution Approach

*"Scientists discover the world that exists; engineers create the world that never was."*
by Thedore Von Karman

## 3.1 Introduction

The experimental data needed to develop thermodynamic models are often scarce for complex and large molecules. Moreover, experimental measurements can be extremely costly and time consuming. Therefore, predictive thermodynamic models play an important role in process design and development of complex products. Accurate prediction of the physical properties of candidate molecular structures is an integral part of computer aided molecular design, in which optimal molecules with a desired set of properties are designed. Group contribution (GC) methods are widely used predictive tools in both process and molecular design. The framework of each group contribution approach is that a system, which can be a pure component or mixture, is treated at the level of representative functional groups, and the properties of the system are obtained by considering the separate contributions that the involved groups make to the overall molecular properties.

GC methods are the most widely used techniques for estimating and predicting thermophysical properties of pure compounds and mixtures [1]. Use of the GC principle in models for phase equilibrium calculations can greatly enhance their predictive capabilities.

## 3.2 Overview of GC Approaches Applied to SAFT

Throughout the last decades, different GC concepts have been applied directly within the framework of an EoS to develop a predictive thermodynamic theory. Various popular methods have been proposed in which a GC activity coefficient approach (such as UNIFAC) is used to obtain a mixing rule for the calculation of the mixture parameters within a given EoS. The resulting theories, so-called EoS-$G^E$ methods, become predictive as no fitting binary interaction parameter is needed. Nevertheless, knowledge of the pure compound parameter is necessary for the application of these methods, which limits their applicability. One popular EoS-$G^E$ model is the predictive Soave-Redlich-Kwong (PSRK) approach [2], in which the SRK EoS [3] is combined with UNIFAC for the calculation of the attractive mixture parameter. Other EoS-$G^E$ model include MHV2 [4,5], LCVM [6], and the method of Orbey *et al.* [7]. Among the first attempts, one may find the GC-EoS by Skjold-Jorgensen [8]; later modified by Gros *et al.* [9], who added an additional associating term. 35 different chemical groups are treated within the GC EoS and various other extensions have been presented [10, 11]. The model covers wide temperature ranges and pressures below 25 MPa.

Implementation of GC concepts within an EoS where a group contribution scheme is applied directly to the calculation of the molecular parameters of the theory, enhances the predictive capability of the EoS. High and Danner [12,13] developed a group contribution lattice-fluid (GCLF) EoS for polymer solutions. A number of modifications followed their original article in order to apply the method to VLE of polymer–solvents [14,15]. Coniglio *et al.* [16,17] examined the popular cubic Peng-Robinson (PR) [18] EoS. Another approach proposed by Elvassore *et al.* [19] combines a GC method with the perturbed-hard-sphere-chain (PHSC) EoS developed by Song *et al.* [20]. The characteristic molecular EoS parameters were obtained by fitting both vapour pressures and saturated liquid densities from which the GC values were determined. This approach provided satisfactory results and improved the PHSC theory allowing modelling of VLE and LLE of mixtures of high $M_w$ compounds. Elliott and Natarajan [21] developed a GC form of the Elliott-Suresh-Donohue (ESD) EoS and applied it to various polymer solutions. 88 group contributions were presented to estimate the ESD shape parameter complementing in this way existing GC methods for the solubility parameters and molar volume. This GC EoS has been applied primarily to polymer solutions (mostly VLE).

One of the first applications of a GC formalism within a SAFT EoS is the work of Lora *et al.* [22] in the context of a study of the fluid properties of poly(alkylacrylates) in ethylene and $CO_2$. The contributions of $CH_3$, $CH_2$, CH, and the acrylate AC groups were determined to make the overall molecular chain-length ($m$), and the segment size ($\nu^{00}$) parameters for investigated hydrocarbon systems. However, because the energy parameters were not treated at the GC level, this method lacked full predictive capability. Vijande *et al.* [23] described in this work all three model parameters within a complete GC context

by using the PC-SAFT EoS for the pure compound VLE modeling of hydrofluoroethers including $CH_3$, $CH_2$, $CF_3$, $CF_2$, and the ether–O group.

In 2004, a GC method presented by Tamouza *et al.* [24] was coupled with two versions of SAFT: the original SAFT [25], and SAFT-VR [26]. During recent years, this GC SAFT approach has been extended to binary mixtures [27], esters [28], and aromatic compounds [29], and also applied to various polar compounds with the PC-SAFT model [29–32]. Despite the fact that this method yields good results for several classes of compounds, the method has not yet been tested for polymer systems. The relevant equations of this approach will be addressed in Section 3.4.

All the existing GC approaches are based on a *homonuclear* version of the theory. Here, all of the segments making up the chain are identical (homonuclear) each with the same "average" parameter. Lymperiadis *et al.* [33] developed a predictive GC SAFT-$\gamma$ by extending the SAFT-VR [26] to treat *heteronuclear* molecules which are formed from tangentially *fused* segments of different types. See Figure 3.1.

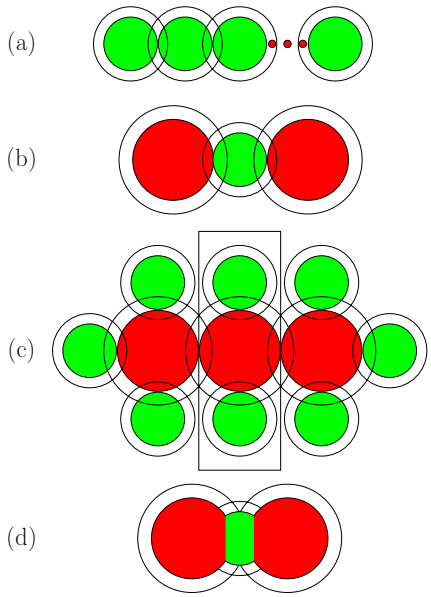


Figure 3.1: Schematic illustration of various molecular models. (a) Homonuclear chain of united-atom segments. (b) Tangent heteronuclear united-atom representation of propane. (c) Tangent heteronuclear all-atom representation of propane where the box indicates the $CH_2$ group. (d) Fused heteronuclear united-atom representation of propane. Illustration freely adopted from [33].

The use of the SAFT-$\gamma$ formalism introduces an extra shape parameter $S_k$ per group $k$, which denotes the extent to which each group contributes to the overall molecular properties. This approach is the first of its kind. Functional groups described in this approach are $CH_3$, $CH_2$, $CH_3CH$, ACH, $ACCH_2$, $CH_2$=, CH=, and OH, together with the different energy parameters between groups of different types. In the case of associating groups, additional hydrogen bonding energy and range parameters have to be specified. The approach is found to describe accurately the VLE for the $n$-alkanes, branched alkanes, $n$-alkylbenzenes, mono- and di-unsaturated hydrocarbons, 2-ketones, carboxylic acids, primary amines, and 1-alcohols.

Before ending this short overview of the implementation of the GC concept within the SAFT formalism, it is important to recall that the use of transferable atom group parameters is well suited to a SAFT description of the thermodynamic properties of homologous series. These transferable SAFT parameters have also been used in the same manner to describe not only the thermodynamic properties of $n$-alkanes [34], siloxane, and their mixtures [35,36], but more complex fluid phase behaviour of polymer solutions, copolymers, and blends [37–39].

## 3.3 The Constantinou-Gani GC Method

In this work, the Constantinou-Gani GC method [40] is used in combination with sPC-SAFT to determine the three characteristic molecular PC-SAFT parameters. This choice is made because, unlike other approaches found in the literature, this GC methodology includes two levels of contributions; both first-order groups (FOG) and second-order groups (SOG) that can, to some extent, capture proximity effects[1] and distinguish among structural isomers.
In general, group contribution methods can be divided into two classes:

1. Methods in the first class are those that estimate the property of a compound as a summation of the contributions of simple first-order groups (FOG) that may occur in the molecular structure, such as $CH_2$ and OH. This approach is necessary when there is no theoretical basis for group's identification and the groups are not able to capture proximity effects or isomer differences.

2. The second class includes methods that attempt to capture fine structural differences by additionally introducing, in a consistent manner, the so-called second-order groups (SOG).

A method that belongs to this second class of models was developed by Constantinou and Gani in 1994 [40]. Only the basic principle of this method is presented in the following. The method is applicable when predicting physical and thermodynamic properties

[1] The fact that two or more strong functional groups situated on two neighbouring carbon atoms will have different properties than if the groups are spaced far apart.

of simple compounds. This is done at two levels. The basic level has contributions from first-order functional groups. The next level has a set of SOG, which have the FOG as building blocks. The SOG should be as small and simple as possible. The definition and identification of SOG are theoretically based on the concept of conjugation operators according to the ABC theory [41], whose basic property is the standard enthalpy of formation at 298 K.

According to the method of Constantinou and Gani [40], the molecular structure of a compound is viewed as a hybrid of a number of conjugate (also known as resonance, alternative formal arrangement of valence electrons) forms. It may therefore contain fractional charges and bonds which are delocalized, and stronger or weaker than ideal integer-order bonds. The property of such a compound is a linear combination of these conjugate form contributions. Each conjugate form is an idealized structure with integer-order localized bonds and integer charges on the atoms. The purely covalent conjugate form is the *dominant conjugate* form that is defined as the arrangement of electron pairs, which results in the maximum number of bonds. The ionic forms are the *recessive conjugates*, which can be obtained from the dominant form by a rearrangement of electron pairs. A *conjugate operator* defines a particular pattern of electron rearrangements and, when applied to a dominant conjugate, yields an entire class of recessive conjugates. As an example, Figure 3.2 illustratively presents identification of a dominant conjugate, its generated recessive conjugate and the corresponding conjugate operator of *n*-propane.

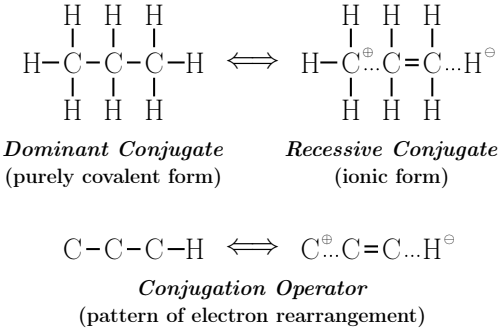


Figure 3.2: Illustration of a dominant conjugate, its generated recessive conjugate, and the corresponding conjugate operator of *n*-propane. The figure is freely adopted from [40].

The group identification follows precise principles and focuses on the operators with significantly higher contributions than the other operators. The structure of the SOG should incorporate the distinct subchain of at least one important conjugation operator; for example, the $CH_3COCH_2$ SOG incorporates the O=C–C, the O=C–C–H, and the C–C–C–H operators.

The methodology for the definition of SOG is:

1. Identification of all FOG present in the syntactic type of a given compound.
2. Definition of all possible substructures of two or three adjacent FOG.
3. Identification of all two-bond and three-bond conjugation operators in the substructures.
4. Estimation of the conjugation operator energy of all substructures by addition of the energies of all of the conjugation operators.
5. Identification of substructures with much higher conjugation energy than the other substructures. These substructures then become the SOG.

On the basis of this method, Constantinou and Gani [40] have presented extensive lists of FOG and SOG. One molecule has definitely FOG but may or may not have SOG. However, it is worth mentioning that because of the physical background of this approach, the group parameters can easily be transferred, which means that the contribution of e.g. a $CH_2$ group in an alkane, has the same contribution to the EoS parameter values as in an alcohol or in an olefin.

The main advantage of this method is the ability to determine the SOG contributions independently of any FOG. Therefore, the method is applicable to existing GC approaches. In general, this method gives sufficiently good results when used to predict temperature-dependent properties of pure organic compounds, such as vapour pressure, liquid density, heat of vapourisation, etc.

Another thing to emphasize at this point is the need for consistent group tables. An important contribution of Constantinou and Gani [40] was the consistent use of the UNIFAC group table [42]. Consistent, in the sense that the same description in terms of groups is applied to the same molecules, regardless of whether it is one or another property that is considered. This approach eliminates the need for accommodating separate group tables and for translation of the one group structure into the other.

### 3.3.1 Constantinou-Gani Method into an EoS

The Constantinou-Gani [40] GC method has been combined with the novel Non-Random Hydrogen-Bonding (NRHB) [43] EoS from Stefanis *et al.* [44]. In this EoS model, the characteristic constants of pure fluids are $\epsilon^*$, $\nu^{**}$, and $\nu^*_{sp}$, which are related to the equivalent set of $T^*$, $P^*$, and $\rho^*$ with the following equations:

$$\epsilon^* = RT^* \tag{3.1}$$

$$\nu^* = \frac{\epsilon^*}{P^*} \tag{3.2}$$

$$\nu^*_{sp} = \frac{1}{\rho^*} \tag{3.3}$$

where $\epsilon^*$ is the average interaction energy per molecular segment, $\nu^*$ is the average segment volume, $\nu^*_{sp}$ is the hard-core specific volume, $T^*$ is the scaling temperature, $P^*$ is the scaling pressure, $\rho^*$ is the scaling density, and $R$ is the universal constant.

The scaling constants for 334 organic compounds (of carbon number between 5 and 15) belonging to 14 different families of compounds are calculated through regression using data from the DIPPR database [45] following the methodology given in the original paper [40]. These scaling constants are then used in the group contribution regression for obtaining FOG and SOG contributions to the $\epsilon^*$, $\nu^*$, and $\nu^*_{sp}$ scaling constants. Using the linear least-square analysis, the equations that give the characteristic scaling constants are obtained to be:

$$\epsilon^* = \sum_i n_i F_i + \Phi \sum_j m_j F_j + 4438\,\mathrm{J/mol} \tag{3.4}$$

$$\nu^* = \sum_i n_i F_i + \Phi \sum_j m_j F_j + 8.8303\,\mathrm{cm^3/mol} \tag{3.5}$$

$$\nu^*_{sp} = \sum_i n_i F_i + \Phi \sum_j m_j F_j + 1.19155\,\mathrm{cm^3/g} \tag{3.6}$$

where $\Phi = 0$ when SOG are not present, or $\Phi = 1$ when SOG are present. $F_i$ is the contribution of the FOG of type $i$ that appears $n_i$ times, and $F_j$ is the contribution of the SOG of type $j$ that appears $m_j$ times. The relevant group contributions and all other equations are reported in the paper. The method is applied to estimate the scaling constants used by the NRHB theory to predict temperature-dependent properties of pure organic compounds such as vapour pressure, liquid density, surface tension, heat of vapourisation in a wide range of temperatures.

## 3.4 The Tamouza *et al.* GC Approach

In the Group Contribution method proposed by Tamouza *et al.* [24], the three molecular parameters for the PC-SAFT model are calculated through averages using the Lorentz-Berthelot combining rules, where energy parameters are averaged geometrically and size parameters are averaged arithmetically.

$$\epsilon_{molecule} = \sqrt[\mathcal{C}]{\prod_{i=1}^{n_{groups}} \epsilon_i^{n_i}} \quad \text{where} \quad \mathcal{C} = \sum_{i=1}^{n_{groups}} n_i \tag{3.7}$$

$$\sigma_{molecule} = \frac{\sum_{i=1}^{n_{groups}} n_i \sigma_i}{\sum_{i=1}^{n_{groups}} n_i} \tag{3.8}$$

where the subscript $i$ refers to a specific chemical group, so that $n_i$ is the number of chemical groups of type $i$, while $n_{groups}$ is the total number of chemical groups in the molecule.

The chain parameter, $m$, fits neither the carbon atom nor generally an integer value. It is assumed to be computed linearly with the number of considered chemical groups in the following way:

$$m_{molecule} = \sum_{i=1}^{n_{groups}} n_i R_i \tag{3.9}$$

where $R_i$ is the contribution of group $i$ to the chain length of the molecular model. The associating parameters ($\epsilon^{AB}$ and $\kappa^{AB}$) are taken to be identical for all the 1-alkanols, which are treated with an association model denoted as 3B by Huang and Radosz [46]. Here, any effects that the carbon chain may have on the chemical group –O–H are neglected. Additionally, when polar compounds are treated with this approach, such as esters [28] and polyaromatic hydrocarbons [29], an additional polar term is introduced accounting for multi-polar interactions, resulting with some additional adjustable parameters. The dipole moment, which was correlated to the COO chemical group position in the ester chain, is introduced for light and heavy esters, while the quadrupolar moment term of alkylbenzene ($Q_{AB}$), benzene ring ($Q_{BR}$), and polyaromatic ($Q_{PA}$) is introduced for polyaromatic hydrocarbons.

Each group is characterized by three parameters. The separate contributions that the various groups make to the overall model's parameters are obtained by optimising the description of the vapour pressure and liquid density of pure compounds. For example, the $CH_2$ and $CH_3$ groups contribution were determined by experimental VLE data regression of the $n$-alkane family and so on.

## 3.5 Final Comments

The literature review presented in this chapter demonstrates the large amount of research that has been devoted to the development of GC methods. By incorporating the GC concept within EoS, one avoids the limitations of the GC activity coefficient models, such as problematic application at high pressures or in the critical region, while adding a predictive and convenient character to the EoS.

While the combination of the Constantinou-Gani method with the NRHB theory [44] predicts scaling constants that are temperature-independent as input to the NRHB model, which in turn evaluates the desired thermo physical properties, the other analogous methods presented in this chapter predict those temperature-dependent thermophysical properties directly. Therefore, no direct comparison can be made between the GC methods. Hence, the main goal of this work is the implementation of the Constantinou-Gani method into sPC-SAFT EoS which would be applicable to a wide array of compounds and this will be further elaborated in the next chapters.

## References

[1] D. Boudouris, L. Constantinou, and C. Panayiotou, "A Group Contribution Estimation of the Thermodynamic Properties of Polymer," *Ind. Eng. Chem. Res.*, vol. 36, pp. 3968–3973, 1997.

[2] T. Holderbaum and J. Gmehling, "PSRK: A Group Contribution Equation of State Based on UNIFAC," *Fluid Phase Equilibria*, vol. 70, pp. 251–265, 1991.

[3] G. Soave, "Equilibrium Constant from a Modified Redlich-Kwong Equation of State," *Chem. Eng. Sci.*, vol. 27, pp. 1197–1203, 1972.

[4] S. Dahl and M. L. Michelsen, "High-Pressure Vapor-Liquid Equilibrium with a UNIFAC-Based Equation of State," *AIChE J.*, vol. 36, pp. 1829–1836, 1990.

[5] S. Dahl, A. Fredenslund, and P. Rasmussen, "MHV2 model. A UNIFAC-Based Equation of State Model for Prediction of Gas Solubility and Vapor-Liquid Equilibria at Low and High Pressures," *Ind. Eng. Chem. Res.*, vol. 30, pp. 1936–1945, 1991.

[6] C. Boukouvalas, N. Spiliotis, P. Coutsikos, N. Tzouvaras, and D. Tassios, "Prediction of Vapor-Liquid Equilibrium with the LCVM Model: A Linear Combination of the Vidal and Michelsen Mixing Rules Coupled with the Original UNIFAC and t-mPR Equation of State," *Fluid Phase Equlibria*, vol. 92, pp. 75–106, 1994.

[7] N. Orbey, S. Sandler, and D. S. H. Wong, "Accurate Equation of State Predictions at High Temperatures and Pressures Using the Existing UNIFAC Model," *Fluid Phase Equilibria*, vol. 85, pp. 41–54, 1993.

[8] S. Skjold-Jorgensen, "Gas Solubility Calculations. II. Application of a New Group-Contribution Equation of State," *Fluid Phase Equilibria*, vol. 16, pp. 317–353, 1984.

[9] H. P. Gros, S. Bottini, and E. Brignole, "A Group Contribution Equation of State for Associating Mixtures," *Fluid Phase Equilibria*, vol. 116, pp. 537–544, 1996.

[10] S. Espinosa, G. M. Foco, A. Bermudez, and T. Fornari, "Revision and Extension of the Group Contribution Equation of State to New Solvent Groups and Higher Molecular Weight Alkanes," *Fluid Phase Equilibria*, vol. 172, pp. 129–143, 2000.

[11] S. Espinosa, T. Fornari, S. B. Bottini, and E. A. Brignole, "Phase Equilibria in Mixtures of Fatty Oils and Derivatives with near Critical Fluids Using the GC-EOS Model," *Supercritical Fluids*, vol. 23, pp. 91–102, 2002.

[12] M. S. High and R. P. Danner, "A Group Contribution Equation of State for Polymer Systems," *Fluid Phase Equilibria*, vol. 53, pp. 323–330, 1989.

[13] M. S. High and R. P. Danner, "Application of the Group Contribution Lattice-Fluid EoS for Polymer Solution," *AIChE J.*, vol. 36, pp. 1625–1632, 1990.

[14] B. C. Lee and R. P. Danner, "Predictions of Polymer-Solvent Phase Equilibria by a Modified Group-Contribution Lattice-Fluid Equation of State," *AIChE J.*, vol. 42, pp. 837–849, 1996.

[15] B. C. Lee and R. P. Danner, "Group-Contribution Lattice-Fluid EoS: Prediction of LLE in Polymer Solutions," *AIChE J.*, vol. 42, pp. 3223–3230, 1996.

[16] L. Coniglio, E. Rauzy, and C. Berro, "Representation and Prediction of Thermophysical Properties of Heavy Hydrocarbons," *Fluid Phase Equilibria*, vol. 87, pp. 53–88, 1993.

[17] L. Coniglio, L. Trassy, and E. Rauzy, "GENERAL RESEARCH – Estimation of Thermophysical Properties of Heavy Hydrocarbons through a Group Contribution Based Equation of State," *Ind. Chem. Eng. Res.*, vol. 39, pp. 5037–5048, 2000.

[18] D. Y. Peng and D. B. Robinson, "New Two-Constant Equation of State," *Ind. Eng. Chem. Fundam.*, vol. 15, pp. 59–64, 1976.

[19] N. Elvassore, A. Bertucco, and M. Fermeglis, "Phase-Equilibria Calculations by Group-Contribution Perturbed-Hard-Sphere-Chain Equation of State," *AIChE J.*, vol. 48, pp. 359–368, 2002.

[20] Y. Song, S. M. Lambert, and J. M. Prausnitz, "A Perturbed-Hard-Sphere-Chain Equation of State for Normal Fluids and Polymers," *Ind. Eng. Chem. Res.*, vol. 33, pp. 1047–1057, 1994.

[21] J. R. Elliott and R. N. Natarajan, "Extension of the Elliott-Suresh-Donohue Equation of State to Polymer Solutions," *Ind. Eng. Chem. Res.*, vol. 41, pp. 1043–1050, 2002.

[22] M. Lora, F. Rindfleisch, and M. A. McHugh, "Influence of the Alkyl Tail on the Solubility of Poly(alkyl acrylates) in Ethylene and $CO_2$ at High Pressures: Experiments and Modeling," *J. Appl. Poly. Sci.*, vol. 73, pp. 1979–1991, 1999.

[23] J. Vijande, M. M. Pineiro, D. Bessieres, H. Saint-Guirons, and J. L. Legido, "Description of PVT Behaviour of Hydrofluoroethers Using the PC-SAFT EoS," *Phys. Chem. Chem. Phys.*, vol. 6, pp. 766–770, 2004.

[24] S. Tamouza, J.-P. Passarello, P. Tobaly, and J.-C. de Hemptinne, "Group Contribution Method with SAFT EoS Applied to Vapor Liquid Equilibria of Various Hydrocarbon Series," *Fluid Phase Equilibria*, vol. 222-223, pp. 67–76, 2004.

[25] W. G. Chapman, K. E. Gubbins, G. Jackson, and M. Radosz, "New Reference Equation of State for Associating Liquids," *Ind. Eng. Chem. Res.*, vol. 29, pp. 1709–1721, 1990.

[26] A. Gil-Villegas, A. Galindo, P. J. Whitehead, S. J. Mills, G. Jackson, and A. N. Burgess, "Statistical Associating Fluid Theory for Chain Molecules with Attractive Potentials of Variable Range," *J. Chem. Phys.*, vol. 106, pp. 4168–4186, 1997.

[27] S. Tamouza, J.-P. Passarello, P. Tobaly, and J.-C. de Hemptinne, "Application to Binary Mixtures of a Group Contribution SAFT EoS (GC-SAFT)," *Fluid Phase Equilibria*, vol. 228-229, pp. 409–419, 2005.

[28] T. X. Nguyen Thi, S. Tamouza, J.-P. Passarello, P. Tobaly, and J.-C. de Hemptinne, "Application of Group Contribution SAFT Equation of State (GC-SAFT) to Model Phase Behaviour of Light and Heavy Esters," *Fluid Phase Equilibria*, vol. 238, pp. 254–261, 2005.

[29] D. N. Huynh, M. Benamira, J.-P. Passarello, P. Tobaly, and J.-C. de Hemptinne, "Application of GC-SAFT EOS to Polycyclic Aromatic Hydrocarbons," *Fluid Phase Equilibria*, vol. 254, pp. 60–66, 2007.

[30] C. Le Thi, S. Tamouza, J.-P. Passarello, P. Tobaly, and J.-C. de Hemptinne, "Modeling Phase Equilibrium of $H_2$+$n$-Alkane and $CO_2$+$n$-Alkane Binary Mixtures Using a Group Contribution Statistical Association Fluid Theory Equation of State GC-SAFT-EoS with a $k_{ij}$ Group Contribution Method," *Ind. Eng. Chem. Res.*, vol. 45, pp. 6803–6810, 2006.

[31] D. N. Huynh, J.-P. Passarello, P. Tobaly, and J.-C. de Hemptinne, "Application of GC-SAFT EOS to Polar Systems Using a Segment Approach," *Fluid Phase Equilibria*, vol. 264, pp. 62–75, 2008.

[32] D. N. Huynh, A. Falaix, J.-P. Passarello, P. Tobaly, and J.-C. de Hemptinne, "Predicting VLE of Heavy Esters and Their Mixtures Using GC-SAFT," *Fluid Phase Equilibria*, vol. 264, pp. 184–200, 2008.

[33] A. Lymperiadis, C. S. Adjiman, A. Galindo, and G. Jackson, "A Group Contribution Method for Associating Chain Molecules Based on the Statistical Associating Fluid Theory (SAFT-$\gamma$)," *J. Chem. Phys.*, vol. 127, pp. 234903–2349032, 2007.

[34] A. Galindo, P. J. Whitehead, and G. Jackson, "Predicting the High-Pressure Phase Equilibria of Water+$n$-Alkanes Using a Simplified SAFT Theory with Transferable Intermolecular Interaction Parameters," *J. Phys. Chem.*, vol. 100, pp. 6781–6792, 1996.

[35] A. L. Archer, M. D. Amos, G. Jackson, and I. A. McLure, "The Theoretical Prediction of the Cricital Points of Alkanes, Perfluoroalkanes, and Their Mixtures Using Bonded Hard-Sphere (BHS) Theory," *Int. J. Thermophys.*, vol. 17, pp. 201–211, 1996.

[36] P. J. Clements, S. Zafar, A. Galindo, G. Jackson, and I. M. McLure, "Thermodynamics of Ternary Mixtures Exhibiting Tunnel Phase Behaviour Part 3. Hexane– Hexamethyldisiloxane– Perfluorohexane," *J. Chem. Soc. Faraday Trans.*, vol. 93, pp. 1331–1339, 1997.

[37] M. Banaszak, C. K. Chen, and M. Radosz, "Copolymer SAFT Equation of State. Thermodynamic Perturbation Theory Extended to Heterobonded Chains," *Macromolecules*, vol. 29, pp. 6481–6486, 1996.

[38] C. K. Chen, M. Banaszak, and M. Radosz, "Statistical Associating Fluid Theory Equation of State with Lennard-Jones Reference Applied to Pure and Binary $n$-Alkane Systems," *J. Phys. Chem. B*, vol. 102, pp. 2427–2431, 1998.

[39] H. Adidharma and M. Radosz, "Prototype of an Engineering Equation of State for Heterosegmented Polymers," *Ind. Eng. Chem. Rev.*, vol. 37, pp. 4453–4462, 1998.

[40] L. Constantinou and R. Gani, "New Group Contribution Method for Estimating Properties of Pure Compounds," *AIChE J.*, vol. 40, pp. 1697–1710, 1994.

[41] M. L. Mavrovouniotis, "Estimation of Properties of Conjugate Forms of Molecular Structures," *Ind. Eng. Chem. Res.*, vol. 32, pp. 1734–1746, 1990.

[42] A. Fredenslund, R. L. Jones, and J. M. Prauznitz, "Group-Contribution Estimation of Activity Coefficients in Nonideal Liquid Mixtures," *AIChE J.*, vol. 21, pp. 1086–1099, 1975.

[43] P. Paricaud, A. Galindo, and G. Jackson, "Nonrandom Hydrogen-Bonding Model of Fluids and Their Mixtures. 1. Pure Fluid," *Ind. Eng. Chem. Res.*, vol. 43, pp. 6592–6606, 2004.

[44] E. Stefanis, L. Constantinou, I. Tsivintzelis, and C. Panayiotou, "New Group-Contribution Method for Predicting Temperature-Dependent Properties of Pure Organic Compounds," *Int. J. Thermophys.*, vol. 26, pp. 1369–1388, 2005.

[45] AIChE J., *DIPPR Table of Physical and Thermodynamic Properties of Pure Compounds*. New York, USA, 1998.

[46] S. H. Huang and M. Radosz, "Equation of State for Small, Large, Polydisperse, and Associating Molecules," *Ind. Eng. Chem. Res.*, vol. 29, pp. 2284–2294, 1990.

# Chapter 4

# Extension of the PC-SAFT Parameter Table

*"But although, as a matter of history, statistical mechanics owes its origin to investigations in thermodynamics, it seems eminently worthy of an independent development, both on account of the elegance and simplicity of its principles, and because it yields new results and places old truths in a new light in departments quite outside of thermodynamics."* by J.W. Gibbs

## 4.1 Introduction

Equation of state parameters for pure compounds are generally determined from available vapour pressure and liquid density data as mentioned in the previous chapters. One of the reasons why the version of SAFT with the implementation of Huang and Radosz [1] has gained substantial popularity is the extended list of parameters covering 100 real fluids which is available in one single article. Similarly, the first articles about PC-SAFT contain parameters for around 120 compounds.

Hydrocarbons are the major components of petroleum. Recent developments in drilling technology allow the extraction of petroleum reservoirs at greater depths up to 10 km. These new reservoirs present specific characteristics regarding temperature, pressure and compositions. It is possible to encounter reservoir temperatures up to 473 K, pressures up to 200 MPa, and asymmetric fluid compositions, with mole fractions of methane up to 0.60 and the presence of long chain $n$-alkanes reaching up to $C_{60}$. These reservoirs are known as *hyperbaric reservoirs* [2]. Therefore, it can be of major industrial importance to be able to correctly model the phase behaviour of such asymmetric fluids at elevated conditions in order to be able to extrapolate work toward more extreme conditions of temperature and pressure.

An important point to this investigation is that long-chain alkanes are oligomers that bridge the gap between simple molecules and polymers. Unlike polymer systems, mix-

tures of long-chain alkanes and solvents are well-defined, and have quantifiable liquid and vapour compositions. However, unlike mixtures of simple molecules, these systems exhibit considerable solvent-solute size asymmetry.

The purpose of the work presented in this chapter is to extend the existing PC-SAFT parameter table with numerous compounds so that in a subsequent step, a group-contribution scheme for parameter estimation can be developed. The aim is not to analyze and enhance the performance of the model, but to give an idea of the performance of the model when necessary parameters are calculated by different approaches. This will make comparisons with the new proposed GC sPC-SAFT model easier at a later stage and provide a foundation of an evaluation of what the new method has to offer.

## 4.2 Complete Parameter Table

Parameter estimations for new non-associating compounds and corresponding modelling results for phase equilibria of binary systems obtained with sPC-SAFT are presented in the following sections. The PC-SAFT pure component parameters for numerous non-associating compounds have been obtained by fitting vapour-pressure and liquid-densities extracted mainly from the DIPPR correlations [3] in a reduced temperature range of $0.5 \leq T_r \leq 0.9$. These parameters are listed in Table 4.1 including molecular weight ($M_w$), temperature range covered by the experimental data, and correlation errors in the vapour pressure and liquid density. The complete PC-SAFT table currently consists of about 500 newly estimated parameters for different families of non-associating compounds: *n*-alkanes, branched alkanes, alkenes, alkynes, benzene derivatives, gases, ethers, esters, ketones, cyclo- and fluorinated hydrocarbons, polynuclear aromatics, nitroalkanes, sulphides, and plasticizers.

Table 4.1: Pure component parameters for the PC-SAFT Equation of State. t.w. = this work.

| CAS-nr. | DIPPR nr. | Compound | $M_w$ [g/mol] | $m$ [−] | $\sigma$ [Å] | $\epsilon/k$ [K] | $T$ range [K] | AAD $(V_L/P^{sat})$ [%] | Ref. |
|---|---|---|---|---|---|---|---|---|---|
| | | | *n-alkanes* | | | | | | |
| 74–82–8 | 1 | methane | 16.04 | 1.0000 | 3.7039 | 150.03 | 97–300 | 0.67/0.36 | [4] |
| 74–84–0 | 2 | ethane | 30.07 | 1.6069 | 3.5206 | 191.42 | 90–305 | 0.57/0.30 | [4] |
| 74–98–6 | 3 | propane | 44.10 | 2.002 | 3.6184 | 208.11 | 85–523 | 0.77/1.29 | [4] |
| 106–97–8 | 5 | butane | 58.12 | 2.3316 | 3.7086 | 222.88 | 135–573 | 1.59/0.75 | [4] |
| 109–66–0 | 7 | pentane | 72.15 | 2.6896 | 3.7729 | 231.2 | 143–469 | 0.78/1.45 | [4] |
| 110–54–3 | 11 | hexane | 86.18 | 3.0576 | 3.7983 | 236.77 | 177–503 | 0.76/0.31 | [4] |
| 142–82–5 | 17 | heptane | 100.20 | 3.4831 | 3.8049 | 238.4 | 182–623 | 2.10/0.34 | [4] |
| 111–65–9 | 27 | octane | 114.23 | 3.8176 | 3.8373 | 242.78 | 216–569 | 1.59/0.77 | [4] |
| 111–84–2 | 46 | nonane | 128.25 | 4.2079 | 3.8448 | 244.51 | 219–595 | 0.32/0.89 | [4] |
| 124–18–5 | 56 | decane | 142.29 | 4.6627 | 3.8384 | 243.87 | 243–617 | 1.18/0.24 | [4] |
| 1120–21–4 | 63 | undecane | 156.31 | 4.9082 | 3.8893 | 248.82 | 247–639 | 0.69/2.02 | [4] |
| 112–40–3 | 64 | dodecane | 170.34 | 5.306 | 3.8959 | 249.21 | 263–658 | 0.93/2.10 | [4] |
| 629–50–5 | 65 | tridecane | 184.37 | 5.6877 | 3.9143 | 249.78 | 267–675 | 1.77/3.15 | [4] |
| 629–59–4 | 66 | tetradecane | 198.39 | 5.9002 | 3.9396 | 254.21 | 279–693 | 1.28/4.80 | [4] |
| 629–62–9 | 67 | pentadecane | 212.42 | 6.2855 | 3.9531 | 254.14 | 283–708 | 5.35/1.04 | [4] |
| 544–76–3 | 68 | hexadecane | 226.45 | 6.6485 | 3.9552 | 254.7 | 291–723 | 0.75/4.88 | [4] |
| 629–78–7 | 69 | heptadecane | 240.47 | 6.9809 | 3.9675 | 255.65 | 295–736 | 0.69/5.35 | [4] |
| 593–45–3 | 70 | octadecane | 254.40 | 7.3271 | 3.9668 | 256.2 | 301–747 | 1.19/4.99 | [4] |
| 629–92–5 | 71 | nonadecane | 268.53 | 7.7175 | 3.9721 | 256.00 | 305–758 | 0.64/5.08 | [4] |
| 112–95–8 | 74 | eicosane | 282.55 | 7.9849 | 3.9869 | 257.75 | 309–775 | 1.13/7.65 | [4] |
| 646–31–1 | 77 | tetracosane | 338.65 | 9.822 | 3.937 | 253.18 | 325–804 | 0.47/0.65 | [5] |
| 630–06–8 | 2086 | hexatriacontane | 506.97 | 13.86 | 4.014 | 256.37 | 350–874 | 2.10/14.70 | [5] |
| | | | *branched alkanes* | | | | | | |
| 75–28–5 | 4 | isobutane | 58.12 | 2.2616 | 3.7574 | 216.53 | 113–407 | 1.47/0.55 | [4] |
| 78–78–4 | 8 | isopentane | 72.15 | 2.562 | 3.8296 | 230.75 | 113–460 | 1.53/0.40 | [4] |
| 463–82–1 | 9 | neopentane | 72.15 | 2.3543 | 3.955 | 225.69 | 256–433 | 0.38/0.04 | [4] |
| 75–83–2 | 14 | 2,2-dimethylbutane | 86.18 | 2.6008 | 4.0042 | 243.51 | 174–488 | 0.21/0.32 | [4] |
| 79–29–8 | 15 | 2,3-dimethylbutane | 86.18 | 2.6853 | 3.9545 | 246.07 | 145–500 | 0.46/0.38 | [4] |

*Continues on next page*

| CAS-nr. | DIPPR nr. | Compound | $M_w$ [g/mol] | $m$ [−] | $\sigma$ [Å] | $\epsilon/k$ [K] | $T$ range [K] | AAD $(V_L/P^{sat})$ [%] | Ref. |
|---|---|---|---|---|---|---|---|---|---|
| 107–83–5 | 12 | 2-methylpentane | 86.18 | 2.9317 | 3.8535 | 235.58 | 119–498 | 0.59/0.61 | [4] |
| 96–14–0 | 13 | 3-methylpentane | 86.18 | 2.8852 | 3.8605 | 240.48 | 110–504 | 0.65/0.33 | [4] |
| 565–59–3 | 22 | 2,3-dimethylpentane | 100.20 | 3.0643 | 3.9278 | 249.83 | 280–500 | 0.52/0.22 | t.w. |
| 464–06–2 | 25 | 2,2,3-trimethylbutane | 100.20 | 2.7373 | 4.0914 | 258.65 | 170–560 | 0.17/0.08 | t.w. |
| 617–78–7 | 20 | 3-ethylpentane | 100.20 | 3.1396 | 3.9068 | 249.17 | 210–570 | 0.63/2.56 | t.w. |
| 589–34–4 | 19 | 3-methylhexane | 100.20 | 3.2570 | 3.8543 | 243.02 | 280–480 | 0.57/0.18 | t.w. |
| 590–35–2 | 21 | 2,2-dimethylpentane | 100.20 | 2.9552 | 4.0094 | 246.30 | 260–465 | 0.16/0.56 | t.w. |
| 108–08–7 | 23 | 2,4-dimethylpentane | 100.20 | 3.1426 | 3.9250 | 238.91 | 260–465 | 0.32/0.21 | t.w. |
| 562–49–2 | 24 | 3,3-dimethylpentane | 100.20 | 2.8915 | 4.0355 | 254.43 | 275–475 | 0.70/0.21 | t.w. |
| 591–76–4 | 18 | 2-methylhexane | 100.20 | 3.3478 | 3.8612 | 237.42 | 154–530 | 1.44/0.74 | [4] |
| 564–02–3 | 40 | 2,2,3-trimethylpentane | 114.23 | 3.0954 | 4.0670 | 260.59 | 280–500 | 0.63/0.18 | t.w. |
| 584–94–1 | 33 | 2,3-dimethylhexane | 114.23 | 3.4634 | 3.9298 | 249.02 | 160–500 | 0.14/0.12 | t.w. |
| 583–48–2 | 37 | 3,4-dimethylhexane | 114.23 | 3.4026 | 3.9431 | 253.13 | 280–560 | 0.13/0.15 | t.w. |
| 565–75–3 | 43 | 2,3,4-trimethylpentane | 114.23 | 3.2154 | 4.0164 | 257.82 | 280–560 | 0.25/0.20 | t.w. |
| 560–21–4 | 42 | 2,3,3-trimethylpentane | 114.23 | 3.0170 | 4.1001 | 268.00 | 250–530 | 0.19/0.13 | t.w. |
| 590–73–8 | 32 | 2,2-dimethylhexane | 114.23 | 3.4476 | 3.9603 | 243.00 | 230–490 | 0.23/1.04 | t.w. |
| 540–84–1 | 41 | 2,2,4-trimethylpentane | 114.23 | 3.1413 | 4.0862 | 249.77 | 230–490 | 0.21/1.76 | t.w. |
| 592–27–8 | 28 | 2-methylheptane | 114.23 | 3.7035 | 3.8676 | 241.21 | 280–500 | 0.15/0.20 | t.w. |
| 589–81–1 | 29 | 3-methylheptane | 114.23 | 3.6225 | 3.8810 | 245.39 | 280–505 | 0.23/0.17 | t.w. |
| 589–53–7 | 30 | 4-methylheptane | 114.23 | 3.6536 | 3.8703 | 243.36 | 280–505 | 0.09/0.28 | t.w. |
| 592–13–2 | 35 | 2,5-dimethylhexane | 114.23 | 3.5480 | 3.9280 | 240.85 | 280–490 | 0.25/0.24 | t.w. |
| 609–26–7 | 38 | 2-methyl-3-ethylpentane | 114.23 | 3.3320 | 3.9610 | 254.65 | 285–505 | 0.67/0.20 | t.w. |
| 1067–08–9 | 39 | 3-methyl-3-ethylpentane | 114.23 | 3.0983 | 4.0683 | 266.66 | 285–515 | 0.13/0.13 | t.w. |
| 594–82–1 | 44 | 2,2,3,3-tetramethylbutane | 114.23 | 2.9241 | 4.1423 | 266.48 | 280–510 | 0.51/0.96 | t.w. |
| 619–99–8 | 31 | 3-ethylhexane | 114.23 | 3.5658 | 3.8849 | 247.45 | 290–505 | 0.40/0.23 | t.w. |
| 589–43–5 | 34 | 2,4-dimethylhexane | 114.23 | 3.4949 | 3.9447 | 242.99 | 280–498 | 0.31/0.22 | t.w. |
| 563–16–6 | 36 | 3,3-dimethylhexane | 114.23 | 3.2197 | 4.0177 | 256.55 | 280–505 | 0.90/0.19 | t.w. |
| 540–84–1 | 41 | 2,2,4-trimethylpentane | 114.23 | 3.1366 | 4.0875 | 249.987 | 270–510 | 0.10/0.10 | [6] |
| 1070–87–7 | 53 | 2,2,4,4-tetramethylpentane | 128.26 | 3.1746 | 4.2086 | 262.92 | 180–570 | 0.21/0.65 | t.w. |
| 3522–94–9 | 47 | 2,2,5-trimethylhexane | 128.26 | 3.7620 | 3.9841 | 241.10 | 230–510 | 0.29/3.57 | t.w. |
| 1071–26–7 | 96 | 2,2-dimethylheptane | 128.26 | 3.8706 | 3.9496 | 243.30 | 230–515 | 0.27/1.76 | t.w. |
| 16747–32–3 | 190 | 2,2-dimethyl-3-ethylpentane | 128.26 | 3.4503 | 4.0698 | 259.84 | 250–530 | 0.21/2.14 | t.w. |

*Continues on next page*

| CAS-nr. | DIPPR nr. | Compound | $M_w$ [g/mol] | $m$ [–] | $\sigma$ [Å] | $\epsilon/k$ [K] | $T$ range [K] | AAD $(V_L/P^{sat})$ [%] | Ref. |
|---|---|---|---|---|---|---|---|---|---|
| 3221–61–2 | 91 | 2-methyloctane | 128.26 | 4.0707 | 3.8889 | 243.85 | 295–525 | 0.35/0.80 | t.w. |
| 2216–33–3 | 92 | 3-methyloctane | 128.26 | 3.9748 | 3.9126 | 247.57 | 295–525 | 0.45/0.86 | t.w. |
| 2216–34–4 | 93 | 4-methyloctane | 128.26 | 3.9538 | 3.9162 | 247.13 | 295–520 | 0.33/0.65 | t.w. |
| 1072–05–5 | 176 | 2,6-dimethylheptane | 128.26 | 4.0443 | 3.8888 | 239.47 | 290–520 | 0.12/0.39 | t.w. |
| 1068–87–7 | 192 | 2,4-dimethyl-3-ethylpentane | 128.26 | 3.5106 | 4.0456 | 259.44 | 295–530 | 0.31/0.40 | t.w. |
| 15869–80–4 | 94 | 3-ethylheptane | 128.26 | 3.9113 | 3.9254 | 248.56 | 295–530 | 0.15/0.43 | t.w. |
| 7154–79–2 | 51 | 2,2,3,3-tetramethylpentane | 128.26 | 3.1245 | 4.1789 | 279.57 | 310–540 | 0.16/0.43 | t.w. |
| 1186–53–4 | 52 | 2,2,3,4-tetramethylpentane | 128.26 | 3.2491 | 4.1459 | 267.81 | 305–530 | 0.10/0.10 | t.w. |
| 16747–38–9 | 54 | 2,3,3,4-tetramethylpentane | 128.26 | 3.1835 | 4.1606 | 277.47 | 305–540 | 0.16/0.34 | t.w. |
| 16747–30–1 | 49 | 2,4,4-trimethylhexane | 128.26 | 3.4059 | 4.1091 | 258.97 | 295–520 | 0.37/0.31 | t.w. |
| 15869–87–1 | 72 | 2,2-dimethyloctane | 142.28 | 4.0461 | 4.0217 | 251.01 | 255–540 | 0.36/2.83 | t.w. |
| 871–83–0 | 86 | 2-methylnonane | 142.28 | 4.5569 | 3.8664 | 242.57 | 310–545 | 0.42/1.18 | t.w. |
| 5911–04–6 | 85 | 3-methylnonane | 142.28 | 4.4407 | 3.8840 | 246.30 | 315–540 | 0.14/0.10 | t.w. |
| 17301–94–9 | 87 | 4-methylnonane | 142.28 | 4.3810 | 3.9151 | 246.42 | 315–540 | 0.65/0.36 | t.w. |
| 15869–85–9 | 88 | 5-methylnonane | 142.28 | 4.3272 | 3.9261 | 247.94 | 315–540 | 0.43/1.01 | t.w. |
| 7146–60–3 | 2095 | 2,3-dimethyloctane | 142.28 | 4.1480 | 3.9779 | 252.62 | 310–550 | 0.54/0.26 | t.w. |
| 4032–94–4 | 2096 | 2,4-dimethyloctane | 142.28 | 4.3750 | 3.9220 | 240.62 | 310–540 | 0.74/0.84 | t.w. |
| 15869–89–3 | 2097 | 2,5-dimethyloctane | 142.28 | 4.1938 | 3.9681 | 247.67 | 310–540 | 0.46/0.78 | t.w. |
| 2051–30–1 | 2098 | 2,6-dimethyloctane | 142.28 | 4.3242 | 3.9403 | 244.67 | 310–540 | 0.77/0.46 | t.w. |
| 1072–16–8 | 2099 | 2,7-dimethyloctane | 142.28 | 4.2935 | 3.9439 | 245.33 | 310–540 | 0.28/0.20 | t.w. |
| 1067–20–5 | 50 | 3,3-diethylpentane | 156.31 | 3.2334 | 4.1403 | 278.43 | 310–545 | 0.05/0.18 | t.w. |
| | | *cycloalkanes* | | | | | | | |
| 75–19–4 | 101 | cyclopropane | 42.02 | 1.8258 | 3.5084 | 234.45 | 145–395 | 0.36/0.10 | t.w. |
| 287–23–0 | 102 | cyclobutane | 56.11 | 2.0988 | 3.6189 | 254.45 | 185–490 | 0.96/.073 | t.w. |
| 287–92–3 | 104 | cyclopentane | 70.13 | 2.3655 | 3.7114 | 265.83 | 193–503 | 0.20/0.69 | [4] |
| 110–82–7 | 137 | cyclohexane | 84.15 | 2.5303 | 3.8499 | 278.11 | 279–533 | 3.12/0.53 | [4] |
| 96–37–7 | 105 | methylcyclopentane | 84.16 | 2.613 | 3.8253 | 265.12 | 183–532 | 0.37/0.88 | [4] |
| 1640–89–7 | 107 | ethylcyclopentane | 98.18 | 2.9062 | 3.8873 | 270.5 | 134–569 | 0.75/2.55 | [4] |
| 108–87–2 | 138 | methylcyclohexane | 98.18 | 2.6637 | 3.9993 | 282.33 | 203–572 | 0.31/1.91 | [4] |
| 291–64–5 | 159 | cycloheptane | 98.19 | 2.6975 | 3.9336 | 296.09 | 180–510 | 0.24/0.46 | t.w. |
| 1638–26–2 | 108 | 1,1-dimethylcyclopentane | 98.19 | 2.7863 | 3.9460 | 264.12 | 280–490 | 0.38/0.38 | t.w. |

*Continues on next page*

| CAS-nr. | DIPPR nr. | Compound | $M_w$ [g/mol] | $m$ [–] | $\sigma$ [Å] | $\epsilon/k$ [K] | $T$ range [K] | AAD $(V_L/P^{sat})$ [%] | Ref. |
|---|---|---|---|---|---|---|---|---|---|
| 1192–18–3 | 109 | *cis*-1,2-dimethylcyclopentane | 98.19 | 2.8090 | 3.9180 | 272.78 | 285–505 | 0.39/0.21 | t.w. |
| 822–50–4 | 110 | *trans*-1,2-dimethylcyclopentane | 98.19 | 2.8607 | 3.9202 | 263.27 | 285–500 | 0.46/0.16 | t.w. |
| 590–66–9 | 141 | 1,1-dimethylcyclohexane | 112.21 | 2.7196 | 4.1593 | 290.06 | 240–590 | 0.85/0.72 | t.w. |
| 292–64–8 | 160 | cyclooctane | 112.21 | 2.8856 | 4.0117 | 307.03 | 290–640 | 0.86/0.72 | t.w. |
| 3875–51–2 | 115 | isopropylcyclopentane | 112.21 | 3.0320 | 4.0022 | 278.15 | 165–590 | 0.26/0.26 | t.w. |
| 2040–96–2 | 114 | propylcyclopentane | 112.21 | 3.2639 | 3.9042 | 270.48 | 200–590 | 0.27/0.09 | t.w. |
| 2207–01–4 | 142 | *cis*-1,2-dimethylcyclohexane | 112.21 | 2.7880 | 4.1065 | 294.75 | 305–545 | 1.00/1.00 | t.w. |
| 6876–23–9 | 143 | *trans*-1,2-dimethylcyclohexane | 112.21 | 2.7483 | 4.1487 | 291.38 | 305–535 | 0.66/0.64 | t.w. |
| 2207–03–6 | 145 | *trans*-1,3-dimethylcyclohexane | 112.21 | 2.8762 | 4.0753 | 285.17 | 305–530 | 0.95/1.01 | t.w. |
| 638–04–0 | 144 | *cis*-1,3-dimethylcyclohexane | 112.21 | 2.8686 | 4.1003 | 281.56 | 300–530 | 0.57/0.80 | t.w. |
| 624–29–3 | 146 | *cis*-1,4-dimethylcyclohexane | 112.21 | 2.8645 | 4.0814 | 285.61 | 300–530 | 0.76/0.89 | t.w. |
| 2207–04–7 | 147 | *trans*-1,4-dimethylcyclohexane | 112.21 | 2.7970 | 4.1387 | 284.87 | 300–530 | 0.44/0.64 | t.w. |
| 1678–91–7 | 140 | ethylcyclohexane | 112.22 | 2.8256 | 4.1039 | 294.04 | 263–609 | 1.04/2.38 | [4] |
| 2040–95–1 | 122 | butylcyclopentane | 126.24 | 3.6442 | 3.9149 | 269.66 | 170–620 | 0.42/0.83 | t.w. |
| 696–29–7 | 150 | isopropylcyclohexane | 126.24 | 3.2678 | 4.0418 | 284.66 | 185–625 | 0.63/0.15 | t.w. |
| 1678–92–8 | 149 | propylcyclohexane | 126.24 | 3.2779 | 4.0499 | 285.91 | 180–630 | 0.37/1.18 | t.w. |
| 493–01–6 | 153 | *cis*-decahydronaphthalene | 138.25 | 2.9850 | 4.1803 | 331.18 | 230–700 | 0.65/0.81 | t.w. |
| 493–02–7 | 154 | *trans*-decahydronaphthalene | 138.25 | 2.9477 | 4.2365 | 325.91 | 245–685 | 0.70/0.85 | t.w. |
| 1678–93–9 | 152 | butylcyclohexane | 140.27 | 3.6023 | 4.0637 | 285.97 | 200–660 | 0.26/1.08 | t.w. |
| 1795–16–0 | 158 | decylcyclohexane | 224.43 | 6.0329 | 4.0083 | 272.23 | 280–750 | 0.65/0.93 | t.w. |
| | | *alkenes* | | | | | | | |
| 74–85–1 | 201 | 1-ethylene | 28.05 | 1.593 | 3.445 | 176.47 | 104–400 | 2.61/1.16 | [4] |
| 513–81–5 | 319 | 2,3-dimethyl-1,3-butadiene | 28.14 | 2.7005 | 3.7841 | 257.70 | 220–470 | 0.32/0.96 | t.w. |
| 463–49–0 | 301 | propadiene | 40.06 | 1.5506 | 3.7082 | 257.73 | 140–390 | 1.77/2.15 | t.w. |
| 115–07–1 | 202 | propylene | 42.08 | 1.9597 | 3.5356 | 207.19 | 87–364 | 1.41/0.66 | [4] |
| 590–19–2 | 302 | 1,2-butadiene | 54.09 | 2.2979 | 3.5395 | 239.01 | 230–400 | 1.20/0.52 | t.w. |
| 106–99–0 | 303 | 1,3-butadiene | 54.09 | 2.2309 | 3.5892 | 228.60 | 170–420 | 0.58/0.17 | t.w. |
| 106–98–9 | 204 | 1-butene | 56.11 | 2.2864 | 3.6431 | 222. | 87–419 | 0.52/0.69 | [4] |
| 107–01–7 | 206 | 2-butene | 56.11 | 2.3842 | 3.564 | 226.296 | 150–390 | 0.40/0.70 | [6] |
| 115–11–7 | 207 | isobutene | 56.11 | 2.2826 | 3.6442 | 221.58 | 210–375 | 0.30/0.13 | t.w. |
| 78–79–5 | 309 | 2-methyl-1,3-butadiene | 68.12 | 2.3837 | 3.7501 | 249.88 | 245–430 | 0.38/0.97 | t.w. |

*Continues on next page*

| CAS-nr. | DIPPR nr. | Compound | $M_w$ [g/mol] | $m$ [–] | $\sigma$ [Å] | $\epsilon/k$ [K] | $T$ range [K] | AAD $(V_L/P^{sat})$ [%] | Ref. |
|---|---|---|---|---|---|---|---|---|---|
| 1574–41–0 | 305 | *cis*-1,3-pentadiene | 68.12 | 2.4704 | 3.7070 | 253.73 | 255–445 | 0.68/1.77 | t.w. |
| 2004–70–8 | 306 | *trans*-1,3-pentadiene | 68.12 | 2.3591 | 3.7913 | 258.26 | 255–450 | 0.57/2.18 | t.w. |
| 591–93–5 | 307 | 1,4-pentadiene | 68.12 | 2.3128 | 3.8357 | 246.23 | 245–430 | 2.17/2.61 | t.w. |
| 591–95–7 | 304 | 1,2-pentadiene | 68.12 | 2.4867 | 3.6949 | 253.50 | 260–450 | 0.47/1.82 | t.w. |
| 591–96–8 | 308 | 2,3-pentadiene | 68.12 | 2.7682 | 3.5581 | 241.21 | 250–445 | 0.72/1.06 | t.w. |
| 598–25–4 | 311 | 3-methyl-1,2-butadiene | 68.12 | 2.6171 | 3.6389 | 242.43 | 250–440 | 1.01/1.17 | t.w. |
| 563–45–1 | 213 | 3-methyl-1-butene | 70.13 | 2.4541 | 3.8146 | 231.15 | 110–450 | 0.37/0.25 | t.w. |
| 563–46–2 | 212 | 2-methyl-1-butene | 70.13 | 2.6485 | 3.6924 | 231.13 | 240–415 | 0.50/0.13 | t.w. |
| 513–35–9 | 214 | 2-methyl-2-butene | 70.13 | 2.6431 | 3.6916 | 237.55 | 240–415 | 0.27/0.15 | t.w. |
| 109–67–1 | 209 | 1-pentene | 70.13 | 2.6006 | 3.7399 | 231.99 | 108–464 | 1.04/0.31 | [4] |
| 592–45–0 | 313 | 1,4-hexadiene | 82.14 | 2.8076 | 3.7739 | 247.98 | 260–455 | 0.83/0.16 | t.w. |
| 592–42–7 | 310 | 1,5-hexadiene | 82.14 | 2.6060 | 3.8764 | 253.78 | 260–455 | 0.21/0.52 | t.w. |
| 5194–50–3 | 320 | *cis*,*trans*-2,4-hexadiene | 82.14 | 2.8920 | 3.7275 | 259.09 | 270–480 | 0.98/0.49 | t.w. |
| 5194–51–4 | 314 | *trans*,*trans*-2,4-hexadiene | 82.14 | 2.9256 | 3.7198 | 256.16 | 270–480 | 0.64/0.79 | t.w. |
| 760–20–3 | 222 | 3-methyl-1-pentene | 84.16 | 2.6583 | 3.9175 | 245.25 | 140–440 | 0.30/0.23 | t.w. |
| 563–78–0 | 230 | 2,3-dimethyl-1-butene | 84.16 | 2.9529 | 3.7347 | 247.15 | 120–500 | 0.62/1.09 | t.w. |
| 763–29–1 | 221 | 2-methyl-1-pentene | 84.16 | 2.8761 | 3.8011 | 241.33 | 255–450 | 0.40/0.78 | t.w. |
| 625–27–4 | 224 | 2-methyl-2-pentene | 84.16 | 2.9916 | 3.7446 | 240.24 | 260–460 | 0.42/0.86 | t.w. |
| 691–37–2 | 223 | 4-methyl-1-pentene | 84.16 | 2.7316 | 3.8841 | 241.15 | 250–440 | 0.18/0.10 | t.w. |
| 563–79–1 | 232 | 2,3-dimethyl-2-butene | 84.16 | 2.9546 | 3.7334 | 247.03 | 265–470 | 0.56/1.03 | t.w. |
| 760–21–4 | 229 | 2-ethyl-1-butene | 84.16 | 2.9398 | 3.7577 | 240.63 | 260–460 | 0.40/0.84 | t.w. |
| 7688–21–3 | 217 | *cis*-2-hexene | 84.16 | 3.0051 | 3.7407 | 240.53 | 260–460 | 0.59/0.53 | t.w. |
| 4050–45–7 | 218 | *trans*-2-hexene | 84.16 | 2.9747 | 3.7693 | 241.09 | 260–460 | 0.50/0.66 | t.w. |
| 691–38–3 | 227 | 4-methyl-*cis*-2-pentene | 84.16 | 2.8277 | 3.8311 | 238.83 | 255–445 | 0.19/0.54 | t.w. |
| 674–76–0 | 228 | 4-methyl-*trans*-2-pentene | 84.16 | 2.9017 | 3.8003 | 237.14 | 255–450 | 0.19/0.46 | t.w. |
| 592–41–6 | 216 | 1-hexene | 84.62 | 2.9853 | 3.7753 | 236.81 | 133–504 | 1.23/0.42 | [4] |
| 592–76–7 | 234 | 1-heptene | 98.00 | 3.3637 | 3.7898 | 240.62 | 174–534 | 0.99/0.95 | [7] |
| 3404–61–3 | 240 | 3-methyl-1-hexene | 98.19 | 3.3079 | 3.8017 | 236.03 | 150–525 | 0.23/0.59 | t.w. |
| 6094–02–6 | 238 | 2-methyl-1-hexene | 98.19 | 3.2338 | 3.8321 | 244.69 | 270–480 | 0.48/0.28 | t.w. |
| 3769–23–1 | 226 | 4-methyl-1-hexene | 98.19 | 3.2965 | 3.7985 | 238.60 | 270–480 | 0.19/0.47 | t.w. |
| 3404–71–5 | 233 | 2-ethyl-1-pentene | 98.19 | 3.0561 | 3.8958 | 254.37 | 275–480 | 0.10/0.82 | t.w. |
| 816–79–5 | 239 | 3-ethyl-2-pentene | 98.19 | 3.3065 | 3.7784 | 236.57 | 270–470 | 0.38/0.32 | t.w. |

*Continues on next page*

| CAS-nr. | DIPPR nr. | Compound | $M_w$ [g/mol] | $m$ [–] | $\sigma$ [Å] | $\epsilon/k$ [K] | $T$ range [K] | AAD $(V_L/P^{sat})$ [%] | Ref. |
|---|---|---|---|---|---|---|---|---|---|
| 14686–13–6 | 236 | *trans*-2-heptene | 98.19 | 3.2073 | 3.8565 | 249.79 | 275–480 | 0.67/0.41 | t.w. |
| 6443–92–1 | 235 | *cis*-2-heptene | 98.19 | 3.0679 | 3.9183 | 256.49 | 280–493 | 1.25/0.51 | t.w. |
| 14686–14–7 | 237 | *trans*-3-heptene | 98.19 | 3.8359 | 3.2596 | 246.08 | 275–485 | 0.58/0.26 | t.w. |
| 7642–10–6 | 249 | *cis*-3-heptene | 98.19 | 3.1306 | 3.8852 | 251.81 | 275–485 | 0.68/0.39 | t.w. |
| 627–58–7 | 329 | 2,5-dimethyl-1,5-hexadiene | 110.20 | 3.3690 | 3.8822 | 253.76 | 285–510 | 0.60/0.48 | t.w. |
| 764–13–6 | 330 | 2,5-dimethyl-2,4-hexadiene | 110.20 | 3.4490 | 3.8277 | 265.66 | 300–530 | 0.14/1.40 | t.w. |
| 107–39–1 | 256 | 2,4,4-trimethyl-1-pentene | 112.21 | 3.0650 | 4.0683 | 256.32 | 230–490 | 0.38/1.82 | t.w. |
| 15870–10–7 | 2252 | 2-methyl-1-heptene | 112.21 | 3.4081 | 3.9348 | 253.96 | 285–510 | 0.88/0.71 | t.w. |
| 107–40–4 | 257 | 2,4,4-trimethyl-2-pentene | 112.21 | 3.3401 | 3.9343 | 247.35 | 285–490 | 0.16/0.22 | t.w. |
| 1632–16–2 | 258 | 2-ethyl-1-hexene | 112.21 | 3.4236 | 3.9141 | 254.18 | 290–515 | 0.45/0.46 | t.w. |
| 13389–42–9 | 251 | *trans*-2-octene | 112.21 | 3.3323 | 3.9757 | 261.12 | 290–515 | 0.91/0.38 | t.w. |
| 7642–04–8 | 276 | *cis*-2-octene | 112.21 | 3.4103 | 3.9427 | 258.10 | 290–510 | 1.35/1.11 | t.w. |
| 14919–01–8 | 277 | *trans*-3-octene | 112.21 | 3.3614 | 3.9690 | 258.69 | 290–515 | 0.87/0.47 | t.w. |
| 14850–22–7 | 280 | *cis*-3-octene | 112.21 | 3.4131 | 3.9321 | 256.24 | 290–510 | 0.67/0.84 | t.w. |
| 14850–23–8 | 279 | *trans*-4-octene | 112.21 | 3.3646 | 3.9683 | 257.89 | 290–515 | 0.83/0.97 | t.w. |
| 7642–15–1 | 278 | *cis*-4-octene | 112.21 | 3.4444 | 3.9184 | 254.85 | 290–510 | 0.64/1.15 | t.w. |
| 111–66–0 | 250 | 1-octene | 112.22 | 3.7424 | 3.8133 | 243.02 | 171–567 | 0.75/0.79 | [4] |
| 124–11–8 | 259 | 1-nonene | 126.00 | 3.99 | 3.8746 | 249.27 | 232–592 | 0.60/1.04 | [7] |
| 872–05–9 | 259 | 1-decene | 140.00 | 4.37 | 3.8908 | 250.35 | 207–607 | 0.85/1.83 | [7] |
| 821–95–4 | 261 | 1-undecene | 154.29 | 4.8572 | 3.8615 | 248.68 | 325–570 | 0.45/0.87 | t.w. |
| 112–41–4 | 262 | 1-dodecene | 168.00 | 4.988 | 3.947 | 255.14 | 278–638 | 0.84/1.53 | [7] |
| 2437–56–1 | 263 | 1-tridecene | 182.35 | 5.6086 | 3.8861 | 250.46 | 340–600 | 0.66/0.86 | t.w. |
| 1120–36–1 | 264 | 1-tetradecene | 196.00 | 5.7437 | 3.96 | 256.66 | 280–680 | 1.44/3.23 | [7] |
| 13360–61–7 | 265 | 1-pentadecene | 210.40 | 6.3945 | 3.8951 | 251.16 | 360–630 | 0.59/2.04 | t.w. |
| 629–73–2 | 266 | 1-hexadecene | 224.00 | 6.5 | 3.9748 | 256.7 | 277–702 | 1.40/2.31 | [7] |
| 6765–39–5 | 281 | 1-heptadecene | 238.45 | 6.9620 | 3.9523 | 254.67 | 390–660 | 0.76/1.96 | t.w. |
| 112–88–9 | 267 | 1-octadecene | 252.48 | 7.2901 | 3.9687 | 255.58 | 410–660 | 0.79/2.44 | t.w. |
| 18435–45–5 | 283 | 1-nonadecene | 266.51 | 7.8402 | 3.9359 | 253.51 | 380–680 | 0.76/2.27 | t.w. |
| 3452–07–1 | 284 | 1-eicosene | 280.53 | 8.2012 | 3.9425 | 253.74 | 390–680 | 0.67/2.21 | t.w. |
| | | *cycloalkenes* | | | | | | | |
| 542–92–7 | 315 | cyclopentadiene | 66.10 | 1.9327 | 3.8126 | 294.29 | 190–505 | 0.51/2.07 | t.w. |

*Continues on next page*

| CAS-nr. | DIPPR nr. | Compound | $M_w$ [g/mol] | $m$ [–] | $\sigma$ [Å] | $\epsilon/k$ [K] | $T$ range [K] | AAD $(V_L/P^{sat})$ [%] | Ref. |
|---|---|---|---|---|---|---|---|---|---|
| 142–29–0 | 257 | cyclopentene | 68.11 | 2.2934 | 3.6668 | 267.76 | 223–393 | 0.07/0.14 | [4] |
| 592–57–4 | 331 | 1,3-cyclohexadiene | 80.13 | 2.5354 | 3.6946 | 280.68 | 165–550 | 1.34/0.26 | t.w. |
| 26519–91–5 | 312 | methylcyclopentadiene | 80.13 | 2.7727 | 3.5933 | 260.55 | 150–540 | 0.14/0.48 | t.w. |
| 628–41–1 | 332 | 1,4-cyclohexadiene | 80.13 | 3.1349 | 3.3922 | 255.23 | 290–510 | 0.48/1.00 | t.w. |
| 110–83–8 | 270 | cyclohexene | 82.14 | 2.4475 | 3.8085 | 287.44 | 170–560 | 0.52/0.43 | t.w. |
| 693–89–0 | 286 | methylcyclopentene | 82.14 | 2.7028 | 3.7044 | 264.50 | 275–485 | 0.10/0.47 | t.w. |
| 628–92–2 | 273 | cycloheptene | 96.17 | 2.9438 | 3.7689 | 279.23 | 220–590 | 0.66/0.77 | t.w. |
| 100–40–3 | 285 | vinylcyclohexene | 108.18 | 2.8461 | 3.9732 | 291.41 | 170–590 | 1.00/1.05 | t.w. |
| 111–78–4 | 333 | 1,5-cyclooctadiene | 108.18 | 3.2217 | 3.7647 | 290.33 | 325–570 | 1.52/0.96 | t.w. |
| 931–88–4 | 274 | cyclooctene | 110.20 | 3.0110 | 3.8277 | 296.24 | 215–630 | 2.76/0.86 | t.w. |
| | | *alkynes* | | | | | | | |
| 74–86–2 | 401 | ethyne | 26.04 | 2.4870 | 2.7578 | 156.17 | 195–300 | 0.16/2.08 | t.w. |
| 74–99–7 | 402 | 1-propyne | 40.06 | 2.4826 | 3.1024 | 205.18 | 170–400 | 0.41/0.51 | t.w. |
| 646–05–9 | 421 | 1-pentene-3-yne | 66.10 | 2.1395 | 3.8483 | 291.31 | 150–520 | 3.80/0.88 | t.w. |
| 691–37–2 | 420 | 1-pentene-4-yne | 66.10 | 1.9914 | 3.8972 | 288.00 | 155–500 | 0.92/0.28 | t.w. |
| 598–23–2 | 414 | 3-methyl-1-butyne | 66.10 | 2.7145 | 3.6141 | 227.51 | 185–460 | 1.04/0.61 | t.w. |
| 627–19–0 | 405 | 1-pentyne | 68.13 | 2.8902 | 3.5105 | 228.48 | 170–480 | 2.77/0.81 | t.w. |
| 627–21–4 | 412 | 2-pentyne | 68.13 | 2.3963 | 3.7472 | 269.25 | 165–510 | 1.52/1.87 | t.w. |
| 693–02–7 | 413 | 1-hexyne | 82.14 | 3.1555 | 3.5961 | 237.56 | 145–515 | 0.12/0.75 | t.w. |
| 764–35–2 | 407 | 2-hexyne | 82.14 | 2.8604 | 3.7368 | 261.66 | 185–545 | 1.34/1.38 | t.w. |
| 928–49–4 | 406 | 3-hexyne | 82.14 | 2.9295 | 3.7000 | 255.43 | 175–540 | 0.32/0.68 | t.w. |
| 628–71–7 | 2414 | 1-heptyne | 96.17 | 3.2242 | 3.7744 | 252.76 | 200–550 | 0.68/1.63 | t.w. |
| 629–05–0 | 416 | 1-octyne | 110.20 | 3.7647 | 3.7327 | 247.34 | 195–585 | 0.23/1.05 | t.w. |
| | | *benzene derivatives* | | | | | | | |
| 71–43–2 | 501 | benzene | 78.11 | 2.4653 | 3.6478 | 287.35 | 278–562 | 1.42/0.64 | [4] |
| 108–88–3 | 502 | toluene | 92.14 | 2.8149 | 3.7169 | 285.69 | 178–594 | 1.35/2.41 | [4] |
| 100–41–4 | 504 | ethylbenzene | 106.17 | 3.0799 | 3.7974 | 287.35 | 178–617 | 1.05/0.41 | [4] |
| 108–38–3 | 506 | *m*-xylene | 106.17 | 3.1861 | 3.7563 | 283.98 | 225–619 | 1.05/1.08 | [4] |
| 95–47–6 | 505 | *o*-xylene | 106.17 | 3.1362 | 3.76 | 291.05 | 248–630 | 1.15/0.64 | [4] |
| 106–42–3 | 507 | *p*-xylene | 106.17 | 3.1723 | 3.7781 | 283.77 | 286–616 | 0.58/2.09 | [4] |

*Continues on next page*

| CAS-nr. | DIPPR nr. | Compound | $M_w$ [g/mol] | $m$ [–] | $\sigma$ [Å] | $\epsilon/k$ [K] | $T$ range [K] | AAD $(V_L/P^{sat})$ [%] | Ref. |
|---|---|---|---|---|---|---|---|---|---|
| 108–67–8 | 516 | 1,3,5-trimethyl benzene | 120.19 | 3.7547 | 3.7032 | 274.21 | 340–570 | 0.70/1.26 | t.w. |
| 526–73–8 | 514 | 1,2,3-trimethyl benzene | 120.19 | 3.4688 | 3.7574 | 295.37 | 340–590 | 0.21/1.00 | t.w. |
| 95–63–6 | 515 | 1,2,4-trimethyl benzene | 120.19 | 3.5204 | 3.7770 | 287.45 | 330–580 | 0.76/0.56 | t.w. |
| 98–82–8 | 510 | cumene | 120.19 | 3.3198 | 3.8675 | 284.09 | 320–565 | 0.96/0.59 | t.w. |
| 620–14–4 | 512 | 1-methyl-3-ethyl benzene | 120.19 | 3.4593 | 3.8198 | 284.20 | 325–570 | 1.19/0.87 | t.w. |
| 611–14–3 | 511 | 1-ethyl-2-methyl benzene | 120.19 | 3.3408 | 3.8426 | 293.07 | 325–580 | 0.89/1.08 | t.w. |
| 622–96–8 | 513 | 1-ethyl-4-methyl benzene | 120.19 | 3.3364 | 3.8708 | 290.23 | 325–575 | 0.92/0.63 | t.w. |
| 103–65–1 | 509 | *n*-propyl benzene | 120.19 | 3.3438 | 3.8438 | 288.13 | 173–638 | 1.19/1.29 | [4] |
| 119–64–2 | 701 | tetralin | 132.21 | 3.3131 | 3.875 | 325.07 | 237–720 | 0.54/1.06 | [4] |
| 98–06–6 | 521 | *tert*-butyl benzene | 134.22 | 3.4461 | 3.9669 | 287.79 | 270–590 | 0.86/2.24 | t.w. |
| 99–87–6 | 524 | *p*-cymene | 134.22 | 3.6022 | 3.9247 | 285.59 | 330–580 | 0.87/0.59 | t.w. |
| 535–77–3 | 523 | *m*-cymene | 134.22 | 3.4623 | 3.9730 | 290.71 | 335–590 | 0.92/0.89 | t.w. |
| 527–84–4 | 522 | *o*-cymene | 134.22 | 3.4251 | 3.9696 | 295.04 | 335–590 | 1.08/0.99 | t.w. |
| 141–93–5 | 525 | *m*-diethyl benzene | 134.22 | 3.6407 | 3.9049 | 287.43 | 335–590 | 0.96/0.93 | t.w. |
| 135–01–3 | 526 | *o*-diethyl benzene | 134.22 | 3.6217 | 3.6876 | 290.32 | 340–590 | 0.81/1.28 | t.w. |
| 105–05–5 | 527 | *p*-diethylbenzene | 134.22 | 3.7494 | 3.8741 | 284.27 | 340–590 | 1.20/0.52 | t.w. |
| 110–57–6 | 576 | 2-ethyl-*m*-xylene | 134.22 | 3.8260 | 3.8033 | 286.28 | 330–600 | 0.94/0.21 | t.w. |
| 1758–88–9 | 577 | 2-ethyl-*p*-xylene | 134.22 | 3.9306 | 3.7845 | 279.78 | 335–590 | 0.94/1.12 | t.w. |
| 874–41–9 | 578 | 4-ethyl-*m*-xylene | 134.22 | 3.8626 | 3.8134 | 283.30 | 335–590 | 1.11/0.97 | t.w. |
| 934–80–5 | 579 | 4-ethyl-*o*-xylene | 134.22 | 3.8007 | 3.8949 | 282.91 | 335–595 | 0.89/0.39 | t.w. |
| 934–74–7 | 575 | 5-ethyl-*m*-xylene | 134.22 | 3.8293 | 3.8383 | 281.01 | 330–585 | 1.20/0.46 | t.w. |
| 135–98–8 | 520 | *sec*-butyl benzene | 134.22 | 3.1800 | 4.0867 | 303.58 | 355–590 | 0.62/1.68 | t.w. |
| 95–93–2 | 532 | 1,2,4,5-tetramethyl benzene | 134.22 | 3.9480 | 3.7777 | 285.77 | 350–600 | 1.20/0.45 | t.w. |
| 933–98–2 | 580 | 1-ethyl-2,3-dimethylbenzene | 134.22 | 3.7826 | 3.8250 | 290.74 | 345–610 | 1.14/0.65 | t.w. |
| 538–93–2 | 519 | 2-methylpropyl benzene | 134.22 | 3.6917 | 3.8900 | 278.86 | 330–580 | 0.62/0.85 | t.w. |
| 104–51–8 | 518 | *n*-butyl benzene | 134.22 | 3.7662 | 3.8727 | 283.07 | 185–660 | 1.32/0.60 | [4] |
| 538–68–1 | 567 | *n*-pentyl benzene | 148.24 | 3.9635 | 3.9350 | 288.02 | 340–610 | 0.78/1.37 | t.w. |
| 92–52–4 | 558 | biphenyl | 154.21 | 3.8877 | 3.8151 | 327.42 | 342–773 | 1.14/0.94 | [4] |
| 1746–23–2 | 621 | *p*-*tert*-butyl styrene | 160.26 | 3.8619 | 4.0487 | 303.56 | 300–600 | 0.98/3.97 | t.w. |
| 1077–16–3 | 568 | *n*-hexylbenzene | 162.27 | 4.3760 | 3.9298 | 284.07 | 355–625 | 0.78/1.16 | t.w. |
| 1078–71–3 | 549 | *n*-heptyl benzene | 176.30 | 4.5241 | 4.0149 | 289.08 | 360–540 | 1.26/1.89 | t.w. |
| 2189–60–8 | 569 | *n*-octyl benzene | 190.32 | 5.0295 | 3.9752 | 282.80 | 370–650 | 1.00/1.95 | t.w. |

*Continues on next page*

| CAS-nr. | DIPPR nr. | Compound | $M_w$ [g/mol] | $m$ [–] | $\sigma$ [Å] | $\epsilon/k$ [K] | $T$ range [K] | AAD $(V_L/P^{sat})$ [%] | Ref. |
|---|---|---|---|---|---|---|---|---|---|
| 1081–77–2 | 570 | *n*-nonyl benzene | 204.35 | 5.4290 | 3.9718 | 280.64 | 390–630 | 0.84/2.00 | t.w. |
| 104–72–3 | 554 | *n*-decyl benzene | 218.38 | 5.9324 | 3.9448 | 276.10 | 380–675 | 1.00/1.88 | t.w. |
| 6742–54–7 | 571 | *n*-undecyl benzene | 232.40 | 6.4419 | 3.9192 | 272.31 | 385–680 | 0.81/1.87 | t.w. |
| 123–01–3 | 574 | *n*-dodecyl benzene | 246.43 | 6.7475 | 3.9410 | 272.53 | 395–700 | 0.91/1.09 | t.w. |
| 123–02–4 | 572 | *n*-tridecyl benzene | 260.46 | 7.0833 | 3.9538 | 272.38 | 395–710 | 0.91/1.56 | t.w. |
| 1459–10–5 | 573 | *n*-tetradecyl benzene | 274.48 | 7.4567 | 3.9570 | 271.19 | 405–720 | 0.90/1.36 | t.w. |
| 2131–18–2 | 2575 | *n*-pentadecyl benzene | 288.51 | 7.8646 | 3.9550 | 269.89 | 410–710 | 0.85/1.90 | t.w. |
| 1459–09–2 | 2576 | *n*-hexadecyl benzene | 302.54 | 8.3513 | 3.9416 | 267.76 | 430–735 | 0.54/1.00 | t.w. |
| 14752–75–1 | 2577 | *n*-heptadecyl benzene | 316.56 | 8.3475 | 3.9989 | 271.69 | 440–742 | 0.46/0.96 | t.w. |
| 4445–07–2 | 2578 | *n*-octadecyl benzene | 330.59 | 8.5544 | 4.0163 | 272.99 | 450–750 | 0.41/0.89 | t.w. |
| | | *polynuclear aromatics* | | | | | | | |
| 95–13–6 | 803 | indene | 116.16 | 2.8969 | 3.8800 | 334.88 | 272–687 | 2.19/1.23 | t.w. |
| 496–11–7 | 820 | indane | 118.18 | 3.1093 | 3.8233 | 316.99 | 220–680 | 1.05/0.17 | t.w. |
| 91–20–3 | 701 | naphthalene | 128.17 | 3.0047 | 3.9133 | 353.63 | 354–748 | 0.74/0.51 | t.w. |
| 281–23–2 | 810 | adamantane | 136.23 | 1.8837 | 4.7979 | 452.13 | 545–740 | 3.31/0.80 | t.w. |
| 79–92–5 | 839 | camphene | 136.23 | 3.0322 | 4.1470 | 300.83 | 325–635 | 0.57/0.23 | t.w. |
| 90–12–0 | 702 | 1-methyl naphthalene | 142.20 | 3.5975 | 3.8173 | 335.57 | 390–690 | 0.54/0.59 | t.w. |
| 91–57–6 | 703 | 2-methyl naphthalene | 142.20 | 3.3234 | 3.9533 | 347.55 | 310–760 | 1.08/1.02 | t.w. |
| 83–32–9 | 808 | acenaphthene | 154.21 | 3.6387 | 3.8560 | 355.50 | 400–720 | 1.28/0.55 | t.w. |
| 1127–76–0 | 704 | 1-ethyl naphthalene | 156.22 | 3.7865 | 3.8809 | 333.55 | 260–776 | 0.33/1.50 | t.w. |
| 132–64–9 | 1480 | dibenzofuran | 168.19 | 2.3829 | 4.5718 | 452.21 | 420–750 | 3.23/2.05 | t.w. |
| 2765–18–6 | 718 | 1-propyl naphthalene | 170.25 | 3.8084 | 4.0307 | 338.48 | 270–780 | 0.83/0.96 | t.w. |
| 120–12–7 | 804 | anthracene | 178.23 | 3.3811 | 4.1423 | 411.47 | 490–870 | 0.83/1.50 | t.w. |
| 1634–09–9 | 713 | 1-butyl naphthalene | 184.28 | 4.6950 | 3.8582 | 311.66 | 255–790 | 0.35/0.34 | t.w. |
| 129–00–0 | 717 | pyrene | 202.25 | 3.7597 | 4.1574 | 421.04 | 290–935 | 3.67/0.77 | t.w. |
| 605–02–7 | 710 | 1-phenyl naphthalene | 204.27 | 4.9170 | 3.8225 | 331.06 | 320–845 | 1.08/0.53 | t.w. |
| 2876–53–1 | 714 | 1-hexyl naphthalene | 212.33 | 5.5795 | 3.8581 | 300.40 | 260–810 | 0.39/0.48 | t.w. |
| 26438–26–6 | 711 | 1-nonyl naphthalene | 254.41 | 5.5274 | 4.1881 | 319.52 | 285–840 | 2.03/0.75 | t.w. |
| 26438–27–7 | 712 | 1-decyl naphthalene | 268.44 | 5.7671 | 4.2172 | 318.51 | 290–860 | 2.16/0.84 | t.w. |

*Continues on next page*

| CAS-nr. | DIPPR nr. | Compound | $M_w$ [g/mol] | $m$ [–] | $\sigma$ [Å] | $\epsilon/k$ [K] | $T$ range [K] | AAD $(V_L/P^{sat})$ [%] | Ref. |
|---|---|---|---|---|---|---|---|---|---|
| | | | *halogenated hydrocarbons* | | | | | | |
| 74–87–3 | 1502 | methyl chloride | 50.49 | 1.9297 | 3.2293 | 240.56 | 175–416 | 1.55/0.48 | [4] |
| 75–00–3 | 1503 | chloroethane | 64.51 | 2.2638 | 3.416 | 245.43 | 134–460 | 1.77/1.63 | [4] |
| 75–29–6 | 1530 | 2-chloropropane | 78.54 | 2.4151 | 3.6184 | 251.47 | 156–489 | 0.61/2.89 | [4] |
| 75–09–2 | 1511 | dichloromethane | 84.93 | 2.2632 | 3.3380 | 274.20 | 180–510 | 1.53/1.18 | t.w. |
| 126–99–8 | 1583 | 2-chloro-1,3-butadiene | 88.54 | 2.1489 | 3.8432 | 290.65 | 265–460 | 0.91/0.16 | t.w. |
| 109–69–3 | 1586 | 1-chlorobutane | 92.57 | 2.8585 | 3.6424 | 258.66 | 150–537 | 1.14/0.99 | [4] |
| 78–86–4 | 1587 | 2-chlorobutane | 92.57 | 2.6874 | 3.7138 | 258.80 | 265–450 | 0.52/1.17 | t.w. |
| 507–20–0 | 1535 | 2-chloro-2-methylpropane | 92.57 | 2.4250 | 3.8665 | 259.27 | 265–450 | 0.14/0.33 | t.w. |
| 107–06–2 | 1523 | 1,2-dichloroethane | 98.96 | 2.5964 | 3.4463 | 285.01 | 300–500 | 0.89/0.34 | t.w. |
| 543–59–9 | 1588 | 1-chloropentane | 106.59 | 2.7513 | 3.9027 | 284.31 | 290–500 | 1.07/0.53 | t.w. |
| 108–90–7 | 1571 | chlorobenzene | 112.56 | 2.6929 | 3.7367 | 312.11 | 230–630 | 0.46/0.29 | t.w. |
| 108–90–7 | 1571 | chlorobenzene | 112.56 | 2.6485 | 3.7533 | 315.04 | 228–632 | 0.66/2.59 | [4] |
| 67–66–3 | 1521 | chloroform | 119.38 | 2.5038 | 3.4709 | 271.625 | 250–490 | 0.38/0.78 | [8] |
| 7415–31–8 | 1598 | 1,3-dichloro-*t*-2-butene | 125.00 | 2.8316 | 3.7365 | 300.04 | 315–530 | 0.49/2.61 | t.w. |
| 1476–11–5 | 1593 | 1,4-dichloro-*c*-2-butene | 125.00 | 3.2115 | 3.5775 | 297.27 | 320–570 | 1.73/0.50 | t.w. |
| 110–57–6 | 1505 | 1,4-dichloro-*t*-2-butene | 125.00 | 3.1752 | 3.5967 | 302.26 | 325–570 | 1.77/0.45 | t.w. |
| 760–23–6 | 1597 | 3,4-dichloro-1-butene | 125.00 | 3.1083 | 3.6114 | 273.60 | 300–530 | 0.84/0.41 | t.w. |
| 616–21–7 | 1536 | 1,2-dichlorobutane | 127.01 | 2.9616 | 3.7239 | 286.55 | 300–530 | 0.14/0.15 | t.w. |
| 110–56–5 | 1508 | 1,4-dichlorobutane | 127.01 | 3.1317 | 3.6791 | 300.85 | 330–560 | 1.37/0.38 | t.w. |
| 7581–97–7 | 1537 | 2,3-dichlorobutane | 127.01 | 2.9240 | 3.7730 | 284.28 | 325–535 | 1.40/0.33 | t.w. |
| 71–55–6 | 1527 | 1,1,1-trichloroethane | 133.40 | 2.4646 | 3.7558 | 279.13 | 270–540 | 0.52/0.32 | t.w. |
| 109–65–9 | 1655 | 1-bromobutane | 137.02 | 2.7452 | 3.7491 | 282.47 | 290–510 | 0.76/1.04 | t.w. |
| 78–76–2 | 2638 | 2-bromobutane | 137.02 | 3.1836 | 3.5234 | 253.14 | 290–490 | 1.50/0.43 | t.w. |
| 628–76–2 | 1509 | 1,5-dichloropentane | 141.04 | 3.6536 | 3.6703 | 291.04 | 335–600 | 1.09/0.43 | t.w. |
| 95–50–1 | 1572 | *o*-dichloro benzene | 147.01 | 2.8409 | 3.8470 | 338.40 | 260–705 | 1.23/1.48 | t.w. |
| 56–23–5 | 1501 | carbon tetrachloride | 153.82 | 2.32521 | 3.8055 | 292.134 | 260–510 | 0.32/0.48 | [8] |
| 108–86–1 | 1680 | bromobenzene | 157.01 | 2.6456 | 3.836 | 334.37 | 242–670 | 1.44/1.27 | [4] |
| 108–86–1 | 1680 | bromobenzene | 157.01 | 2.5899 | 3.8534 | 338.55 | 340–600 | 0.78/0.96 | t.w. |
| 106–38–7 | 2661 | *p*-bromotoluene | 171.03 | 3.3482 | 3.7082 | 308.97 | 350–625 | 0.39/2.15 | t.w. |
| 629–04–9 | 1667 | 1-bromoheptane | 179.10 | 3.9421 | 3.7907 | 273.68 | 325–580 | 0.15/1.02 | t.w. |
| 591–50–4 | 1691 | iodobenzene | 204.01 | 2.7326 | 3.8793 | 352.85 | 365–645 | 0.75/0.23 | t.w. |

*Continues on next page*

| CAS-nr. | DIPPR nr. | Compound | $M_w$ [g/mol] | $m$ [–] | $\sigma$ [Å] | $\epsilon/k$ [K] | $T$ range [K] | AAD $(V_L/P^{sat})$ [%] | Ref. |
|---|---|---|---|---|---|---|---|---|---|
| 90–11–9 | 1697 | 1-bromonaphthalene | 207.07 | 3.6549 | 3.8328 | 358.20 | 420–740 | 1.06/0.55 | t.w. |
| 108–36–1 | 1678 | *m*-dibromobenzene | 235.90 | 2.8807 | 3.9138 | 363.31 | 385–680 | 0.23/0.77 | t.w. |
| | | *ethers* | | | | | | | |
| 115–10–6 | 1401 | dimethyl ether | 46.07 | 2.3071 | 3.2528 | 211.06 | 200–400 | 0.8/0.25 | [4] |
| 107–25–5 | 1470 | vinyl methyl ether | 58.08 | 2.7079 | 3.2431 | 215.05 | 220–390 | 0.08/0.51 | t.w. |
| 60–29–7 | 1402 | diethyl ether | 74.12 | 2.9686 | 3.5147 | 220.09 | 240–467 | 0.94/0.46 | [4] |
| 557–17–5 | 1415 | methyl-*n*-propyl ether | 74.12 | 3.0087 | 3.4569 | 222.73 | 220–476 | 1.99/1.04 | [4] |
| 557–17–5 | 1415 | methyl-*n*-propyl ether | 74.12 | 3.1934 | 3.3897 | 215.43 | 220–476 | 0.97/0.63 | t.w. |
| 123–91–1 | 1421 | *p*-dioxane | 88.11 | 2.9724 | 3.3762 | 275.88 | 305–525 | 0.34/0.80 | t.w. |
| 111–43–3 | 1446 | dipropyl ether | 102.17 | 3.4930 | 3.6928 | 234.16 | 150–530 | 0.008/0.18 | t.w. |
| 108–20–3 | 1403 | diisopropyl ether | 102.17 | 3.7102 | 3.4577 | 219.63 | 188–500 | 0.07/1.99 | [4] |
| 628–80–8 | 1429 | methyl-*n*-pentyl ether | 102.17 | 3.8886 | 3.5478 | 227.85 | 150–540 | 0.34/0.48 | t.w. |
| 142–96–1 | 1404 | dibutyl ether | 130.23 | 4.6200 | 3.6404 | 228.48 | 180–580 | 0.16/0.77 | t.w. |
| 539–30–0 | 1460 | benzyl ethyl ether | 136.19 | 4.0145 | 3.6513 | 277.75 | 280–660 | 0.27/1.61 | t.w. |
| 101–84–8 | 1465 | diphenyl ether | 170.21 | 3.5961 | 4.0205 | 340.40 | 300–760 | 1.60/1.47 | t.w. |
| 103–50–4 | 1463 | dibenzyl ether | 198.26 | 7.0830 | 3.3098 | 258.77 | 280–770 | 1.96/2.77 | t.w. |
| | | *fluorinated hydrocarbons* | | | | | | | |
| 75–10–5 | 1614 | difluoromethane | 52.02 | 2.5229 | 2.7852 | 168.401 | — | 0.46/0.28 | [9] |
| 75–37–6 | 1640 | difluoroethane | 66.05 | 2.1772 | 3.3554 | 216. | 170–370 | 2.24/2.80 | [10] |
| 75–46–7 | 1615 | trifluoromethane | 70.01 | 2.9404 | 2.7213 | 141.13 | — | 0.40/0.22 | [9] |
| 75–45–6 | 1601 | difluorochloromethane | 86.47 | 2.1012 | 3.3104 | 203.3215 | — | 0.41/0.40 | [9] |
| 75–73–0 | 1616 | carbon tetra fluoride | 88.00 | 2.1779 | 3.1383 | 122.65 | 115–205 | 0.16/0.18 | t.w. |
| 421–14–7 | — | trifluoromethyl methyl ether | 100.40 | 2.8808 | 3.2403 | 181.69 | 197–353 | -/[11] | |
| 116–14–3 | 1630 | tetrafluoroethane | 102.03 | 1.9793 | 3.1418 | 189.14 | — | 0.58/0.31 | [9] |
| 76–16–4 | 2693 | hexafluoroethane | 138.01 | 2.7543 | 3.3459 | 141.69 | 160–260 | 0.54/1.23 | t.w. |
| 22410–44–2 | — | pentafluoroethyl methyl ether | 150.05 | 3.565 | 3.3342 | 177.02 | — | 0.15/0.10 | [11] |
| 392–56–3 | 1864 | perfluorobenzene | 186.05 | 3.2897 | 3.5601 | 239.92 | 288–313 | 0.00/0.39 | t.w. |
| 76–19–7 | 2652 | octafluoropropane | 188.02 | 3.4547 | 3.3031 | 154.20 | 180–305 | 0.20/1.48 | t.w. |
| 115–25–3 | 2654 | octafluorocyclobutane | 200.03 | 3.7354 | 3.3674 | 164.66 | 200–345 | 0.24/0.45 | t.w. |
| 375–03–1 | — | heptafluoropropyl methyl ether | 200.06 | 4.7413 | 3.2622 | 171.44 | — | /0.05 | [11] |

*Continues on next page*

| CAS-nr. | DIPPR nr. | Compound | $M_w$ [g/mol] | $m$ [–] | $\sigma$ [Å] | $\epsilon/k$ [K] | $T$ range [K] | AAD $(V_L/P^{sat})$ [%] | Ref. |
|---|---|---|---|---|---|---|---|---|---|
| 434–64–0 | — | perfluorotoluene | 236.06 | 4.4079 | 3.4490 | 215.95 | 288–313 | 0.13/0.86 | t.w. |
| 355–25–9 | 1622 | decafluorobutane | 238.03 | 3.8326 | 3.5361 | 162.28 | 195–340 | 0.70/0.38 | t.w. |
| 163702–07–6 | — | nonafluorobutyl methyl ether | 250.07 | 6.9892 | 3.036 | 163.98 | — | — | [11] |
| 355–42–0 | — | perfluoro-*n*-hexane | 338.04 | 4.9669 | 3.6172 | 171.45 | 288–313 | 0.09/1.40 | t.w. |
| 163702–07–6 | — | nonafluorobutyl ethyl ether | 364.10 | 7.1779 | 3.1467 | 168.62 | 283–350 | 0.04/0.04 | [11] |
| 335–65–9 | — | 1H-perfluoro-*n*-octane | 420.07 | 5.3504 | 3.8249 | 195.41 | 288–313 | 0.22/0.62 | t.w. |
| 306–94–5 | — | perfluorodecalin | 462.08 | 2.2527 | 3.4135 | 341.35 | 288–313 | 0.17/2.77 | t.w. |
| 375–96–2 | — | perfluoro-*n*-nonane | 488.06 | 5.9846 | 3.8425 | 188.62 | 288–313 | 0.01/0.70 | t.w. |
| 307–43–7 | — | 1Br-perfluoro-*n*-octane | 498.96 | 4.4272 | 4.2492 | 229.97 | 288–313 | 0.07/2.12 | t.w. |
| | | *nitroalkanes* | | | | | | | |
| 75–05–8 | 1772 | acetonitrile | 41.05 | 1.6092 | 3.6162 | 190.21 | 230–545 | 0.89/0.41 | [12] |
| 75–05–8 | 1772 | acetonitrile | 41.05 | 1.9693 | 3.3648 | 344.90 | 275–470 | 0.39/1.89 | t.w. |
| 75–52–5 | 1760 | nitromethane | 61.04 | 2.5325 | 3.1174 | 314.19 | 245–590 | 3.44/1.63 | t.w. |
| 79–24–3 | 1761 | nitroethane | 75.07 | 2.9556 | 3.2322 | 290.55 | 185–590 | 2.21/0.76 | t.w. |
| 108–03–2 | 1762 | 1-nitropropane | 89.09 | 3.1377 | 3.4066 | 289.01 | 170–605 | 0.85/1.93 | t.w. |
| 79–46–9 | 1763 | 2-nitropropane | 89.09 | 3.1019 | 3.4243 | 281.65 | 171–590 | 1.69/1.13 | t.w. |
| 98–95–3 | 1886 | nitrobenzene | 123.11 | 3.1442 | 3.6415 | 344.88 | 280–715 | 2.72/1.09 | t.w. |
| 99–08–1 | 1780 | *m*-nitrotoluene | 137.14 | 3.5459 | 3.6719 | 331.95 | 290–730 | 2.64/5.14 | t.w. |
| 88–72–2 | 1778 | *o*-nitrotoluene | 137.14 | 3.9917 | 3.5014 | 306.03 | 270–720 | 2.16/2.51 | t.w. |
| 509–14–8 | 1768 | tetranitromethane | 151.04 | 4.0979 | 3.2294 | 290.53 | 184–593 | 2.13/0.78 | t.w. |
| 99–65–0 | 2740 | *m*-dinitrobenzene | 168.11 | 6.0678 | 3.0025 | 293.97 | 364–805 | 0.75/0.79 | t.w. |
| 528–29–0 | 2741 | *o*-dinitrobenzene | 168.11 | 6.2837 | 3.0511 | 297.61 | 390–831 | 0.50/0.65 | t.w. |
| 100–25–4 | 2742 | *p*-dinitrobenzene | 168.11 | 6.4161 | 3.0433 | 283.69 | 450–800 | 0.23/0.66 | t.w. |
| | | *esters* | | | | | | | |
| 107–31–3 | 1301 | methyl methanoate | 60.05 | 2.6784 | 3.0875 | 242.63 | 174–487 | 1.48/1.17 | [4] |
| 109–94–4 | 1302 | ethyl methanoate | 74.08 | 2.8876 | 3.3109 | 246.47 | 193–508 | 1.80/0.92 | [4] |
| 79–20–9 | 1312 | methyl acetate | 74.08 | 3.1421 | 3.1888 | 235.75 | 200–500 | 0.95/1.10 | [6] |
| 108–05–4 | 1321 | vinyl acetate | 86.09 | 3.4674 | 3.2482 | 231.45 | 180–515 | 0.52/0.53 | t.w. |
| 96–33–3 | 1341 | methyl acrylate | 86.09 | 3.1365 | 3.3462 | 250.65 | 270–480 | 0.23/1.04 | t.w. |
| 141–78–6 | 1313 | ethyl acetate | 88.11 | 3.6000 | 3.2719 | 228.92 | 190–520 | 0.54/0.68 | t.w. |

*Continues on next page*

| CAS-nr. | DIPPR nr. | Compound | $M_w$ [g/mol] | $m$ [−] | $\sigma$ [Å] | $\epsilon/k$ [K] | $T$ range [K] | AAD $(V_L/P^{sat})$ [%] | Ref. |
|---|---|---|---|---|---|---|---|---|---|
| 141–78–6 | 1313 | ethyl acetate | 88.11 | 3.5375 | 3.3079 | 230.8 | 180–533 | 2.24/1.30 | [4] |
| 554–12–1 | 1322 | methyl propanoate | 88.11 | 3.4793 | 3.3142 | 234.96 | 185.53–1.87 | 1.26/[4] | |
| 110–74–7 | 1322 | propyl methanoate | 88.11 | 3.2088 | 3.4168 | 246.46 | 270–538 | 1.01/0.95 | [4] |
| 110–74–7 | 1303 | *n*-propyl formate | 88.11 | 3.2858 | 3.3803 | 243.42 | 270–480 | 0.45/1.12 | t.w. |
| 591–87–7 | 1318 | allyl acetate | 100.12 | 3.3340 | 3.5146 | 254.64 | 140–555 | 1.22/2.11 | t.w. |
| 105–38–4 | 1331 | vinyl propionate | 100.12 | 3.8051 | 3.3433 | 232.13 | 280–490 | 0.47/0.51 | t.w. |
| 80–62–6 | 1351 | methyl methacrylate | 100.12 | 3.2385 | 3.5269 | 257.06 | 315–480 | 0.92/1.17 | t.w. |
| 109–60–4 | 1314 | propyl acetate | 102.13 | 3.7861 | 3.4227 | 235.76 | 290–543 | 1.07/1.22 | [4] |
| 108–21–4 | 1319 | isopropyl acetate | 102.13 | 3.6084 | 3.4818 | 231.91 | 199–532 | 1.09/4.82 | t.w. |
| 105–37–3 | 1323 | ethyl propanoate | 102.13 | 3.3837 | 3.4031 | 232.78 | 199–546 | 1.07/2.18 | [4] |
| 623–42–7 | 1332 | methyl butanoate | 102.13 | 3.6758 | 3.4437 | 240.62 | 187–554 | 0.94/1.36 | [4] |
| 547–63–7 | 2332 | methyl isobutyrate | 102.13 | 3.6605 | 3.444 | 234.109 | 20–510 | 0.60/0.80 | [6] |
| 592–84–7 | 1304 | *n*-butyl formate | 102.13 | 3.6969 | 3.4388 | 241.79 | 270–500 | 0.26/0.86 | t.w. |
| 589–40–2 | 2305 | *sec*-butyl formate | 102.13 | 3.7042 | 3.4274 | 233.07 | 270–490 | 0.24/0.78 | t.w. |
| 762–75–4 | 2306 | *tert*-butyl formate | 102.13 | 3.2023 | 3.6341 | 243.32 | 290–485 | 1.31/0.55 | t.w. |
| 925–60–0 | 1343 | *n*-propyl acrylate | 114.14 | 4.2864 | 3.3799 | 230.53 | 285–510 | 0.19/0.57 | t.w. |
| 123–86–4 | 1315 | *n*-butyl acetate | 116.16 | 3.9808 | 3.5427 | 242.52 | 199–579 | 1.26/2.03 | [4] |
| 110–19–0 | 1316 | isobutyl acetate | 116.16 | 4.2012 | 3.4519 | 229.69 | 175–560 | 0.21/1.22 | t.w. |
| 105–46–4 | 1320 | *sec*-butyl acetate | 116.16 | 4.1424 | 3.4735 | 228.31 | 175–560 | 0.20/1.10 | t.w. |
| 106–36–5 | 1324 | *n*-propyl propanoate | 116.16 | 4.1155 | 3.4875 | 235.6 | 220–568 | 0.73/3.53 | [4] |
| 638–49–3 | 1306 | *n*-pentyl formate | 116.16 | 4.0048 | 3.5391 | 245.57 | 300–510 | 1.46/0.58 | t.w. |
| 540–88–5 | 2321 | *tert*-butyl acetate | 116.16 | 3.9416 | 3.5064 | 225.11 | 300–485 | 0.86/1.16 | t.w. |
| 97–62–1 | 2337 | ethyl isobutyrate | 116.16 | 3.9660 | 3.5351 | 232.10 | 290–495 | 0.41/1.09 | t.w. |
| 4351–54–6 | 2311 | cyclohexyl formate | 128.17 | 3.4949 | 3.7095 | 285.26 | 325–580 | 0.83/0.32 | t.w. |
| 141–32–2 | 1344 | *n*-butyl acrylate | 128.17 | 3.9771 | 3.6645 | 253.90 | 330–510 | 1.39/1.36 | t.w. |
| 106–63–8 | 2384 | isobutyl acrylate | 128.17 | 4.3238 | 3.5334 | 237.54 | 300–520 | 0.18/0.43 | t.w. |
| 2210–28–8 | 1353 | *n*-propyl methacrylate | 128.17 | 3.9401 | 3.6466 | 252.04 | 305–530 | 0.54/0.45 | t.w. |
| 123–92–2 | 1317 | isopentyl acetate | 130.18 | 4.1790 | 3.6303 | 244.76 | 200–595 | 0.37/0.52 | t.w. |
| 628–63–7 | 1357 | pentyl acetate | 130.18 | 4.7077 | 3.4729 | 234.57 | 205–595 | 0.15/0.57 | t.w. |
| 629–33–4 | 2307 | *n*-hexyl formate | 130.18 | 4.6713 | 3.4747 | 239.13 | 310–540 | 0.32/0.57 | t.w. |
| 105–66–8 | 1327 | *n*-propyl *n*-butyrate | 130.18 | 4.1319 | 3.6474 | 245.90 | 305–525 | 0.59/0.49 | t.w. |
| 644–49–5 | 1336 | *n*-propyl *n*-isobutyrate | 130.18 | 4.0428 | 3.6800 | 243.56 | 310–530 | 0.48/0.61 | t.w. |

*Continues on next page*

| CAS-nr. | DIPPR nr. | Compound | $M_w$ [g/mol] | $m$ [–] | $\sigma$ [Å] | $\epsilon/k$ [K] | $T$ range [K] | AAD $(V_L/P^{sat})$ [%] | Ref. |
|---|---|---|---|---|---|---|---|---|---|
| 108–64–5 | 1347 | ethyl isovalerate | 130.18 | 4.4745 | 3.5526 | 230.77 | 305–525 | 1.01/0.96 | t.w. |
| 104–57–4 | 2350 | benzyl formate | 136.15 | 4.0732 | 3.5237 | 290.32 | 355–620 | 1.05/0.41 | t.w. |
| 93–58–3 | 1390 | methyl benzoate | 136.15 | 3.6922 | 3.6377 | 303.46 | 355–620 | 1.32/1.07 | t.w. |
| 622–45–7 | 2364 | cyclohexyl acetate | 142.20 | 4.2248 | 3.6151 | 263.35 | 195–645 | 0.13/0.56 | t.w. |
| 97–88–1 | 1389 | *n*-butyl methacrylate | 142.20 | 4.5525 | 3.6067 | 244.68 | 310–550 | 0.33/0.55 | t.w. |
| 97–86–9 | 1388 | isobutyl methacrylate | 142.20 | 4.0377 | 3.7721 | 254.81 | 310–540 | 0.39/0.34 | t.w. |
| 624–48–6 | 2387 | dimethyl maleate | 144.13 | 5.0101 | 3.2679 | 262.83 | 255–675 | 1.02/0.30 | t.w. |
| 97–85–8 | 1360 | isobutyl isobutyrate | 144.21 | 4.3798 | 3.7321 | 239.135 | 250–560 | 1.10/1.60 | [6] |
| 142–92–7 | 1363 | *n*-hexyl acetate | 144.21 | 4.8447 | 3.5834 | 241.42 | 195–615 | 0.43/0.75 | t.w. |
| 112–23–2 | 2308 | *n*-heptyl formate | 144.21 | 4.1488 | 3.7096 | 256.39 | 345–560 | 0.90/1.70 | t.w. |
| 109–21–7 | 1385 | *n*-butyl *n*-butyrate | 144.21 | 4.4071 | 3.7006 | 249.14 | 315–550 | 0.24/0.41 | t.w. |
| 140–11–4 | 1359 | benzyl acetate | 150.17 | 4.3419 | 3.6165 | 283.70 | 225–700 | 1.73/0.50 | t.w. |
| 112–06–1 | 1367 | *n*-heptyl acetate | 158.24 | 5.3796 | 3.5874 | 239.08 | 225–635 | 0.87/1.47 | t.w. |
| 112–32–3 | 1308 | *n*-octyl formate | 158.24 | 4.1067 | 3.9853 | 279.89 | 350–510 | 1.01/1.15 | t.w. |
| 591–68–4 | 1346 | *n*-butyl valerate | 158.24 | 5.4038 | 3.5643 | 235.66 | 325–540 | 0.08/1.57 | t.w. |
| 105–53–3 | 1394 | diethyl malonate | 160.17 | 5.3090 | 3.4069 | 247.80 | 340–560 | 0.83/1.36 | t.w. |
| 2315–68–6 | 2392 | *n*-propyl benzoate | 164.20 | 4.6655 | 3.6530 | 281.56 | 225–710 | 1.00/0.30 | t.w. |
| 141–05–9 | 2386 | diethyl maleate | 172.18 | 5.3643 | 3.5877 | 257.45 | 265–680 | 0.57/4.39 | t.w. |
| 103–09–3 | 1358 | ethylhexyl acetate | 172.26 | 5.9074 | 3.5313 | 231.85 | 185–635 | 0.97/0.72 | t.w. |
| 112–14–1 | 1368 | *n*-octyl acetate | 172.26 | 5.9596 | 3.5603 | 236.43 | 235–650 | 0.25/0.91 | t.w. |
| 659–70–1 | 1361 | isopentyl isovalerate | 172.26 | 4.7649 | 3.8179 | 252.55 | 380–570 | 0.72/2.01 | t.w. |
| 5451–92–3 | 1309 | *n*-nonyl formate | 172.27 | 5.6297 | 3.6378 | 243.93 | 365–570 | 0.35/2.02 | t.w. |
| 123–25–1 | 2378 | diethyl succinate | 174.19 | 6.2233 | 3.3197 | 238.21 | 255–665 | 0.17/0.99 | t.w. |
| 136–60–7 | 1365 | butyl benzoate | 178.23 | 4.9127 | 3.7073 | 283.08 | 255–720 | 0.63/2.29 | t.w. |
| 103–11–7 | 1386 | 2-ethylhexyl acrylate | 184.28 | 5.7355 | 3.6697 | 242.08 | 380–580 | 0.29/2.20 | t.w. |
| 143–13–5 | 1369 | *n*-nonyl acetate | 186.29 | 6.8356 | 3.4950 | 227.63 | 250–660 | 0.34/1.21 | t.w. |
| 110–42–9 | 1395 | methyl decanoate | 186.29 | 6.0382 | 3.6480 | 244.17 | 345–590 | 0.41/0.60 | t.w. |
| 5451–52–5 | 1310 | *n*-decyl formate | 186.30 | 6.2919 | 3.5897 | 240.31 | 395–600 | 0.18/1.67 | t.w. |
| 131–11–3 | 2377 | dimethyl phthalate | 194.18 | 5.6798 | 3.4496 | 284.56 | 275–765 | 0.85/1.96 | t.w. |
| 1459–93–4 | 1377 | dimethyl isophthalate | 194.18 | 3.7729 | 3.9445 | 347.75 | 400–670 | 2.58/1.66 | t.w. |
| 120–61–6 | 1381 | dimethyl terephthalate | 194.18 | 4.4909 | 3.7491 | 320.95 | 435–660 | 0.43/2.64 | t.w. |
| 999–21–3 | 2381 | diallyl maleate | 196.20 | 7.3289 | 3.2317 | 235.29 | 230–693 | 0.27/0.62 | t.w. |

*Continues on next page*

| CAS-nr. | DIPPR nr. | Compound | $M_w$ [g/mol] | $m$ [–] | $\sigma$ [Å] | $\epsilon/k$ [K] | $T$ range [K] | AAD $(V_L/P^{sat})$ [%] | Ref. |
|---|---|---|---|---|---|---|---|---|---|
| 2432–63–5 | 2388 | dipropyl maleate | 200.23 | 7.2628 | 3.1371 | 235.22 | 250–691 | 0.45/1.68 | t.w. |
| 112–17–4 | 1370 | *n*-decyl acetate | 200.32 | 6.8956 | 3.5745 | 234.94 | 260–675 | 0.17/3.62 | t.w. |
| 120–51–4 | 1364 | benzyl benzoate | 212.24 | 5.7986 | 3.6609 | 299.33 | 295–820 | 2.14/0.77 | t.w. |
| 50623–57–9 | 1345 | *n*-butyl nonanoate | 214.34 | 7.8355 | 3.4778 | 215.50 | 340–580 | 0.88/0.72 | t.w. |
| 111–82–0 | 2385 | methyl dodecanoate | 214.34 | 6.1495 | 3.6422 | 260.31 | 370–630 | 1.41/0.93 | t.w. |
| 110–27–0 | 1396 | isopropyl myristate | 214.34 | 8.0669 | 3.8004 | 245.69 | 400–640 | 0.28/1.07 | t.w. |
| 84–66–2 | 2375 | diethyl phthalate | 222.24 | 6.8389 | 3.4744 | 262.72 | 270–755 | 1.25/0.36 | t.w. |
| 105–76–0 | 2382 | dibutyl maleate | 228.28 | 8.2638 | 3.3552 | 234.78 | 280–715 | 0.69/3.5 | t.w. |
| 131–16–8 | 1375 | dipropyl phthalate | 250.29 | 6.9781 | 3.6095 | 268.80 | 245–765 | 0.48/1.40 | t.w. |
| 84–74–2 | 2376 | dibutyl phthalate | 278.34 | 7.7283 | 3.6571 | 265.37 | 238–781 | 0.45/3.84 | t.w. |
| 112–62–9 | 1362 | methyl oleate | 296.49 | 9.6659 | 3.6507 | 240.45 | 295–760 | 0.69/7.98 | t.w. |
| 109–43–3 | 1384 | dibutyl sebacate | 314.46 | 10.2719 | 3.5908 | 237.05 | 265–765 | 1.70/8.77 | t.w. |
| 110–33–8 | 2379 | dihexyl adipate | 314.46 | 10.5322 | 3.5584 | 234.09 | 255–765 | 1.05/5.46 | t.w. |
| 123–95–5 | 1383 | *n*-butyl stearate | 340.58 | 9.7890 | 3.8554 | 238.32 | 425–685 | 0.49/1.12 | t.w. |
| 103–23–1 | 3379 | di(2-ethyl hexyl)adipate | 370.57 | 9.8744 | 3.9007 | 264.12 | 165–845 | 0.46/6.89 | t.w. |
| | | *ketones* | | | | | | | |
| 67–64–1 | 1051 | acetone | 58.08 | 2.77409 | 3.2557 | 253.406 | 250–480 | 1.95/0.99 | [8] |
| 57–57–8 | 1091 | *beta*-propiolactone | 72.06 | 2.9031 | 3.1538 | 336.84 | 240–680 | 2.04/0.45 | t.w. |
| 78–93–3 | 1052 | 2-butanone | 72.11 | 2.9093 | 3.4473 | 260.07 | 200–490 | 1.86/1.47 | [8] |
| 78–84–2 | 1006 | 2-methylpropanal | 72.11 | 3.5582 | 3.2003 | 222.71 | 210–505 | 0.83/0.49 | t.w. |
| 674–82–8 | 1099 | diketene | 84.07 | 3.8331 | 3.0270 | 258.60 | 270–612 | 0.42/2.32 | t.w. |
| 120–92–3 | 1079 | cyclopentanone | 84.12 | 2.8092 | 3.5344 | 307.24 | 225–630 | 1.25/0.32 | t.w. |
| 96–22–0 | 1053 | 3-pentanone | 86.13 | 3.35652 | 3.4778 | 252.726 | 280–530 | 1.39/1.28 | [8] |
| 108–10–1 | 1054 | methyl isobutyl ketone | 100.16 | 3.3628 | 3.6799 | 259.89 | 190–570 | 0.97/1.50 | t.w. |
| 108–24–7 | 1291 | acetic anhydride | 102.09 | 4.2175 | 3.1329 | 250.93 | 200–600 | 1.63/0.36 | t.w. |
| 100–52–7 | 1041 | benzaldehyde | 106.12 | 3.1474 | 3.5760 | 321.19 | 350–620 | 0.91/0.28 | t.w. |
| 105–60–2 | 1880 | caprolactam | 113.16 | 4.30008 | 3.3014 | 330.112 | 400–740 | 0.77/0.76 | [13] |
| 108–55–4 | 1296 | glutaric anhydride | 114.10 | 4.1265 | 3.1949 | 353.59 | 330–830 | 1.83/2.63 | t.w. |
| 110–43–0 | 1063 | 2-heptanone | 114.19 | 3.7965 | 3.6415 | 259.346 | 300–550 | 0.10/0.10 | [6] |
| 565–80–0 | 1069 | diisopropyl ketone | 114.19 | 3.70638 | 3.5532 | 251.843 | 250–540 | 1.36/0.48 | [8] |
| 925–54–2 | 1016 | 2-methylhexanal | 114.19 | 4.4290 | 3.4976 | 238.15 | 230–590 | 0.54/0.51 | t.w. |

*Continues on next page*

| CAS-nr. | DIPPR nr. | Compound | $M_w$ [g/mol] | $m$ [–] | $\sigma$ [Å] | $\epsilon/k$ [K] | $T$ range [K] | AAD $(V_L/P^{sat})$ [%] | Ref. |
|---|---|---|---|---|---|---|---|---|---|
| 104–87–0 | 1040 | *p*-tolualdehyde | 120.15 | 4.1695 | 3.4261 | 289.34 | 290–680 | 1.09/0.54 | t.w. |
| 123–05–7 | 1013 | 2-ethyl hexanal | 128.21 | 4.8693 | 3.5037 | 236.37 | 200–600 | 0.57/0.55 | t.w. |
| 123–62–6 | 1292 | propionic anhydride | 130.14 | 4.8138 | 3.3220 | 244.80 | 230–620 | 1.30/1.38 | t.w. |
| 623–27–8 | 1044 | terephthaldehyde | 134.13 | 5.1570 | 3.1091 | 286.91 | 390–735 | 1.80/0.63 | t.w. |
| 78–59–1 | 1077 | isophorone | 138.21 | 3.2635 | 4.0318 | 328.86 | 270–710 | 1.00/3.22 | t.w. |
| 108–83–8 | 1068 | diisobutyl ketone | 142.24 | 4.6179 | 3.7032 | 243.72 | 260–600 | 0.64/1.03 | [14] |
| 76–22–2 | 2850 | camphor | 152.23 | 3.7441 | 3.8866 | 301.73 | 460–705 | 0.37/4.62 | t.w. |
| 106–31–0 | 1293 | butyric anhydride | 158.19 | 5.2497 | 3.5274 | 246.88 | 200–640 | 1.36/0.83 | t.w. |
| | | *sulfides* | | | | | | | |
| 7783–06–4 | 1922 | hydrogen sulfide | 34.08 | 1.6941 | 3.0214 | 226.79 | 190–373 | 0.31/0.36 | t.w. |
| 463–58–1 | 1893 | carbon sulfide | 44.08 | 1.5799 | 3.4631 | 240.33 | 135–380 | 0.37/0.32 | t.w. |
| 75–18–3 | 1820 | dimethyl sulfide | 62.14 | 2.1985 | 3.4975 | 273.25 | 175–503 | 0.14/0.44 | t.w. |
| 75–15–0 | 1938 | carbon disulfide | 76.14 | 1.7072 | 3.6171 | 333.44 | 165–550 | 0.52/0.87 | t.w. |
| 624–89–5 | 1813 | methyl ethyl sulfide | 76.16 | 2.5289 | 3.6109 | 271.40 | 168–533 | 0.80/0.91 | t.w. |
| 352–93–2 | 1818 | diethyl sulfide | 90.19 | 2.9078 | 3.6599 | 266.25 | 170–555 | 0.42/0.33 | t.w. |
| 3877–15–4 | 1814 | methyl-*n*-propyl sulfide | 90.19 | 2.9283 | 3.6524 | 267.83 | 160–565 | 0.72/0.19 | t.w. |
| 624–92–0 | 1828 | dimethyl disulfide | 94.20 | 2.6430 | 3.5836 | 300.67 | 190–605 | 0.85/0.61 | t.w. |
| 628–29–5 | 2815 | methyl-*n*-butyl sulfide | 104.21 | 3.2429 | 3.7186 | 270.11 | 175–590 | 0.46/0.31 | t.w. |
| 6163–64–0 | 1815 | methyl-*t*-butyl sulfide | 104.21 | 2.8002 | 3.9090 | 273.18 | 190–570 | 0.14/0.71 | t.w. |
| 111–47–7 | 1817 | dipropyl sulfide | 118.24 | 3.5494 | 3.7766 | 267.42 | 170–608 | 0.45/0.38 | t.w. |
| 638–46–0 | 2816 | ethyl-*t*-butyl sulfide | 118.24 | 3.1483 | 3.9335 | 268.45 | 185–588 | 0.16/0.43 | t.w. |
| 1741–83–9 | 1816 | methyl-*t*-pentyl sulfide | 118.24 | 2.9650 | 4.0306 | 299.81 | 155–632 | 0.79/0.38 | t.w. |
| 110–81–6 | 1824 | diethyl disulfide | 122.25 | 3.1372 | 3.7905 | 297.77 | 175–640 | 0.70/0.49 | t.w. |
| 629–19–6 | 1829 | dipropyl disulfide | 150.31 | 3.9145 | 3.8224 | 285.78 | 188–675 | 0.75/0.48 | t.w. |
| | | *Si-compounds* | | | | | | | |
| 7803–62–5 | 1982 | silane | 32.12 | 1.2356 | 3.8939 | 191.99 | 89–265 | 2.32/1.14 | t.w. |
| 992–94–9 | 3984 | methyl silane | 46.14 | 1.9149 | 3.6541 | 198.36 | 120–350 | 0.49/0.60 | t.w. |
| 1111–74–6 | 3985 | dimethyl silane | 60.17 | 1.7821 | 4.0532 | 241.95 | 125–400 | 0.91/1.52 | t.w. |
| 1590–87–0 | 1980 | disilane | 62.22 | 1.4751 | 4.0212 | 284.00 | 145–430 | 0.72/0.66 | t.w. |
| 993–07–7 | 3986 | trimethyl silane | 74.20 | 2.2372 | 3.9955 | 230.66 | 140–430 | 0.73/0.44 | t.w. |

*Continues on next page*

| CAS-nr. | DIPPR nr. | Compound | $M_w$ [g/mol] | $m$ [–] | $\sigma$ [Å] | $\epsilon/k$ [K] | $T$ range [K] | AAD $(V_L/P^{sat})$ [%] | Ref. |
|---|---|---|---|---|---|---|---|---|---|
| 993–00–0 | 3935 | methyl chlorosilane | 80.60 | 2.0443 | 3.7866 | 251.97 | 140–440 | 0.88/0.66 | t.w. |
| 75–76–3 | 1984 | tetramethyl silane | 88.22 | 2.7440 | 3.9150 | 217.89 | 175–450 | 0.30/0.36 | t.w. |
| 1066–35–9 | 3987 | dimethyl chlorosilane | 94.62 | 2.5167 | 3.7771 | 240.78 | 165–470 | 0.11/1.29 | t.w. |
| 4109–96–0 | 1935 | dichloro silane | 101.01 | 2.0805 | 3.6551 | 251.49 | 155–455 | 1.31/1.63 | t.w. |
| 75–77–4 | 3988 | trimethyl chlorosilane | 108.64 | 2.9076 | 3.8116 | 235.77 | 220–495 | 1.23/0.27 | t.w. |
| 75–54–7 | 3936 | methyl dichlorosilane | 115.03 | 2.4390 | 3.7565 | 251.73 | 185–480 | 1.0/1.44 | t.w. |
| 75–78–5 | 3989 | dimethyl dichlorosilane | 129.06 | 3.0756 | 3.6923 | 238.85 | 200–520 | 0.57/0.32 | t.w. |
| 10025–78–2 | 1936 | trichloro silane | 135.45 | 2.4885 | 3.6894 | 241.65 | 145–475 | 0.43/0.67 | t.w. |
| 631–36–7 | 2994 | tetraethyl silane | 144.33 | 3.7427 | 4.0716 | 259.04 | 190–600 | 0.17/2.04 | t.w. |
| 75–79–6 | 3937 | methyl trichlorosilane | 149.48 | 2.6034 | 3.8815 | 259.26 | 200–515 | 0.7/1.83 | t.w. |
| 999–97–3 | 1964 | hexamethyl disilazane | 161.39 | 4.4767 | 3.9173 | 219.01 | 295–540 | 0.43/0.63 | t.w. |
| 107–46–0 | 1965 | hexamethyl disiloxane | 162.38 | 4.0530 | 4.0466 | 214.19 | 205–515 | 0.08/2.09 | t.w. |
| 10026–04–7 | 1937 | tetrachloro silane | 169.90 | 2.7298 | 3.7680 | 246.27 | 205–505 | 0.13/0.19 | t.w. |
| | | *S-compounds* | | | | | | | |
| 110–02–1 | 1821 | thiophene | 84.14 | 2.4013 | 3.5401 | 299.01 | 290–520 | 0.46/0.93 | t.w. |
| 110–01–0 | 1843 | tetrahydrothiophene | 88.17 | 2.3554 | 3.6959 | 333.18 | 320–568 | 0.94/0.72 | t.w. |
| 616–44–4 | 2845 | 3-methyl thiophene | 98.17 | 2.7257 | 3.6314 | 298.37 | 307–550 | 0.17/0.46 | t.w. |
| 554–14–3 | 2844 | 2-methyl thiophene | 98.17 | 2.7094 | 3.6520 | 296.78 | 305–648 | 0.78/0.73 | t.w. |
| 126–33–0 | 1845 | sulfolane | 120.17 | 3.3306 | 3.5058 | 393.88 | 430–767 | 1.87/0.43 | t.w. |
| 872–93–5 | 1847 | 3-methyl sulfolane | 134.2 | 3.9202 | 3.4896 | 348.53 | 410–730 | 1.35/0.55 | t.w. |
| 95–15–8 | 1822 | benzo thiophene | 134.2 | 2.9313 | 3.8360 | 363.28 | 380–678 | 2.35/0.57 | t.w. |
| 598–03–8 | 1848 | di-*n*-propyl sulfone | 150.24 | 5.3670 | 3.3672 | 288.28 | 385–685 | 0.82/0.48 | t.w. |
| 598–04–9 | 1849 | di-*n*-butyl sulfone | 178.29 | 6.3200 | 3.4062 | 273.93 | 385–690 | 0.35/0.69 | t.w. |
| 132–65–0 | 2823 | dibenzo thiophene | 184.26 | 3.7015 | 3.9596 | 386.77 | 450–807 | 0.39/0.87 | t.w. |
| 6012–97–1 | 4877 | tetrachloro thiophene | 221.92 | 4.1136 | 3.5422 | 308.43 | 380–677 | 0.35/1.08 | t.w. |
| | | *mercaptans/thiols* | | | | | | | |
| 75–33–2 | 1810 | isopropyl mercaptan | 76.16 | 2.4302 | 3.6762 | 264.82 | 260–465 | 0.31/1.05 | t.w. |
| 107–03–9 | 1803 | *n*-propyl mercaptan | 76.16 | 2.4564 | 3.6540 | 276.82 | 285–482 | 0.85/0.95 | t.w. |
| 109–79–5 | 1841 | *n*-butyl mercaptan | 90.19 | 2.7253 | 3.7499 | 281.41 | 285–513 | 0.56/1.04 | t.w. |
| 513–44–0 | 1805 | isobutyl mercaptan | 90.19 | 2.6846 | 3.7706 | 275.51 | 280–503 | 0.59/0.86 | t.w. |

*Continues on next page*

| CAS-nr. | DIPPR nr. | Compound | $M_w$ [g/mol] | $m$ [–] | $\sigma$ [Å] | $\epsilon/k$ [K] | $T$ range [K] | AAD $(V_L/P^{sat})$ [%] | Ref. |
|---|---|---|---|---|---|---|---|---|---|
| 110–66–7 | 1827 | *n*-pentyl mercaptan | 104.21 | 3.1788 | 3.7578 | 275.26 | 300–538 | 0.92/0.77 | t.w. |
| 108–98–5 | 1842 | phenyl mercaptan | 110.18 | 3.2933 | 3.5183 | 307.03 | 345–620 | 0.55/2.75 | t.w. |
| 1569–69–3 | 1811 | cyclohexyl mercaptan | 116.23 | 2.7597 | 3.9610 | 323.53 | 340–597 | 0.71/0.15 | t.w. |
| 111–31–9 | 1807 | *n*-hexyl mercaptan | 118.24 | 3.4471 | 3.8209 | 278.90 | 315–560 | 0.62/0.44 | t.w. |
| 100–53–8 | 1812 | benzyl mercaptan | 124.20 | 3.5557 | 3.6078 | 307.93 | 356–640 | 0.83/0.95 | t.w. |
| 1639–09–4 | 1839 | *n*-heptyl mercaptan | 132.27 | 3.8330 | 3.8372 | 276.75 | 330–580 | 0.68/0.91 | t.w. |
| 111–88–6 | 1809 | *n*-octyl mercaptan | 146.29 | 4.1432 | 3.8728 | 277.22 | 335–600 | 0.57/0.63 | t.w. |
| 1455–21–6 | 1808 | *n*-nonyl mercaptan | 160.32 | 4.6257 | 3.8494 | 272.37 | 340–610 | 0.64/0.87 | t.w. |
| 143–10–2 | 1826 | *n*-decyl mercaptan | 174.35 | 5.0016 | 3.8442 | 271.70 | 350–626 | 0.16/0.51 | t.w. |
| | | *gases* | | | | | | | |
| 1333–74–0 | 902 | hydrogen | 2.02 | 1.0000 | 2.986 | 19.2775 | 462–583 | — | [7] |
| 630–08–0 | 908 | carbon monoxide | 28.01 | 1.3097 | 3.2507 | 92.15 | 80–133 | 1.38/2.21 | [4] |
| 7727–37–9 | 905 | nitrogen | 28.01 | 1.2053 | 3.313 | 90.96 | 63–126 | 1.5/0.34 | [4] |
| 7782–44–7 | 901 | oxygen | 32.00 | 1.1217 | 3.2098 | 114.96 | 55–154 | 0.32/0.18 | t.w. |
| 7440–37–1 | 914 | argon | 39.95 | 0.9285 | 3.4784 | 122.23 | 84–151 | 0.68/0.32 | [4] |
| 124–38–9 | 909 | carbon dioxide | 44.01 | 2.0729 | 2.7852 | 169.21 | 216–304 | 2.73/2.78 | [4] |
| 7446–09–5 | 910 | sulfur dioxide | 64.07 | 2.8611 | 2.6826 | 205.35 | 198–431 | 1.33/1.82 | [4] |
| 7782–50–5 | 918 | chlorine | 70.91 | 1.5514 | 3.3672 | 265.67 | 172–417 | 0.57/0.99 | [4] |
| 75–15–0 | 1938 | carbon disulfide | 76.14 | 1.7173 | 3.6107 | 332.23 | 150–550 | 0.47/0.87 | t.w. |
| 75–15–0 | 1938 | carbon disulfide | 76.14 | 1.6919 | 3.6172 | 334.82 | 200–552 | 0.77/2.26 | [4] |
| 7439–90–9 | 920 | krypton | 83.80 | 0.9610 | 3.6634 | 167.26 | 110–185 | 0.52/0.40 | t.w. |
| 7440–63–3 | 959 | xenon | 131.29 | 0.9025 | 4.0892 | 239.69 | 148–260 | 0.97/0.56 | t.w. |

## 4.3 Heavy Alkanes

Accurate experimental results of the thermodynamic properties, e.g. vapour pressures and liquid densities, of light/medium $M_w$ alkanes are available. Properties of heavier alkanes are more irregular and less reliable due to their thermal instability at temperatures above 650 K making experimental investigations difficult [15]. For this reason, in order to obtain a complete picture of the thermodynamic properties of not only alkanes, but other families of compounds, various theoretical approaches have been developed for extrapolating the existing experimental data. As mentioned earlier, the suggested solution to this problem is to develop a group contribution scheme for estimating the model parameters from low $M_w$ compounds for which data is available and then extrapolate to complex molecules.

The scope of the original work of von Solms *et al.* [16] on $n$-alkanes up to $n$-eicosane is here extended to $n$-hexatriacontane. Correlations of the PC-SAFT parameters are first obtained to enable extrapolation to longer members of the homologous series. The parameters for all $n$-alkanes (excluding methane exhibiting anomalous behaviour) up to hexatriacontane are shown graphically as a function of $M_w$ in Figure 4.1.

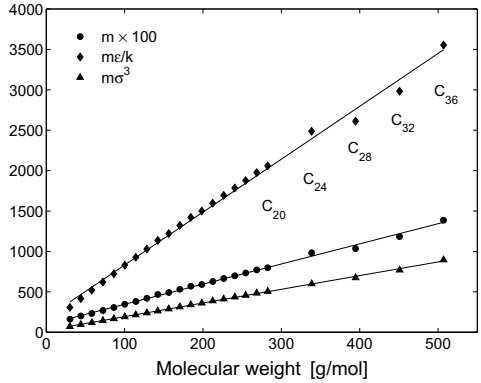


Figure 4.1: Parameters $m$, $m\sigma^3$, and $m\epsilon/k$ vs. $M_w$ for $n$-alkanes up to $C_{36}$. Symbols are PC-SAFT parameters obtained from various studies and the lines are linear fits described by Equations (4.1)–(4.3).

The three parameters are all shown to vary linearly with $M_w$ of the $n$-alkane molecules:

$$m = 0.0249M_w + 0.9711 \tag{4.1}$$

$$m\epsilon/k = 6.5446M_w + 177.92 \tag{4.2}$$

$$m\sigma^3 = 1.6947M_w + 23.27 \tag{4.3}$$

Units of $\sigma$ and $\epsilon/k$ are in Å and K, respectively. Equations (4.1)–(4.3) provide a standard way to obtain parameters for SAFT-type models for higher members of $n$-alkane series for which no experimental data exist. Similar expressions were obtained for $n$-alkanes by Gross and Sadowski [4], though only selected $n$-alkanes from ethane to $n$-eicosane were studied. It is noticed that this trend of linearity has also been observed for other SAFT-family models, for example SAFT-VR [17].

Several investigations have previously been reported on the estimation of pure component PC-SAFT parameters for heavy alkanes. The parameters estimated by these different investigations are summarized in Table 4.2.

Table 4.2: Pure component PC-SAFT parameters for heavy $n$-alkanes estimated with various methods.

| Compound | $m$ [–] | $\sigma$ [Å] | $\epsilon/k$ [K] | $T$ range [K] | AAD $P^{sat}/V_L$ [a] [%] | Ref. |
|---|---|---|---|---|---|---|
| Eicosane | 7.9850 | 3.9870 | 257.75 | 318–768 | 5.6/1.6 | [18] |
| $C_{20}H_{42}$ | 7.9849 | 3.9869 | 257.75 | 309–775 | 7.7/1.1 | [4] |
| | 8.4092 | 3.9120 | 251.92 | 400–690 | 2.3/0.2 | [b] |
| | 8.0765 | 3.9764 | 257.78 | 309–775 | 8.9/0.7 | [16] |
| | 8.0316 | 3.9688 | 252.39 | — | 7.4/0.6 | [5] |
| Docosane | 8.9601 | 3.9511 | 254.31 | 400–700 | 2.6/0.9 | [b] |
| $C_{22}H_{46}$ | 8.7880 | 3.9856 | 258.9924 | 400–700 | 15.9/1.0 | [16] |
| | 8.7067 | 3.9820 | 225.390 | 400–700 | 10.4/0.7 | [c] |
| Tetracosane | 9.8820 | 3.8890 | 252.8 | 450–600 | 1.0/1.5 | [18] |
| $C_{24}H_{50}$ | 9.8220 | 3.9370 | 253.18 | — | 0.7/0.5 | [5] |
| | 9.6836 | 3.9709 | 254.69 | 450–720 | 0.8/0.4 | [b] |
| | 9.4997 | 3.9934 | 260.018 | 450–720 | 18.4/2.0 | [16] |
| | 9.4034 | 3.9896 | 254.61 | 450–720 | 20.7/1.1 | [c] |
| Octacosane | 11.0830 | 3.9789 | 255.62 | 460–720 | 1.9/0.2 | [b] |
| $C_{28}H_{58}$ | 10.9230 | 4.0059 | 261.6 | 460–710 | 27.6/1.4 | [16] |
| | 10.8004 | 4.0019 | 255.67 | 460–710 | 20.4/0.9 | [c] |
| | 10.3620 | 4.0217 | 252.0 | — | 23.3/1.7 | [19] |
| Hexatriacontane | 13.4880 | 4.015 | 259.35 | 500–600 | 2.5/0.8 | [18] |
| $C_{36}H_{74}$ | 14.3320 | 3.8836 | 252.89 | 510–720 | 10.8/4.9 | [b] |
| | 13.7699 | 4.0229 | 263.946 | 510–770 | 35.7/2.1 | [16] |
| | 13.5946 | 4.0189 | 257.15 | 510–770 | 6.0/1.3 | [c] |
| | 13.8600 | 4.014 | 256.37 | — | 14.7/2.1 | [5] |

[a] AAD [%] $P^{sat} = 100 \times \sum_{data} \left(\left|P^{sat}_{exp} - P^{sat}_{calc}\right|\right) / P^{sat}_{exp}$ and similar for AAD [%] $V_L$.
[b] Estimated in present work by direct fitting of vapour-pressure and saturated liquid-density data using DIPPR [3].
[c] Estimated in present work using Equations (4.1)–(4.3).

It is not unusual for SAFT-type models that more than one set of parameters may provide equally accurate correlation of experimental data [8]. Due to the existence of different sets of parameters proposed for heavy alkanes, an investigation is made in order to select the best set of parameters. Thus, vapour pressure predictions with sPC-SAFT

for a few heavy alkanes are performed for which reliable experimental vapour pressure data are available [20]. Table 4.3 shows the result of the comparison.

Table 4.3: Comparison of calculated vapour pressure of heavy $n$-alkanes using different PC-SAFT parameter sets with the experimental data from Morgan and Kobayashi [20].

| Alkane | $M_w$ [g/mol] | $T$ range [K] | AAD $P$ [%] | Ref. |
|---|---|---|---|---|
| Eicosane $C_{20}H_{42}$ | 282.55 | 433–583 | 2.5 | [18] |
| | | | 1.3 | [3] |
| | | | 3.2 | [a] |
| | | | 11.1 | [16] |
| | | | 22.3 | [b] |
| Docosane $C_{22}H_{46}$ | 310.60 | 453–573 | 2.3 | [3] |
| | | | 1.5 | [a] |
| | | | 16.2 | [16] |
| | | | 42.7 | [b] |
| Tetracosane $C_{24}H_{50}$ | 338.65 | 453–588 | 1.7 | [18] |
| | | | 1.0 | [3] |
| | | | 2.2 | [a] |
| | | | 21.0 | [16] |
| | | | 29.6 | [b] |
| Octacosane $C_{28}H_{58}$ | 394.76 | 483–588 | 2.0 | [3] |
| | | | 3.0 | [a] |
| | | | 32.7 | [16] |
| | | | 24.3 | [b] |

[a] Estimated in present work by direct fitting of vapour-pressure and saturated liquid-density data using DIPPR [3].
[b] Estimated in present work using Equations (4.1)–(4.3).

The differences in the reported AAD values among various parameter sets may indicate use of different sources of experimental data for their estimation. At the same time, the results show that the sensitivity of pure alkanes' saturation pressure to the parameters of PC-SAFT is rather high. Results are generally good when the parameters have been obtained from direct fitting to experimental data, while they are less satisfactory when these have been obtained from various extrapolation methods, i.e. correlations similar to Equations (4.1)–(4.3). Nevertheless, it is of interest to test the validity of PC-SAFT parameters obtained by the extrapolation, as in many other cases, these parameters could not be obtained from direct fitting to experimental data. The implications of this sensitivity is further evaluated in the following Section 4.3.1 through a comparison between sPC-SAFT predictions obtained with the parameters from the linear correlation, Equations (4.1)–(4.3), and the parameters obtained from direct fitting of vapour-pressure and saturated liquid density data.

### 4.3.1 Sensitivity Analysis

This section presents results on how the PC-SAFT parameter sets from Table 4.2 affect the modelling of the phase behaviour of heavy alkanes. More specifically, the ability of sPC-SAFT to predict the phase behaviour of asymmetric systems, such as the light alkanes–heavy alkanes and gases–heavy alkanes mixtures is investigated.

#### 4.3.1.1 VLE with Light Alkanes

The performance of sPC-SAFT is tested when modelling systems containing propane with a series of alkanes and hexane with two heavy alkanes, tetratriacontane and hexacontane. Binary VLE correlations for *n*-propane systems are presented in Table 4.4, where the overall average deviation is 1.5 %.

Table 4.4: VLE predictions of propane–*n*-alkane binary systems.

| *n*-Alkane | $x$ (*n*-Alkane) | $T$ range [K] | AAD $P$ [%] | Ref. |
|---|---|---|---|---|
| Eicosane | 0.2448 | 293–350 | 2.7 | [21] |
| | 0.3445 | 304–357 | 2.4 | |
| Tetratriacontane | 0.0112 | 320–366 | 0.1 | [22] |
| | 0.3969 | 336–427 | 1.2 | |
| Hexacontane | 0.2405 | 365–419 | 1.7 | [23] |
| | 0.3902 | 368–413 | 1.0 | |

Table 4.5 shows the AAD % between sPC-SAFT predictions using different pure component parameters and the experimental data reported by Joyce *et al.* [24]. The results show that sPC-SAFT reproduces the experimental data equally well when using different parameter sets for heavy alkanes. The deviations are slightly higher when using the parameters fitted directly to experimental data; especially at high temperatures and higher asymmetries. Therefore, it has been decided to use the parameters based on Equations (4.1)–(4.3) for further modelling of mixtures with heavy alkanes, since focus is less on the quality of the fit of pure components but more on the parameter behaviour and trends when used by sPC-SAFT for mixture phase behaviour.

Table 4.6 shows the optimised binary interaction parameters and the AAD % between experimental and calculated vapour pressure for mixtures with short alkanes and heavy alkanes. The overall AAD % for vapour pressure is 3.8 % when using a temperature-independent interaction parameter, which emphasizes the success of sPC-SAFT to reproduce the experimental data. Furthermore, the optimised $k_{ij}$ values slightly decrease with increasing system asymmetry and they are closer to zero than $k_{ij}$'s reported by other authors [18]. The excellent agreement obtained in many of the cases between the experimental data and the sPC-SAFT predictions is encouraging. The same sets of parameters are used in the subsequent calculations.

Table 4.5: PC-SAFT parameters' sensitivity analysis for asymmetric systems. $C_X$ represents a $n$-alkane with $X$ number of carbon atoms.

| Sources of parameters | $C_6$–$C_{24}$ | | $C_6$–$C_{36}$ | |
|---|---|---|---|---|
| | AAD $P$ [%] (473.7 K) | AAD $P$ [%] (524.1 K) | AAD $P$ [%] (521.7 K) | AAD $P$ [%] (573.1 K) |
| [18] | 1.1 | 6.3 | 2.0 | 3.0 |
| [5] | 1.5 | 5.1 | 1.8 | 3.0 |
| [16] | 1.1 | 6.1 | 4.2 | 6.2 |
| t.w., direct fitting[a] | 1.7 | 5.0 | 3.5 | 4.4 |
| t.w., interpolation[b] | 1.7 | 4.7 | 1.9 | 2.7 |

[a] Estimated in present work by direct fitting of vapour-pressure and saturated liquid-density data using DIPPR [3].
[b] Estimated in present work using Equations (4.1)–(4.3).

Table 4.6: VLE results for different light alkane–heavy alkanes binary systems. $C_X$ represents a $n$-alkane with $X$ number of carbon atoms.

| System | $T$ [K] | $k_{ij}$ [–] | AAD $P$ [%] | Ref. |
|---|---|---|---|---|
| $C_1$–$C_{16}$ | 623.15 | 0.130 | 4.0 | [25] |
| $C_1$–$C_{20}$ | 323.15 | 0.025 | 4.9 | [26] |
| | 353.15 | | 5.0 | |
| $C_1$–$C_{30}$ | 374.15 | 0.035 | 4.2 | [2] |
| $C_2$–$C_{10}$ | 377.16 | 0.000 | 4.9 | [27] |
| $C_6$–$C_{16}$ | 472.3 | 0.000 | 1.1 | [28] |
| | 524.4 | | 0.8 | |
| | 572.3 | | 2.1 | |
| | 623.0 | | 2.2 | |
| $C_6$–$C_{24}$ | 473.0 | 0.000 | 1.7 | [24] |
| | 524.4 | | 4.7 | |
| | 573.0 | | 8.4 | |
| | 622.9 | | 8.7 | |
| $C_6$–$C_{36}$ | 521.7 | 0.000 | 1.9 | [24] |
| | 573.1 | | 2.7 | |
| AAD [%] overall | | | 3.8 | |

#### 4.3.1.2 VLE with Light Gases

It has been shown earlier [4] that mixtures with carbon dioxide, which is a strong quadrupolar compound, could be well described with PC-SAFT, even when the specific quadrupolar interactions are not explicitly taken into account. Mixture data of carbon dioxide with two heavy alkanes, octacosane and hexatriacontane, are used for further testing of the reliability of pure component parameters for heavy alkanes and are presented in Figure 4.2.

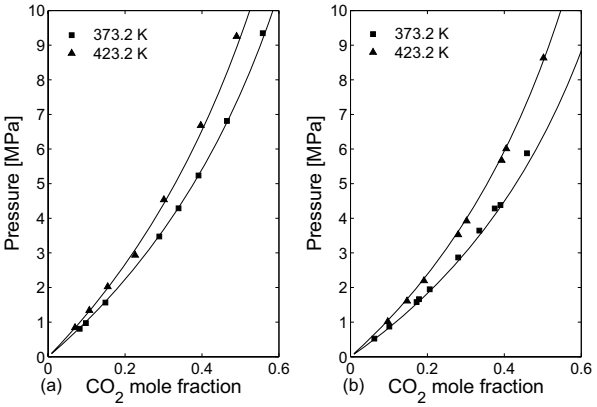


Figure 4.2: VLE of (a) $CO_2$–octacosane and (b) $CO_2$–hexatriacontane mixtures. Symbols are experimental data [29] and lines are sPC-SAFT correlations with $k_{ij} = 0.055$ and 0.04, respectively.

A further illustration of the predictive capability of the heavy alkanes' parameters is shown in Table 4.7 that contains results for other light gases–heavy alkane systems. The light gases include hydrogen, hydrogen sulphide, carbon monoxide, nitrogen, methane, ethane, and ethylene.

Table 4.7: VLE results of light gases–heavy alkanes binary systems with sPC-SAFT.

| Heavy alkane | Light gas | $T$ [K] | $k_{ij}$ | AAD $P$ [%] | Ref. |
|---|---|---|---|---|---|
| Eicosane | $H_2$ | 323.2 | | 0.9 | [30] |
| | | 373.2 | –0.43 | 0.9 | |
| | | 423.2 | | 2.9 | |
| | $H_2S$ | 322.9 | 0.035 | 2.8 | [31] |
| | | 361.3 | 0.02 | 5.9 | |
| | | 423.2 | 0.015 | 4.8 | |
| | $N_2$ | 323.3 | | 0.8 | [32] |
| | | 373.2 | 0.095 | 1.9 | |
| | | 423.2 | | 1.6 | |
| | CO | 323.3 | 0.01 | 1.2 | [33] |
| | | 373.2 | 0.04 | 1.4 | |
| | | 423.2 | 0.095 | 1.0 | |
| | $CO_2$ | 323.2 | 0.00 | 1.5 | [29] |
| | | 373.2 | 0.055 | 2.2 | |
| | $CH_4$ | 323.3 | 0.02 | 2.1 | [34] |
| | | 373.2 | 0.03 | 1.7 | |
| | | 423.2 | 0.035 | 0.5 | |

*Continues on next page*

| Heavy alkane | Light gas | $T$ [K] | $k_{ij}$ | AAD $P$ [%] | Ref. |
|---|---|---|---|---|---|
| Eicosane | $C_2H_4$ | 373.3 | | 2.2 | [35] |
| | | 473.2 | 0.00 | 2.2 | |
| | | 573.2 | | 3.8 | |
| | $C_2H_6$ | 373.3 | | 3.2 | [36] |
| | | 473.2 | 0.00 | 4.2 | |
| | | 573.2 | | 1.7 | |
| Octacosane | $H_2$ | 323.2 | | 2.9 | [30] |
| | | 373.2 | –0.45 | 0.8 | |
| | | 423.2 | | 0.7 | |
| | $N_2$ | 348.3 | | 0.6 | [32] |
| | | 373.2 | 0.095 | 0.9 | |
| | | 423.2 | | 1.5 | |
| | CO | 348.3 | 0.01 | 3.6 | [33] |
| | | 373.2 | 0.035 | 1.4 | |
| | | 423.2 | 0.075 | 1.0 | |
| | $CO_2$ | 348.2 | | 5.1 | [29] |
| | | 373.2 | 0.055 | 1.0 | |
| | | 423.2 | | 2.8 | |
| | $CH_4$ | 348.3 | | 3.1 | [34] |
| | | 373.2 | 0.025 | 1.5 | |
| | | 423.2 | | 2.5 | |
| | $C_2H_4$ | 373.3 | | 1.6 | [35] |
| | | 473.2 | 0.005 | 4.0 | |
| | | 573.2 | | 2.7 | |
| | $C_2H_6$ | 348.2 | | 5.8 | [36] |
| | | 373.2 | 0.00 | 2.2 | |
| | | 423.2 | | 0.7 | |
| Hexatriacontane | $H_2$ | 373.3 | –0.45 | 1.5 | [30] |
| | | 423.2 | | 2.5 | |
| | $N_2$ | 373.3 | 0.095 | 0.9 | [32] |
| | | 423.2 | | 1.0 | |
| | CO | 373.3 | 0.01 | 1.5 | [33] |
| | | 423.2 | 0.065 | 0.5 | |
| | $CO_2$ | 373.2 | 0.04 | 4.1 | [29] |
| | | 423.2 | | 3.0 | |
| | $CH_4$ | 373.3 | 0.025 | 1.9 | [34] |
| | | 423.2 | 0.030 | 1.7 | |
| | $C_2H_4$ | 373.3 | | 1.9 | [35] |
| | | 473.2 | 0.00 | 1.1 | |
| | | 573.2 | | 1.1 | |
| | $C_2H_6$ | 373.2 | 0.00 | 2.4 | [36] |
| | | 423.2 | | 2.9 | |
| AAD [%] overall | | | | 2.1 | |

The following points summarize observations from Table 4.7:

- The behaviour of nitrogen–alkanes and ethane– and ethylene–alkanes are interesting as the same values of $k_{ij}$ can be used at higher asymmetries and/or temperatures. A temperature-independent $k_{ij} = 0.095$ accurately predicts nitrogen solubility with

increasing carbon number of the alkane solvent, and $k_{ij} = 0$ (pure prediction) for ethane and ethylene mixtures.

- For CO–alkanes, $k_{ij}$ values slightly increase with increasing temperature.
- A comment should be made for the rather peculiar behaviour of hydrogen–alkanes. A very high negative $k_{ij}$ value is needed to correlate hydrogen containing mixtures. This could be attributed to hydrogen's special features compared to other gases. At the same time, the vapour-liquid coexistence for pure hydrogen occurs at very low temperatures (4–15 K). The PC-SAFT parameters for hydrogen are fitted to these data, and such parameters may not be equally successful at higher temperatures. The hydrogen parameters used in these calculations are $m = 1$, $\sigma = 2.986$ Å, and $\epsilon/k = 19.2775$ K, taken from Ghosh *et al.* [7]. Considering the extremely low solubility of hydrogen at the tested conditions (close to $10^{-4}$ mole fraction), the obtained results are quite good. Similar results have been obtained applying another version of SAFT to mixtures of hydrogen with heavy *n*-alkanes [7, 37].
- The overall AAD % for vapour pressure is only 2.0 %, which shows the success of sPC-SAFT to represent the experimental data for light gas–heavy alkanes.
- From those results, it is clear that the weak light gases–alkane interactions together with the very different properties of the involved molecules require use of compound-dependent binary interaction parameter to obtain accurate correlations.

Hydrogen sulphide is found in substantial amounts in many natural gases and crude oils. It is an undesirable compound that makes the gas sour. Hydrogen sulphide, being highly toxic and corrosive, affects the economical proportions of the hydrocarbons in the reservoir. Therefore, it should be eliminated or removed. The procedures for gas sweetening require accurate knowledge of mixture phase behaviour [38], which is affected by the hydrogen-bonding ability of hydrogen sulphide. Thus, VLE of hydrogen sulphide–alkanes is of interest.

PC-SAFT parameters for pure hydrogen sulphide are not taken from the literature, where normally hydrogen sulphide is assumed to be a self-associating compound [39], but instead estimated in this work as a non-associating compound. The predictive capabilities of sPC-SAFT to predict VLE of these systems are considered as well as the ability to obtain successful correlations. The obtained results presented in Table 4.8 are satisfactory. They include hydrogen sulphide–pentadecane and hydrogen sulphide–eicosane, which are highly asymmetric systems.

Figure 4.3 compares experimental [42] and sPC-SAFT VLE of the propane–hydrogen sulphide binary system at different temperatures. sPC-SAFT correlates well the complex azeotropic behaviour of this mixture with a single binary interaction parameter ($k_{ij} = 0.055$) over a wide temperature range. The model can accurately calculate the location

Table 4.8: VLE predictions and correlations of binary $H_2S$ systems with sPC-SAFT.

| System | $T$ | $N_{DP}$ | $k_{ij}=0$ | | $k_{ij}$ | AAD | AAD | Ref. |
|---|---|---|---|---|---|---|---|---|
| | | | AAD $P$ | AAD $y$ | | $P$ | $y$ | |
| | [K] | | [%] | [–] | | [%] | [–] | |
| $H_2S$–eicosane | 323 | 8 | 10.3 | 0.004 | 0.035 | 2.8 | 0.001 | [31] |
| $H_2S$–butane | 366 | 13 | 11.8 | 0.027 | 0.045 | 3.5 | 0.053 | [40] |
| $H_2S$–isobutane | 363 | 12 | 6.1 | 0.087 | 0.026 | 3.7 | 0.059 | [40] |
| $H_2S$–hexane | 323 | 8 | 20.1 | 0.015 | 0.048 | 2.6 | 0.002 | [41] |
| $H_2S$–cyclohexane | 323 | 7 | 32.1 | 0.011 | 0.061 | 2.2 | 0.006 | [41] |
| $H_2S$–benzene | 323 | 8 | 4.3 | 0.002 | 0.010 | 0.7 | 0.003 | [41] |
| $H_2S$–pentadecane | 422 | 8 | 9.6 | 0.004 | 0.030 | 2.8 | 0.001 | [41] |
| AAD [%] overall | | | 13.5 | | | 2.6 | | |

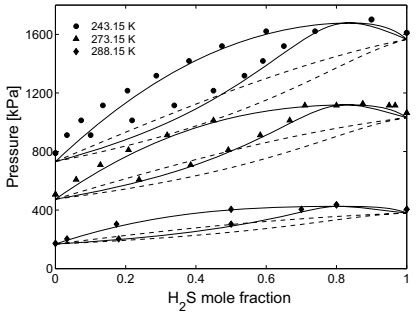


Figure 4.3: Isothermal VLE of propane–$H_2S$. Symbols represent experimental data [42], where the dotted lines are predictions ($k_{ij}=0.0$) and the solid lines are correlations ($k_{ij}=0.055$) with sPC-SAFT.

of the azeotrope at the different temperatures studied even when hydrogen sulphide is modelled as a non-associating compound. For $n$-alkanes larger than propane, sPC-SAFT does not predict an azeotrope which is in agreement with available experimental data [31, 40, 41].

Mixtures such as $n$-alkanes with carbon dioxide, nitrogen, or hydrogen sulphide considered in this work are rather difficult tests for the predictive capability of the sPC-SAFT model because of the complex intermolecular effects rising from the quadrupolar character of the molecules, the existance of hydrogen bonding, as well as size and shape effects. To summarize, sPC-SAFT can rather accurately predict VLE for most of the asymmetric systems studied. This acts in favour of the reliability of PC-SAFT parameters for heavy alkanes estimated from Equations (4.1)–(4.3). It is evident that the fitted interaction parameters are relatively small and approach a constant value as the chains of the alkanes

are increased. Whether this holds to higher carbon numbers can only be answered once the experimental data for longer chain alkanes systems have been studied.

### 4.3.2 Evaluation of $\gamma^{\infty}$

The aim of this section is to evaluate the ability of sPC-SAFT to describe the activity of a long-chain molecule using the newly estimated parameters for heavy alkanes. As experimental polymer activities are not available, the mole fraction activity coefficient at infinite dilution ($\gamma_2^{\infty}$) can provide a way to test the model in the "polymer" end, which is of importance when performing e.g. LLE calculations in polymer mixtures where the activities of all the components in the mixture are involved. Moreover, $\gamma^{\infty}$ is important for:

- Characterizing the behaviour of liquid mixtures.
- Fitting $G^E$-model parameters (e.g. Margules, van Laar, Wilson, NRTL, and UNIQUAC).
- Predicting the existence of an azeotrope.
- Estimation of mutual solubilities.
- Providing incisive information for the statistical thermodynamics.
- Analytical chromatographers.
- Screening solvents for extraction and extractive distillation processes.
- Calculation of limiting separation factors necessary for the reliable design of distillation processes.
- Calculation of Henry constants and partition coefficients.
- Development of predictive methods, as was the case with UNIFAC.

Calculations of $\gamma_2^{\infty}$ have been performed with the sPC-SAFT model for mixtures of heavy hydrocarbons ($C_{12}$–$C_{36}$). Calculations using newly estimated and previously obtained parameters are compared with those results obtained when using the original PC-SAFT EoS. Additionally, calculation of $\gamma_1^{\infty}$ of light alkanes ($C_4$–$C_{10}$) in heavy ones ($C_{30}$ and $C_{36}$) are also performed. The extended database of experimental $\gamma_2^{\infty}$ available in the literature is used in this study [43, 44]. The extensive literature data [43, 45] for $\gamma_1^{\infty}$, obtained from gas-liquid chromatography measurements, are used as well.

Table 4.9 summarizes the results, while the results of the individual systems are presented in Figures 4.4–4.8 where only new parameters are used. Notice that all calculations

Table 4.9: AAD % between experimental data and predicted ($k_{ij} = 0$) $\gamma_i^\infty$ with two versions of PC-SAFT [4, 16] using newly estimated pure compound parameters and old parameters. $C_X$ indicates an alkane with $X$ carbon atoms.

| AAD [%] | Fig. | sPC-SAFT new | original PC-SAFT new | sPC-SAFT old | original PC-SAFT old |
|---|---|---|---|---|---|
| $C_{12}$–$C_{36}$ in hexane | 4.4 | 10 | 11 | 16 | 8 |
| $C_{16}$–$C_{32}$ in cyclohexane | 4.5 | 30 | 16 | 30 | 15 |
| $C_{18}$–$C_{36}$ in heptane | 4.6 | 8 | 11 | 15 | 6 |
| $C_4$–$C_{10}$ in $C_{30}$ | 4.7 | 2 | 5 | 5 | 3 |
| $C_4$–$C_{10}$ in $C_{36}$ | 4.8 | 3 | 5 | 6 | 2 |

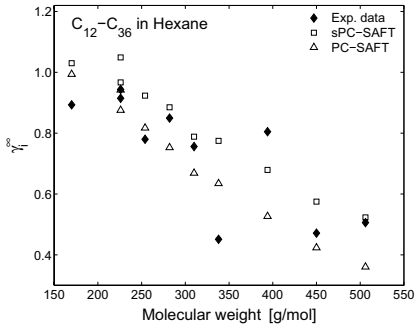


Figure 4.4: Experimental and predicted $\gamma_2^\infty$ for heavy $n$-alkanes in $n$-hexane as a function of the $M_w$ of the heavy alkanes.

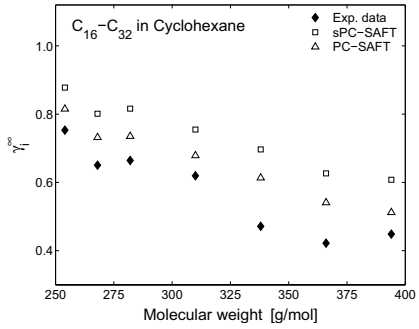


Figure 4.5: Experimental and predicted $\gamma_2^\infty$ for heavy $n$-alkanes in cyclohexane as a function of $M_w$ of the heavy alkanes.

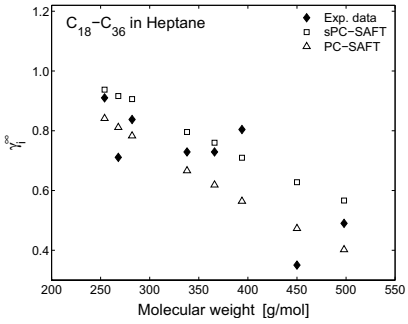


Figure 4.6: Experimental and predicted $\gamma_2^\infty$ for heavy $n$-alkanes in $n$-heptane as a function of the $M_w$ of the heavy alkanes.

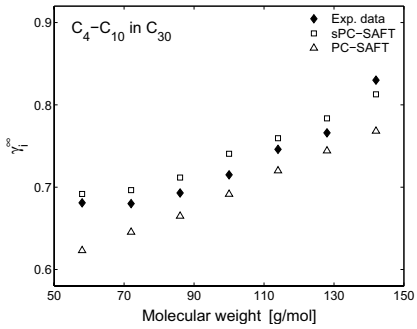


Figure 4.7: Experimental and predicted $\gamma_1^\infty$ for light alkanes in $n$-$C_{30}$ as a function of the $M_w$ of the light alkane.

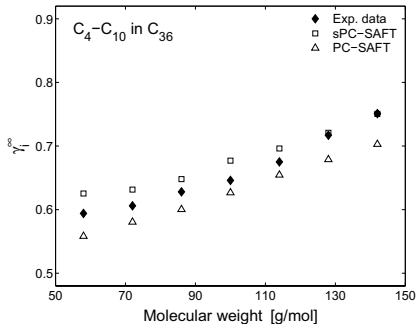


Figure 4.8: Experimental and predicted $\gamma_1^\infty$ for light alkanes in $n$-$C_{36}$ as a function of the $M_w$ of the light alkane.

have been performed with $k_{ij} = 0$. "Old parameters" refer to those taken from von Solms *et al.* [16], while "new parameters" are calculated from Equations (4.1)–(4.3).

From Table 4.9 and Figures 4.4–4.8 it is observed that it is difficult to represent experimental data for these asymmetric systems with the same accuracy. The sPC-SAFT model predicts $\gamma_2^\infty$ values that are close to the experimental values, with the exceptions of the cases where very low values of $\gamma_2^\infty$ have been measured, like $C_{24}$ in hexane, $C_{16}$ and $C_{30}$ in cyclohexane, and $C_{32}$ in heptane. There is also a tendency that the model overestimates the experimental data.

The deviation of sPC-SAFT from original PC-SAFT is more obvious when $M_w$ of the heavy $n$-alkanes increases; in other words, when the size-difference between the two components is greater. Table 4.9 shows that the best performance in the majority of the studied systems is by sPC-SAFT when using newly estimated parameters for heavy $n$-alkanes. It is noted that the experimental points that deviate from the general trend of the rest are excluded when calculating AAD %.

This investigation provides a preliminary study of the activity coefficient values that will later be encountered in relation to polymer–solvent LLE calculations. Furthermore, a detailed evaluation of sPC-SAFT to predict activity coefficient values to numerous asymmetric systems will be addressed in Chapter 7, as well as in polymer mixtures when using the pure compound parameters calculated from the GC scheme.

## 4.4 Correlations of Parameters for Other Families

In order to continue the extent of the parameter database, it has been investigated whether other compounds belonging to the same chemical family can be analysed in the same way as $n$-alkanes. The results are presented graphically in Figures 4.9–4.11 and the linear

equations of estimated PC-SAFT parameters of all the tested families of compounds are summarized in Table 4.10.

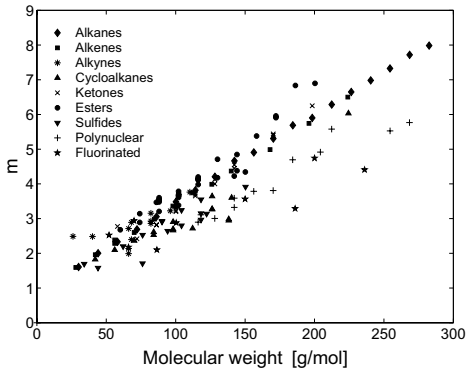


Figure 4.9: The segment number $m$ vs. $M_w$ for different families of compounds.

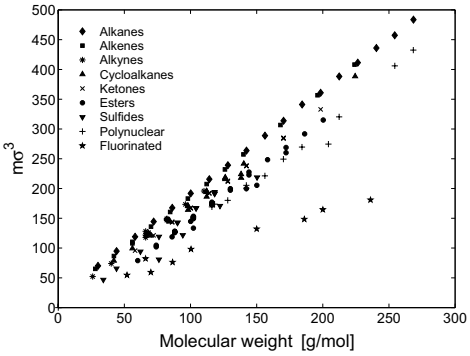


Figure 4.10: The segment number $m\sigma^3$ vs. $M_w$ for different families of compounds.

Although there is some scatter, it can be concluded that linear relationships of sPC-SAFT parameters can be employed for many classes of compounds. Fluorinated compounds exhibit significantly different slopes, which may be related to the substitution of hydrogen with fluorine on the carbon backbone. The success of this extrapolation further underlines the sound physical basis of the EoS.

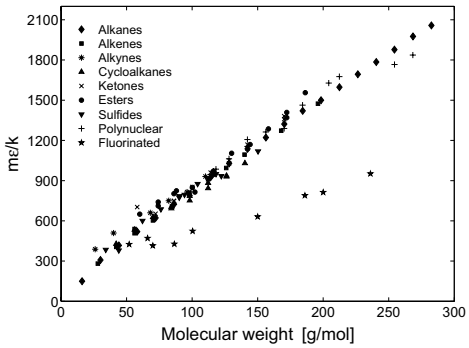


Figure 4.11: The segment number $m\epsilon/k$, vs. $M_w$ for different families of compounds.

Table 4.10: Linear correlations for PC-SAFT parameters for different families of compounds.

| Family of compounds | $N_{DP}$ | $m$ | $m\sigma^3$ | $m\epsilon/k$ |
|---|---|---|---|---|
| Alkanes | 23 | $0.0249M_w$+0.9711 | $1.6947M_w$+23.27 | $6.5446M_w$+177.92 |
| Alkenes | 13 | $0.0247M_w$+0.9173 | $1.7575M_w$+11.983 | $6.9348M_w$+119.25 |
| Alkynes | 8 | $0.0170M_w$+1.7585 | $1.7223M_w$+6.5264 | $6.1464M_w$+242.59 |
| Cycloalkanes | 10 | $0.0223M_w$+0.6646 | $1.7092M_w$+2.1664 | $6.4676M_w$+147.52 |
| Ketones | 9 | $0.0282M_w$+0.6646 | $1.6774M_w$–0.8076 | $6.9060M_w$+176.09 |
| Esters | 13 | $0.0309M_w$+0.6355 | $1.6799M_w$–21.492 | $7.1101M_w$+167.66 |
| Sulfides | 10 | $0.0204M_w$+0.9247 | $1.4849M_w$+1.4107 | $6.5816M_w$+162.94 |
| Fluorinated | 9 | $0.0121M_w$+1.634 | $0.6888M_w$+22.895 | $2.9412M_w$+230.1 |
| Polynuclear aromatic | 11 | $0.0203M_w$+0.607 | $1.7024M_w$–39.059 | $5.8932M_w$+325.34 |

### 4.4.1 Various Binary Mixtures

Phase equilibrium calculations are performed for several families of compounds such as ethers, ketones, aromatic compounds, nitroalkanes, fluorinated compounds, siloxanes, and plasticizers, in order to further investigate the reliability of the newly estimated parameters. Results obtained for some representative mixtures are shown in Table 4.11. The overall AAD % for vapour pressure is 1.8 % and 0.1 % for mole fractions. These results are considered to be satisfactory.

The ability of sPC-SAFT EoS to model other families of compounds will be discussed in more detail in the proceeding sections.

Table 4.11: Correlation results for binary VLE of different systems with sPC-SAFT.

| System | $T$ [K] | $N_{DP}$ | $k_{ij}$ [–] | AAD $P$ [%] | AAD $y$ [–] | Ref. |
|---|---|---|---|---|---|---|
| *Ethers* | | | | | | |
| Dipropyl ether–benzene | 323 | 20 | –0.004 | 0.9 | 0.0 | [46] |
| Dipropyl ether–toluene | 343 | 19 | –0.002 | 0.4 | 0.0 | [46] |
| Dipropyl ether–ethyl benzene | 323 | 10 | 0.00 | 0.7 | 0.1 | [46] |
| Dipropyl ether–octane | 363 | 11 | 0.008 | 3.7 | 0.1 | [46] |
| Dipropyl ether–nonane | 363 | 11 | 0.00 | 4.7 | 0.0 | [46] |
| Diisopropyl ether–benzene | 323 | 17 | 0.00 | 0.6 | 0.0 | [46] |
| Diisopropyl ether–toluene | 333 | 13 | –0.002 | 1.2 | 0.0 | [46] |
| *Ketones* | | | | | | |
| Methyl isobutyl ketone–benzene | 353 | 14 | 0.00 | 2.3 | 0.1 | [46] |
| Methyl isobutyl ketone–toluene | 323 | 28 | –0.0075 | 1.4 | 0.1 | [46] |
| Methyl isobutyl ketone –cyclohexane | 353 | 13 | 0.0038 | 2.1 | 0.1 | [46] |
| *Aromatic compounds* | | | | | | |
| 1-Methylnaphthalene –naphthalene | 463 | 10 | 0.01 | 0.4 | 0.0 | [47] |
| 1-Methylnaphthalene–biphenyl | 463 | 10 | 0.008 | 0.3 | 0.0 | [47] |
| Tetralin–1-methylnaphthalene | 463 | 11 | 0.003 | 0.6 | 0.0 | [47] |
| Tetralin–naphthalene | 443 | 11 | 0.003 | 0.5 | 0.0 | [48] |
| Tetralin–acenaphthene | 443 | 10 | 0.00 | 0.6 | 0.0 | [48] |
| Tetralin–dibenzofuran | 443 | 10 | 0.01 | 1.0 | 0.0 | [48] |
| *Nitroalkanes* | | | | | | |
| Nitrobenzene–chlorobenzene | 353 | 12 | 0.01 | 4.4 | 0.0 | [49] |
| Acetonitrile–toluene | 343 | 19 | 0.02 | 3.2 | 0.1 | [50] |
| Acetonitrile–1,4-dioxane | 313 | 16 | 0.003 | 2.1 | 0.1 | [51] |
| *Fluorinated compounds* | | | | | | |
| Perfluorohexane–pentane | 293 | 15 | 0.077 | 3.3 | 0.0 | [52] |
| Perfluorohexane–hexane | 298 | 18 | 0.077 | 3.3 | 0.1 | [52] |
| *Si-compounds* | | | | | | |
| Tetraethyl silane–acetone | 308 | 9 | 0.04 | 2.9 | 0.4 | [53] |
| Tetrachloro silane–hexane | 308 | 14 | 0.01 | 1.0 | — | [54] |
| Hexamethyl disiloxane–hexane | 308 | 8 | –0.005 | 0.2 | 0.0 | [55] |
| *Plasticizers* | | | | | | |
| Benzyl benzoate–benzene | 453 | 13 | 0.00 | 1.6 | — | [56] |
| Benzyl benzoate–toluene | 453 | 13 | 0.004 | 2.0 | — | [56] |
| Benzyl benzoate–benzaldehyde | 453 | 13 | 0.004 | 3.6 | — | [56] |
| AAD [%] overall | | | | 1.8 | 0.1 | |

### 4.4.2 Fluorocarbon Mixtures

The present section extends the study toward a specific family of compounds, namely *n*-fluorocarbons. Despite their similar formulas, fluorocarbons and hydrocarbons posses totally different structures and properties and express their reciprocal phobicity and incompatibility in a number of interesting phenomena because of the existing intrinsic atomic properties of fluorine and carbon [57]. Fluorocarbons are used in different fields, e.g. in biomedical applications as artificial blood and synthetic oxygen carriers, due to their high intramolecular (covalent) and low intermolecular (van der Waals) forces that characterize them. They are much more stable than their corresponding hydrocarbons, with low surface tension, low dielectric constants and refractive indexes, high vapour pressures, high compressibility, and high respiratory gas solubilities [57–59].

The modelling of fluorocarbons' thermodynamic properties is of great importance, because there are features of these compounds that are still not completely understood, and their thermodynamic modelling is quite difficult. Recently, highly fluorinated compounds have been modelled using different versions of SAFT [60–63], but not sPC-SAFT. The reliability of sPC-SAFT parameters for perfluorohexane estimated from recent published data [64] has been tested by predicting VLE of its mixtures with different alkanes. For these calculations, the $k_{ij}$ value is optimised so that the difference between experimental and calculated azeotrope pressure is minimised. Figure 4.12 shows the good agreement achieved between experimental data [52] and sPC-SAFT estimations. The occurrence and location of the azeotropes are well captured by the model.

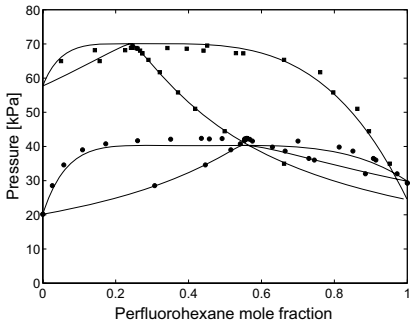


Figure 4.12: VLE of perfluorohexane–$C_5$ at 293.15 K and perfluorohexane–$C_6$ at 298.65 K [52]. Lines are sPC-SAFT correlations ($k_{ij} = 0.077$).

Moreover, calculations of the solubility of two gases, xenon and oxygen, in three perfluoroalkanes are shown in Figures 4.13 and 4.14. Binary interaction parameters are used in the modelling of all mixtures. sPC-SAFT provides satisfactory results for xenon–

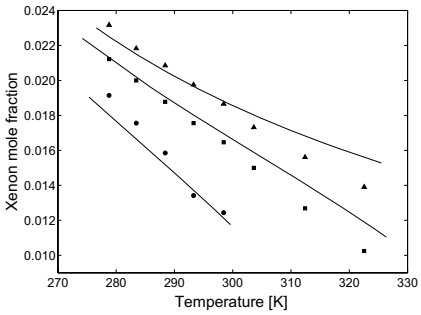


Figure 4.13: Solubility of Xe in perfluorohexane (circles), perfluoroheptane (squares) and perfluorooctane (triangles) at 101.3 kPa [65]. Lines are sPC-SAFT correlations using $k_{ij} = 0.098$, 0.085, and 0.07, respectively.

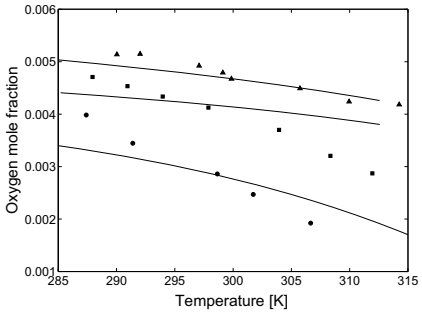


Figure 4.14: Solubility of $O_2$ in perfluorohexane (circles), perfluoroheptane (squares) and perfluorooctane (triangles) at 101.3 kPa [62]. Lines are sPC-SAFT correlations using $k_{ij} = 0.12$, 0.085, and 0.06, respectively.

perfluoroalkanes, as well as for alkanes–perfluorohexane mixtures (see Figure 4.12). This is possibly because xenon is considered as the first member of the *n*-alkane series, methane, in terms of its phase equilibria properties [66], and behaves like one. Further examples of the similarity between xenon and methane in terms of phase equilibria can be found in mixtures with alcohols [67], namely methanol. This similarity is observed in other microscopic properties. The diameter of the xenon atom measured in terms of van der Waals radii agrees well with that of the cross-sectional diameter of the *n*-alkanes. Also, the dielectric polarisability of xenon (the relation between the dipole moment and the incident electric field) fits well with the linear dependency on $n$ exhibited by the *n*-alkanes.

For the oxygen–perfluoroalkanes mixtures, sPC-SAFT does not provide satisfactory results regardless of the value of the binary interaction parameter, as shown in Figure 4.14. The modelling of these systems is done without including cross-association effects. It turns out that for these particular systems such effects need to be included in order to capture the strong interactions present between molecular oxygen and the carbon atoms of the perfluorocarbon chains [62].

Furthermore, calculations of LLE are performed for the three perfluorohexane–*n*-alkane systems and presented in Figure 4.15. sPC-SAFT overpredicts the upper critical solution temperature (UCST), and although many experimental points are located in the critical region, it is observed that the shape of the curve is correct and the correlations can be considered satisfactory; at least in the low-temperature region.

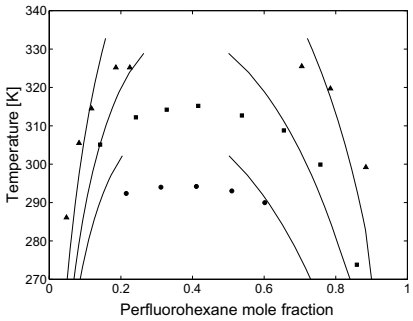


Figure 4.15: LLE of perfluorohexane–$n$-alkanes [52]; $n$-hexane (circles), $n$-heptane (squares) and $n$-octane (triangles). Lines are sPC-SAFT correlations ($k_{ij} = 0.073$).

### 4.4.3 Hexane–Acetone System

Acetone contains a carbonyl group which has a dipole moment particular to the molecular axis and is therefore a self-associating compound [68]. In this work, acetone is assumed to be a non-associating compound and PC-SAFT parameters are taken from [8]. The binary system of acetone with $n$-hexane exhibits large deviations from ideality resulting from dipole-dipole interactions of acetone molecules. The phase equilibria for this binary system has been measured in the range of 20–120 kPa and 253–323 K. Fourteen phase equlibrium datasets for this system can be collected covering both the VLE and LLE behaviour. In fact, there are 110 experimental VLE data [69–72] and a few LLE data [73].

Thus, various possibilities exist in terms of how the data may best be fitted. In the procedure which is found to yield good results, the optimisation proceeds in two steps. First, VLE data are treated to determine the optimum $k_{ij}$. With this $k_{ij}$ value, sPC-SAFT correlates the LLE data, while in the other step, LLE data are treated to determine the optimum $k_{ij}$ and with this $k_{ij}$ sPC-SAFT correlates the VLE data. Examples that illustrate the effective reproduction of experimental results are given in Figure 4.16.

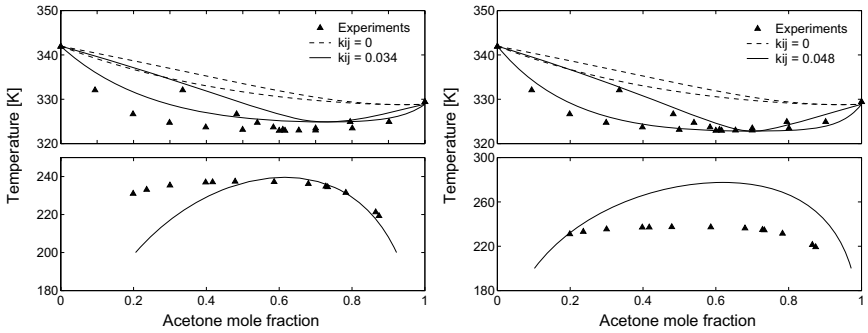


Figure 4.16: sPC-SAFT correlations of phase behaviour of acetone in $n$-hexane with $k_{ij} = 0.034$ optimised from LLE data [71] (left), and $k_{ij} = 0.048$ optimised from VLE data [73] (right).

As shown in Figure 4.17, very good accuracy is obtained when representing experimental pressure–mole fraction of acetone–$n$-hexane at 268.15 and 293.15 K [70] with the temperature independent $k_{ij} = 0.048$. Even when using $k_{ij} = 0.034$ optimised from LLE data, the location of the azeotrope is well captured by the model.

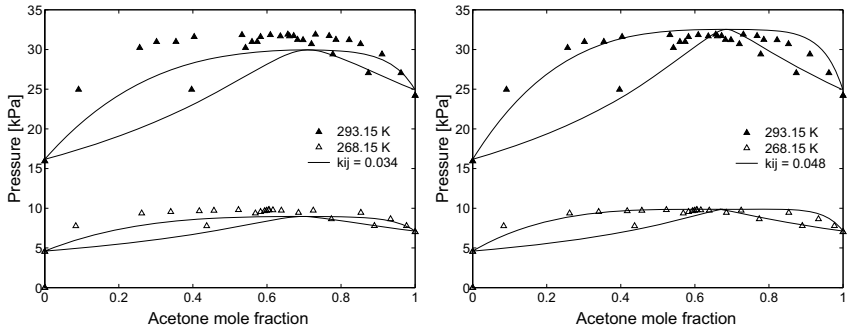


Figure 4.17: sPC-SAFT correlations of VLE of acetone–$n$-hexane with $k_{ij} = 0.034$ optimised from LLE data [71] (left) and $k_{ij} = 0.048$ optimised from VLE data [70] (right).

Additionally, calculations of LLE are performed for the four acetone–$n$-alkane systems and presented in Figures 4.18–4.21. sPC-SAFT satisfactorily represents experimental data [73] with a single $k_{ij} = 0.034$. The overall AAD for the temperature is 3.5 % for all four systems.

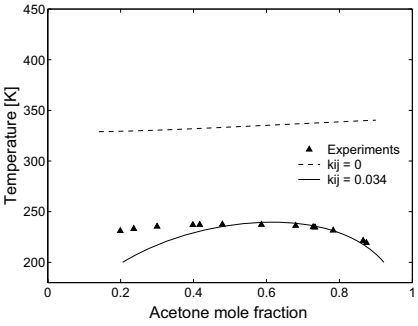


Figure 4.18: LLE of acetone–*n*-hexane [73].

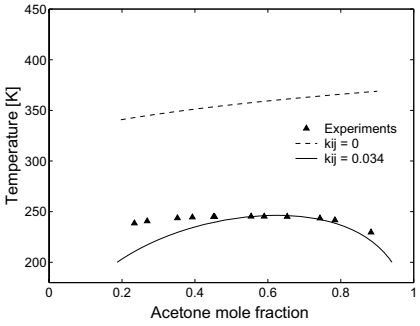


Figure 4.19: LLE of acetone–*n*-heptane [73].

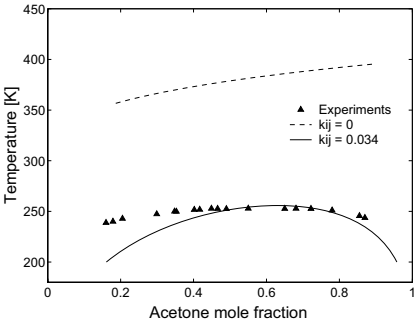


Figure 4.20: LLE of acetone–*n*-octane [73].

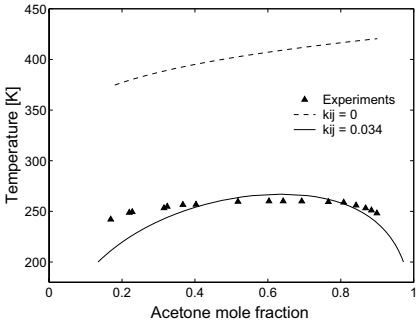


Figure 4.21: LLE of acetone–*n*-nonane [73].

The overall study of acetone–*n*-alkane systems indicates that the sPC-SAFT model requires a fitted $k_{ij}$ to model both VLE and LLE. The temperature and system independent $k_{ij}$ optimised to LLE data can be used to VLE providing satisfactory correlations over a wide temperature and pressure range, and vise versa. Furthermore, the optimised $k_{ij}$ values for these mixtures are closer to zero than $k_{ij} = 0.063$ reported by other authors [68].

## 4.5 Prediction of Binary Interaction Parameters ($k_{ij}$)

It has been demonstrated that the Lorentz-Berthelot combining rules; see Equations (4.4)–(4.5), provide a good representation of the phase equilibria of binary mixtures when studied with the sPC-SAFT EoS. As discussed in Section 2.2.1.4, the binary interaction parameter $k_{ij}$ determined by fitting to experimental mixture phase equilibrium data is often introduced to improve their applicability by correcting the mean-field energy contri-

bution of the SAFT EoS. However, as experimental data are not available for all mixtures of interest, constructing a more predictive way to calculate these $k_{ij}$ values is required. There are several empirical correlations for $k_{ij}$ presented in the literature. A detailed discussion of these correlations can be found elsewhere [74, 75] and is not provided here.

$$\sigma_{ij} = \frac{\sigma_i + \sigma_j}{2} \tag{4.4}$$

$$\epsilon_{ij} = \sqrt{\epsilon_{ii}\epsilon_{jj}}\,(1 - k_{ij}) \tag{4.5}$$

In the recent work of Haslam *et al.* [76], a method where the Hudson-McCoubrey combining rules [77] are used in the framework of the SAFT-VR EoS [78] for modelling fluid mixtures is presented. At first, a derivation of the Hudson-McCoubrey combining rules to the intermolecular potentials that are not of Lennard-Jones form is provided as these combining rules are originally determined assuming the Lennard-Jones potential. Secondly, various improvements in their predictions for mixtures compared with those made when using the most applied Lorentz-Berthelot rules are given.

Additionally, Haslam and coworkers [76] have looked at the possibility of applying the new method to sPC-SAFT as well. Assuming that although the potential model in sPC-SAFT is not exactly of Lennard-Jones form, it is defined by the two analogous parameters, $\epsilon/k$ and $\sigma$, and therefore the original Hudson-McCoubrey rules provide means of predicting $k_{ij}$ for sPC-SAFT. The following Equation (4.6) is used to calculate a predictive binary interaction parameter, $k_{ij}$, for sPC-SAFT:

$$k_{ij} = 1 - \left\{ 2^7 \left( \frac{(I_i I_j)^{1/2}}{I_i + I_j} \right) \left( \frac{\sigma_{ii}^3 \sigma_{jj}^3}{(\sigma_{ii} + \sigma_{jj})^6} \right) \right\} \tag{4.6}$$

where $\sigma_i$ is a molecular-size parameter in Å, and $I_i$ is the ionisation potential of compound $i$ expressed in eV.

For a more detailed explanation of the applied Hudson-McCoubrey combining rules and the derivation of Equation (4.6), please see references [76, 77].

Continuing their observations [76] when looking at the modelling results with sPC-SAFT, the original Hudson-McCoubrey rules' applicability to sPC-SAFT is further tested here by comparison with available binary interaction parameters from the studies presented in this chapter and with new calculations for some binary mixtures.

Table 4.12 presents predicted binary-interaction parameters for $n$-alkane mixtures calculated using Equation (4.6), which seem to be close to zero when alkanes are near neighbours in the homologous series as expected according to the theory. For these calculations, values of ionisation potential are taken from Reference [79].

New VLE calculations for the methane–$n$-octane systems at three temperatures are performed in order to illustrate the sensitivity of calculated phase equilibria to $k_{ij}$ values of such small magnitude. Figure 4.22 shows the predictions with sPC-SAFT using $k_{ij} = 0$,

Table 4.12: Predicted $k_{ij}$ for binary mixtures of $n$-alkanes from $C_1$ to $C_8$.

| $n$-Alkane | Methane | Ethane | Propane | $n$-Butane | $n$-Pentane | $n$-Hexane | $n$-Heptane |
|---|---|---|---|---|---|---|---|
| Ethane | 0.00287 | | | | | | |
| Propane | 0.00289 | 0.00093 | | | | | |
| $n$-Butane | 0.00405 | 0.00311 | 0.00065 | | | | |
| $n$-Pentane | 0.00545 | 0.00530 | 0.00181 | 0.00029 | | | |
| $n$-Hexane | 0.00644 | 0.00648 | 0.00252 | 0.00062 | 0.00006 | | |
| $n$-Heptane | 0.00763 | 0.00738 | 0.00308 | 0.00092 | 0.00020 | 0.00005 | |
| $n$-Octane | 0.00882 | 0.00893 | 0.00412 | 0.00152 | 0.00050 | 0.00022 | 0.00008 |

as well as the correlations using the predictive $k_{ij} = 0.00882$. The results of this system show that the correlations using the predicted $k_{ij}$ provide an overall better description of the experimental data.

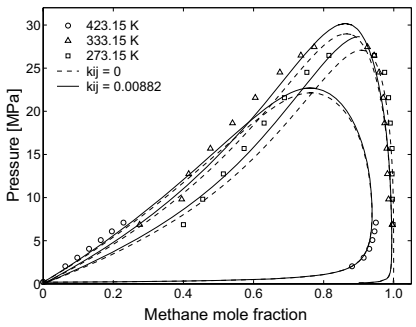


Figure 4.22: Pressure-composition isotherms for the methane–$n$-octane system. Symbols are experimental data, while lines are sPC-SAFT modelling results.

Based on this evidence, the following calculations are performed for several other alkane systems. The results are summarized in Table 4.13.

Calculations for these mixtures using fitted $k_{ij}$ are expected to provide correct representations of phase equilibria, as previously demonstrated in this chapter for different $n$-alkane mixtures. It is not expected that the predicted $k_{ij}$ values will match exactly those obtained by fitting, but they should improve the correlations with sPC-SAFT rather than using $k_{ij} = 0$ in accordance with the smaller AAD values listed in Table 4.13.

Another test is performed on the binary mixtures of $H_2S$ with various hydrocarbons. Calculations of VLE of these mixtures with sPC-SAFT are previously presented in Table 4.8 listing the fitted $k_{ij}$ values. The fitted and predicted $k_{ij}$ values of these systems are graphically compared in Figure 4.23 showing that the $k_{ij}$ values do not match but follow the same trends.

Table 4.13: Comparison of experimental [46] and calculated VLE data for binary mixtures of $n$-alkanes from $C_1$ to $C_8$ using the predicted $k_{ij}$ values from Table 4.12.

| System | AAD [%] | |
|---|---|---|
| | $k_{ij} = 0$ | $k_{ij}$ from Table 4.12 |
| $C_1$–$C_2$ | 0.9 | 0.3 |
| $C_1$–$C_3$ | 2.7 | 2.1 |
| $C_1$–$C_4$ | 4.4 | 3.5 |
| $C_1$–$C_5$ | 7.4 | 5.2 |
| $C_1$–$C_6$ | 11.3 | 8.3 |
| $C_1$–$C_7$ | 7.7 | 5.2 |
| $C_1$–$C_8$ | 7.8 | 5.1 |
| $C_2$–$C_3$ | 1.6 | 1.6 |
| $C_2$–$C_4$ | 2.8 | 2.1 |
| $C_2$–$C_5$ | 2.6 | 1.3 |
| $C_2$–$C_6$ | 6.6 | 4.7 |
| $C_2$–$C_7$ | 3.7 | 1.9 |
| $C_2$–$C_8$ | 6.2 | 1.5 |
| $C_3$–$C_4$ | 1.4 | 1.2 |
| $C_3$–$C_5$ | 4.5 | 4.2 |
| $C_3$–$C_6$ | 2.0 | 0.8 |
| $C_4$–$C_5$ | 3.9 | 3.0 |
| AAD [%] overall | 4.6 | 3.1 |

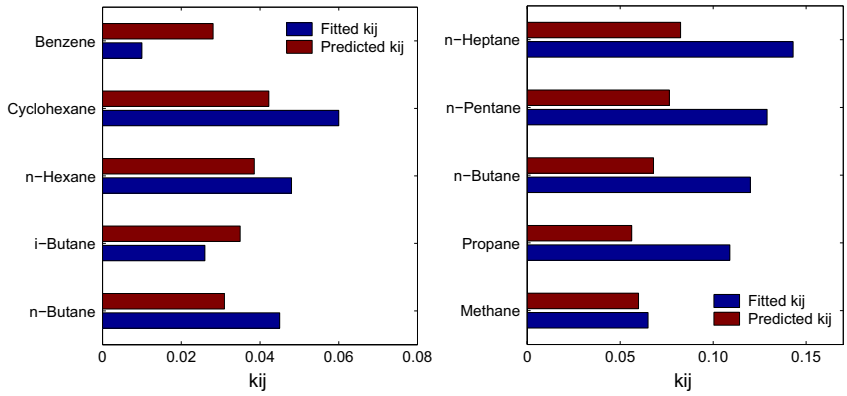


Figure 4.23: Fitted and predicted $k_{ij}$ values for $H_2S$ (left) and $CO_2$ (right) systems.

Particularly, the investigated theory suggests an increasing $k_{ij}$ for increasing asymmetric $CO_2$–$n$-alkane mixtures except for methane that exhibit higher ionisation potential of 12.61 eV than the other alkanes. This is due to the steady increase in ionisation potential

of $n$-alkanes with chain length, whereas $CO_2$ has a relatively large ionisation potential of 13.78 eV [79]. The same trend is observed with the fitted $k_{ij}$ values as presented in Figure 4.23.

As the potential model in sPC-SAFT is not exactly of Lennard-Jones form, one cannot draw a firm conclusion from this study. However, the study presents a possibility to predict $k_{ij}$ values using the information on the properties of pure compounds alone. Further work and some improvements of the present theory are required for reliable prediction of binary interaction parameters in fluid mixtures. Unfortunately, this approach is limited to available ionisation potential energy values for compounds under consideration. The known ionisation potentials for most heavy hydrocarbons are not very accurate, and they are found to vary proportionally with $1/\sigma^3$, as discussed in [74]. In order to be applicable, for example, for polymer–solvent mixtures, it is necessary that these values are extrapolated from the values for non-polymer compounds. This possibility is briefly investigated on the binary PE mixtures both with SAFT-VR and sPC-SAFT [76]. The $k_{ij}$ values for binary PE–gas mixtures obtained by adjusting to experimental data [8, 16] and the predicted $k_{ij}$ values calculated by Equation (4.6) are compared, and the trends are qualitatively captured using the Hudson-McCoubrey rules.

## 4.6 Final Comments

sPC-SAFT has been applied to phase equilibria modelling, especially VLE, of numerous non-associating compounds. Special attention has been given to the estimation of the models' pure compound parameters. The pure compound parameters of 500 non-associating compounds are determined by simultaneously fitting vapour pressure and liquid density data. Good agreement is obtained for light gases–heavy alkanes systems using a constant value of the binary interaction parameters. Using those new estimated PC-SAFT parameters, the results justify the capability of sPC-SAFT in describing asymmetric systems.

It is shown that sPC-SAFT can correlate binary mixtures of alkanes and perfluoroalkanes by adjusting a temperature-independent interaction parameter. The same is true with binary mixtures of xenon and perfluoroalkanes. Even when modelling phase equilibria of polar low $M_w$ compounds, such as acetone–$n$-alkanes, sPC-SAFT generally performs well using a fitted $k_{ij}$ value. The application of the model to mixtures with more than one polar compound is troublesome, and requires higher values of $k_{ij}$ for the optimal description. Implementing an additional polar term to account for dipole-dipole interactions, as discussed by other authors [68, 80–82], may improve these results and provide more predictive capability of the model. Moreover, as the focus of engineers in the near future is moved to more complex biological processes with polar and aqueous solutions, the further extension of the model toward these systems is quite essential.

Generally satisfactory estimations are obtained for the tested binary systems using

the newly estimated parameters (with or without $k_{ij}$). Moreover, a suitable predictive form of the $k_{ij}$ parameter based on the Hudson-McCoubrey rules is presented. Further work and some improvements of the present theory are required for reliable prediction of binary interaction parameters in fluid mixtures.

## References


[1] S. H. Huang and M. Radosz, "Equation of State for Small, Large, Polydisperse, and Associating Molecules," *Ind. Eng. Chem. Res.*, vol. 29, pp. 2284–2294, 1990.

[2] J. J. B. Machado and T. W. de Loos, "Liquid-Vapour and Solid-Fluid Equilibria for the System of Methane + Triacontane at High Temperature and High Pressure," *Fluid Phase Equilibria*, vol. 222–223, pp. 261–267, 2004.

[3] AIChE J., *DIPPR Table of Physical and Thermodynamic Properties of Pure Compounds*. New York, USA, 1998.

[4] J. Gross and G. Sadowski, "Perturbed-Chain SAFT: An Equation of State Based on Perturbation Theory for Chain Molecules," *Ind. Eng. Chem. Res.*, vol. 40, pp. 1244–1260, 2001.

[5] P. D. Ting, C. P. Joyce, P. K. Jog, W. G. Chapman, and M. C. Thies, "Phase Equilibrium Modeling of Mixtures of Long-Chain and Short-Chain Alkanes Using Peng-Robinson and SAFT," *Fluid Phase Equilibria*, vol. 206, pp. 267–286, 2003.

[6] I. A. Kouskoumvekaki, N. von Solms, T. Lindvig, M. L. Michelsen, and G. M. Kontogeorgis, "Novel Method for Estimating Pure-Component Parameters for Polymers: Application to the PC-SAFT Equation of State," *Ind. Chem. Eng. Res.*, vol. 43, pp. 2830–2838, 2004.

[7] A. Ghosh, W. G. Chapman, and R. N. French, "Gas solubility in Hydrocarbons – A SAFT-based Approach," *Fluid Phase Equlibria*, vol. 209, pp. 229–243, 2003.

[8] I. A. Kouskoumvekaki, N. von Solms, M. L. Michelsen, and G. M. Kontogeorgis, "Application of a Simplified Perturbed Chain SAFT Equation of State to Complex Polymer Systems Using Simplified Mixing Rules," *Fluid Phase Equilibria*, vol. 215, pp. 71–78, 2004.

[9] P. Arce and M. Aznar, "Modeling the Phase Behavior of Commercial Biodegradable Polymers and Copolymer in Supercritical Fluids," *Fluid Phase Equilibria*, vol. 238, pp. 242–253, 2005.

[10] N. von Solms, M. L. Michelsen, and G. M. Kontogeorgis, "Prediction and Correlation of High-Pressure Gas Solubility in Polymers with Simplified PC-SAFT," *Ind. Eng. Chem. Res.*, vol. 44, pp. 3330–3335, 2005.

[11] J. Vijande, M. M. Pineiro, D. Bessieres, H. Saint-Guirons, and J. L. Legido, "Description of PVT Behaviour of Hydrofluoroethers Using the PC-SAFT EoS," *Phys. Chem. Chem. Phys.*, vol. 6, pp. 766–770, 2004.

[12] O. Spuhl, S. Herzog, J. Gross, I. Smirnova, and W. Arlt, "Reactive Phase Equilibria in Silica Aerogel Synthesis: Experimental Study and Prediction of the Complex Phase Behavior Using the PC-SAFT Equation of State," *Ind. Eng. Chem. Res.*, vol. 43, pp. 4457–4464, 2004.

[13] I. A. Kouskoumvekaki, G. J. P. Krooshof, M. L. Michelsen, and G. M. Kontogeorgis, "Application of the Simplified PC-SAFT Equation of State to the Vapor-Liquid Equilibria of Binary and Ternary Mixtures of Polyamide 6 with Several Solvents," *Ind. Chem. Eng. Res.*, vol. 43, pp. 826–834, 2004.

[14] N. von Solms, I. A. Kouskomvekaki, T. Lindvig, M. L. Michelsen, and G. M. Kontogeorgis, "A Novel Approach to Liquid-Liquid in Polymer Systems with Application to Simplified PC-SAFT," *Fluid Phase Equlibria*, vol. 222–223, pp. 87–93, 2004.

[15] M. J. Anselme, M. Gude, and A. S. Teja, "The Critical Temperatures and Densities of the *n*-Alkanes from Pentane to Octadecane," *Fluid Phase Equlibria*, vol. 57, pp. 317–326, 1990.

[16] N. von Solms, M. L. Michelsen, and G. M. Kontogeorgis, "Computational and Physical Performance of a Modified PC-SAFT Equation of State for Highly Asymmetric and Associating Mixtures," *Ind. Eng. Chem. Res.*, vol. 42, pp. 1098–1105, 2003.

[17] C. McCabe and G. Jackson, "SAFT-VR Modelling of the Phase Equlibria of Long-Chain *n*-Alkanes," *Phys. Chem. Chem. Phys*, vol. 1, pp. 2057–2064, 1999.

[18] E. C. Voutsas, G. D. Pappa, K. Magoulas, and D. P. Tassios, "Vapor Liquid Equilibrium Modeling of Alkane Systems with Equations of State: "Simplicity versus Complexity"," *Fluid Phase Equilibria*, vol. 240, pp. 127–139, 2006.

[19] R. Agarwal, D. Prasad, S. Maity, K. Gayen, and S. Ganguly, "Experimental Measurments and Model Based Inferencing of Solubility of Polyethylene in Xylene," *J. Chem. Eng. Jpn.*, vol. 37, pp. 1427–1435, 2004.

[20] D. L. Morgan and R. Kobayashi, "Direct Vapor Pressure Measurements of Ten *n*-Alkanes in the $C_{10}$–$C_{28}$ Range," *Fluid Phase Equilibria*, vol. 97, pp. 211–242, 1994.

[21] J. Gregorowicz, T. W. de Loos, and J. de Swaan Arons, "System Propane + Eicosane. P, T, and x Measurements in the Temperature Range 288–358 K," *J. Chem. Eng. Data.*, vol. 37, pp. 356–358, 1992.

[22] C. J. Peters, T. W. de Loos, and J. de Swaan Arons, "Measurements and Calculations of Phase Equilibria in Binary Mixtures of Propane + Tetratriacontane," *Fluid Phase Equilibria*, vol. 72, pp. 251–266, 1992.

[23] C. J. Peters, T. W. de Loos, and J. de Swaan Arons, "Phase Equilibria in Binary Mixtures of Propane and Hexacontane," *Fluid Phase Equilibria*, vol. 85, pp. 301–312, 1993.

[24] P. C. Joyce, J. Gordon, and M. C. Thies, "Vapor-Liquid Equilibria for the Hexane + Tetracosane and Hexane + Hexatriacontane Systems at Elevated Temperatures and Pressures," *J. Chem. Eng. Data*, vol. 45, pp. 424–427, 2000.

[25] H. M. Lin, H. M. Sebastian, and K. C. Chao, "Gas-Liquid Equilibrium in Hydrogen + *n*-Hexadecane and Methane + *n*-Hexadecane at Elevated Temperatures and Pressures," *J. Chem. Eng. Data.*, vol. 25, pp. 252–254, 1980.

[26] H. J. van der Kooi, E. Flöter, and T. W. de Loos, "High-Pressure Phase Equilibria of $(1-x)CH_4+xCH_3(CH_2)_{18}CH_3$," *J. Chem. Thermodyn.*, vol. 27, pp. 847–861, 1995.

[27] H. H. Reamer and B. H. Sage, "Phase Equilibria in Hydrocarbon Systems. Volumetric and Phase Behaviour of the Ethane–*n*-Decane System," *Phase Equilib. Mol. Transp. Thermodyn.*, vol. 7, pp. 161–168, 1962.

[28] P. C. Joyce and M. C. Thies, "Vapor-Liquid Equilibria for the Hexane + Hexadecane and Hexane + 1-Hexadecanol Systems at Elevated Temperatures and Pressures," *J. Chem. Eng. Data*, vol. 4, pp. 819–822, 1998.

[29] K. A. M. Gasem and R. L. Robinson, "Solubilities of Carbon Dioxide in Heavy Normal Paraffins ($C_{20}$–$C_{44}$) at Pressures to 9.6 MPa and Temperatures from 323 to 423 K," *J. Chem. Eng. Data.*, vol. 30, pp. 53–56, 1985.

[30] J. Park, R. L. Robinson, and K. A. M. Gasem, "Solubilities of Hydrogen in Heavy Normal Paraffins at Temperatures from 323.2 to 423.2 K and Pressures to 17.4 MPa," *J. Chem. Eng. Data.*, vol. 40, pp. 241–244, 1995.

[31] G.-X. Feng and A. E. Mather, "Solubility of Hydrogen Sulfide in *n*-Eicosane at Elevated Pressure," *J. Chem. Eng. Data.*, vol. 37, pp. 412–413, 1992.

[32] J. Tong, W. Gao, R. L. Robinson, and K. A. M. Gasem, "Solubilities of Nitrogen in Heavy Normal Paraffins from 323 to 423 K at Pressures to 18.0 MPa," *J. Chem. Eng. Data.*, vol. 44, pp. 784–787, 1999.

[33] S. Strivatsan, X. Yi, R. L. Robinson, and K. A. M. Gasem, "Solubilities of Carbon Monoxide in Heavy Normal Paraffins at Temperatures from 311 to 423 K and Pressures to 10.2 MPa," *J. Chem. Eng. Data.*, vol. 40, pp. 237–240, 1995.

[34] N. A. Darwish, J. Fathikalajski, K. A. M. Gasem, and R. L. Robinson, "Solubility of Methane in Heavy Normal Paraffins at Temperature from 323 to 423 K and Pressure to 10.7 MPa," *J. Chem. Eng. Data.*, vol. 38, pp. 44–48, 1993.

[35] J. S. Chou and K. Chao, "Solubility of Ethylene in *n*-Eicosane, *n*-Octacosane, and *n*-Hexatriacontane," *J. Chem. Eng. Data.*, vol. 34, pp. 68–70, 1989.

[36] K. A. M. Gasem, B. A. Bufkin, A. M. Raff, and R. L. Robinson, "Solubilities of Ethane in Heavy Normal Paraffins at Pressures to 7.8 MPa and Temperatures from 348 to 423 K," *J. Chem. Eng. Data.*, vol. 34, pp. 187–191, 1989.

[37] L. F. Vega, L. J. Florusse, C. J. Peters, J. C. Pámies, and H. Meijer, "Solubility of Hydrogen in Heavy *n*-Alkanes: Experiments and SAFT Modeling," *AIChE J.*, vol. 49, pp. 3260–3269, 2003.

[38] H. H. Reamer, B. H. Sage, and B. H. Lacey, "Phase Equilibria in Hydrocarbon Systems," *Ind. Eng. Chem.*, vol. 43, pp. 976–989, 1951.

[39] S. Apparicio-Martinez and K. R. Hall, "Use of PC-SAFT for Global Phase Diagrams in Binary Mixtures Relevant to Natural Gases. 3. Alkane + Non-Hydrocarbons," *Ind. Eng. Chem. Res.*, vol. 46, pp. 291–296, 2007.

[40] A. Leu and D. B. Robinson, "Equilibrium Phase Properties of the *n*-Butane–Hydrogen Sulfide and Isobutane–Hydrogen Sulfide Binary Systems," *J. Chem. Eng. Data.*, vol. 34, pp. 315–319, 1989.

[41] S. Laugier and D. Richon, "Vapor-Liquid Equilibria for Hydrogen Sulfide + Hexane, + Cyclohexane, + Benzene, + Pentadecane, and + (Hexane + Pentadecane)," *J. Chem. Eng. Data.*, vol. 40, pp. 153–159, 1995.

[42] J. J. Carroll and A. E. Mather, "An Examination of the Vapor-Liquid Equilibrium in the System Propane–Hydrogen Sulfide," *Fluid Phase Equlibria*, vol. 81, pp. 187–204, 1992.

[43] K. Kniaz, "Influence of the Size and Shape Effect on the Solubility of Hydrocarbons: The Role of the Combinatorial Entropy," *Fluid Phase Equilibria*, vol. 68, pp. 35–46, 1991.

[44] K. Kniaz, "Solubility of *n*-Docosane in *n*-Hexane and Cyclohexane," *J. Chem. Eng. Data*, vol. 36, pp. 471–482, 1991.

[45] J. F. Parcher, P. H. Weiner, C. L. Hussey, and T. N. Westlake, "Specific Retention Volumes and Limited Activity Coefficients of $C_4$–$C_8$ Alkane Solutes in $C_{22}$–$C_{36}$ *n*-Alkane Solvents," *J. Chem. Eng. Data*, vol. 20, pp. 145–151, 1975.

[46] J. Gmehling, U. Onken, and W. Arlt, *Vapor-Liquid Equilibrium Data Collection*. DECHEMA Chemistry data serie, vol. I–IV, Frankfurt: DECHEMA, 1979.

[47] A. Gupta, F. R. Groves, and E. McLaughlin, "Isothermal Vapor-Liquid Equilibrium of Binary and Ternary Systems Composed of Heavy Aromatic Compounds," *J. Chem. Eng. Data.*, vol. 37, pp. 32–36, 1992.

[48] A. Gupta, S. Gupta, F. R. Groves, and E. McLaughlin, "Measurement of Vapor-Liquid Equilibrium for Binary Systems Containing Polynuclear Aromatic Compounds," *Fluid Phase Equilibria*, vol. 65, pp. 305–326, 1991.

[49] B. Varughese and J. T. Sommerfeld, "Vapor-Liquid Equilibria for the Chlorobenzene–Nitrobenzene System at 80.0 and 95.0°C," *J. Chem. Eng. Data.*, vol. 34, pp. 21–25, 1989.

[50] J. P. Monfort, "Vapor-Liquid Equilibriums for Benzene–Acetonitrile and Toluene–Acetonitrile Mixtures at 343.15 K," *J. Chem. Eng. Data.*, vol. 28, pp. 24–27, 1983.

[51] R. Francesconi and F. Comelli, "Excess Thermodynamic Properties for the Binary System 1,4-Dioxane–Acetonitrile at 40°C," *J. Chem. Eng. Data.*, vol. 33, pp. 80–83, 1988.

[52] C. Duce, M. R. Tinè, L. Lepori, and E. Matteoli, "VLE and LLE of Perfluoroalkane + Alkane mixtures," *Fluid Phase Equilibria*, vol. 199, pp. 197–212, 2002.

[53] N. Bjerrum and E. Jozefowicz, "Studies on Ionic Separation Coefficients. II. Solubilities of Tetraethylsilane and Tetraethylammonium Halogenides in Different Means of Solution," *Phys. Chem. (Leipzig)*, vol. 159, pp. 194–222, 1932.

[54] D. V. S. Jain and O. P. Yadav, "Thermodynamics of *n*-Alkane Solutions: Part VIII – Vapour Pressures and Excess Free Energies for the $SiCl_4$/*n*-Hexane System," *Indian J. Chem.*, vol. 11, pp. 28–30, 1973.

[55] E. Dickinson, I. A. McLure, and B. H. Powell, "Thermodynamics of Alkane–Dimethyl Siloxane Mixtures. 2. Vapor Pressures and Enthalpies of Mixing," *J. Chem. Soc., Faraday Trans. 1*, vol. 70, pp. 2321–2333, 1974.

[56] B. Nienhaus, R. Witting, R. Bölts, S. H. Niemann, A. B. de Haan, and J. Gmehling, "Vapor-Liquid Equilibria at 453.25 K and Excess Enthalpies at 363.15 K and 413.15 K for Mixtures of Benzene, Toluene, Phenol, Benzaldehyde, and Benzyl Alcohol with Benzyl Benzoate," *J. Chem. Eng. Data.*, vol. 3, pp. 303–308, 1999.

[57] P. Lo Nostro, "Aggregates from Semifluorinated *n*-Alkanes: How Incompatibility Determines Self-Assembly," *Curr. Opin. Colloid Interface Sci.*, vol. 8, pp. 223–226, 2003.

[58] P. Lo Nostro, "Phase Separation Properties of Fluorocarbons, Hydrocarbons and Their Copolymers," *Adv. Colloid Interface Sci.*, vol. 56, pp. 245–287, 1995.

[59] M. P. Krafft, "Fluorocarbons and Fluorinated Amphiphiles in Drug Delivery and Biomedical Research," *Adv. Drug Delivery Rev.*, vol. 47, pp. 209–228, 2001.

[60] F. J. Blas and L. F. Vega, "Thermodynamic Behaviour of Homonuclear and Heteronuclear Lennard-Jones Chains with Association Sites from Simulation and Theory," *Mol. Phys.*, vol. 92, pp. 135–150, 1997.

[61] F. J. Blas and L. F. Vega, "Prediction of Binary and Ternary Diagrams Using the Statistical Associating Fluid Theory (SAFT) Equation of State," *Ind. Eng. Chem. Res.*, vol. 37, pp. 660–674, 1998.

[62] A. M. A. Dias, M. Freire, J. A. P. Coutinho, and I. M. Marrucho, "Solubility of Oxygen in Liquid Perfluorocarbons," *Fluid Phase Equlibria*, vol. 222/223, pp. 325–330, 2004.

[63] A. M. A. Dias, J. C. Pámies, J. A. P. Coutinho, I. M. Marrucho, and L. Vega, "SAFT Modeling of the Solubility of Gases in Perfluoroalkanes," *J. Phys. Chem. B*, vol. 108, pp. 1450–1457, 2004.

[64] A. M. A. Dias, C. M. B. Gancalves, A. I. Caco, L. M. N. B. F. Santos, M. M. Pineiro, L. F. Vega, J. A. P. Coutinho, and I. M. Marrucho, "Densities and Vapor Pressures of Highly Fluorinated Compounds," *J. Chem. Eng. Data*, vol. 50, pp. 1328–1333, 2005.

[65] R. P. Kennan and G. L. Pollack, "Solubility of Xenon in Perfluoroalkanes: Temperature Dependence and Thermodynamics," *J. Chem. Phys.*, vol. 89, pp. 517–521, 1988.

[66] E. J. M. Filipe, L. M. B. Dias, J. C. G. Calado, C. McCabe, and G. Jackson, "Is Xenon an "Ennobled" Alkane?," *Phys. Chem. Chem. Phys.*, vol. 4, pp. 1618–1621, 2002.

[67] T. A. Gricus, K. D. Luks, and C. L. Patton, "Liquid-Liquid-Vapor Phase Equilibrium Behavior of Binary Xenon + 1-Alkanol Mixtures," *Fluid Phase Equilibria*, vol. 108, pp. 219–229, 1995.

[68] F. Tumakaka and G. Sadowski, "Application of the Perturbed-Chain SAFT Equation of State to Polar Systems," *Fluid Phase Equilibria*, vol. 217, pp. 233–239, 2004.

[69] K. Schafer and W. Rall, "Dampfdruckuntersuchungen und Aktivitaetskoeffizienten des Systems Aceton–*n*-Hexan," *Z. Elektrochem.*, vol. 62, pp. 1090–1092, 1958.

[70] W. Rall and K. Schafer, "Thermodynamische Untersuchungen an fluessigen Mischsystemen von Aceton und *n*-Pentan sowie von. Aceton und *n*-Hexan," *Z. Electrochem.*, vol. 63, pp. 1019–1024, 1959.

[71] L. S. Kudryavtseva and M. P. Susarev, "Liquid-Vapor Equilibrium in the Systems Acetone–Hexane and Hexane–Ethyl Alcohol at 35, 45 and 55 deg. and 760 mmHg," *Zh. Prikl. Khim.*, vol. 36, pp. 1471–1477, 1963.

[72] S. K. Ogorodnikov, V. B. Kogan, and M. S. Nemtsov, "Separation of $C_5$ Hydrocarbons by Azeotropic and Extractive Fractionation. III. Liquid Equilibrium in Binary Systems Formed by Hydrocarbons with Acetone," *Zh. Prikl. Khim*, vol. 34, pp. 323–331, 1961.

[73] G. Spinolo and R. Riccardi, "Liquid-Liquid Equilibria in Propanone and *n*-Alkane Mixtures," *International DATA Series, Selected Data on Mixtures*, vol. A, pp. 91–94, 1977.

[74] J. A. P. Coutinho, G. Kontogeorgis, and E. H. Stenby, "Binary Interaction parameters for Nonpolar Systems with Cubic Equation of State: A Theoretical Approach 1. $CO_2$/Hydrocarbons using SRK Equation of State," *Fluid Phase Equilibria*, vol. 102, pp. 31–60, 1994.

[75] J. A. P. Coutinho, P. M. Vlamos, and G. Kontogeorgis, "General Form of the Cross-Energy Parameter of Equations of State," *Ind. Eng. Chem. Res.*, vol. 39, pp. 3076–3082, 2000.

[76] A. J. Haslam, A. Galindo, and G. Jackson, "Prediction of Binary Intermolecular Potential Parameters for Use in Modelling Fluid Mixtures," *Fluid Phase Equilibria*, vol. 266, pp. 105–128, 2008.

[77] G. H. Hudson and J. C. McCoubrey, "Intermolecular Forces Between Unlike Molecules. A More Complete Form of the Combining Rules," *Trans. Faraday Soc.*, vol. 56, pp. 761–766, 1960.

[78] A. Gil-Villegas, A. Galindo, P. J. Whitehead, S. J. Mills, G. Jackson, and A. N. Burgess, "Statistical Associating Fluid Theory for Chain Molecules with Attractive Potentials of Variable Range," *J. Chem. Phys.*, vol. 106, pp. 4168–4186, 1997.

[79] D. R. Lide, *CRC Handbook of Chemistry and Physics*. Taylor and Francis, Boca Raton, Florida, USA, 2005.

[80] N. von Solms, M. L. Michelsen, and G. M. Kontogeorgis, "Applying Association Theories to Polar Fluids," *Ind. Eng. Chem. Res.*, vol. 43, pp. 1803–1806, 2004.

[81] A. Dominik, W. G. Chapman, M. Kleiner, and G. Sadowski, "Modeling of Polar Systems with the Perturbed-Chain SAFT Equation of State. Investigation of the Performance of Two Polar Terms," *Ind. Eng. Chem. Res.*, vol. 44, pp. 6928–6938, 2005.

[82] E. K. Karakatsani and I. G. Economou, "Perturbed Chain-Statistical Associating Fluid Theory Extended to Dipolar and Quadrupolar Molecular Fluids," *J. Phys. Chem. B*, vol. 110, pp. 9252–9261, 2006.

# Chapter 5

# Validation of sPC-SAFT in Novel Polymer Applications

*"To dissolve or not to dissolve. That is the question."* by Anonymous
(with apologies to William Shakespeare)

## 5.1 Introduction

The knowledge of the solubility of solvents in polymers is essential for many processes in polymer production and purification. The removal of solvents and unconverted monomers from the polymer at the end of these processes is typically done by vapourization. Important thermodynamic parameters for the design of these processes are the *solvent mole fraction activity coefficient*, $\gamma_1^\infty$, and the *solvent weight fraction activity coefficient at infinite dilution*, $\Omega_1^\infty$, in the polymer. Generally, for highly asymmetric systems like these, $\Omega^\infty$ is much better scaled than $\gamma^\infty$ because of very low mole fractions of dissolved high-molecular-weight compounds, e.g. polymer, in solvents. Additionally, $\Omega^\infty$ is independent of polymer $M_w$.

Often the vapour pressure of a solvent above a polymer solution (solvent activity) is calculated using the *Flory-Huggins Equation*, an activity coefficient model, in which the thermodynamic quantities of the solution are derived from a simple concept of the combinatorial entropy of mixing and a Gibbs energy parameter, the $\chi$-parameter [1].

There are several different EoS that can be used to calculate polymer–solvent phase behaviour but only one is used in this work, the sPC-SAFT EoS. Being widely used in the polymer solution thermodynamics community, it is at the same time a good representative example of the perturbation models used to describe polymer solution behaviour.

Generally, EoS have certain predictive limitations for polymer solutions, and are thus in a state of continuous development. These equations can be used to correlate data, and, with caution, they can be used to simulate other experimental conditions not explicitly

measured. The strength and limitations of the sPC-SAFT EoS modeling of some polymer mixtures are presented in this chapter.

## 5.2 Binary PVC Mixtures

The first task is to evaluate how well the sPC-SAFT EoS represents the data for PVC–solvent and PVC–plasticizer systems and to see if the model can be used to assess miscibility of these systems. For this purpose, results are compared to those of more purely predictive models, such as Group Contribution Lattice-Fluid (GCLF) [2], UNIversal quasichemical Functional group Activity Coefficients–Free Volume (UNIFAC-FV) [3], and Entropic-FV [4], which are based on the group contribution principle and for which calculations can be made without parameter regressions.

The basic characteristics of the molecular and predictive models used for the comparison are summarized in Table 5.1. For more details on the theory behind these thermodynamic models, their different versions and applications, the reader is referred to the original publications [2–4].

Table 5.1: Schematic overview of purely predictive models used in this work, including the presentation of various physical effects and the parameters used in each model.

| **Model** | **Combinatorial effect** | **Free-volume effect** | **Energetic effect** | **Group parameters** | **Group interaction parameters** |
|---|---|---|---|---|---|
| Entropic-FV | Derived from the generalized van der Waals partition function | | UNIFAC | Volume ($R_k$)<br>Surf. area ($Q_k$) | $a_{mn}$ from low $M_w$ binary VLE data |
| UNIFAC-FV | UNIFAC | Obtained from Flory's EoS | UNIFAC | Volume ($R_k$)<br>Surf. area ($Q_k$) | $a_{mn}$ from low $M_w$ binary VLE data |
| GCLF | Derived from Guggenheim's statistical combinatorial formula | | Quasi-chemical theory | Volume ($v_k^*$)<br>Interaction energy ($\epsilon_{kk}$) | $a_{mn}$ from low $M_w$ binary VLE data |

| **Model** | **Combinatorial effect** | **Free-volume effect** | **Energetic effect** | **Pure-component parameters** | **Interaction parameters** |
|---|---|---|---|---|---|
| sPC-SAFT | $1^{st}$ and $2^{nd}$ order perturbation theory | | | $m_i$, $\sigma_i$, $(\epsilon/k)_i$ | One per binary $ij$-pair ($k_{ij} = k_{ji}$) |

The original form of the UNIFAC model [5] may be applied within the temperature range 275–425 K, and the model uses a parameter table with temperature-independent group interaction parameters. The parameter table has been revised and extended by Hansen *et al.* in 1991 [6], where a few new groups have been added. In 1992, Hansen *et al.* [7] introduced changes in the residual term using a linear temperature dependency in the group-interaction parameters. UNIFAC-FV [3] and Entropic-FV [4] use these parameter tables. In this work, when the parameter table of Hansen *et al.* from 1991 [6] is used, this is referred to as "1 coefficient". When the parameter table of Hansen *et al.* from 1992 [7] is used, this is referred to as "2 coefficient". In cases where the original parameter table of Fredenslund *et al.* [5] is used, this is stated as "Fred'75".

### 5.2.1 The "Rule of Thumb"

This summary of the "rule of thumb" [1] briefly discusses the way to assess the miscibility of polymers and solvents. A chemical (1) is often a good solvent for a specific polymer (2), or the two components have a tendency to be miscible if one or more of the following statements are fulfilled:

- Flory-Huggins parameter $\chi_{12} \leq 0.5$ indicates good miscibility.
- The value of the $\Omega_1^\infty$:

$$\begin{aligned} \Omega_1^\infty &\leq 6 : \text{Good solvency} \\ 6 < \Omega_1^\infty &< 8 : \text{Uncertainty} \\ \Omega_1^\infty &\geq 8 : \text{Non-solvency} \end{aligned}$$

- Theta temperatures[1] can be found for many liquid-liquid equilibria (LLE) systems and define the ultimate limit of solubility. For LLE, according to thermodynamics, complete miscibility is achieved if $\left(\frac{\partial^2 \Delta G}{\partial \varphi_1^2}\right)_{T,P} \geq 0$ at all concentrations. The higher the polymer molecular weight ($M_w$), the less miscible are polymer and solvent, or in other words the greater the LLE region (the area below the UCST-curve and above the LCST-curve; see Figure 5.1).
- A plot of the activity which is calculated by thermodynamic models, as a function of the solvent weight fraction, can give us indications of miscibility. If the activity value exceeds one, the system is immiscible according to the thermodynamic model.

[1] With respect to molecular interactions in dilute polymer solutions, theta temperature is the temperature at which the second virial coefficient disappears. That is, the temperature at which the coiled polymer molecules expand to their full contour lengths and become rod-shaped. Also known as the *Flory temperature*.

[2] For conditions of constant pressure, or when pressure effects are negligible, binary LLE is conveniently displayed on a solubility diagram, a plot of $T$ vs. $x_1$. Various types of these diagrams are observed for LLE, which are strongly dependent on the type of specific interactions that are determined in the

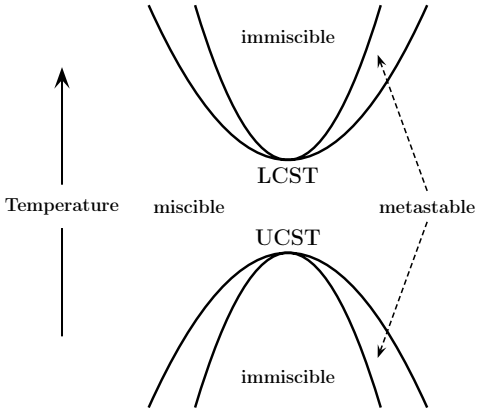


Figure 5.1: Schematic illustration of the UCST–LCST diagram[2].

### 5.2.2 PVC–Solvent Systems

The pure component parameters for PVC are obtained using the method developed by Kouskoumvekaki *et al.* [8]. The basic principle behind the method is explained in Section 2.2.3.2, which at the same time discusses the problematic issues when calculating polymer parameters. The corresponding monomer for PVC is chloroethane. Pure components parameters for PVC used in the following calculations are $m/M_w = 0.02101\,\mathrm{mol/g}$, $\sigma = 3.724\,\text{Å}$, and $\epsilon/k = 315.93\,\mathrm{K}$, while the model's parameters for different solvents can be found in Table 4.1 in Section 4.2.

#### 5.2.2.1 Evaluation of VLE

sPC-SAFT EoS has been applied to VLE for several different PVC–solvent systems. A temperature independent $k_{ij}$ value is used to obtain better correlations of experimental data.

Figure 5.2 shows VLE for the system PVC–toluene where the sPC-SAFT model provides a good correlation with $k_{ij} = -0.016$. Similar modelling results are obtained for the PVC–$CCl_4$ system with the same $k_{ij}$.

system considered. Endothermic systems demix below the binodal (the borderline between the one-phase region and the two-phase region) into two liquid phases. The maximum of the binodal is the upper critical solution temperature (UCST). This temperature exists because the thermal motion increases with temperature and thus overcomes any potential energy advantage in molecules of any type being close together. Exothermic systems demix with increasing temperature, and the minimum of the binodal is the lower critical solution temperature (LCST). LCST correspond to entropically induced phase separations and UCST to enthalpically induced ones.

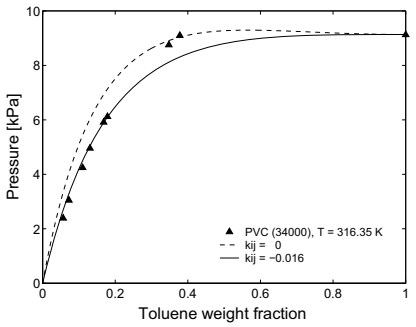


Figure 5.2: Pressure-weight fraction of the PVC–toluene system. Symbols represent experimental data [9], while lines are sPC-SAFT modelling results.

The aim of Figures 5.3 and 5.4 is to evaluate sPC-SAFT for two different PVC–ether systems. The PVC–di-*n*-propyl ether mixture in Figure 5.3 is well correlated by a small negative $k_{ij}$. However, this is not the case with the binary mixture of PVC and di-*n*-butyl ether in Figure 5.4. Even though the underestimation of the prediction is somewhat corrected by a small positive $k_{ij}$, the correlation is still not satisfactory. The $k_{ij}$ value is known to be sensitive to temperature and solvents used, and even small changes in $k_{ij}$ lead to differences as seen in Figure 5.3 for the PVC–di-*n*-propyl ether system.

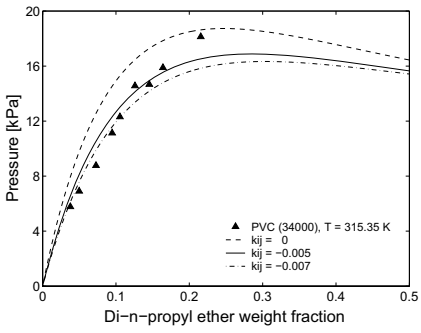


Figure 5.3: Pressure-weight fraction of PVC–di-*n*-propyl ether. Symbols represent experimental data [9], while lines are sPC-SAFT modelling results.

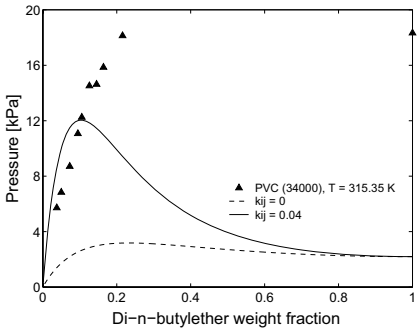


Figure 5.4: Pressure-weight fraction of PVC–di-*n*-butyl ether. Symbols represent experimental data [9], while lines are sPC-SAFT modelling results.

The optimised $k_{ij}$ values for the investigated PVC–solvent systems are listed in Table 5.2. Figure 5.5 shows the linear trend of $k_{ij}$ for PVC–solvent systems with increasing solvent $M_w$. The binary interaction parameter can be calculated using Equation (5.1), where the values for PVC–toluene and PVC–di(1-propyl) ether systems are removed assumed to be outsiders. Furthermore, it is not possible to investigate the temperature dependency of the $k_{ij}$ values, due to unavailable experimental data.

$$k_{ij} = 8.85 \times 10^{-4} M_w - 7.83 \times 10^{-2} \tag{5.1}$$

Table 5.2: Optimised $k_{ij}$ for PVC–solvent systems.

| Solvent | Optimized $k_{ij}$ |
|---|---|
| Toluene | –0.016 |
| Tetrachloromethane | 0.016 |
| Vinyl chloride | –0.025 |
| 1,4-Dioxane | 0.002 |
| Tetrahydrofuran | –0.015 |
| Di(1-propyl) ether | –0.007 |
| Di(1-butyl) ether | 0.040 |

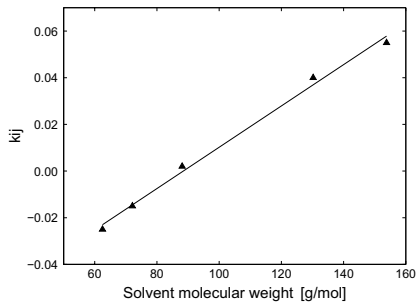


Figure 5.5: Optimized binary interaction parameter ($k_{ij}$) values for PVC–solvent systems as function of solvents' $M_w$. The line represents a linear regression and is described by Equation (5.1).

Now that the optimum $k_{ij}$ is identified by fitting to PVC–solvents mixture data, the same $k_{ij}$ can be used to predict ($\Omega_1^\infty$) for other members of the homologous series and at different temperatures. This assumption is further investigated in the following section where the $\Omega^\infty$ values for the binary PVC–solvent systems are evaluated.

#### 5.2.2.2 Evaluation of $\Omega^{\infty}$

The solvent weight fraction activity coefficient at infinite dilution ($\Omega_1^{\infty}$) is a useful quantity for selection of good solvents, where values below six typically indicate a good solvent, and values above eight indicate a poor solvent (see Section 5.2.1). On the other hand, there is a problem with this kind of approach. The objection stems from the observation that the $\Omega^{\infty}$ values determined by inverse gas chromatography (IGC) are usually obtained at temperatures which may easily be 373.15 K or above the temperature at which one typically wishes the polymer solubility to be assessed [10].

The experimental data [11, 12] for solvents' $\Omega_1^{\infty}$ in 19 PVC–solvent systems are listed in Table 5.3. The values of $\Omega_1^{\infty}$ estimated by the sPC-SAFT model with different $k_{ij}$ values are included as well. The results in Table 5.3 clearly show the significant influence of $k_{ij}$ on the estimation of solvent' $\Omega_1^{\infty}$ of binary PVC–solvent systems. Unfortunately, the correlated results with the optimum $k_{ij}$ calculated using Equation (5.1) provides higher deviations than pure predictions of the model, and thus cannot be used for this type of calculations. While, with temperature and system dependent values of $k_{ij}$, sPC-SAFT successfully correlate experimental data resulting in a total average deviation of 0.5 % contrary to the higher deviations obtained when predicting the $\Omega_1^{\infty}$ values or using $k_{ij}$ from Equation (5.1). In most cases, the optimum $k_{ij}$ assumes a very small negative value, and is rather system specific.

For additional comparison purposes, Table A.1 is presented in Appendix A with values of $\Omega_1^{\infty}$ for various PVC–solvent systems using different thermodynamic models and deviations from the experimental data for each investigated system. The table is adapted from Tihic [13].

Table 5.3: Experimental [11, 12] and calculated $\Omega_1^\infty$ values for PVC–solvent systems with the sPC-SAFT EoS. Values written in *italic* are regarded as outliers.

| No. | System | Exp. $\Omega_1^\infty$ | sPC-SAFT ($k_{ij}=0$) $\Omega_1^\infty$ | AAD [%] | $k_{ij}$ from Eq.(5.1) | sPC-SAFT ($k_{ij}$ Eq.(5.1)) $\Omega_1^\infty$ | AAD [%] | $k_{ij}$ fitted to exp. data | sPC-SAFT (fitted $k_{ij}$) $\Omega_1^\infty$ | AAD [%] |
|---|---|---|---|---|---|---|---|---|---|---|
| 1 | PVC(40000)–monochlorobenzene | 6.197 | 3.7 | 39.8 | 0.054 | 16.5 | 165.0 | 0.0183 | 6.18 | 0.3 |
| 2 | PVC(170000)–chloroform | 6.05 | 19.2 | *225.0* | 0.0291 | 35.8 | *491.0* | –0.057 | 6.07 | 0.3 |
| 3 | PVC(170000)–dichloromethane | 8.16 | 23.7 | 190.0 | –0.0019 | 22.9 | 181.0 | –0.06 | 8.19 | 0.4 |
| 4 | PVC(97000)–nitroethane | 7.56 | 16.1 | 113.0 | –0.0107 | 12.7 | 67.7 | –0.034 | 7.52 | 0.5 |
| 5 | PVC(34000)–1,4-dioxane | 9.61 | 6.79 | 29.3 | 0.0009 | 6.99 | 27.3 | 0.011 | 9.64 | 0.3 |
| 6 | PVC(97000)–tetrahydrofurane | 7.33 | 18.3 | 150.0 | –0.0134 | 13.9 | 89.4 | –0.044 | 7.39 | 0.8 |
| 7 | PVC(34000)–tetrahydrofurane | 7.44 | 8.43 | 13.3 | –0.0134 | 5.77 | 22.4 | –0.047 | 7.4 | 0.5 |
| 8 | PVC(97000)–tetrahydrofurane | 6.89 | 17.9 | 160.0 | –0.0134 | 13.8 | 99.6 | –0.049 | 6.84 | 0.7 |
| 9 | PVC(170000)–tetrahydrofurane | 12.87 | 32.4 | 35.2 | –0.0134 | 24.4 | 89.9 | –0.044 | 12.86 | 0.1 |
| 10 | PVC(97000)–toluene | 7.47 | 17.4 | 133.0 | 0.0046 | 19.6 | 162.0 | –0.033 | 7.41 | 0.8 |
| 11 | PVC(340000)–toluene | 12.22 | 79.8 | *553.0* | 0.0046 | 93.9 | *669.0* | –0.0528 | 12.25 | 0.3 |
| 12 | PVC(97000)–benzene | 7.363 | 17.5 | 138.0 | –0.008 | 14.7 | 99.2 | –0.0393 | 7.34 | 0.3 |
| 13 | PVC(97000)–acetone | 10.82 | 27.7 | 156.0 | –0.0269 | 16.8 | 55.6 | –0.0505 | 10.84 | 0.2 |
| 14 | PVC(41000)–acetone | 11.81 | 11.8 | 0.0 | –0.0269 | 16.0 | 35.6 | 0.0 | 11.81 | 0.0 |
| 15 | PVC(34000)–di-*n*-propyl ether | 26.46 | 19.5 | 26.2 | 0.0137 | 33.3 | 26.0 | 0.0078 | 26.5 | 0.2 |
| 16 | PVC(97000)–*n*-nonane | 34.44 | 45.2 | 31.3 | 0.0371 | 195. | *467.0* | –0.007 | 34.33 | 0.3 |
| 17 | PVC(97000)–*n*-octane | 34.32 | 45.5 | 32.6 | 0.0245 | 108.5 | *216.0* | –0.0071 | 35.39 | 0.1 |
| 18 | PVC(97000)–*n*-pentane | 38.65 | 50.9 | 31.7 | –0.0133 | 37.5 | 2.9 | –0.0012 | 38.67 | 0.1 |
| 19 | PVC(97000)–*n*-heptane | 31.89 | 21.3 | 33.2 | 0.0119 | 31.5 | 1.2 | 0.0122 | 31.89 | 0.0 |
| | Average AAD [%] | | | 110.0 | | | 156.2 | | | 0.5 |
| | Average AAD [%] *without outliers* | | | 77.2 | | | 83.8 | | | 0.5 |

Furthermore, the results in Table 5.4 show that the solubilities between PVC and seven tested solvents predicted by $\Omega_1^\infty$ values are in good agreement with the predictions from the experimental solvent(s)/non-solvent(ns) data [11, 12]. One out of seven miscibility indications is incorrect for sPC-SAFT, and sPC-SAFT compares favorably with the other three thermodynamic models.

Table 5.4: Comparison of results from the assessment of miscibility by predicted $\Omega_1^\infty$ values with experimental solvent activity data [11,12]. Green colour indicates agreement with experiments, while red numbers disagree. 's' means miscible system, while 'ns' indicates immiscible system.

| System | Temp. [K] | Exp. data | E-FV $\Omega_1^\infty$ | U-VF $\Omega_1^\infty$ | GCLF $\Omega_1^\infty$ | sPC-SAFT $\Omega_1^\infty$ |
|---|---|---|---|---|---|---|
| PVC(34000)–toluene | 316.15 | ns | **5.12** | **4.09** | **8.90** | **7.97** |
| PVC(39600)–$CCl_4$ | 338.15 | ns | **1.82** | **1.69** | **9.12** | **5.04** |
| PVC(62500)–vinyl chloride | 340.15 | ns | **1.89** | **1.75** | **9.95** | **18.96** |
| PVC(34000)–1,4-dioxane | 315.15 | ns | **10.25** | **18.32** | **5.61** | **6.79** |
| PVC(34000)–THF | 315.15 | s | **9.26** | **16.51** | **6.65** | **8.43** |
| PVC(34000)–di-*n*-propyl ether | 315.15 | ns | **8.62** | **7.47** | **20.03** | **19.52** |
| PVC(34000)–di-*n*-butyl ether | 315.15 | ns | **7.89** | **8.50** | **22.06** | **21.44** |

Additionally, it is investigated whether solvent selection for PVC at 298 K can be based on the $\Omega_1^\infty$-"rule of thumb" together with *aw*-diagrams, where the activity coefficients are plotted as function of the solvent weight fraction [13]. The $\Omega_1^\infty$ values are predicted by four activity coefficient models, Entropic-FV (E-FV), UNIFAC-FV (U-FV), UNIFAC, and GCLF, which are among the best models for such calculations [13], and compared with predicted values by sPC-SAFT. In these calculations the PVC $M_w$ is set to 50000 $g/mol$ as the value of $\Omega_1^\infty$ varies only slightly with the polymer $M_w$. In Table 5.5, the results from the five models are compared with the experimental solvent(s)/non-solvent(ns) data that are available in the literature [11, 12, 14].

The GCLF and sPC-SAFT ($k_{ij} = 0$) models have most wrong answers for solvent/non-solvent assessment for the PVC systems at 298 K. For an isolated group of compounds, which is *n*-alkanes, sPC-SAFT performs well, as seen in Table 5.5. As expected [13], the two free-volume based activity coefficient models, Entropic-FV and UNIFAC-FV, predict solubility assessments with quite good results with the smallest number of wrong calculations.

Table 5.5: Observed and predicted $\Omega_1^\infty$ and *aw*-indications for PVC(50000)–solvent systems at 298 K. Colour indications: Green agrees with experimental assessments. Red disagrees with experimental assessments. Blue means no available answer or $6 < \Omega_1^\infty < 8$. Regarding *aw*-indications: 's' indicates *soluble* chemicals. The system is *immiscible* if the activity value >1. Numeric values are the maximum on solvent activity over solvent weight fraction curves (meaning insoluble chemicals).

| | Solvent | Exp. | E-FV *2 coefficient* [7] | | U-FV *Fred '75* [5] | | GCLF | UNIFAC *1 coefficient* [6] | | sPC-SAFT $k_{ij} = 0$ |
|---|---|---|---|---|---|---|---|---|---|---|
| | | s/ns | $\Omega_1^\infty$ | $a_1(w)$ | $\Omega_1^\infty$ | $a_1(w)$ | $\Omega_1^\infty$ | $\Omega_1^\infty$ | $a_1(w)$ | $\Omega_1^\infty$ |
| 1 | Monochlorobenzene | s | **5.08** | **s** | **3.08** | **s** | **4.54** | **2.45** | **s** | **8.08** |
| | Chloroform | ns | **2.98** | **s** | **4.44** | **s** | **4.54** | **2.11** | **s** | **8.41** |
| | Dichloromethane | s | **3.79** | **s** | **4.12** | **s** | **4.5** | **2.64** | **s** | **10.28** |
| | 1,2-Dichlorobenzene | s | **2.06** | **s** | **1.58** | **s** | **6.22** | **2.01** | **s** | **5.48** |
| | Vinyl chloride | ns | **2.17** | **s** | **3.93** | **s** | **3.8** | — | — | **19.57** |
| 2 | Butyl acrylate | ns | **3.67** | **s** | **8.65** | **1.02** | **12.78** | **4.08** | **s** | **18.25** |
| | 1,4-Dioxane | s | **12.2** | **s** | **19.08** | **1.34** | **5.76** | **14.5** | **1.22** | **11.05** |
| | Tetrahydrofurane | s | — | — | — | — | **6.67** | **7.32** | **1.01** | **13.8** |
| | Di-*n*-propyl ether | ns | **13.58** | **1.03** | **17.1** | **1.13** | **23.49** | **9.52** | **1.01** | **33.75** |
| 3 | *n*-Nonane | ns | **18.89** | **1.24** | **16.27** | **1.08** | **29.89** | **11.57** | **1.02** | **44.79** |
| | *n*-Octane | ns | **17.72** | **1.2** | **15.72** | **1.06** | **27.34** | **10.72** | **1.01** | **44.28** |
| | *n*-Pentane | ns | **15.98** | **1.2** | **15.88** | **1.02** | **22.56** | **8.71** | **s** | **48.22** |
| | *n*-Heptane | ns | **16.72** | **1.16** | **15.31** | **1.05** | **25.24** | **9.96** | **s** | **16.38** |
| 4 | Toluene | s | **2.54** | **s** | **19.9** | **1.72** | **9.16** | **2.87** | **s** | **7.06** |
| | Benzene | s | **4.64** | **s** | **4.47** | **s** | **8.23** | **3** | **s** | **13.11** |
| | *o*-Xylene | s | **11.26** | **1.17** | **5.16** | **s** | **10.2** | **3.85** | **s** | **11.87** |
| 5 | Acetone | ns | **6.44** | **s** | **9.5** | **s** | **8.45** | **6.02** | **s** | **21.96** |
| | Methyl ethyl ketone | s | **5.09** | **s** | **6.63** | **s** | **9.35** | — | — | **16.32** |
| 6 | Nitroethane | ns | — | — | — | — | — | **5.67** | **s** | **9.9** |
| | Carbon disulfide | ns | — | — | — | — | **4.6** | **7.14** | **s** | **8.21** |
| Number of wrong calculations | | | 4 | 5 | 2 | 4 | 7 | 4 | 9 | 9 |
| Total number of calculations | | | 18 | 17 | 17 | 17 | 19 | 18 | 18 | 20 |

### 5.2.3 PVC–Plasticizer Systems

#### 5.2.3.1 Evaluation of $\Omega^{\infty}$

Similar calculations as in Section 5.2.2 are performed in this section. It is investigated how sPC-SAFT performs in predicting plasticizer $\Omega_1^{\infty}$ in PVC, and how these results can be used to predict the miscibility of PVC in plasticizers based on the "rule of thumb" (presented in Section 5.2.1). As seen in Section 5.2.2, only limited amounts of experimental data for PVC containing systems are available in the literature. In fact, there are no direct phase equilibrium data, e.g. activity coefficients, VLE data, etc., available for PVC–plasticizer systems. Therefore, no direct comparison with the results of sPC-SAFT modelling is possible.

To start with, PC-SAFT parameters for various plasticizers are estimated and presented in Table 4.1. Even though sPC-SAFT correlates experimental vapour pressure data accurately for most of the pure plasticizers studied, higher deviations are obtained in a few cases, such as diethyl maleate, dihexyl adipate, methyl oleate, and dibutyl sebacate. This may however be related to experimental uncertainties of the available data [15].

Table 5.6: Predicted $\Omega_1^{\infty}$ values for different PVC(50000)–plasticizer systems at 298 K by sPC-SAFT.

| No. | Plasticizer | $\Omega_1^{\infty}$ |
|---|---|---|
| 1 | Benzyl benzoate | 6.47 |
| | Butyl benzoate | 9.52 |
| | Propyl benzoate | 9.26 |
| 2 | Diethyl maleate | 13.42 |
| | Dimethyl maleate | 10.17 |
| | Dipropyl maleate | 13.27 |
| | Dibutyl maleate | 15.86 |
| 3 | Dimethyl phthalate | 7.14 |
| | Diethyl phthalate | 9.32 |
| | Dipropyl phthalate | 9.62 |
| | Dibutyl phthalate | 11.92 |
| 4 | Dihexyl adipate | 34.20 |
| | Di(2-ethyl hexyl) adipate | 53.77 |
| 5 | Diethyl succinate | 13.66 |
| 6 | Methyl oleate | 38.26 |
| 7 | Dibutyl sebacate | 33.82 |

Table 5.6 lists predicted $\Omega_1^{\infty}$ for different PVC–plasticizer systems at 298 K. The plasticizers are classified into seven families according to their structure. The results show that sPC-SAFT predicts immiscibility with almost all plasticizers as the values of $\Omega_1^{\infty}$ are larger than 8, except for benzyl benzoate and dimethyl phthalate that lie in the uncertainty range (see Section 5.2.1). Again, there are no direct experimental data available for these systems in order to analyse the performance of sPC-SAFT.

Figure 5.6 shows the connection between the predicted plasticizer $\Omega_1^\infty$ and the size of the plasticizer.

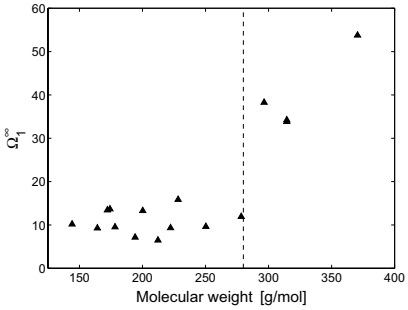


Figure 5.6: Dependency of the plasticizers' $\Omega_1^\infty$ on their $M_w$.

Figure 5.6 shows that the values of $\Omega_1^\infty$ predicted by sPC-SAFT range between 8 and 16 up to the $M_w$ of 280 g/mol. Above this $M_w$, the values of $\Omega_1^\infty$ begin to differ and increase significantly.

In order to arrive at more definite conclusions about the performance of sPC-SAFT in binary PVC systems, it is necessary to have more and better experimental data at different temperatures. Although the models provide highly uncertain activity coefficient predictions, they can be used roughly for pointing out solvents and non-solvents for PVC, either by plotting the entire $aw$-diagram or by using the models in a combination with the semi-empirical "rule of thumb".

## 5.3 Silicone Polymers

The practical applications of selectivity of gas permeation through polymer membranes have generated substantial interest in theoretical methods of studying the underlying molecular mechanisms. Quantitative predictions of permeability and selectivity open the prospect of developing tools for the design of membranes with predefined properties. The properties that determine whether a given polymer is, in practice, suitable for a specific mixture separation are the sorption coefficient, $S$, and the diffusion coefficient, $D$, for each of the mixture components in the polymer. These properties depend strongly on the molecular structure of the polymer and penetrants, and related microscopic properties (i.e. free-volume change, intra- and intermolecular interactions, etc.). The permeability coefficient, $P = DS$, is further used for the calculation of permselectivity[3], $a_{A/B}$, which, for a

[3]The permeation of certain ions in preference to other ions through an ion-exchange membrane determined by difference in the transport rate of various components in the membrane matrix.

specific binary mixture of components A and B, is equal to the ratio of the permeability coefficients of each. For industrial applications, $P_i$ must be as high as possible, whereas, at the same time, $a_{A/B}$ should differ significantly from unity to facilitate separation [16–18].

In most industrial applications, glassy polymers are preferred as permeability is controlled by the diffusivity of the penetrants so that these polymers normally operate by favoring passage of the lighter compound(s) of the mixture. While on the other hand, permeability of rubber polymers is solubility driven and so suitable for separation of heavy component(s).

Poly(dimethylsiloxane) (PDMS) is a widely used rubber polymer for industrial membrane applications. Its derivatives contain the Si–O backbone bonds, which are vulnerable to sulfuric compounds found in natural gases. Another type of polymers contain the $Si(CH_3)_2$ groups attached to the main chains and are distinguished by great gas permeability and diffusion coefficients. These polymers, e.g. poly(dimethyl silamethylene) (PDMSM) are identified as potential membrane materials for the separation of heavy hydrocarbons in natural gas. Figure 5.7 shows the repeating monomer units of PDMS and PDMSM.

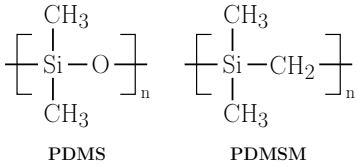


Figure 5.7: Repeating monomer units of PDMS and PDMSM.

The sPC-SAFT model is used to correlate the low pressure phase equilibria of various PDMS–solvent and PDMSM–solvent mixtures. Calculations are compared to experimental data from the literature. Furthermore, the infinite dilution solubility coefficients of various $n$-alkanes, $C_3$–$C_6$, noble gases, and light gases in the two silicone-containing rubber polymers, PDMS and PDMSM, are investigated with sPC-SAFT and compared against available experimental and molecular simulation data.

### 5.3.1 Poly(dimethylsiloxane) (PDMS)

#### 5.3.1.1 Evaluation of PDMS Parameters

As observed in earlier publications [8], and discussed in Section 2.2.3.2 for PVC, pure component polymer parameters for PC-SAFT obtained by methods which use binary phase equilibrium, are not unique for each polymer, but rather depend on the binary system chosen for the regression. The same is demonstrated in Table 5.7 when comparing the

pure component parameters of PDMS obtained from regression over pure polymer PVT data and binary phase equilibrium data in five different ways. The parameter estimation methods are listed in the following:

Case 1: Using only PVT data.

Case 2: Using PVT data and a single binary VLE data set for the system PDMS–*n*-octane.

Case 3: Using PVT data and the same binary VLE data sets as Case 2, with the binary interaction parameter excluded.

Case 4: Using PVT data and ten binary VLE data sets for PDMS with pentane, hexane, heptane, octane, cyclohexane, benzene, and toluene, excluding the binary interaction parameter.

Case 5: Using PVT data and seven binary VLE data are used (with heptane, octane, benzene, and toluene), excluding the binary interaction parameter.

Table 5.7: Values of PC-SAFT parameters and AAD % between calculated and experimental $\rho$ [19] of poly(dimethylsiloxane) (PDMS) using five different data sets for the parameter estimation methods.

| Case | Data set | $m/M_w$ [mol/g] | $\sigma$ [Å] | $\epsilon/k$ [K] | $T$ range [K] | $P$ range [MPa] | AAD $\rho$ [%] |
|---|---|---|---|---|---|---|---|
| 1. | PVT only | 0.03245 | 3.531 | 204.95 | 325–385 | 0.1–100 | 0.1 |
| 2. | PVT + single binary VLE incl. $k_{ij}$ | 0.02240 | 4.070 | 248.77 | 325–385 | 0.1–100 | 0.2 |
| 3. | PVT + single binary VLE excl. $k_{ij}$ | 0.02229 | 4.076 | 248.49 | 325–385 | 0.1–100 | 0.2 |
| 4. | PVT + 10 binary VLE excl. $k_{ij}$ | 0.03998 | 3.225 | 159.65 | 325–385 | 0.1–100 | 2.7 |
| 5. | PVT + 7 binary VLE excl. $k_{ij}$ | 0.02264 | 4.055 | 248.36 | 325–385 | 0.1–100 | 0.2 |

The most commonly used correlation for polymeric PVT data is the *Tait equation* [19]. The Tait equation is able to represent the experimental data for the melt state within the limits of experimental errors, i.e. the maximum deviations between measured and calculated specific volumes are about 0.001–0.002 $\mathrm{cm^3/g}$. As the volumes calculated by the Tait equation do not differ so much from the actual experimental data, the Tait calculated volumes can be considered as equivalent to the experimental values for applications in the present work.

As shown in Table 5.7, the AAD % between sPC-SAFT calculated and experimental liquid density is the lowest when PDMS pure components parameters are based on PVT

data. When using only PVT data for estimation of the parameters, the PDMS parameters are not dependent on any VLE data sets. This gives an opportunity to evaluate the performance of sPC-SAFT on the VLE modeling of PDMS systems with all available solvents. Therefore, the parameter set from Case 1 will be used in the following calculations.

#### 5.3.1.2 Evaluation of VLE

The sPC-SAFT model has been used to calculate the entire composition-pressure diagram for various PDMS–solvent mixtures and results are compared to experimental data. In this case, a binary interaction parameter, $k_{ij}$, has been introduced in order to obtain an accurate correlation with the experimental data.

In Figure 5.8, a representative calculation is shown for the PDMS–*n*-octane mixture at 313 K. Model predictions are in fair agreement with the experiments [20], while $k_{ij} = 0.01$ results in a very accurate correlation of the data over the entire pressure range.

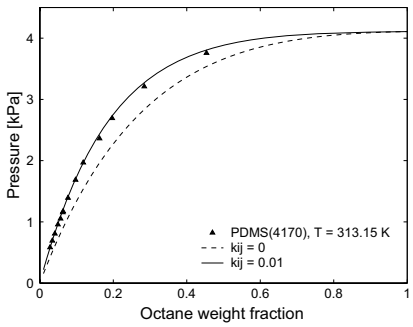


Figure 5.8: Pressure-weight fraction of PDMS–*n*-Octane. Symbols represent experimental data [20], while lines are sPC-SAFT modelling results.

As shown in Figure 5.9, good accuracy is obtained for PDMS–benzene systems at 298, 303, and 313 K with the temperature-independent $k_{ij} = 0.015$. In Figure 5.10, experimental data [20] and sPC-SAFT calculations are shown for PDMS–toluene at 298 and 313 K. The same temperature-independent $k_{ij} = 0.015$ provides a very good correlation of the data.

Modeling results of VLE for all the PDMS–solvent systems with sPC-SAFT are presented in tabulated form in Table 5.8 including optimum $k_{ij}$ values. The overall AAD % for vapour pressure is 32.6 % for predictions and 4.2 % for correlations emphasizing the need to include $k_{ij}$ when modelling PDMS binary systems.

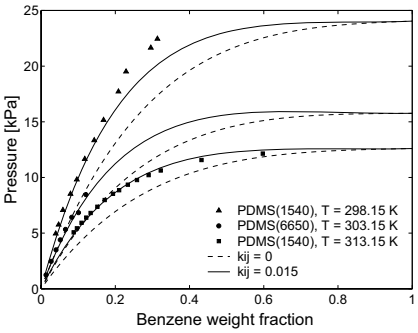


Figure 5.9: Pressure-weight fraction of PDMS–benzene. Symbols represent experimental data [20], while lines are sPC-SAFT modelling results.

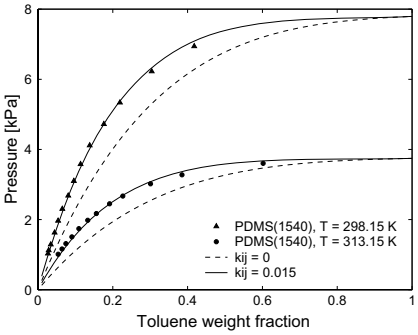


Figure 5.10: Pressure-weight fraction of PDMS–toluene. Symbols represent experimental data [20], while lines are sPC-SAFT modelling results.

Table 5.8: Prediction and correlation of VLE of PDMS–solvent systems with sPC-SAFT.

| System | Temp. [K] | AAD $P$ [%] ($k_{ij} = 0$) | $k_{ij}$ | AAD $P$ [%] | Ref. |
|---|---|---|---|---|---|
| PDMS(1540)–benzene | 298 | 19.2 | 0.015 | 1.5 | [20] |
| | 303 | 30.0 | | 6.2 | |
| | 313 | 26.6 | | 6.7 | |
| PDMS(1540)–toluene | 298 | 24.9 | 0.015 | 3.3 | [20] |
| | 313 | 27.0 | | 2.6 | |
| PDMS(89000)–pentane | 303 | 56.3 | –0.045 | 8.9 | [21] |
| PDMS(4170)–octane | 313 | 29.1 | 0.010 | 2.1 | [20] |
| PDMS(89000)–cyclohexane | 303 | 48.1 | –0.030 | 1.9 | [22] |
| AAD [%] overall | | 32.6 | | 4.2 | |

#### 5.3.1.3 Evaluation of $\Omega^{\infty}$

The sPC-SAFT modelling of full isotherms, from zero up to high solvent concentrations in PDMS mixtures, has been presented in Section 5.3.1.2. In this section, a comparison of sPC-SAFT modelling is conducted against relevant experimental data [11, 12] for the case of infinite dilution.

Solvent weight fraction activity coefficients at infinite dilution ($\Omega_1^{\infty}$) for several PDMS–solvent systems at different temperatures and polymer $M_w$ have been predicted by sPC-SAFT. The results are presented in Table 5.9. It can be observed that the model can predict the $\Omega_1^{\infty}$ within 26 % overall deviation. There is a tendency that sPC-SAFT underestimates the solvent activity for all investigated systems. As the experimental errors of activity coefficint are often rather large for polymer solutions, it is not possible to draw any final conclusions on this matter.

Table 5.9: Experimental [11, 12] and predicted $\Omega_1^\infty$ values for PDMS–solvent systems with sPC-SAFT.

| Solvent | PDMS characteristics | | | Exp. | sPC-SAFT ($k_{ij} = 0$) | |
|---|---|---|---|---|---|---|
| | $M_n$ | $M_w$ | $T$ | $\Omega_1^\infty$ | $\Omega_1^\infty$ | AAD $\Omega_1^\infty$ [%] |
| Pentane | 20700 | 95300 | 303.2 | 5.937 | 5.376 | 9.5 |
| | 208000 | 580000 | 303.2 | 5.964 | 5.418 | 9.1 |
| Benzene | 89000 | — | 303.0 | 6.404 | 4.066 | 36.5 |
| Cyclohexane | 20700 | 95300 | 303.2 | 5.227 | 3.799 | 27.3 |
| | 89000 | — | 303.0 | 5.378 | 3.820 | 29.0 |
| | 208000 | 580000 | 303.2 | 5.208 | 3.823 | 26.6 |
| Hexane | 20700 | 95300 | 303.2 | 5.854 | 4.727 | 19.2 |
| | 89000 | — | 303.0 | 6.023 | 4.761 | 21.0 |
| | 208000 | 580000 | 303.2 | 5.863 | 4.766 | 18.7 |
| Toluene | 89000 | — | 303.0 | 6.457 | 3.721 | 42.4 |
| Methylcyclohexane | 89000 | — | 303.0 | 4.712 | 3.522 | 25.2 |
| Heptane | 20700 | 95300 | 303.2 | 5.927 | 4.358 | 26.5 |
| | 20800 | 580000 | 303.2 | 5.92 | 4.396 | 25.7 |
| Octane | 20700 | 95300 | 303.2 | 6.169 | 4.041 | 34.5 |
| | 20800 | 580000 | 303.2 | 6.14 | 4.041 | 34.2 |
| AAD [%] overall | | | | | | 25.7 |

The results in Table 5.10 show the estimation of $\Omega_1^\infty$ for PDMS–solvent systems when using $k_{ij}$ from finite VLE (see Table 5.8). In fact, this investigation shows that introducing $k_{ij}$ from VLE calculations does not improve the $\Omega_1^\infty$ calculations. As in the case for the PVC binary mixtures, the values of $k_{ij}$ are specific with regards to system and type of calculation.

Table 5.10: Experimental [11, 12] and correlated $\Omega_1^\infty$ values for PDMS–solvent systems using sPC-SAFT with $k_{ij}$ from finite VLE.

| Solvent | PDMS characteristics | | | Exp. | sPC-SAFT ($k_{ij} \neq 0$) | | |
|---|---|---|---|---|---|---|---|
| | $M_n$ | $M_w$ | $T$ | $\Omega_1^\infty$ | $k_{ij}$ | $\Omega_1^\infty$ | AAD $\Omega_1^\infty$ [%] |
| Pentane | 20700 | 95300 | 303.2 | 5.937 | –0.045 | 1.781 | 70.0 |
| | 208000 | 580000 | 303.2 | 5.964 | | 1.784 | 70.2 |
| Benzene | 89000 | — | 303.0 | 6.404 | 0.015 | 5.852 | 8.6 |
| Cyclohexane | 20700 | 95300 | 303.2 | 5.227 | –0.030 | 1.725 | 67.1 |
| | 89000 | — | 303.0 | 5.378 | | 1.723 | 67.8 |
| | 208000 | 580000 | 303.2 | 5.208 | | 1.727 | 66.8 |
| Toluene | 89000 | — | 303.0 | 6.457 | 0.015 | 5.699 | 11.9 |
| Octane | 20700 | 95300 | 303.2 | 6.169 | 0.010 | 5.880 | 4.5 |
| | 20800 | 580000 | 303.2 | 6.14 | | 5.910 | 3.9 |
| AAD [%] overall | | | | | | | 38.0 |

### 5.3.2 Poly(dimethylsilamethylene) (PDMSM)

#### 5.3.2.1 Evaluation of PDMSM Parameters

PDMSM is not a polymer as widely studied as PDMS and therefore only limited melt density data are available. There are no PC-SAFT parameters available for PDMSM in the literature, so the starting point is to obtain these parameters. The analysed estimation methods for obtaining PDMSM parameters are:

Case 1: Two parameters, $m/M_w$ and $\epsilon/k$, are calculated with the Kouskomvekaki *et al.* [8] method using dimethyl silazane as the corresponding monomer. The remaining parameter, $\sigma$, is obtained by fitting to relatively few melt density data available over a narrow temperature and pressure range [17].

Case 2: PDMDM is a non-polar elastomer whose chemical structure closely resembles the structure of polyolefins. Consequently, the energetic interactions between PDMSM segments are expected to be close to those between polyolefin segments. For this reason, previously published PC-SAFT parameters for polyethylene(PE) [8] are used for PDMSM.

Case 3: The $m/M_w$ from Case 1 and $\epsilon/k$ from Case 2 are used as fixed variables, and the remaining $\sigma$ parameter is fitted to the density data.

Case 4: The $\epsilon/k$ from Case 2 is used as a fixed variable, and the other two parameters, $m/M_w$ and $\sigma$, are fitted to the density data.

As shown in Table 5.11, the lowest AAD % between accurate molecular simulation density results [17] in the temperature range 300–400 K and pressures up to 160 MPa, and sPC-SAFT correlation is obtained with the parameters from Case 4.

Table 5.11: Values of PC-SAFT parameters and AAD % between calculated and simulated $\rho$ [17] of poly(dimethylsilamethylene) (PDMSM) using four different approaches for the regression.

| Case | Approach | $m/M_w$ [mol/g] | $\sigma$ [Å] | $\epsilon/k$ [K] | AAD $\rho$ [%] |
|---|---|---|---|---|---|
| 1 | Kouskomvekaki *et al.* [8] | 0.0145 | 4.971 | 347.7 | 3.3 |
| 2 | Parameters equivalent to PE | 0.0254 | 4.107 | 272.4 | 6.0 |
| 3 | Fixed $m/M_w$ and $\epsilon/k$ | 0.0145 | 4.893 | 272.4 | 4.2 |
| 4 | Fixed $\epsilon/k$ | 0.0563 | 3.8054 | 272.4 | 1.0 |

The following calculations are performed in order to check the accuracy of used density data obtained by MS simulations [17] and to compare the values with the values obtained using predictive density approaches, such as the Group-Contribution VOLume (GC-VOL) [23] and the van Krevelen [24] methods. For both of these latter methods, PDMSM is

divided into the following groups: 2×$CH_3$, 1×$CH_2$, and 1×Si per repeating unit as the chemical structure of the polymer is $[(CH_3)_2Si(CH_2)]_n$ (see Figure 5.7).

Table 5.12: Comparison of PDMSM density data predictions from molecular dynamics (MD) with other predictive approaches.

| Temperature [K] | MD [g/cm³] | GC-VOL [g/cm³] | AAD $\rho$ [%] | van Krevelen [g/cm³] | AAD $\rho$ [%] |
|---|---|---|---|---|---|
| 300.1 | 0.918 | 0.803 | 14.3 | 0.844 | 8.8 |
| 350.1 | 0.893 | 0.728 | 22.6 | 0.818 | 9.1 |
| 400.1 | 0.871 | 0.637 | 36.7 | 0.794 | 9.7 |
| AAD [%] overall | | | 24.5 | | 9.2 |

Table 5.12 shows deviations between densities estimated by the GC-VOL and the van Krevelen models, and densities determined by molecular simulation. The overall AAD % for the prediction of PDMSM density is 24.5 % for GC-VOL and 9.2 % for van Krevelen in the tested temperature range. Data are also plotted in Figure 5.11.

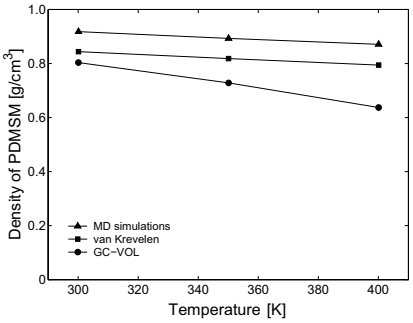


Figure 5.11: Density predictions for PDMSM with different models. Data from Table 5.12.

In this calculation, the GC-VOL method is used to predict densities for amorphous polymers, as the glass transition temperature for PDMSM is 187 K, and as it most closely resembles the liquid density of a solvent at the temperatures between the glass transition temperature and the degradation temperature.

The performance of each parameter set for PDMSM in VLE calculations with sPC-SAFT is further evaluated in the following section.

#### 5.3.2.2 Evaluation of VLE

The sPC-SAFT model is applied to a few binary systems of PDMSM with several *n*-alkanes (methane, propane, butane, and hexane). The four sets of PDMSM parameters from Table 5.11 are used to obtain the following VLE modelling results, which are then compared to the experimental data.

Modeling results of VLE for all the PDMSM–*n*-alkane systems with sPC-SAFT are summarized in Table 5.13 including optimum $k_{ij}$ values and the average deviations for vapour pressure.

Table 5.13: Optimised $k_{ij}$ and AAD % for PDMSM–alkane binary mixtures for Case 1–4.

| System | Parameters from Case no. | $k_{ij}$ | AAD $P$ [%] | Figure |
|---|---|---|---|---|
| PDMSM–hexane | 1 | 0.035 | 19.2 | (5.12) |
| | 2 | –0.01 | 3.5 | (5.13) |
| | 3 | –0.03 | 6.9 | (5.14) |
| | 4 | –0.07 | 10.5 | (5.15) |
| PDMSM–butane | 1 | –0.05 | 24.2 | (5.16) |
| | 2 | –0.014 | 17.0 | (5.17) |
| | 3 | –0.045 | 10.6 | (5.18) |
| | 4 | –0.065 | 18.7 | (5.19) |
| PDMSM–propane | 1 | –0.03 to –0.07 | 72.5, 43.8, 17.2 | (5.20) |
| | 2 | –0.019 | 16.7, 7.2, 6.5 | (5.21) |
| | 3 | –0.035 | 24.7, 12.1, 9.9 | (5.22) |
| | 4 | –0.085 | 3.9, 4.7, 3.5 | (5.23) |
| PDMSM–methane | 1 | –0.22 to –0.15 | 9.8, 7.1, 13.0 | (5.24) |
| | 2 | –0.065 | 12.2, 2.3, 27.6 | (5.25) |
| | 3 | –0.08 to –0.04 | 2.3, 4.5, 9.6 | (5.26) |
| | 4 | –0.19 to –0.15 | 2.1, 1.0, 11.2 | (5.27) |

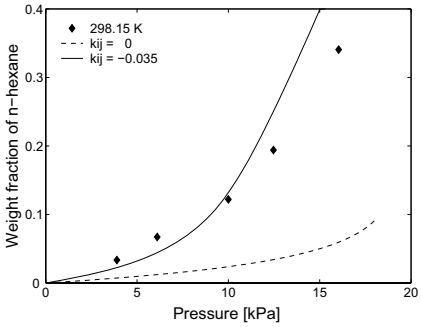


Figure 5.12: Solubility of $n$-hexane in PDMSM. Experiments (symbols) and sPC-SAFT (lines) using parameters from Case 1.

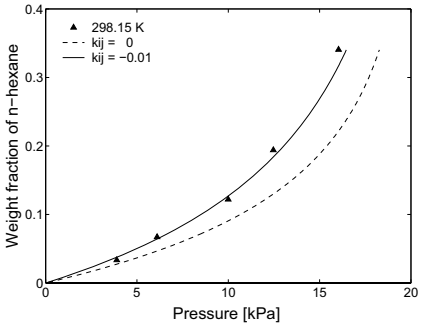


Figure 5.13: Solubility of $n$-hexane in PDMSM. Experiments (symbols) and sPC-SAFT (lines) using parameters from Case 2.

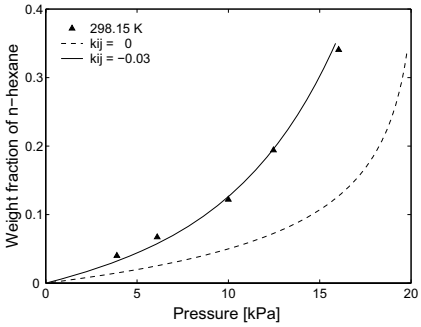


Figure 5.14: Solubility of $n$-hexane in PDMSM. Experiments (symbols) and sPC-SAFT (lines) using parameters from Case 3.

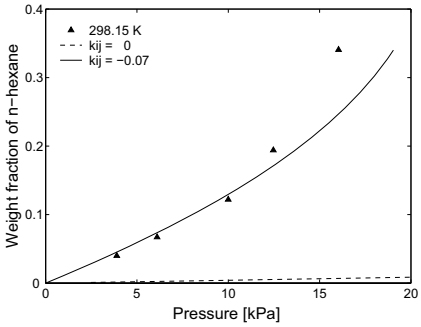


Figure 5.15: Solubility of $n$-hexane in PDMSM. Experiments (symbols) and sPC-SAFT (lines) using parameters from Case 4.

For the PDMSM–$n$-hexane mixture in Figures 5.12–5.15, sPC-SAFT correlation and prediction are in good agreement with the experimental data over the low-pressure range in all four cases, but fails in Case 1 and 4 when the pressure is increased. This is observed in Figures 5.12 and 5.15 requiring rather high $k_{ij}$ values to correlate data.

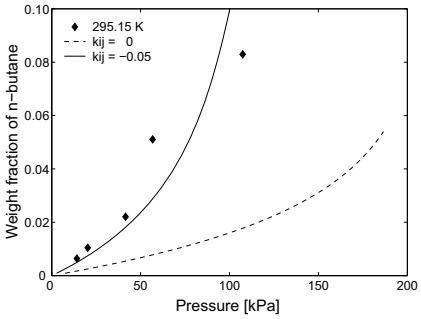


Figure 5.16: Solubility of $n$-butane in PDMSM. Experiments (symbols) and sPC-SAFT (lines) using parameters from Case 1.

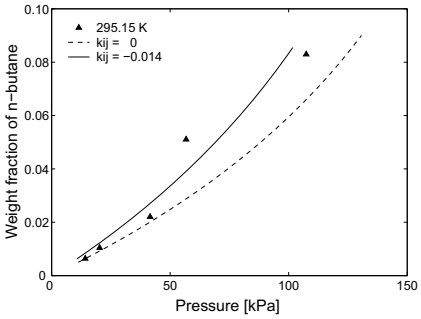


Figure 5.17: Solubility of $n$-butane in PDMSM. Experiments (symbols) and sPC-SAFT (lines) using parameters from Case 2.

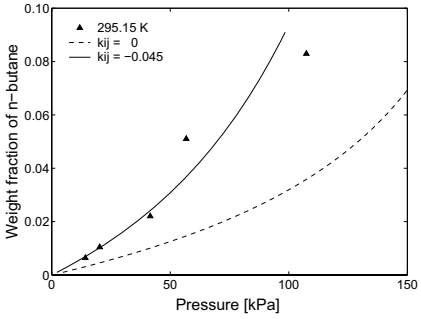


Figure 5.18: Solubility of $n$-butane in PDMSM. Experiments (symbols) and sPC-SAFT (lines) using parameters from Case 3.

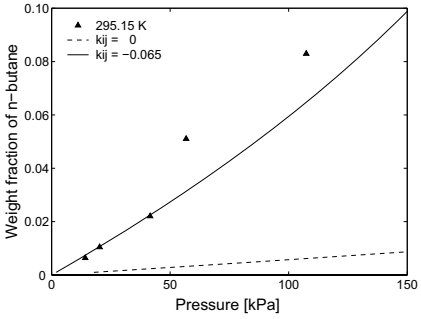


Figure 5.19: Solubility of $n$-butane in PDMSM. Experiments (symbols) and sPC-SAFT (lines) using parameters from Case 4.

For the $n$-butane–PDMSM mixtures in Figures 5.16–5.19, some scatter is observed in the experimental data at higher pressures, which makes the comparison difficult. However, sPC-SAFT can predict the data well over the low-pressure range; especially when using the parameters from Case 2.

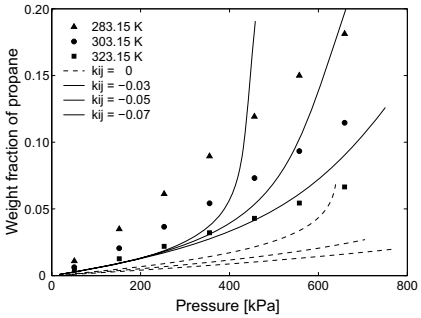


Figure 5.20: Solubility of $n$-propane in PDMSM. Experiments (symbols) and sPC-SAFT (lines) using parameters from Case 1.

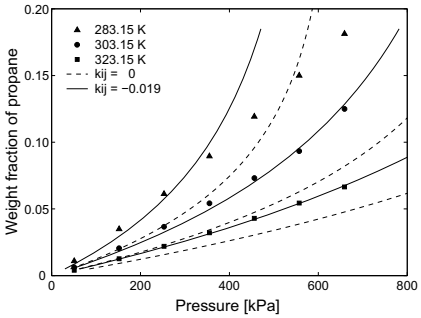


Figure 5.21: Solubility of $n$-propane in PDMSM. Experiments (symbols) and sPC-SAFT (lines) using parameters from Case 2.

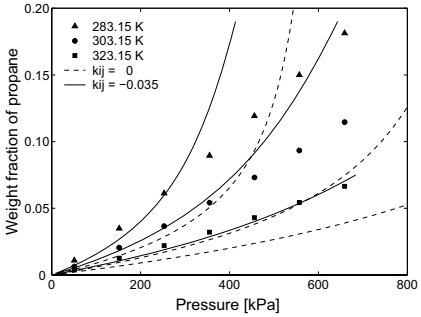


Figure 5.22: Solubility of $n$-propane in PDMSM. Experiments (symbols) and sPC-SAFT (lines) using parameters from Case 3.

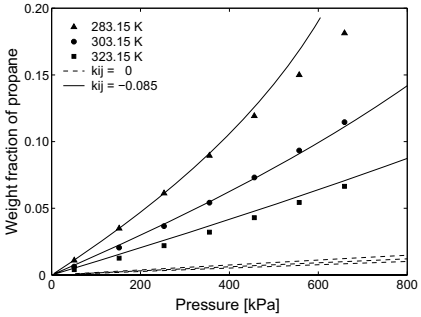


Figure 5.23: Solubility of $n$-propane in PDMSM. Experiments (symbols) and sPC-SAFT (lines) using parameters from Case 4.

The existing experimental data of $n$-propane in PDMSM (Figures 5.20 to 5.23) cover a broader temperature and pressure range than the data of heavier alkanes. sPC-SAFT correlates particularly well the experimental data in Figure 5.23 for Case 4 using a temperature independent binary interaction parameter $k_{ij}$.

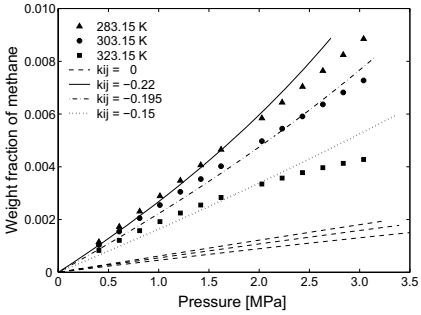


Figure 5.24: Solubility of methane in PDMSM. Experiments (symbols) and sPC-SAFT (lines) using parameters from Case 1.

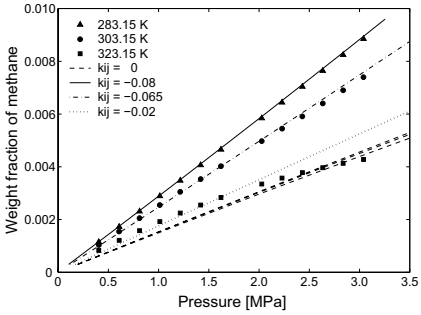


Figure 5.25: Solubility of methane in PDMSM. Experiments (symbols) and sPC-SAFT (lines) using parameters from Case 2.

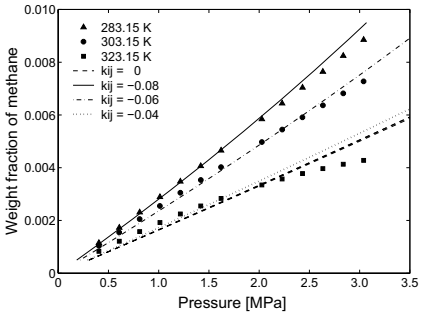


Figure 5.26: Solubility of methane in PDMSM. Experiments (symbols) and sPC-SAFT (lines) using parameters from Case 3.

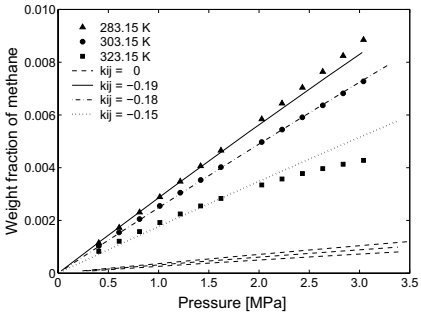


Figure 5.27: Solubility of methane in PDMSM. Experiments (symbols) and sPC-SAFT (lines) using parameters from Case 4.

Solubility values of methane in PDMSM are more than one order of magnitude lower than the solubility values of other higher weight alkanes. sPC-SAFT fails to correlate the experimental data well with a temperature independent $k_{ij}$. Therefore, different values of binary interaction parameters have been used as presented in Figures 5.24 to 5.27. Additionally, sPC-SAFT underpredicts the experimental data in Case 1 and 4.

In this investigation involving Figures 5.12–5.27, the most satisfying modelling results of VLE data with sPC-SAFT are obtained using the parameter sets of Case 4 for PDMSM. Therefore, this parameter set is used in further calculations with PDMSM.

### 5.3.3 Calculation of $S_o$ with sPC-SAFT

In this section, the solubilities of various $n$-alkanes and gases in PDMS and PDMSM are calculated by sPC-SAFT. Pure components parameters for PDMS used in the following calculations are $m/M_w = 0.03245\,\mathrm{mol/g}$, $\sigma = 3.5310\,\text{Å}$, and $\epsilon/k = 204.95\,\mathrm{K}$, while for PDMSM $m/M_w = 0.0563\,\mathrm{mol/g}$, $\sigma = 3.8054\,\text{Å}$, and $\epsilon/k = 272.40\,\mathrm{K}$. Results are compared with results obtained from molecular simulation performed at the isobaric-isothermal (NPT) ensemble [18], and experimental data [25] when available.

Molecular dynamic (MD) simulation results for $S_o$ for all the systems examined are taken from Economou *et al.* [26]. Calculations for PDMSM are reported at 300, 350, and 400 K, while calculations for PDMS are provided over a wider temperature range up to 450 K. Calculations and limited experimental data for $S_o$ of $n$-alkanes in PDMSM and PDMS at 0.1 MPa are shown in Figure 5.28.

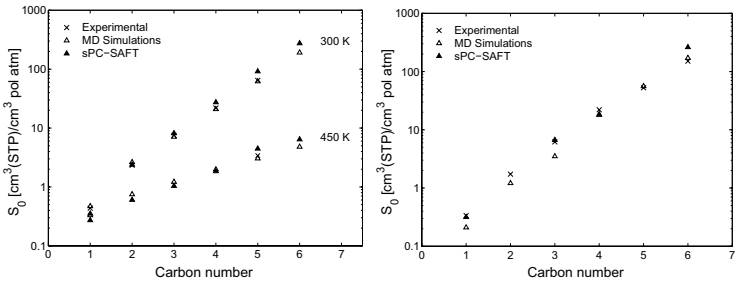


Figure 5.28: The infinite dilution solubility coefficient of $n$-alkanes in PDMS (left) and PDMSM (right) at 0.1 MPa.

The solubility investigation from this work depicts several interesting features. In all cases, solubility increases with $n$-alkane carbon number. The obtained results are in good agreement with available experiment data. Furthermore, for a given $n$-alkane, $S_o$ values are very similar for the two investigated polymers. In other words, the chemical structure of the polymer for these two polymers has very little effect on the solubility of the solvents.

$S_o$ of various solvents in a polymer correlate nicely with the solvent experimental critical temperature ($T_c$) [25]. In Figure 5.29, experimental data [25], molecular simulation calculations, and sPC-SAFT predictions are shown for eight different gases in PDMS. Predictions from sPC-SAFT are in good agreement with the experimental data and MD results in all cases showing that the solubility correlates strongly with the $T_c$ of the solvent. Additionally, from this data, it is observed that the dependency of solubility on $T_c$ diminishes as the temperature of the system increases.

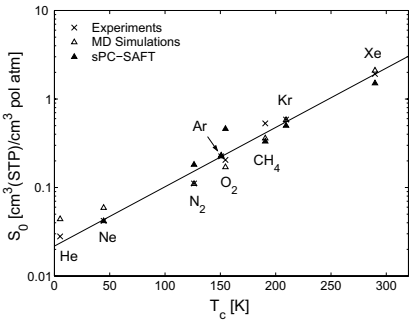


Figure 5.29: Predicted infinite dilution solubility coefficient of gases in PDMS versus their experimental critical temperature at 300 K. The solid line is a linear fit to experimental data.

In Figure 5.30, an interesting temperature dependence on $S_o$ is observed for different solvents. For the lighter gas He solubility increases with temperature. For the intermediate gases, including Ar, $N_2$, and $O_2$, solubility is fairly independent of temperature, while for the heavier ones, such as $CH_4$, Kr, Xe, and beyond, solubility decreases as temperature increases.

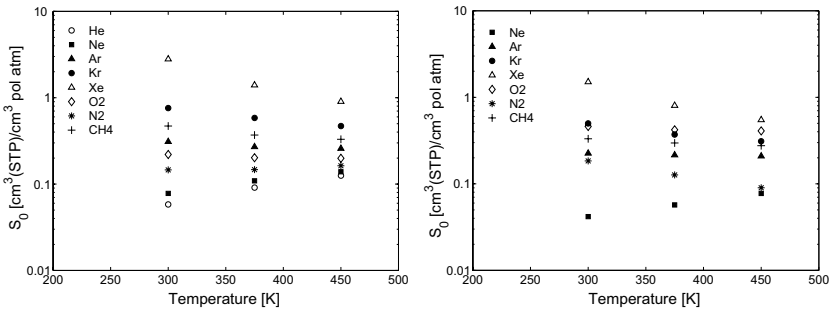


Figure 5.30: The predicted infinite dilution solubility coefficient of gases in PDMS by MD (left) and sPC-SAFT (right) at 300, 375, and 450 K.

In the present investigation, a systematic crossover is observed for both polymers, where the solubility crosses at the single value of the $T_c$ of the solvent. For PDMSM, the crossover temperature is estimated from a least square fit to the data and is around 150–160 K, while for PDMS it is a little lower at around 125–135 K. This behaviour has been observed experimentally by van Amerongen [27] for various gases in natural rubber

where the crossover is estimated to occur between $N_2$ and $O_2$ in the critical temperature range of $T_c = 126 - 154\,\mathrm{K}$. Furthermore, the same phenomenon is predicted by Curro *et al.* [28] for noble gases in PE using an accurate integral equation theory known as polymer reference interaction site (PRISM). PRISM has predicted a crossover value of $T_c = 165\,\mathrm{K}$, which is in good agreement with experiments and predictions shown in their work. With the exceptions of the prediction from PRISM, all sets of data and calculations agree in the temperature range of crossover. The crossover temperature seems to be independent of the nature of the polymer (at least for the two polymers examined) and depends only on the solvent.

A phenomenological explanation for this behaviour can be based on combined energetic and entropic effects. A temperature increase results in a decrease of the polymer density or increase of the free volume accessible to small molecules and so light gases become more soluble. On the other hand, the temperature increase makes heavier solvent molecules behave more like gas molecules with a significant decrease in their density and a substantial decrease in their solubility in polymer [26].

## 5.4 High $T, P$ Polymer–Solvent VLE

Even though high-pressure VLE data for polymer–solvent systems are essential for the design and optimization of various processes such as polymer synthesis and devolatilization, at present, only limited data at high pressures are available in the literature. In addition, only a few publications deal with modelling of this type of systems using the models based on the SAFT EoS. Pure components parameters for LDPE used in the following calculations are $m/M_w = 0.0263\,\mathrm{mol/g}$, $\sigma = 4.0217\,\text{Å}$, and $\epsilon/k = 249.5\,\mathrm{K}$ taken from [29] with the reported AAD % for density of 1.1 %.

VLE data of low density polyethylene (LDPE) with ethylene is presented in Figure 5.31 together with the sPC-SAFT calculations. Model predictions are in fair agreement with the experimental data [30] at all three temperatures. Deviations increase as the temperature of the system increases when the optimum temperature-independent $k_{ij} = 0.013$ is used. Using a temperature dependent $k_{ij}$ does not improve the sPC-SAFT correlations significantly.

Experimental VLE data of LDPE with *n*-pentane, cyclopentane, 3-pentanone, propyl acetate, and isopropyl acetate at temperatures of 423.15 and 473.15 K, and solvent concentration up to 50 % by weight reported by Surana *et al.* [31] are used in the following calculations with sPC-SAFT.

Figure 5.32 shows the VLE data and the modeling results for LDPE with *n*-pentane. For this particular case, sPC-SAFT gives rather good results within lower pressures, but shows considerable underprediction at pressures higher than 1 MPa. At 473.15 K, where *n*-pentane is above its critical temperature, the modeling is not successful.

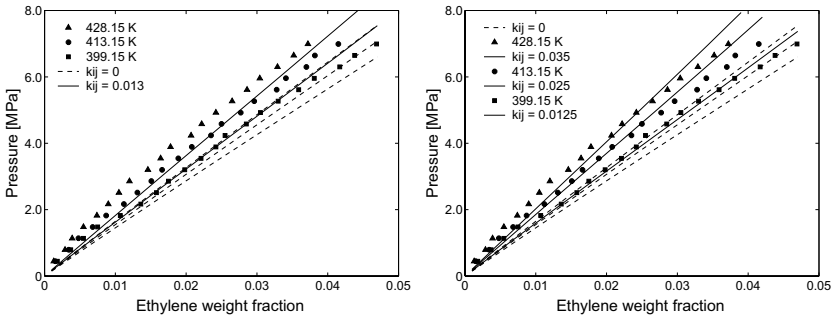


Figure 5.31: Pressure-weight fraction of LDPE and ethylene. Symbols represent experimental data [30], while lines are sPC-SAFT modelling results with temperature-independent $k_{ij}$ (left) and temperature-dependent $k_{ij}$ (right).

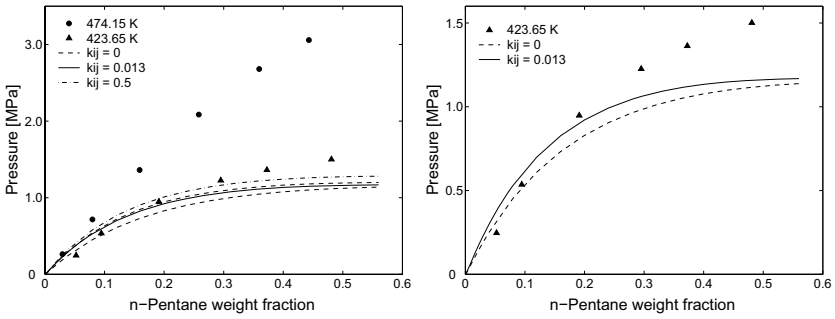


Figure 5.32: Pressure-weight fraction of LDPE and $n$-pentane. Left figure only shows results at 423.65 K. Symbols represent experimental data [31], while lines are sPC-SAFT modelling results.

For cyclopentane, however, sPC-SAFT provides good predictions of experimental data at 425.15 K with the AAD % in the pressure of 9 % over the entire concentration range, as presented in Figure 5.33. More accurate correlations of the data at 473.15 K are obtained by introducting $k_{ij} = 0.015$, which gives the AAD % of 15 % in the pressure.

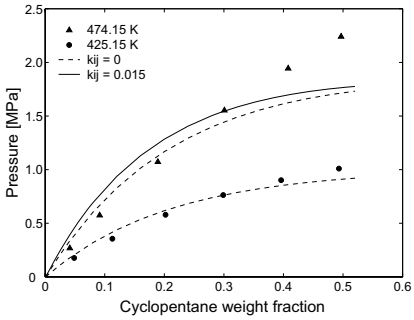


Figure 5.33: Pressure-weight fraction of LDPE and cyclopentane. Symbols represent experimental data [31], while lines are sPC-SAFT modelling results.

Figures 5.34 and 5.35 represent the VLE data and the corresponding sPC-SAFT predictions and correlations for binary mixtures of LDPE with two moderately polar compounds: 3-pentanone and propyl acetate. Despite the polar nature of these compounds, the model performs well for these two systems with the temperature independent $k_{ij}$ of 0.015.

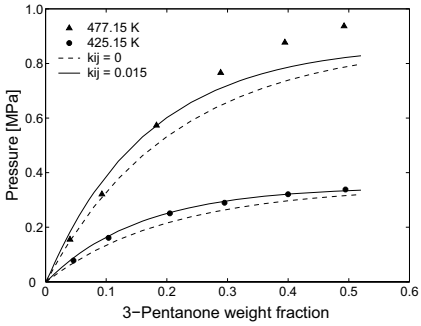


Figure 5.34: Pressure-weight fraction of LDPE and 3-pentanone. Symbols represent experimental data [31], while lines are sPC-SAFT modelling results.

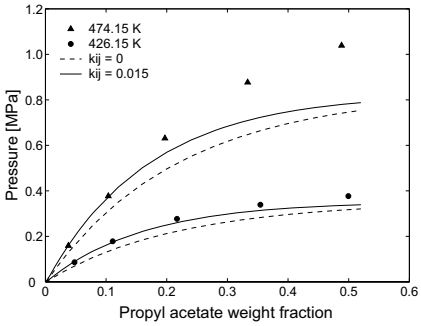


Figure 5.35: Pressure-weight fraction of LDPE and propyl acetate. Symbols represent experimental data [31], while lines are sPC-SAFT modelling results.

In Figure 5.36, experimental VLE and sPC-SAFT calculations are shown for the LDPE–isopropyl amine system. The model cannot represent the data at 473.15 K as the amine here is above its critical temperature of 471.9 K, but the agreement is reasonable at 427.15 K.

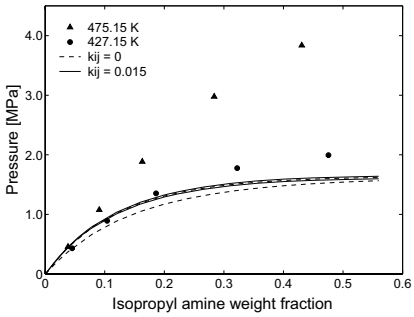


Figure 5.36: Pressure-weight fraction of LDPE and isopropyl amine. Symbols represent experimental data [31], while lines are sPC-SAFT modelling results.

The evaluation of the VLE data of LDPE for a variety of solvents; both nonpolar and polar, at high pressure and temperatures with sPC-SAFT shows that the model is capable of representing the experimental data. The AAD % in pressure are 14.5 and 25.1 % at 423.15 and 473.15 K respectively in the case of the predictions of the model, and 7.5 and 18.3 % for the correlations. It is advisable to use a temperature independent $k_{ij}$ of 0.015 for all binary LDPE systems in order to obtain quantitatively better results. However, it seems that the model cannot represent the experimental results for temperatures above the critical point of the solvents.

## 5.5 Polymer Blends

Polymer blends, by definition, are physical mixtures of structurally different homopolymers or copolymers. In polymer blends or polymer alloys, the mixing of two or more polymers provides a new material with a modified array of properties. Within the past years, the use of polymer blends is constantly increasing due to the numerous chemical and mechanical properties that they exhibit making them suitable for various applications. The study of the blend miscibility is of major importance as it affects the physical properties of the final blend and, at the same time, determines the fields of applications. Polymer blends exhibit very complex phase behaviour due to free-volume, dispersion forces, compressibility effects and specific interactions between the consistent compounds. At low temperatures and in the absence of specific interactions, polymer blends are not miscible

due to dispersion forces. As the temperature increases, these effects diminish and mixing occurs as a result of the entropy of mixing until free-volume effects become important and immiscibility starts to occur. It is not always possible to reach those temperatures experimentally. In typical cases, phase separation should be expected and the majority of the binary polymer blends are hence incompatible over much of the concentration range [32–34].

The study of phase behaviour of polymer blends is hampered by the scarcity of accurate experimental data because experimental measurements of polymer blend miscibility are far more difficult than that of polymer–solvent solutions. Particularly troublesome is the attainment of the equilibrium state after the phase separations, because the high viscosity of polymer blends leads to very slow diffusion. Moreover, traditional methods for measuring phase boundaries, free energy, etc. are not applicable to polymer blends. As a consequence, only few results are available in the literature and limited work has been done from modification of the original Flory-Huggins expression, to cubic and more complex EoS for the prediction and correlation of blend miscibility [35–39]. The results presented in these articles show that it is rather difficult to correlate simultaneously the variation of the binodal curves with respect to $M_w$ and the concentration.

The purpose of this study is to apply sPC-SAFT to LLE calculations of polymer blends which do not exhibit strong specific interactions, and hence investigate the suitability of the model for similar phase equilibria calculations and identify strong points as well as limitations. Only a small number of polymer blends are considered as preliminary examples of the applicability of sPC-SAFT for this kind of mixtures. One should also note that all applied experimental data correspond to nearly monodispersive polymers, having polydispersity indices $<$1.1, which is not expected to have a significant influence on blend miscibility.

Pure components parameters for polymers used in the calculations are listed in Table 5.14.

Table 5.14: Pure polymer parameters for PC-SAFT EoS.

| Polymer | $m/M_w$ [mol/g] | $\sigma$ [Å] | $\epsilon/k$ [K] | $T$ range [K] | AAD $\rho$ [%] | Ref. |
|---|---|---|---|---|---|---|
| PS | 0.0205 | 4.152 | 348.2 | 390–470 | 0.6 | [8] |
| PBD | 0.0245 | 4.097 | 288.84 | 320–380 | 1.0 | t.w. |
| P-$\alpha$MS | 0.0204 | 4.204 | 354.055 | 320–380 | 1.0 | t.w. |
| PMMA | 0.027 | 3.553 | 264.6 | 390–430 | 1.0 | [8] |

The experimental data for the PS–PBD system are rather numerous compared to other polymer blends, and therefore a more detailed investigation of the description of the phase behaviour with sPC-SAFT is performed for this mixture. Additionally, the effect of $M_w$ and the sensitivity of $k_{ij}$ values on the modelling results with sPC-SAFT are investigated.

The effect of $M_w$ on the phase behaviour for the PS–PBD blend is shown in Figure 5.37 where the $M_w$ of PBD is kept constant while varying $M_w$ of PS from 1340 to 4370 g/mol. As $M_w$ increases, mobility of polymer chains and the entropy of the system decreases so that higher temperatures are needed to overcome the enthalpy of mixing and obtain one phase region. Therefore, as presented in Figure 5.37, higher $M_w$ of PS gives higher CST values for the related system.

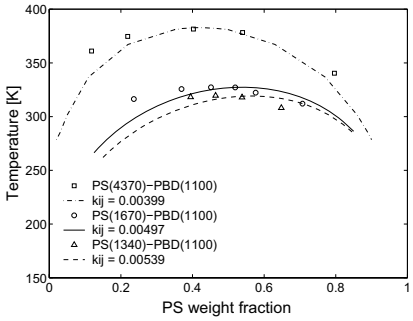


Figure 5.37: Temperature–weight fraction of PS–PBD(1100). Symbols represent experimental data [37], while lines are sPC-SAFT modelling results.

The optimum $k_{ij}$ values determined from UCST data for the PS–PBD blends are plotted versus $M_w$ of the polymer in Figure 5.38. The obtained plot indicates that $k_{ij}$ decreases with increasing $M_w$ of PS but there is some scatter observed. The $k_{ij}$ values can be roughly represented by the linear Equation (5.2) and can consequently be used to predict the UCST for the PS blends with PBD. The predicted versus the experimental UCST values for the systems included in the analysis are plotted in Figure 5.38 where satisfactory correlations can be observed.

$$k_{ij} = -9.07 \times 10^{-7} M_w + 1.61 \times 10^{-3} \tag{5.2}$$

A case where sPC-SAFT has difficulties representing qualitatively the shape of the phase diagram for the PS–PBD blend is presented in Figure 5.39. As this is the only experimental data available, it is not possible to check if the reason for this deviation is due to experimental uncertainties or lack of suitability of the model.

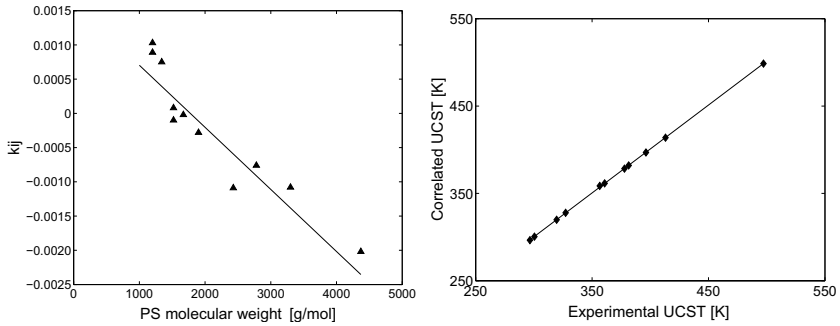


Figure 5.38: Correlated UCTS versus optimum $k_{ij}$ and versus experimental UCST for PS–PBD blends.

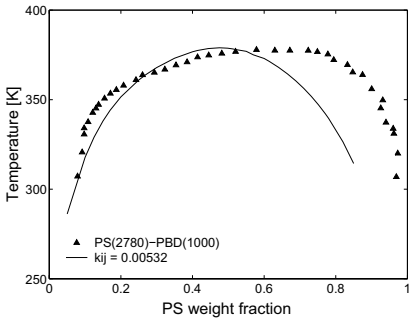


Figure 5.39: Temperature–weight fraction of PS–PBD. Symbols represent experimental data [40], while lines are sPC-SAFT modelling results.

Another blend of PS which exhibits no polarity, hydrogen bonding, or other specific interactions, is with poly($\alpha$-methyl styrene) (P-$\alpha$MS). Figure 5.40 shows that sPC-SAFT models the phase behaviour of this blend quite well and is moreover able to capture the change in $M_w$.

As shown in Figure 5.41 for the blend of PS(1250) with PMMA(6350), sPC-SAFT describes rather accurately the UCST using a single $k_{ij} = -0.0095$.

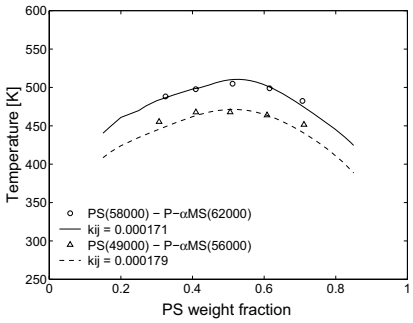


Figure 5.40: Temperature–weight fraction of PS–P-$\alpha$MS. Symbols represent experimental data [41], while lines are sPC-SAFT modelling results.

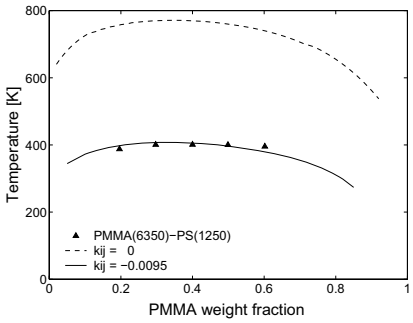


Figure 5.41: Temperature–weight fraction of PS–PMMA. Symbols represent experimental data [35], while lines are sPC-SAFT modelling results.

The phase behavior of the semicrystalline polymer blend composed of isotactic polypropylene (iPP) and linear low density polyethylene (LDPE) is studied where polymers have rather high $M_w$ of 100440 and 152000 g/mol, respectively. Sensitivity of the model on the $k_{ij}$ value is considerably high. Figure 5.42 illustrates the binary phase diagram of this blend showing that the model can correlate UCST well, but the shape of the phase diagram is not in good agreement with the experimental data.

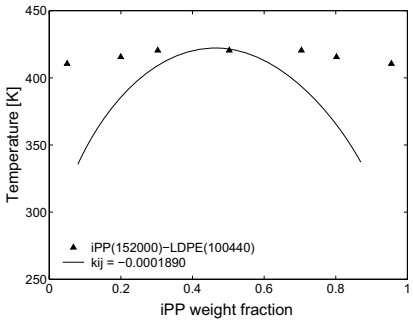


Figure 5.42: Temperature–weight fraction of iPP–LDPE. Symbols represent experimental data [42], while lines are sPC-SAFT modelling results.

Generally, for ordinary non-polar systems, such as PS–P-$\alpha$MS and PS–PBD blends, very satisfactory results are obtained with the sPC-SAFT model. For the *i*PP–LDPE blend the results are less satisfactory. It seems that monomer structural effects, inaccurate polymer parameters estimation (side branches have been neglected) or even high polydispersity of experimental cloud points can have an effect on the modeling results on polymer blends. It is observed that for blends exhibiting both UCST and LCST, the sPC-SAFT model is highly sensitive with respect to the binary interaction parameter ($k_{ij}$). In all investigated cases, pure predictions give large deviations when representing the experimental data.

## 5.6 Final Comments

Describing the complex phase behaviour of polymer solutions and polymer blends is a rather difficult task. The Flory-Huggins theory has been the primary theoretical tool for the past years, although it is known to have deficiencies, which limits its usefulness as a predictive tool.

In this chapter, the sPC-SAFT EoS is used to explain the behaviour of polymer solutions. Despite the complexity and the varying nature of the mixtures considered, the sPC-SAFT model with an adjustable binary interaction parameter generally yields satisfactory results. Additionally, it is observed that the phase diagrams of sPC-SAFT are rather sensitive to small $k_{ij}$ deviations. The model is capable of describing the qualitative aspects of the phase diagram of polymer blends, meaning upper or lower critical solution behaviour, but the exact critical solution temperatures predicted by the model differ significantly from the experimental data.

## References

[1] K. S. Birdi, *Handbook of Surface and Colloidal Chemistry.* 2nd edition, CRC Press Inc., USA, 2003.

[2] B. C. Lee and R. P. Danner, "Predictions of Polymer-Solvent Phase Equilibria by a Modified Group-Contribution Lattice-Fluid Equation of State," *AIChE J.*, vol. 42, pp. 837–849, 1996.

[3] T. Oishi and M. Prausnitz, "Estimation of Solvent Activities in Polymer Solutions Using a Group-Contribution Method," *Ind. Eng. Chem. Process Des. Dev.*, vol. 17, pp. 333–339, 1978.

[4] G. M. Kontogeorgis, A. Fredenslund, and D. P. Tassios, "Simple Activity Coefficient Model for the Prediction of Solvent Activities in Polymer Solutions," *Ind. Eng. Chem. Res.*, vol. 32, pp. 362–372, 1993.

[5] A. Fredenslund, J. Gmehling, and P. Rasmussen, "Group Contribution Estimation of Activity Coefficients in Non-Ideal Liquid Mixtures," *AIChE J.*, vol. 25, pp. 1089–1096, 1975.

[6] H. K. Hansen, P. Rasmussen, A. Fredenslund, M. Schiller, and J. Gmehling, "Vapor-Liquid Equilibria by UNIFAC Group Contribution. 5. Revision and Extension," *Ind. Eng. Chem. Res.*, vol. 30, pp. 2352–2355, 1991.

[7] H. K. Hansen, B. Coto, and B. Kuhlmann, *UNIFAC with Linearly Temperature-Dependent Group-Interaction Parameters.* Internal Report SEP 9212, Department of Chemical Engineering, Technical University of Denmark, DK-2800 Kgs. Lyngby, 1992.

[8] I. A. Kouskoumvekaki, N. von Solms, T. Lindvig, M. L. Michelsen, and G. M. Kontogeorgis, "Novel Method for Estimating Pure-Component Parameters for Polymers: Application to the PC-SAFT Equation of State," *Ind. Chem. Eng. Res.*, vol. 43, pp. 2830–2838, 2004.

[9] P. J. T. Tait and A. M. Abushihada, "Comparative Studies on the Use of Gas Chromatographic and Vapour Pressure Techniques for the Determination of the Interaction Energy Parameter," *Polymer*, vol. 18, pp. 810–816, 1977.

[10] H. S. Elbro, *Phase Equilibria of Polymer Solutions – with Special Emphasis on Free Volume.* Ph. D. Thesis, Department of Chemical Engineering, Technical University of Denmark, DK-2800 Kgs. Lyngby, 1992.

[11] W. Hao, H. S. Elbro, and P. Alessi, *Polymer Solution Data Collection: Vapor Liquid Equilibrium (Dechema Chemistry Data Series : Volume 14, Part 1 and 2).* Scholium Intl., DECHAMA, Germany, 1992.

[12] C. Wohlfarth, *Vapour-Liquid Equilibrium Data for Binary Polymer Solutions (Physical Sciences Data 44).* Elsevier Science, Amsterdam, The Netherlands, 1994.

[13] A. Tihic, *Investigation of the Miscibility of Plasticizers in PVC.* Bachelor Thesis, Department of Chemical Engineering, Technical University of Denmark, DK-2800 Kgs. Lyngby, 2003.

[14] A. M. F. Barton, *Handbook of Solubility Parameters and Other Cohesion Parameters.* CRC Press Inc., Florida, USA, 1983.

[15] AIChE J., *DIPPR Table of Physical and Thermodynamic Properties of Pure Compounds.* New York, USA, 1998.

[16] M. Mulder, *Basic Principle of Membrane Technology.* Kluwer Academic Publichers, London, UK, 1996.

[17] V. E. Raptis, I. G. Economou, D. N. Theodorou, J. Petrou, and J. H. Petropoulos, "Molecular Dynamics Simulation of Structure and Thermodynamic Properties of Poly(dimethylsilamethylene) and Hydrocarbon Solubility Therein: Toward the Development of Novel Membrane Materials for Hydrocarbon Separation," *Macromolecules*, vol. 37, pp. 1102–1112, 2004.

[18] Z. A. Makrodimitri, V. E. Raptis, and I. G. Economou, "Molecular Dynamics Simulation of Structure, Thermodynamic, and Dynamic Properties of Poly(dimethylsilamethylene), Poly(dimethylsilatrimethylene) and Their Alternating Copolymer," *J. Phys. Chem. B.*, vol. 110, pp. 16047–16058, 2006.

[19] P. A. Rodgers, "Pressure Volume Temperature relationships for Polymeric Liquids – A Review of Equations of State and Their Characteristic Parameters for 56 Polymers," *J. Appl. Polym. Sci.*, vol. 48, pp. 1061–1980, 1993.

[20] E. M. Dolch, M. Glaser, A. Heintz, H. Wagner, and R. N. Lichtenthaler, "Thermodynamics of Polydimethylsiloxane Solutions. III. Experimental Results and Theoretical Calculations of Solvent Activities," *Ber Bunsen–Ges. Phys. Chem.*, vol. 88, pp. 479–484, 1984.

[21] O. Pfohl, C. Riebesell, and R. Z. Dohrn, "Measurement and Calculation of Phase Equilibria in the System *n*-Pentane + Poly(dimethylsiloxane) at 308.15–423.15 K," *Fluid Phase Equilibria*, vol. 202, pp. 289–306, 2002.

[22] A. J. Ashworth, C. F. Chien, D. L. Furio, D. Hooker, M. M. Kopecnik, R. J. Laub, and G. J. Price, "Comparison of Static with Gas–Chromatographic Solute Infinite Dilution Activity Coefficients with Poly(Dimethylsiloxane)Solvent," *Macromolecules*, vol. 17, pp. 1090–1094, 1984.

[23] H. S. Elbro, A. Fredenslund, and P. Rasmussen, "Group Contribution Method for the Prediction of Liquid Densities as a Function of Temperature for Solvents, Oligomers, and Polymers," *Ind. Eng. Chem. Res.*, vol. 30, pp. 2576–2582, 1991.

[24] D. W. van Krevelen and P. J. Hoftyzer, *Properties of Polymers. Their Correlation with Chemical Structure.* Elsevier Science, Amsterdam, The Netherlands, 1972.

[25] Y. Kamiya, Y. Naito, K. Terada, K. Mizoguchi, and A. Tsuboi, "Volumetric Properties and Interaction Parameters of Dissolved Gases in Poly(dimethylsiloxane) and Polyethylene," *Macromolecules*, vol. 33, pp. 3111–3119, 2000.

[26] I. G. Economou, Z. A. Makrodimitri, G. M. Kontogeorgis, and A. Tihic, "Solubility of Gases and Solvents in Silicon Polymers: Molecular Simulation and Equation of State Modeling," *Molecular Simulation*, vol. 33, pp. 851–860, 2007.

[27] G. J. van Amerongen, "Diffusion in Elastomers," *Rub. Chem. Technol.*, vol. 37, pp. 1065–1152, 1964.

[28] J. G. Curro, K. G. Honnell, and J. D. McCoy, "Theory of Gases in Polymers: Application to Monatomic Solutes," *Macromolecules*, vol. 30, pp. 145–152, 1997.

[29] J. Gross and G. Sadowski, "Modeling Polymer Systems Using the Perturbed-Chain Statistical Associating Fluid Theory Equation of State," *Ind. Eng. Chem. Res.*, vol. 41, pp. 1084–1093, 2002.

[30] Y. L. Cheng and D. C. Bonner, "Solubility of Ethylene in Liquid, Low-Density Polyethylene to 69 Atmospheres," *J. Polym. Sci., Polym. Phys. Ed.*, vol. 15, pp. 593–600, 1977.

[31] R. K. Surana, R. D. Danner, A. B. de Haan, and N. Bechers, "New Technique to Measure High-Pressure and High-Temperature Polymer–Solvent Vapor-Liquid Equilibrium," *Fluid Phase Equilibria*, vol. 139, pp. 361–370, 1997.

[32] M. M. Coleman, J. F. Graf, and P. C. Painter, *Specific Interactions and the Miscibility of Polymer Blends: Practical Guides for Predicting and Designing Miscible Polymer Mixtures*. Technomic Publishing Company, Inc., USA, 1991.

[33] A. Wakker and M. A. van Dijk, "Predicting Polymer Blend Miscibility: Dispersive Versus Specific Interactions," *Polym. Networks Blends*, vol. 2, pp. 123–133, 1992.

[34] E. C. Voutsas, G. D. Pappa, C. J. Boukouvalas, K. Magoulas, and D. P. Tassios, "Miscibility in Binary Polymer Blends: Correlation and Prediction," *Ind. Eng. Chem. Res.*, vol. 43, pp. 1312–1321, 2004.

[35] V. I. Harismiadis, A. R. D. van Bergen, A. Saraiva, G. M. Kontogeorgis, A. Fredenslund, and D. P. Tassios, "Miscibility of Polymer Blends with Engineering Models," *AIChE J.*, vol. 42, pp. 3170–3180, 1996.

[36] J. Kressler, N. Higashida, K. Shimomai, T. Inoue, and T. Ougizawa, "Temperature Dependence of the Interaction Parameter Between Polystyrene and Poly(methyl methacrylate)," *Macromolecules*, vol. 27, pp. 2448–2453, 1994.

[37] B. H. Chang and Y. C. Bae, "Molecular thermodynamics approach for Liquid-Liquid Equilibria of the Symmetrical Polymer Blend Systems," *Chem. Eng. Sci.*, vol. 58, pp. 2931–2936, 2003.

[38] X. Chen, Z. Sun, J. Yin, and L. An, "Thermodynamics of Blends of PEO with PVAc: Application of the Sanchez-Lacombe Lattice Fluid Theory," *Polymer*, vol. 41, pp. 5669–5674, 2000.

[39] I. G. Economou, "Lattice-Fluid Theory Prediction of High-Density Polyethylene-Branched Polyolefin Blend Miscibility," *Macromolecules*, vol. 33, pp. 4954–4960, 2000.

[40] J. T. Cabral and A. Karim, "Discrete Combinatorial Investigation of Polymer Mixture Phase Boundaries," *Measurement Science and Technology*, vol. 16, pp. 191–198, 2005.

[41] Y. Song, T. Hino, and S. M. Lambert, "Liquid-liquid Equilibria for Polymer Solutions and Blends, including Copolymers," *Fluid Phase Equilibria*, vol. 117, pp. 69–76, 1996.

[42] C. T. Lo, S. Seifert, P. Thiyagarajan, and B. Narasimhan, "Phase Behavior of Semicrystalline Polymer Blends," *Polymer*, vol. 45, pp. 3671–3679, 2004.

# Chapter 6

# The GC sPC-SAFT model

*"If we knew what we were doing, it would not be called research, would it?"* by Albert Einstein

## 6.1 Introduction

In this work, the Constantinou-Gani Group Contribution (GC) approach [1] in combination with the sPC-SAFT EoS [2] is applied in order to determine the three characteristic molecular PC-SAFT parameters that are required in the model to describe a non-associating compound. These parameters are the segment number, $m$, the interaction energy, $\epsilon/k$, and the hard-core segment diameter, $\sigma$.

As mentioned in Section 3.3, the choice is made because, unlike other approaches found in the literature, this GC methodology includes two levels of contributions. These are first-order groups (FOG) and second-order groups (SOG) that can, to some extent, capture proximity effects and distinguish among structural isomers.

The objective of this chapter is twofold: first, to generate a parameter table, whose extent ultimately determines the range of applicability of the model, and second, to evaluate the capability of the GC approach in accurately describing important thermodynamic properties. The methodology behind the GC approach will be presented in this chapter outlining the important steps in the development of the model. Moreover, other approaches which are considered during this work are discussed.

Correlations of experimental data are drawn from DIPPR [3]. These data are referred to as "experimental" even though they may include compilations of real experiments and computational results, and are therefore, in fact, only pseudo-experimental in nature with some uncertainties. Sometimes, measurements are rather difficult to obtain, e.g. vapour pressures of heavy compounds, so they might not be as accurate as desired. This must be kept in mind when interpreting the performance of the current method and the deviations from the so-called "experimental values". Hence, deviations of the order of several percentages should not automatically be considered as a failure of the method.

## 6.2 Parameter Trends

Chapter 4 presented a thorough parameterization of various compounds in the framework of the sPC-SAFT EoS (cf. Table 4.1). The quality of the fit for both vapour pressure ($P^{sat}$) and liquid density ($\rho$) is satisfactory for a three-parameter EoS. However, the focus in this work is not as much on the quality of the fit as on the overall parameter behaviour. This is important because a future challenge lies in estimating the EoS parameters for complex compounds, like polymers, and compounds that are poorly experimentally defined in general, rather than fine-tuning precise values for well-defined pure components. Apart from an unavoidable level of scatter due to inaccuracies in experimental data and fitting itself, the parameter values reported in Table 4.1 are well-behaved and suggest predictable trends for similar compounds with increasing molecular weight, $M_w$.

Numerous sets of PC-SAFT parameters for various polar and non-polar non-associating compounds have been analyzed in order to study possible trends and parameter dependencies on various physical properties such as $M_w$, dipole moment, van der Waals volume, etc.

It has already been shown that the increase of segment number $m$ with increasing $M_w$ is practically linear within each homologous series, cf. Chapter 4. This linear relationship holds for many other investigated chemical families. The parameter groupings $m\sigma^3$ and $m\epsilon/k$ are essentially linear functions of $M_w$ as well. This is an expected finding since $\sigma$ and $\epsilon/k$ do not vary much with chain length and remain almost constant for long chains, and $m$ is a linear function of $M_w$. This means that if there are no accurate PVT data available, which is sometimes the case, the three PC-SAFT parameters can be estimated from $M_w$ alone.

It is well known that dipole interactions have a significant effect on the phase behavior of various chemical systems of industrial importance, such as mixtures containing ketones, esters, ethers, and aldehydes, as well as many polar polymers, copolymers, and different biochemicals. Non-ideal behaviour of a polar compound in a mixture with non-polar compounds is very common due to differences in the intermolecular interactions. This issue will be addressed in Chapter 7. Generally, the deviation from ideal solution can be modelled by various EoS by fitting a binary interaction parameter. To improve existing models for applications with these kinds of mixtures, various types of the SAFT EoS have been developed. One example is the polar version of SAFT [4–6].

In the present study, dipole moments have been collected from the literature to determine if possible parameter dependencies could be observed and, perhaps, applied for extrapolation purposes. The ranges of dipole moments of various polar compounds taken from DIPPR [3] are given in Table 6.1.

Unfortunately, it has not been possible to observe any usable trends as function of $M_w$ or individual or grouped PC-SAFT parameters. However, as presented by Gross and Vrabec [6], the polar PC-SAFT correlation results with compounds that exhibit high

Table 6.1: Ranges of dipole moments ($\mu$) for families of polar compounds.

| Chemical family | Range of $\mu$ [D][a] |
|---|---|
| Esters | 1.7–3.0 |
| Ethers | 1.1–1.4 |
| Ketones | 2.4–4.8 |
| *Halogenated:* | |
| Fluoro | 1.4–3.0 |
| Bromo | 1.0–2.3 |
| Iodo | 1.6–2.1 |

[a] $1\,\mathrm{D} = 3.33564 \times 10^{-30}\,\mathrm{C.m}$

dipole moments above 3 D are improved when dipole interactions are taken into account compared to results with original PC-SAFT. For ethers with weak dipoles, only slight improvement is found.

It is noted that a more comprehensive investigation will not be presented in this thesis, but further progress in the same line can be helpful if the proposed GC methodology is to be extended to polar compounds and their corresponding mixtures.

## 6.3 Program for GC Estimation

The GC parameters are determined using an optimisation program developed by Constantinou [7] and modified by Constantinou and Gani in 1994 [1]. For the current application, the program is adjusted with updated equations. A brief summary of the optimisation method is given in the following.

The objective function is a sum of squares of residuals between the experimental and calculated property $\Psi$, which in this case can be one of the three pure compound PC-SAFT parameters or a grouping of these, e.g. $m$ or $m\sigma^3$. The objective function $F$ for the optimisation then becomes:

$$F = \sum_i \left[\Psi_i^{GC} - \Psi_i^{DIPPR}\right]^2 \tag{6.1}$$

where $i$ represents individual compounds included in the optimisation. The routine applies a Levenberg-Marquard algorithm [8] for the minimization of $F$. The specific program has earlier proven to be a stable and fast tool for calculations of required parameters for group contributions [1, 9].

The parameter estimation is facilitated by Table 4.1 with the extensive list of pure compound PC-SAFT parameters estimated from data ($P^{sat}$ and $\rho$) that are mainly drawn from the DIPPR [3] data bank.

The final outcome of the group contribution scheme depends on the selection and weighting of input data for the optimisation. For the determination of group contribution

parameters, it is not only required to include reliable and consistent data, where estimated pure compounds parameters exhibit minimum errors, but the included compounds must also be represented correctly and in a consistent manner within the same chemical family. Thus, when the database is ready and all molecular structures included are broken down into well-defined chemical groups, the regression will rely on a large number of data points that will ensure dilution of noise from outliers and inter-family variations.

## 6.4 Development of GC sPC-SAFT

The specific methodology applied in this work is as follows:

- Identification and occurrences of FOG and SOG in each compound in the database are defined. In order to obtain a list covering various functional groups, several different families of chemical compounds are included.
- An extensive parameter table for PC-SAFT for numerous non-associating compounds are developed by fitting $P^{sat}$ and $\rho$ data obtained from DIPPR correlations [3] in a reduced temperature range of $0.5 \leq T_r \leq 0.9$. In this way, the vicinity of the critical point is not included because this would deteriorate the quality of the description of temperatures removed from the critical region (cf. Section 2.2.1.1). Here, only experimental data of relatively low $M_w$ compounds ($C_{\geq 5}$) are used that exhibit $<5\,\%$ experimental uncertainty for $P^{sat}$ and $<3\,\%$ for $\rho$. The values obtained are found to have a linear relation with their molecular parameters, as discussed in Chapter 4. The linear relationship of the parameter groupings is used as the basis for developing the present GC method.
- Fitting the three GC based parameters to the corresponding DIPPR fitted parameters using linear regression with the sum of squares of residuals between DIPPR fitted and GC-based values as the objective function.

Assuming that a given molecule contains $n_i$ groups of type $i$, the following linear relations for the three parameter groupings: $m$, $m\sigma^3$, and $m\epsilon/k$, are applied as models for the linear regression:

$$m_{molecule} = \sum_i (n_i m_i)_{FOG} + \Phi \sum_j (n_j m_j)_{SOG} \tag{6.2}$$

$$\left(m\sigma^3\right)_{molecule} = \sum_i \left(n_i m_i \sigma_i^3\right)_{FOG} + \Phi \sum_j \left(n_j m_j \sigma_j^3\right)_{SOG} \tag{6.3}$$

$$(m\epsilon/k)_{molecule} = \sum_i (n_i m_i \epsilon_i/k)_{FOG} + \Phi \sum_j (n_j m_j \epsilon_j/k)_{SOG} \tag{6.4}$$

where $\Phi = 0$ when no SOG are present, and $\Phi = 1$ when SOG are present.

The parameters $m_i$, $\sigma_i$, and $\epsilon_i/k$ represent contributions of the FOG of type $i$ that appears $n_i$ times, and $m_j$, $\sigma_j$, and $\epsilon_j/k$ are the contributions of the SOG of type $j$ that appears $n_j$ times. The multiplication of $\sigma$ and $\epsilon/k$ by $m$ (scaling) is introduced to avoid numerical instabilities during the linear least square analysis.

Figure 6.1 is a schematic illustration of the method in a flow chart form.

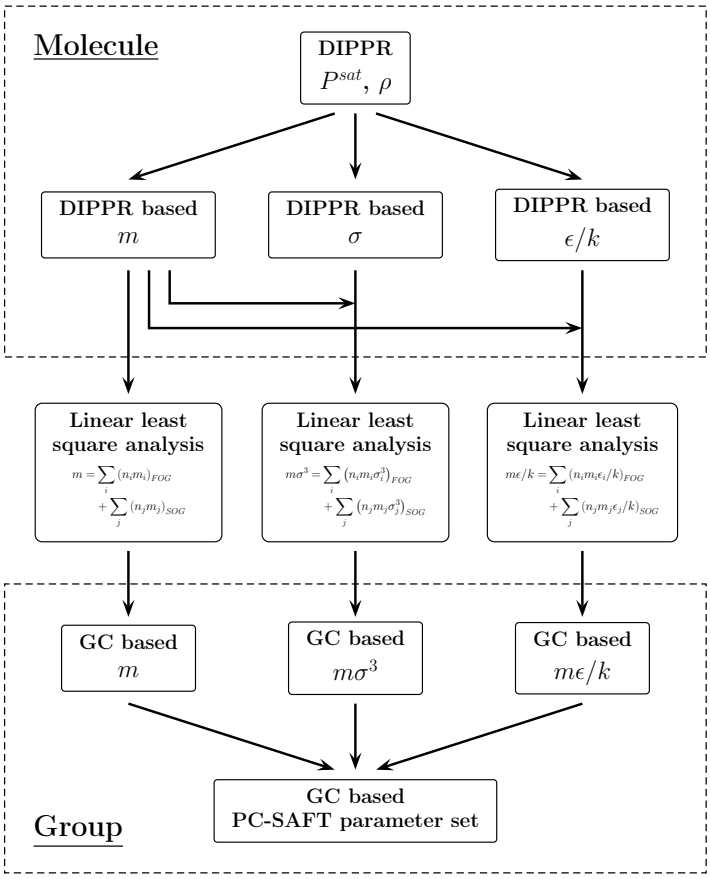


Figure 6.1: Schematic illustration of the GC method in flow chart form used for GC sPC-SAFT.

The first- and second-order group contributions for each of the PC-SAFT parameters are shown in Tables 6.3 and 6.4 respectively. The same FOG have been proposed by Fredenslund *et al.* [10] in the UNIFAC model, and therefore, the group notation from UNIFAC is also provided in the tables as supplementary to the reader who is familiar with the UNIFAC GC approach. Following the interpretation of the GC scheme by Fredenslund *et al.* [10], a group appearing in an aliphatic ring is considered equivalent to its identical non-ring one. So each group has a single contribution independent of the type of the compound involved, acyclic or cyclic. In other words, the contribution of e.g. a $-CH_2$ group in an alkane has the same contribution to the pure parameter of an alcohol as an olefin. This justifies the use of all families of compounds for the fitting of a specific group rather than selecting a single family as representative of that specific group, e.g. using only alkanes to fit $-CH_3$ and $-CH_2$ groups.

Screening through Tables 6.3 and 6.4, it is observed that the resulting GC parameter values follow physically meaningful trends. The values of the three parameter groupings, $m$, $m\sigma^3$, and $m\epsilon/k$, of a group $i$ decrease with decreasing size of groups such as $-CH_3$, $-CH_2$, $-CH<$, and $>C<$. Moreover, it is noted as well that a few FOG contributions exhibit negative values. Similar behaviour has been observed by Elbro *et al.* [11] and Stefanis *et al.* [9].

Table 6.2 gives the standard deviations, the average errors, and the average absolute deviations for the FOG and SOG approximations. These results indicate an overall improvement of the estimation of groups' approximations achieved after the introduction of SOG in the estimation method. Therefore, it can be argued that the contribution of the SOG serves as a correction to the FOG approximation.

Table 6.2: Statistical results with the GC method implemented in the sPC-SAFT EoS.

| Parameter | $N_{DP}$ | Std. dev.[a] | | AAE[a] | | AAD[a] [%] | |
|---|---|---|---|---|---|---|---|
| | | FOG | FOG+SOG | FOG | FOG+SOG | FOG | FOG+SOG |
| $m$ | 399 | 0.27 | 0.26 | 0.19 | 0.18 | 5.11 | 4.54 |
| $m\sigma^3$ | 399 | 4.11 | 3.94 | 2.77 | 2.55 | 1.38 | 1.25 |
| $m\epsilon/k$ | 399 | 41.7 | 36.6 | 31.1 | 27.8 | 3.26 | 2.87 |

[a] Std. dev. $= \sqrt{\sum \left(X^{est} - X^{exp}\right) / \left(N_{DP} - 1\right)}$; AAE $= (1/N_{DP}) \sum \left|X^{est} - X^{exp}\right|$; AAD $= (1/N_{DP}) \sum \left(\left|X^{est} - X^{exp}\right| / X^{exp}\right) 100\,\%$. $N_{DP}$ is the number of experimental data points; $X^{est}$ is the estimated value of the property $X$, and $X^{exp}$ is the experimental value of the property $X$.

Table 6.3: First-Order Group (FOG) contributions from the parameters $m$, $m\sigma^3$, and $m\epsilon/k$.

| First-order group (FOG) | Contribution | | | UNIFAC notation [10] | Sample group assignment (occurrences) |
|---|---|---|---|---|---|
| | $m$ [–] | $m\sigma^3$ [Å$^3$] | $m\epsilon/k$ [K] | | |
|  | 0.644362 | 34.16955 | 129.3866 | "–$CH_3$" | propane (2) |
|  | 0.384329 | 24.33981 | 102.3238 | "–$CH_2$" | *n*-butane (2) |
|  | 0.043834 | 13.95391 | 68.2084 | "–CH<" | *i*-butene (1) |
|  | –0.492080 | 2.325415 | –10.9830 | ">C<" | neopentane (1) |
|  | 1.031502 | 52.08640 | 240.7577 | "$CH_2$=CH–" | propylene (1) |
|  | 0.900577 | 39.68639 | 257.6914 | "–CH=CH–" | *cis*-2-butane (1) |
|  | 0.739720 | 40.85726 | 214.9811 | "$CH_2$=C<" | *i*-butene (1) |
|  | 0.513621 | 29.69589 | 208.6538 | "–CH=C<" | 2-methyl-2-butene (1) |
|  | 0.377151 | 17.07079 | 212.3236 | ">C=C<" | 2,3-dimethyl-2-butene (1) |
| 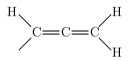 | 1.588361 | 67.46085 | 412.7788 | "$CH_2$=C=CH–" | 1,2-butadiene (1) |

*Continues on next page*

| First-order group (FOG) | Contribution | | | UNIFAC notation [10] | Sample group assignment (occurrences) |
|---|---|---|---|---|---|
| | $m$ [–] | $m\sigma^3$ [Å$^3$] | $m\epsilon/k$ [K] | | |
| 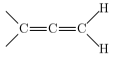 | 1.328356 | 57.76490 | 375.6868 | "$CH_2$=C=C<" | 3-methyl-1,2-butadiene (1) |
| 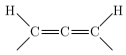 | 1.479486 | 56.35690 | 408.9468 | "CH=C=CH–" | 2,3-pentadiene (1) |
| 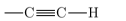 | 1.172342 | 41.80054 | 287.8396 | "CHEC–" | propyne (1) |
| 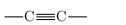 | 0.715504 | 33.17167 | 276.7768 | "CEC" | 2-butyne (1) |
|  | 0.366330 | 19.81753 | 106.9481 | "ACH" | benzene (6) |
|  | 0.010721 | 10.51468 | 87.93008 | "AC" | napthalene (2) |
| 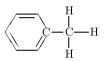 | 0.836861 | 43.57497 | 235.0636 | "$ACCH_3$" | toluene (1) |
|  | 0.389760 | 34.49823 | 171.3898 | "$ACCH_2$–" | *m*-ethyltoluene (1) |
|  | –0.036170 | 27.22617 | 109.9270 | "ACH<" | *sec*-butylbenzene (1) |
|  | 1.793821 | 61.90347 | 496.6067 | "$CH_3CO$" | methyl ethyl ketone (1) |
|  | 1.552067 | 52.18521 | 444.9888 | "$CH_2CO$" | cyclopentanone (1) |

*Continues on next page*

| First-order group (FOG) | Contribution | | | UNIFAC notation [10] | Sample group assignment (occurrences) |
|---|---|---|---|---|---|
| | $m$ [–] | $m\sigma^3$ [Å$^3$] | $m\epsilon/k$ [K] | | |
|  | 1.085097 | 15.63589 | 347.6752 | "CHCO" | diisopropyl ketone (1) |
|  | 1.889630 | 31.06693 | 436.2165 | "CHO" | 1-butanal (1) |
| 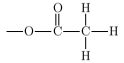 | 2.362557 | 65.59442 | 538.0440 | "$CH_3COO$" | ethyl acetate (1) |
| 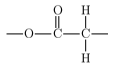 | 1.952796 | 54.80990 | 462.7927 | "$CH_2COO$" | methyl propionate (1) |
|  | 1.745841 | 43.39209 | 426.2767 | "HCOO" | *n*-propyl formate (1) |
|  | 1.439110 | 32.51328 | 351.1344 | "COO" | ethyl acetate (1) |
|  | 1.527003 | 38.22602 | 330.7321 | "$CH_3O$" | methyl ethyl ether (1) |
|  | 1.226298 | 28.97937 | 277.2849 | "$CH_2O$" | ethyl vinyl ether (1) |
| 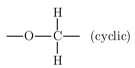 (cyclic) | 1.101871 | 32.85569 | 307.6912 | "$CH_2O$ (cyclic)" | 1,4-dioxane (2) |
|  | 1.544171 | 16.26332 | 321.8993 | "CHO" | diisopropyl ether (1) |
| —O— (except as above) | –0.088640 | 14.50239 | –21.2312 | "O (except as above)" | divinyl ether (1) |

*Continues on next page*

| First-order group (FOG) | Contribution | | | UNIFAC notation [10] | Sample group assignment (occurrences) |
|---|---|---|---|---|---|
| | $m$ [–] | $m\sigma^3$ [Å$^3$] | $m\epsilon/k$ [K] | | |
|  | 1.391979 | 61.46831 | 428.3381 | "$CH_3S$" | methyl ethyl sulfide (1) |
|  | 0.970886 | 51.07098 | 341.3012 | "$CH_2S$" | diethyl sulfide (1) |
|  | 0.928117 | 40.55489 | 363.4252 | "CHS" | diisopropyl sulfide (1) |
| —I | 0.890179 | 49.92270 | 341.5094 | "I" | isopropyl iodide (1) |
| —Br | 0.888904 | 35.94299 | 276.4405 | "Br" | 2-bromopropane (1) |
|  | 1.209673 | 53.65876 | 368.3897 | "$CH_2Cl$" | $n$-butyl chloride (1) |
|  | 0.810132 | 43.14092 | 272.4527 | "CHCl" | isopropyl chloride (1) |
|  | 0.713602 | 41.17843 | 273.3549 | "ACCl" | $m$-dichlorobenzene (2) |
|  | 1.458050 | 49.34937 | 254.5159 | "ACF" | fluorobenzene (1) |
|  | 0.615750 | 46.22000 | 118.2550 | "$CF_3$" | $n$-perfluorohexane (2) |
|  | 0.933850 | 35.65825 | 153.7675 | "$CF_2$" | perfluoromethylcyclohexane (5) |

*Continues on next page*

| First-order group (FOG) | Contribution | | | UNIFAC notation [10] | Sample group assignment (occurrences) |
|---|---|---|---|---|---|
| | $m$ [–] | $m\sigma^3$ [Å$^3$] | $m\epsilon/k$ [K] | | |
|  | 2.210123 | 65.58354 | 702.2415 | "$CH_2NO_2$" | 1-nitropropane (1) |
| 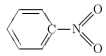 | 2.340985 | 48.05376 | 687.6930 | "$ACNO_2$" | nitrobenzene (1) |

Table 6.4: Second-Order Group (SOG) contributions from the parameters $m$, $m\sigma^3$, and $m\epsilon/k$.

| Second-order group (SOG) | Contribution | | | UNIFAC notation [10] | Sample group assignment (occurrences) |
|---|---|---|---|---|---|
| | $m$ [–] | $m\sigma^3$ [Å$^3$] | $m\epsilon/k$ [K] | | |
|  | 0.016263 | 0.280872 | –9.83615 | "$(CH_3)_2$–CH–" | *i*-butane (1) |
|  | 0.041437 | 1.472296 | –6.89516 | "$(CH_3)_3$–C–" | neopentane (1) |
|  | –0.046340 | –2.464521 | –6.81456 | "–CH($CH_3$)–CH($CH_3$)–" | 2,3-dimethylbutane (1) |
|  | –0.101480 | –1.913722 | –4.68034 | "–CH($CH_3$)–C($CH_3$)$_2$–" | 2,2,3-trimethylpentane (1) |
|  | –0.183290 | –7.464243 | 23.72792 | "–C($CH_3$)$_2$–C($CH_3$)$_2$–" | 2,2,3,3-tetramethylpentane (1) |

*Continues on next page*

| Second-order group (SOG) | Contribution | | | UNIFAC notation [10] | Sample group assignment (occurrences) |
|---|---|---|---|---|---|
| | $m$ [–] | $m\sigma^3$ [Å$^3$] | $m\epsilon/k$ [K] | | |
|  | 0.672813 | 5.826574 | 121.08870 | "ring of 3 carbons" | cyclopropane (1) |
|  | 0.506911 | 2.643507 | 101.78980 | "ring of 4 carbons" | cyclobutane (1) |
|  | 0.309498 | 1.015915 | 61.40257 | "ring of 5 carbons" | cyclopentane (1) |
|  | 0.064237 | –0.636912 | 29.24676 | "ring of 6 carbons" | cyclohexane (1) |
|  | 0.121577 | –4.990554 | 52.68976 | "ring of 7 carbons" | cycloheptane (1) |
| 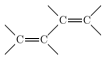 | –0.112200 | -0.955843 | –19.75390 | "–C=CC=C–" | 1,3-butadiene (1) |
|  | 0.013538 | 0.342635 | 1.52891 | "$CH_3$–C=" | *i*-butene (2) |
|  | –0.043500 | 0.658982 | –5.93727 | "–$CH_2$–C=" | 1-butene (1) |
|  (X = H or C) | 0.087414 | –0.806591 | –0.98985 | "–C{H or C}–C=" | 3-methyl-1-butene (1) |

*Continues on next page*

| Second-order group (SOG) | Contribution | | | UNIFAC notation [10] | Sample group assignment (occurrences) |
|---|---|---|---|---|---|
| | $m$ [–] | $m\sigma^3$ [Å$^3$] | $m\epsilon/k$ [K] | | |
| 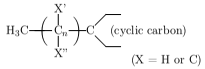 (X = H or C) | –0.14510 | –0.220100 | –5.71982 | "string in cyclic" | ethylcyclohexane (1) |
|  | 0.254933 | 4.322626 | 24.83824 | ">CHCHO" | 2-methyl butyraldehyde (1) |
| 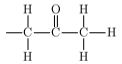 | –0.03869 | –1.234490 | –6.90654 | "$CH_3(CO)CH_2$–" | 2-pentanone (1) |
| 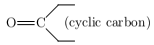 | –0.030920 | –0.169280 | 32.29944 | "C(cyclic)==O" | cyclopentanone (1) |
| 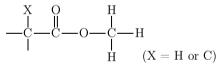 (X = H or C) | 0.088960 | –1.218040 | –18.93980 | "$CH_3(CO)OC\{H$ or $C\}<$" | *i*-butyric acid (1) |
| 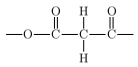 | –0.010910 | 3.553918 | 47.56669 | "$(CO)C\{H_2\}COO$" | ethyl acetoacetate (1) |
| 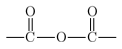 | –0.077070 | 3.242018 | –13.21250 | "(CO)O(CO)" | propanoic anhydride (1) |
|  | –0.242220 | –0.313420 | –8.35346 | "ACHO" | benzaldehyde (1) |
|  | –0.123261 | 0.424762 | –37.97600 | "ACBr" | bromotoluene (1) |
| 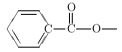 | –0.080001 | 1.303279 | –23.83030 | "ACCOO" | benzoic acid ethyl ester (1) |

*Continues on next page*

| Second-order group (SOG) | Contribution | | | UNIFAC notation [10] | Sample group assignment (occurrences) |
|---|---|---|---|---|---|
| | $m$ [–] | $m\sigma^3$ [Å$^3$] | $m\epsilon/k$ [K] | | |
|  | –0.000133 | 0.665582 | 5.95001 | "AC($ACH_m$)$_2$AC($ACH_n$)$_2$" | benzoic acid ethyl ester (1) |
|  (cyclic structure) | 0.363529 | 3.423997 | –0.92222 | "O(cyclic)–C(cyclic)=O" | diketene (1) |

Using the above linear relations in Equation (6.3) and (6.4), the $\sigma$ and $\epsilon/k$ parameters for each investigated compound can then be calculated. Calculated average errors for the $\sigma$ and $\epsilon/k$ parameters, when compared to DIPPR fitted values, are about 0.5 and 3.3 %, respectively, when only FOG are included, and 0.4 and 2.8 % when both FOG and SOG contributions are taken into account. The observed improvement of ∼10 % when using SOG is typical for the Constantinou-Gani GC method [1]. It is important to say that the performance of SOG is directly related to the extent that the database contains molecular structures with SOG. The smaller the number of compounds with SOG, the lower the accuracy of the SOG contributions.

Figure 6.2 presents comparisons with corresponding experimental reference values from DIPPR [3] in terms of linear correlations and % deviations of GC estimated parameters for the almost 400 different molecules that have been included in the derivation of the GC schemes in Tables 6.3 and 6.4.

Linear correlations between the GC estimated parameters and the reference values from DIPPR are clearly obtained; especially for $m$ and $\sigma$ with coefficient of determination values ($R^2$)[1] of 0.9740 and 0.9878 respectively. The linear correlation of $\epsilon/k$ is less pronounced, but even so, $R^2 > 0.9$ is considered to be satisfactory. The scatter plots to the right in Figure 6.2 show % deviations of individual datapoints. Dashed lines mark ranges that are considered to embrase low deviations and provide a mean of comparison with alternative GC approaches considered later in this work.

The number of datapoints that exhibit low deviations, i.e. datapoints lying within the dashed lines in Figure 6.2 (right), includes 90.2 % of the GC estimated $m$ parameters that, hence, deviate <10 % from their corresponding experimental reference values. Similarly, 98.2 % of the GC estimated $\sigma$ parameters deviate <2 % from their reference values, while 83.9 % of the GC estimated $\epsilon/k$ parameters yield <5 % deviation.

A higher accuracy of the GC estimated $\epsilon/k$ parameters would be desired. However, since the current accuracy is considered to be acceptable, rigorous testing and evaluation of the current GC scheme is given higher priority than attempts to further improve the GC scheme. Nevertheless, Section 6.5 addresses ongoing attempts to improve the accuracy of $\epsilon/k$ using different updated approaches.

### 6.4.1 Predictions of $P^{sat}$ and $\rho$

In the previous section, it was described how the GC scheme in Tables 6.3 and 6.4 is combined with the sPC-SAFT EoS in order to yield the "GC sPC-SAFT EoS". Before considering the description of binary mixtures with the model, the attention is focused on pure component properties in terms of $P^{sat}$ and $\rho$, and trends within some selected chemical families.

[1] The coefficient of determination is a measure of how well the regression line represents the data.

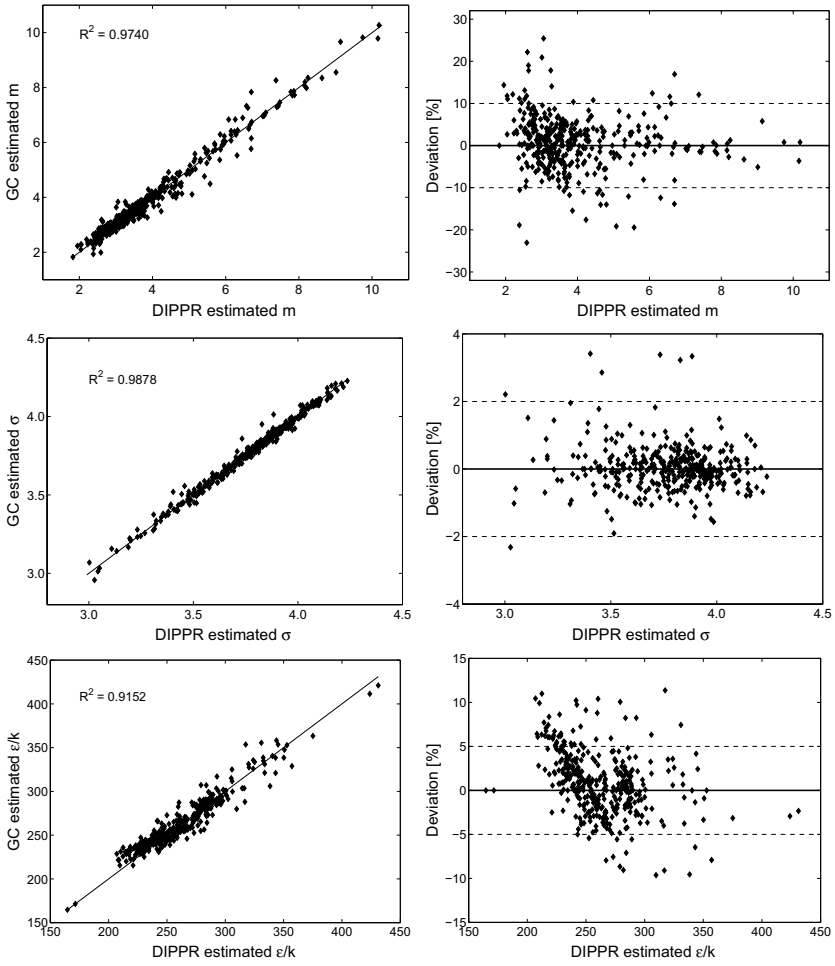


Figure 6.2: Scatter plots showing linear correlations (left) and % deviations (right) of GC- vs. DIPPR-estimated PC-SAFT parameters $m$ (top), $\sigma$ (middle), and $\epsilon/k$ (bottom) using the proposed GC method. Dashed lines (right) mark ranges of deviating datapoints; see text.

In the following, predictions of experimental $P^{sat}$ and $\rho$ for several families of chemical compounds are investigated, including $n$-alkanes, $n$-alkenes, $n$-alkynes, branched alkanes, 2-alkyl benzenes, and alkyl acetate esters. Results from each chemical family will be discussed separately.

#### 6.4.1.1 *n*-Alkanes

The agreement of the GC sPC-SAFT description of the fluid phase equilibria with the experimental data obtained for the *n*-alkanes is summarised in Table 6.5. The overall AAD %, obtained as an average of the AADs for individual compounds, is found to be 24 % for $P^{sat}$ and 0.9 % for $\rho$ of *n*-pentane to *n*-eicosane. The presented results indicate that representation of experimental data is improving with increasing *n*-alkane carbon number.

Table 6.5: GC estimated PC-SAFT parameters for various *n*-alkanes and the resulting AAD % of $P^{sat}$ and $\rho$ predictions when compared to values from DIPPR [3].

| *n*-Alkane | $N_{DP}$ | GC estimated parameters | | | $T$ range | AAD [%] | AAD [%] |
|---|---|---|---|---|---|---|---|
| | | $m$ [–] | $\sigma$ [Å] | $\epsilon/k$ [K] | [K] | $P^{sat}$ | $\rho$ |
| *n*-Pentane | 20 | 2.4417 | 3.8685 | 231.70 | 235–422 | 66.7 | 2.0 |
| *n*-Hexane | 20 | 2.8260 | 3.8849 | 236.39 | 260–450 | 56.2 | 1.9 |
| *n*-Heptane | 21 | 3.2104 | 3.8973 | 239.97 | 280–480 | 46.9 | 1.7 |
| *n*-Octane | 23 | 3.5947 | 3.9070 | 242.78 | 290–510 | 40.7 | 1.4 |
| *n*-Nonane | 24 | 3.9790 | 3.9147 | 245.04 | 300–530 | 34.7 | 1.2 |
| *n*-Decane | 25 | 4.3634 | 3.9211 | 246.91 | 310–550 | 30.5 | 0.8 |
| *n*-Undecane | 26 | 4.7477 | 3.9264 | 248.48 | 320–570 | 25.2 | 0.7 |
| *n*-Dodecane | 25 | 5.1320 | 3.9310 | 249.81 | 350–590 | 18.2 | 0.5 |
| *n*-Tridecane | 25 | 5.5163 | 3.9349 | 250.95 | 340–580 | 16.2 | 0.6 |
| *n*-Tetradecane | 27 | 5.9007 | 3.9382 | 251.95 | 350–610 | 11.5 | 0.4 |
| *n*-Pentadecane | 26 | 6.2850 | 3.9412 | 252.82 | 360–610 | 9.2 | 0.4 |
| *n*-Hexadecane | 27 | 6.6693 | 3.9438 | 253.59 | 370–630 | 3.4 | 0.5 |
| *n*-Heptadecane | 27 | 7.0537 | 3.9461 | 254.28 | 370–630 | 1.8 | 0.4 |
| *n*-Octadecane | 28 | 7.4380 | 3.9482 | 254.90 | 380–660 | 3.5 | 0.5 |
| *n*-Nonadecane | 30 | 7.8223 | 3.9501 | 255.46 | 390–680 | 9.7 | 0.6 |
| *n*-Eicosane | 30 | 8.2066 | 3.9518 | 255.96 | 390–680 | 8.9 | 0.6 |
| AAD [%] overall | | | | | | 23.9 | 0.9 |

The satisfactory description of $P^{sat}$ and $\rho$ for *n*-alkanes is also evident from Figure 6.3.

Heavier *n*-alkanes ($C_{>10}$) are also included in the estimation of the $–CH_3$ and $–CH_2$ group parameters, but one may be concerned that these compounds will introduce a bias in the objective function owing to their larger relative deviations in experimental data arising from limited or older measurements and from the fact that these compounds have very low vapour pressures. A more detailed analysis on this matter has been presented in Section 4.3. The agreement with experimental data may be improved by not including these compounds, but as the GC approach aims to be applied to heavier compounds, only heavy *n*-alkanes with accurately reported experimental data are included.

Calculations of heavier compounds using the GC approach are a pertinent test of the predictive capability of the proposed method. With the PC-SAFT parameters for

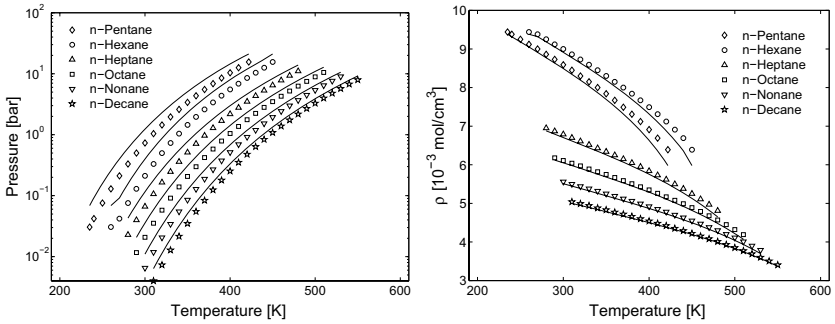


Figure 6.3: Vapour pressures (left) and liquid densities (right) of light $n$-alkanes. The symbols represent the experimental data [3], while the solid curves correspond to the GC sPC-SAFT description with the parameters estimated in this work.

heavy alkanes, listed in Table 6.5, the $P^{sat}$ and $\rho$ are calculated for heavy $n$-alkanes up to $n$-eicosane. The calculation results, graphically shown in Figure 6.4, indicate that representation of experimental data is improving with increasing $n$-alkanes carbon number. The same trend is observed for light $n$-alkanes as well.

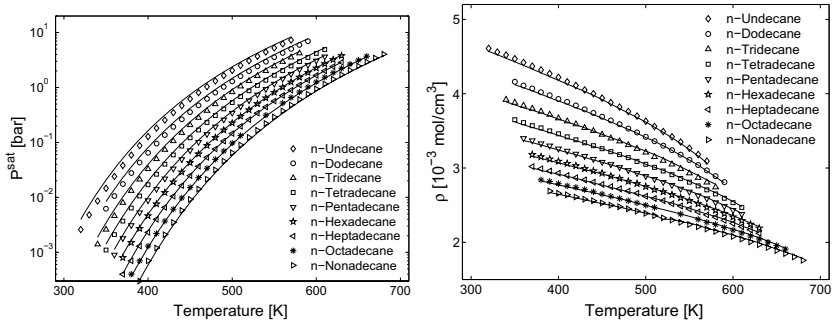


Figure 6.4: Vapour pressures (left) and liquid densities (right) of heavy $n$-alkanes. The symbols represent the experimental data [3], while the solid curves correspond to the GC sPC-SAFT description with the parameters estimated in this work.

Examination of the results obtained for $n$-alkanes shows that the deviations remain relatively stable when the chain length increases, making the first indications that the GC method can be applied successfully to polymers, as presented in Section 7.5 of the following chapter. As a matter of fact, the GC deviations decrease slightly with chain length for the other families as well. This is also observed in the following calculations.

#### 6.4.1.2 1-Alkenes

Unsaturated hydrocarbons (mono- and di-) are considered here, which means that the two additional groups –$CH_2$=CH and –CH=CH– are now included in the analysis. The deviations from the experimental $P^{sat}$ and $\rho$ for 1-alkenes are summarised in Table 6.6.

Table 6.6: GC estimated PC-SAFT parameters for 1-alkenes and the resulting AAD % of $P^{sat}$ and $\rho$ predictions when compared to values from DIPPR [3].

| 1-Alkene | $N_{DP}$ | GC estimated parameters | | | $T$ range | AAD [%] | AAD [%] |
|---|---|---|---|---|---|---|---|
| | | $m$ [–] | $\sigma$ [Å] | $\epsilon/k$ [K] | [K] | $P^{sat}$ | $\rho$ |
| 1-Butene | 16 | 2.0602 | 3.7723 | 229.33 | 230–375 | 24.4 | 0.8 |
| 1-Pentene | 17 | 2.4445 | 3.8075 | 235.13 | 250–410 | 21.6 | 0.6 |
| 1-Hexene | 18 | 2.8289 | 3.8328 | 239.36 | 280–450 | 19.7 | 0.6 |
| 1-Heptene | 20 | 3.2132 | 3.8517 | 242.58 | 290–480 | 17.2 | 1.1 |
| 1-Octene | 20 | 3.5975 | 3.8665 | 245.10 | 320–510 | 12.9 | 1.5 |
| 1-Nonene | 23 | 3.9818 | 3.8784 | 247.14 | 310–530 | 11.2 | 1.2 |
| 1-Decene | 23 | 4.3662 | 3.8881 | 292.21 | 330–550 | 14.9 | 0.8 |
| AAD [%] overall | | | | | | 17.4 | 0.9 |

The respective fluid phase behaviours are graphically presented in Figure 6.5 showing a better agreement with the experimental values than observed for the corresponding light $n$-alkanes.

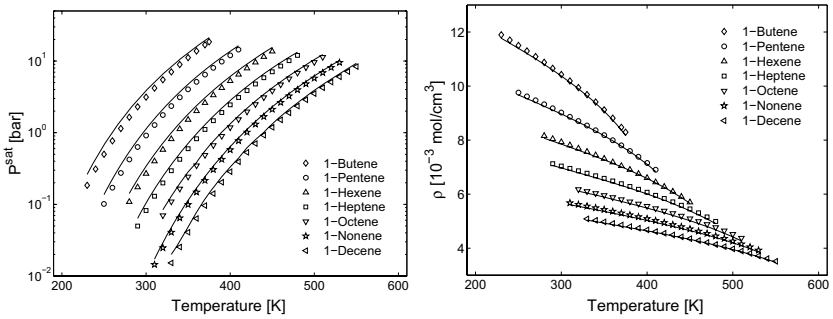


Figure 6.5: Vapour pressures (left) and liquid densities (right) of 1-alkenes. The symbols represent the experimental data [3], while the solid curves correspond to the GC sPC-SAFT description with the parameters estimated in this work.

#### 6.4.1.3 1-Alkynes

With the GC estimated parameters of a few alkynes listed in Table 6.7, sPC-SAFT calculates their $P^{sat}$ and $\rho$ with good accuracy, as shown in Figure 6.6.

Table 6.7: GC estimated PC-SAFT parameters for 1-alkynes and the resulting AAD % of $P^{sat}$ and $\rho$ predictions when compared to values from DIPPR [3].

| 1-Alkyne | $N_{DP}$ | GC estimated parameters | | | $T$ range | AAD [%] | AAD [%] |
|---|---|---|---|---|---|---|---|
| | | $m$ [–] | $\sigma$ [Å] | $\epsilon/k$ [K] | [K] | $P^{sat}$ | $\rho$ |
| 1-Pentyne | 19 | 2.5854 | 3.6396 | 229.33 | 250–430 | 11.1 | 2.7 |
| 1-Hexyne | 16 | 2.9697 | 3.6882 | 235.13 | 310–460 | 4.3 | 1.2 |
| 1-Heptyne | 18 | 2.3540 | 3.7248 | 239.36 | 350–500 | 4.2 | 0.6 |
| 1-Octyne | 20 | 3.7383 | 3.7534 | 242.58 | 350–520 | 2.2 | 1.7 |
| 2-Hexyne | 17 | 2.7729 | 3.7836 | 266.94 | 290–490 | 2.8 | 1.5 |
| AAD [%] overall | | | | | | 4.9 | 1.5 |

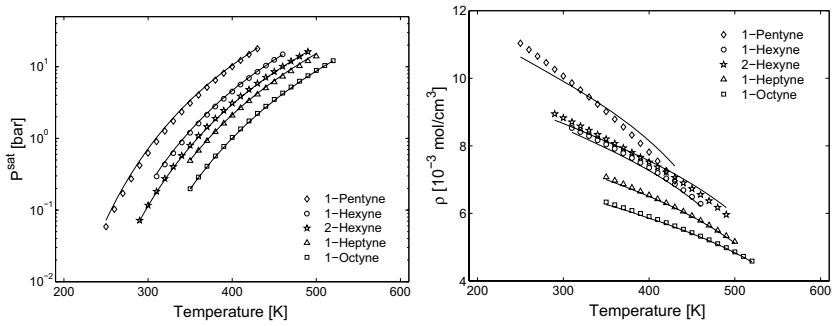


Figure 6.6: Vapour pressures (left) and liquid densities (right) of 1-alkynes. The symbols represent the experimental data [3], while the solid curves correspond to the GC sPC-SAFT description with the parameters estimated in this work.

Predictions of $P^{sat}$ and $\rho$ of the five investigated 1-alkynes in Table 6.7 generally exhibit low deviations from experimental data; especially when compared to the corresponding predictions of $n$-alkanes and 1-alkenes as presented in Sections 6.4.1.1 and 6.4.1.2 respectively.

#### 6.4.1.4 2-Methyl Alkanes

In the case of the 2-methyl alkanes, the new group –$CH_3CH$ is included in the parameter calculations. GC estimated parameters for these compounds, as well as the deviations from the experimental $P^{sat}$ and $\rho$ are summarised in Table 6.8. The overall AAD % for all investigated compounds of this family is 12 % for $P^{sat}$ and 0.7 % for $\rho$. Moreover, accurate representations of both properties are seen in Figure 6.7.

Table 6.8: GC estimated PC-SAFT parameters for 2-methyl alkanes and the resulting AAD % of $P^{sat}$ and $\rho$ predictions when compared to values from DIPPR [3].

| 2-Methyl Alkane | $N_{DP}$ | GC estimated parameters | | | $T$ range | AAD [%] | AAD [%] |
|---|---|---|---|---|---|---|---|
| | | $m$ | $\sigma$ | $\epsilon/k$ | | | |
| | | [–] | [Å] | [K] | [K] | $P^{sat}$ | $\rho$ |
| 2-Methyl butane | 19 | 2.3612 | 3.9068 | 236.61 | 230–410 | 24.5 | 0.5 |
| 2-Methyl pentane | 21 | 2.7456 | 3.9181 | 240.76 | 250–447 | 17.2 | 0.9 |
| 2-Methyl hexane | 22 | 3.1299 | 3.9266 | 243.89 | 270–477 | 11.8 | 0.7 |
| 2-Methyl heptane | 23 | 3.5142 | 3.9331 | 246.33 | 280–500 | 8.3 | 0.4 |
| 2-Methyl octane | 24 | 3.8986 | 3.9384 | 248.29 | 290–520 | 6.3 | 0.8 |
| 2-Methyl decane | 24 | 4.2829 | 3.9427 | 249.90 | 310–545 | 3.1 | 1.1 |
| AAD [%] overall | | | | | | 11.9 | 0.7 |

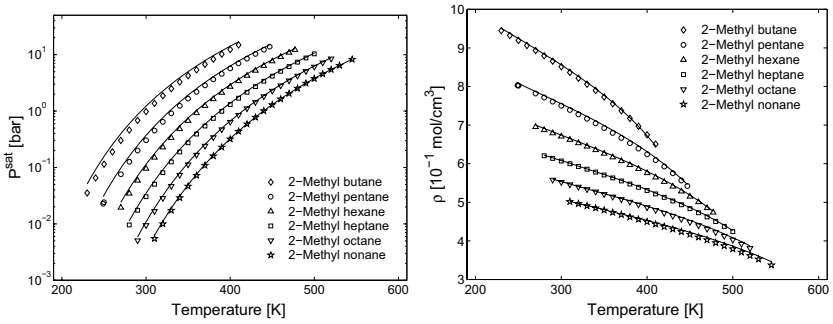


Figure 6.7: Vapour pressures (left) and liquid densities (right) of 2-methyl alkanes. The symbols represent the experimental data [3], while the solid curves correspond to the GC sPC-SAFT description with the parameters estimated in this work.

#### 6.4.1.5 $n$-Alkyl Benzenes

Description of the vapour-liquid coexistence of aromatic compounds is a more rigorous test for the GC method as these compounds have very distinct chemical properties, such

as more significant quadropole moments and the possibility of interactions between $\pi$-electrons. In this case, two new groups, ACH and $ACH_2$, are required for calculating pure compound parameters of some $n$-alkyl benzenes (from ethyl benzene to $n$-decyl benzene). PC-SAFT parameters calculated using the proposed GC scheme are listed in Table 6.9.

Results presented in Table 6.9 indicate rather good adequacy of the model in describing $P^{sat}$ and $\rho$ of this chemical family. This can also be seen in Figure 6.8.

Table 6.9: GC estimated PC-SAFT parameters for $n$-alkyl benzenes and the resulting AAD % of $P^{sat}$ and $\rho$ predictions when compared to values from DIPPR [3].

| $n$-alkyl benzene | $N_{DP}$ | GC estimated parameters | | | $T$ range | AAD [%] | AAD [%] |
|---|---|---|---|---|---|---|---|
| | | $m$ [–] | $\sigma$ [Å] | $\epsilon/k$ [K] | [K] | $P^{sat}$ | $\rho$ |
| Ethyl benzene | 25 | 2.8658 | 3.8828 | 291.55 | 310–550 | 28.9 | 1.2 |
| $n$-Propyl benzene | 25 | 3.2501 | 3.8953 | 288.56 | 320–570 | 14.5 | 0.7 |
| $n$-Butyl benzene | 25 | 3.6344 | 3.9051 | 286.20 | 340–590 | 10.5 | 0.7 |
| $n$-Pentyl benzene | 26 | 4.0188 | 3.9130 | 284.29 | 345–610 | 6.9 | 0.5 |
| $n$-Hexyl benzene | 26 | 4.4031 | 3.9195 | 282.71 | 350–628 | 2.0 | 0.6 |
| $n$-Heptyl benzene | 26 | 4.7874 | 3.9249 | 281.39 | 360–640 | 4.3 | 0.9 |
| $n$-Octyl benzene | 26 | 5.1717 | 3.9295 | 280.27 | 365–656 | 6.2 | 0.8 |
| $n$-Nonyl benzene | 27 | 5.5561 | 3.9334 | 279.29 | 370–665 | 7.6 | 1.0 |
| $n$-Decyl benzene | 25 | 5.9404 | 3.9369 | 278.45 | 380–677 | 11.9 | 1.1 |
| AAD [%] overall | | | | | | 10.3 | 0.8 |

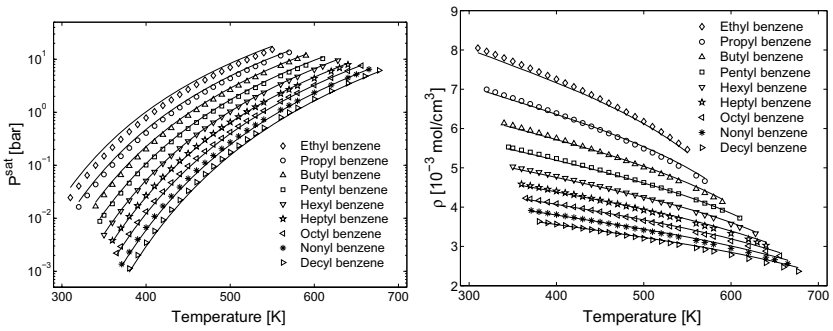


Figure 6.8: Vapour pressures (left) and liquid densities (right) of $n$-alkyl benzenes. The symbols represent the experimental data [3], while the solid curves correspond to the GC sPC-SAFT description with the parameters estimated in this work.

Predictions of $P^{sat}$ and $\rho$ of the nine investigated $n$-alkyl benzenes generally exhibit low deviations from experiments, with the overall deviations of 10.3 % and 0.8 % respectively.

#### 6.4.1.6 Alkyl Acetate Esters

The final class of compounds examined in this part of the work is acetate esters with varying alkyl chain length. For this family, an extra group –$CH_3COO$ is considered.

Table 6.10 lists GC estimated parameters and AAD % of $P^{sat}$ and $\rho$ predictions for the investigated acetates. The results in Figure 6.9 show decreasing predicted values of $P^{sat}$ with increasing alkyl carbon number going from 2 to 6, but the deviation begins to increase again at alkyl carbon numbers >7. This is similarly observed for *n*-alkyl benzenes in Section 6.4.1.5. Predictions of $\rho$ seem to be more accurate when the alkyl chain contains fewer carbon atoms, but deviations are very low in the first place.

Table 6.10: GC estimated PC-SAFT parameters for alkyl acetates and the resulting AAD % of $P^{sat}$ and $\rho$ predictions when compared to values from DIPPR [3].

| Alkyl Acetates | $N_{DP}$ | GC estimated parameters | | | $T$ range | AAD [%] | AAD [%] |
|---|---|---|---|---|---|---|---|
| | | $m$ [–] | $\sigma$ [Å] | $\epsilon/k$ [K] | [K] | $P^{sat}$ | $\rho$ |
| Ethyl acetate | 20 | 3.3912 | 3.3200 | 226.98 | 280–470 | 42.6 | 0.4 |
| Propyl acetate | 23 | 3.7756 | 3.4004 | 230.98 | 270–490 | 29.9 | 0.0 |
| Butyl acetate | 24 | 4.1599 | 3.4632 | 234.24 | 290–520 | 16.5 | 0.5 |
| Pentyl acetate | 21 | 4.5442 | 3.5137 | 236.94 | 330–530 | 8.7 | 1.1 |
| Hexyl acetate | 21 | 4.9286 | 3.5552 | 239.23 | 350–550 | 1.7 | 0.3 |
| Heptyl acetate | 24 | 5.3129 | 3.5899 | 241.18 | 320–550 | 1.8 | 1.3 |
| Octyl acetate | 26 | 5.6972 | 3.6195 | 242.87 | 330–580 | 6.9 | 0.8 |
| Nonyl acetate | 27 | 6.0816 | 3.6449 | 244.35 | 340–590 | 19.7 | 2.5 |
| Decyl acetate | 27 | 6.4659 | 3.6670 | 245.65 | 350–600 | 18.8 | 1.1 |
| AAD [%] overall | | | | | | 16.3 | 0.8 |

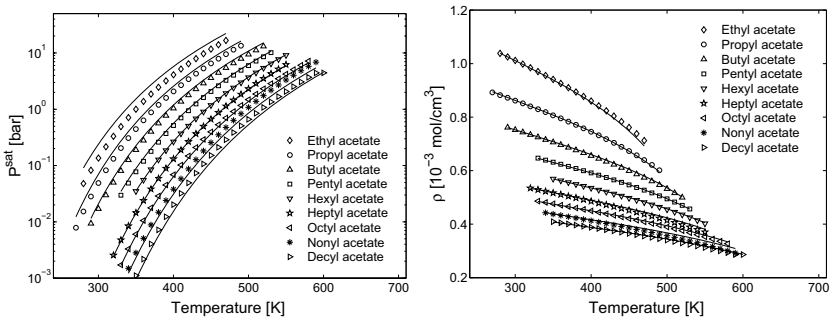


Figure 6.9: Vapour pressures (left) and liquid densities (right) of alkyl acetates. The symbols represent the experimental data [3], while the solid curves correspond to the GC sPC-SAFT description with the parameters estimated in this work.

In the work presented by Nguyen Huynh *et al.* [12], several heavy esters and their mixtures are treated with their version of the GC PC-SAFT EoS, and the resulting predictions of $P^{sat}$ and $\rho$ are in the same range as the ones from this work. The overall deviations are reported to be around 6 % for $P^{sat}$ and 3 % for $\rho$. However, in addition to the usual terms of the EoS, they use a multi polar term as well, which improves the predictive capability of their GC approach. This does not come unexpected when the number of model parameters is increased. Moreover, they have also reported significantly higher deviations for nonyl acetate and decyl acetate compared to other alkyl acetates, which is similar to this work (cf. Table 6.10). This might indicate an inconsistency of the experimental results for these two compounds rather than shortcomings by the models.

The description of the fluid phase behaviour with the currently proposed GC scheme is not comparable with the calculations reported by Tamouza *et al.* [13] (see Section 3.4) using their GC version of the PC-SAFT EoS, where the reported overall deviations for the $P^{sat}$ and $\rho$ are somewhat lower than deviations reported in this work. A more detailed comparison at this stage is not provided because of the use of different experimental data sets and temperature ranges.

### 6.4.2 Inspiration from the Tamouza *et al.* Approach

One of the most complete GC treatments within the SAFT formalism is that of Tamouza *et al.* (see Section 3.4). In this case, separate contributions from various groups to the overall chain length, segment size, dispersive energy, and association parameters are obtained by optimising the description of $P^{sat}$ and $\rho$ of pure components. Numerous chemical families are considered with their approach. An excellent description of the fluid phase behaviour of the pure components and representative mixtures of these systems is obtained.

Therefore, inspired by the approach presented by Tamouza *et al.* [13] (see Section 3.4), the three PC-SAFT parameters are calculated through averages by the Lorentz-Berthelot combining rules. In these rules, energy parameters are averaged geometrically, whereas size parameters are averaged arithmetically.

Applying their method using FOG and SOG defined in this work, the relations for the calculation of pure compound GC parameters become as follows. The chain-length parameter $m$ is calculated as a sum of group contributions as presented in Equation (6.5). The energy parameter $\epsilon/k$ of a molecule is obtained from Equation (6.6) by a geometric average of FOGs present in the molecule, whereas the segment diameter $\sigma$ is calculated as an arithmetic average in Equation (6.7) including both FOG and SOG.

$$m_{molecule} = \sum_i (n_i m_i)_{FOG} + \Phi \sum_j (n_j m_j)_{SOG} \tag{6.5}$$

$$(\epsilon/k)_{molecule} = \left( \mathcal{C} \sqrt{\prod_i (\epsilon_i/k)^{n_i}} \right)_{FOG} \qquad \text{where} \qquad \mathcal{C} = \sum_i n_i \tag{6.6}$$

$$\sigma_{molecule} = \frac{\sum_i (n_i \sigma_i)_{FOG} + \Phi \sum_j (n_j \sigma_j)_{SOG}}{\sum_{i,j} (n_i + n_j)} \tag{6.7}$$

where $\Phi = 0$ when no SOG are present, and $\Phi = 1$ when SOG are present.

The parameters $m_i$, $\sigma_i$, and $\epsilon_i/k$ represent the contributions of the FOG of type $i$ that appears $n_i$ times, and $m_j$ and $\sigma_j$ are the contributions of the SOG of type $j$ that appears $n_j$ times. Equation (6.6) does not contain a contribution from SOG, because this lead to numerical instabilities during the linear least square analysis. A solution to this problem has not been sought, since it is not expected that contributions from SOG will lead to significant improvements of the resulting GC scheme.

GC parameters for FOG and SOG are now calculated using the correlations in Equations (6.5)–(6.7) with the methodology explained in Section 6.4. The resulting GC scheme with values of $m$, $\sigma$, and $\epsilon/k$ is found in Tables B.1 and B.2 in Appendix B together with statistical results in Table B.3. Since values of $\sigma$ and $\epsilon/k$ are directly fitted in the current approach instead of the parameter groupings $m\sigma^3$ and $m\epsilon/k$, the statistical results in Table B.3 are not directly comparable with statistical results from the original approach in Table 6.2.

Figure 6.10 shows linear correlations and % deviations of GC estimated parameters for about 400 different molecules, obtained from the GC scheme in Tables B.1 and B.2, with corresponding experimental reference values from DIPPR [3].

The results in Figure 6.10 should be compared to the scatter plots presented in Figure 6.2 on page 144 for the GC approach based on the linear equations in (6.2)–(6.4) proposed in this work. The linear correlation of $m$ and corresponding % deviations in Figure 6.10 (top) are more or less identical to the result obtained in Figure 6.2 (top). This does not come as a surprise since the underlying equations for $m$, i.e. Equations (6.2) and (6.5), are identical, so the small differences observed can only arise from slight deviations in the set of experimental data used for the linear regression.

However, for the $\sigma$ and $\epsilon/k$ parameters in Figure 6.10, the linear correlations with experimental reference values have deteriorated compared to the results in Figure 6.2; especially for $\epsilon/k$, where the value of $R^2 = 0.7116$ is considered unacceptable for further application of this approach. In addition, only 71.7 and 70.2 % of the $\sigma$ and $\epsilon/k$ datapoints,

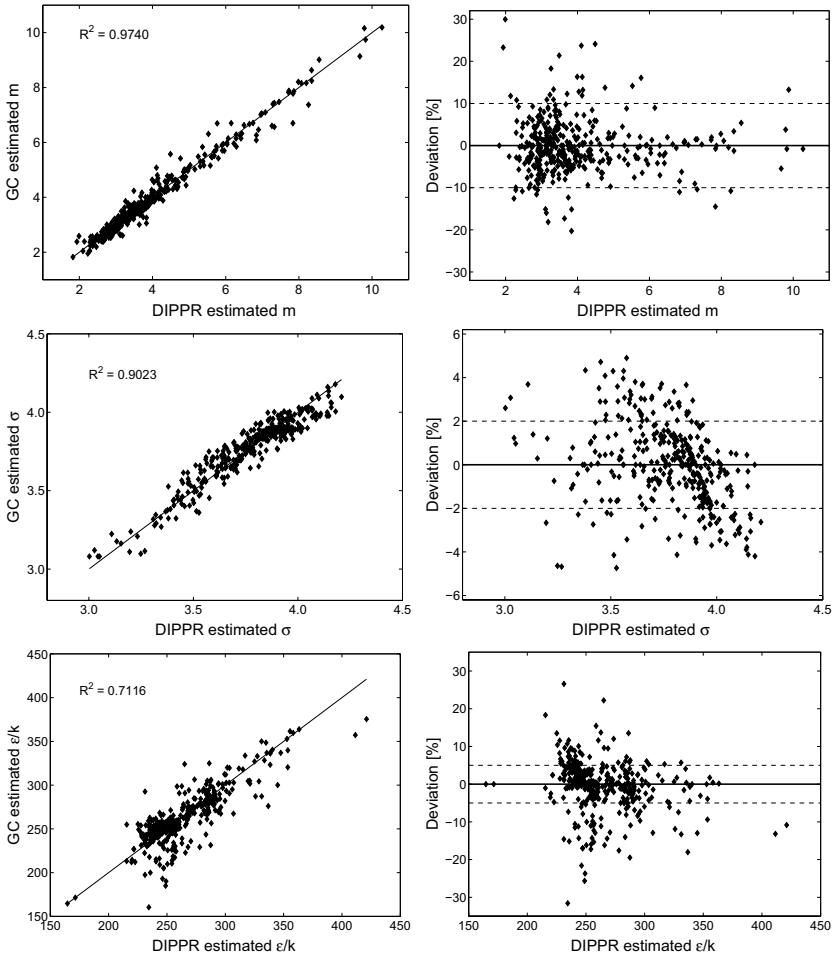


Figure 6.10: Scatter plots showing linear correlations (left) and % deviations (right) of GC- vs. DIPPR-estimated PC-SAFT parameters $m$ (top), $\sigma$ (middle), and $\epsilon/k$ (bottom), using the Tamouza *et al.* approach [13]. Dashed lines (right) mark ranges of deviating datapoints and are used to compare different GC approaches; see text.

respectively, lie within the ranges of the dashed lines that are considered to mark the limits of *low devations*; as discussed previously in Section 6.4. This is in contrast to 98.2 and 83.9 % for the GC estimated $\sigma$ and $\epsilon/k$ parameters from Figure 6.2.

Considering the poor linear correlation between the GC estimated $\epsilon/k$ parameters and reference values from DIPPR, it is concluded that Equations (6.5)–(6.7), based on proposals from Tamouza *et al.* [13], do not perform as well as the equations proposed in this work, i.e. Equations (6.2)–(6.4), when applied to the current GC methodology; at least when numerous groups are regressed at the same time.

## 6.5 Ongoing Attempts to Improve the GC Scheme

There have been some difficulties obtaining a solid linear correlation between GC estimated $\epsilon/k$ parameters and reference values from DIPPR. This can be observed in the scatter plots in Figure 6.2 (bottom) for the currently proposed GC approach, and in Figure 6.10 (bottom) for the application of the GC approach proposed by Tamouza *et al.* [13]. Moreover, it is the experience of the author that GC sPC-SAFT model predictions are generally more sensitive to the value of $\epsilon/k$ than the $m$ and $\sigma$ parameters, and hence, also sensitive to deviations of the $\epsilon/k$ parameter. Therefore, attempts to improve the current GC scheme have been focused on the accuracy of $\epsilon/k$.

This part of the work has been carried out after finishing detailed testing and analysis of the proposed GC scheme in Tables 6.3 and 6.4; the results of which will be the subject of the proceeding Chapter 7. It has resulted in what appears to be a further improvement of the existing GC scheme, but within the time limitations of the project it has not been possible to complete testing of this potential improvement of the GC scheme in a more consistent way. Therefore, it is regarded as supplementary to this thesis, and is, hence, presented in Appendix C from where it can serve as a springboard for future work within the subject.

## 6.6 Final Comments

The first-order group and second-order group contributions have been estimated following the procedure described in this chapter, and the accuracy of the fluid phase behaviour description of the compounds included in the fitting database has been examined. Two tables have been compiled including the contributions of 45 FOG and 26 SOG for each of the three parameter groupings, $m$, $m\sigma^3$, and $m\epsilon/k$.

The quality of the GC sPC-SAFT description of the pure compound data has been assessed for selected chemical families. It has been demonstrated that the GC approach provides a good representation of the fluid phase equilibria of the various compounds examined, and, particularly, for heavier members of the investigated families with observed low overall deviations from the experimental data. For almost all investigated compounds, AAD of $P^{sat}$ decreases with increasing carbon number. Predictions of $\rho$ are very accurate and in range of the AAD obtained when predicting $\rho$ using DIPPR estimated parameter sets (reported in Table 4.1).

In this chapter, the accuracy of the fluid phase behaviour of the compounds included in the optimisation database has been examined. In the next chapter, the predictive capability of the GC sPC-SAFT EoS is tested. The estimated parameters are used in a more predictive manner for the treatment of compounds not included in the database and for some selected binary mixtures.

## References


[1] L. Constantinou and R. Gani, "New Group Contribution Method for Estimating Properties of Pure Compounds," *AIChE J.*, vol. 40, pp. 1697–1710, 1994.

[2] N. von Solms, M. L. Michelsen, and G. M. Kontogeorgis, "Computational and Physical Performance of a Modified PC-SAFT Equation of State for Highly Asymmetric and Associating Mixtures," *Ind. Eng. Chem. Res.*, vol. 42, pp. 1098–1105, 2003.

[3] AIChE J., *DIPPR Table of Physical and Thermodynamic Properties of Pure Compounds.* New York, USA, 1998.

[4] E. K. Karakatsani, T. Spyriouni, and I. G. Economou, "Extended SAFT Equations of State for Dipolar Fluids," *AIChE. J.*, vol. 51, pp. 2328–2342, 2005.

[5] E. K. Karakatsani and I. G. Economou, "Perturbed Chain-Statistical Associating Fluid Theory Extended to Dipolar and Quadrupolar Molecular Fluids," *J. Phys. Chem. B*, vol. 110, pp. 9252–9261, 2006.

[6] J. Gross and J. Vrabec, "An Equation of State Contribution for Polar Components: Dipolar Molecules," *AIChE J.*, vol. 52, pp. 1194–1204, 2006.

[7] L. A. Constantinou, *Estimation of Properties of Acyclic Organic Compounds Through Conjugation.* PhD Thesis, Institute for Systems Research, University of Maryland, USA, 1993.

[8] D. Marquardt, "An Algorithm for Least Squares Estimation on Nonlinear Parameters," *SIAM (Soc. Ind. Appl. Math.) J. Appl. Math.*, vol. 11, pp. 431–441, 1936.

[9] E. Stefanis, L. Constantinou, I. Tsivintzelis, and C. Panayiotou, "New Group-Contribution Method for Predicting Temperature-Dependent Properties of Pure Organic Compounds," *Int. J. Thermophys.*, vol. 26, pp. 1369–1388, 2005.

[10] A. Fredenslund, R. L. Jones, and J. M. Prauznitz, "Group-Contribution Estimation of Activity Coefficients in Nonideal Liquid Mixtures," *AIChE J.*, vol. 21, pp. 1086–1099, 1975.

[11] H. S. Elbro, A. Fredenslund, and P. Rasmussen, "Group Contribution Method for the Prediction of Liquid Densities as a Function of Temperature for Solvents, Oligomers, and Polymers," *Ind. Eng. Chem. Res.*, vol. 30, pp. 2576–2582, 1991.

[12] D. N. Huynh, J.-P. Passarello, P. Tobaly, and J.-C. de Hemptinne, "Application of GC-SAFT EOS to Polar Systems Using a Segment Approach," *Fluid Phase Equilibria*, vol. 264, pp. 62–75, 2008.

[13] S. Tamouza, J.-P. Passarello, P. Tobaly, and J.-C. de Hemptinne, "Group Contribution Method with SAFT EoS Applied to Vapor Liquid Equilibria of Various Hydrocarbon Series," *Fluid Phase Equilibria*, vol. 222-223, pp. 67–76, 2004.

# Chapter 7

# Analysis and Applications of GC sPC-SAFT

*"When you come to the end of all the light you know, and it's time to step into the darkness of the unknown, faith is knowing that one of two things shall happen: Either you will be given something solid to stand on or you will be taught to fly."* by Edward Teller

## 7.1 Introduction

The GC method presented in Chapter 6 is now used for the treatment of binary mixtures where the quality of the phase behaviour modeling with the sPC-SAFT model is assessed through comparison with experimental data. For this final assessment, selected systems will be investigated representing a broad range of classes of industrially important mixtures. Even though the list of investigated compounds is far from exhaustive it should provide the reader with a good impression of the applicability of the method for binary systems.

## 7.2 Complex Binary Systems

In the previous chapter the correlative capability of the GC sPC-SAFT EoS has been investigated demonstrating satisfactory description of the fluid behaviour of the compounds used in the regression. However, the main objective of the GC approach is to function as a predictive tool for complex compounds or mixtures not necessarily included in the database but which can be formed from the various functional groups. Thus, emphasis is given to the predictive capability of the GC sPC-SAFT EoS without use of any binary interaction parameters. As supplementary help to the reader Table D.1 in Appendix D shows chemical structures of the complex compounds and monomer units of polymers investigated in this chapter together with their FOG and SOG descriptions.

### 7.2.1 Aromatic Esters

Aromatic esters belong to a family of valuable compounds with a number of important technological applications. The presence of the polarizable aromatic group (electron systems in the vicinity of the dipolar ester group) together with their hydrophobic character, confers to these compounds a highly selective solvent ability that is used for applications in fields such as cosmetic formulations, polymer science, and several synthesis processes among others [1, 2]. Aromatic esters with various chemical structures are tested in order to observe the effects of the alkylic chain length or the presence of the aromatic ring and its influence on the pure compounds' properties. Ester compounds investigated in this work are: methyl, ethyl, propyl, butyl benzoate, and phenyl acetate (See Table D.1 in Appendix D for their molecular structures). The experimental PVT behavior of the investigated aromatic esters reported by Aparicio *et al.* [3] is used for comparison with modelling results.

Table 7.1: Pure component PC-SAFT parameters for investigated aromatic esters and AAD % of $P^{sat}$ and $\rho$ for aromatic esters with various metods.

| Compound | $m$ [–] | $\sigma$ [Å] | $\epsilon/k$ [K] | AAD [%] $P^{sat}/\rho$ | Method |
|---|---|---|---|---|---|
| Methyl benzoate | 3.9654 | 3.5674 | 279.67 | 24.5/1.8 | FOG |
| | 3.8751 | 3.5934 | 281.62 | 26.0/1.6 | FOG+SOG |
| | 3.657 | 3.6412 | 304.91 | 2.8/0.5 | fitted to [3] |
| | 3.6922 | 3.6377 | 303.46 | 1.3/1.1 | fitted to [4] |
| Ethyl benzoate | 4.3488 | 3.6073 | 278.30 | 22.6/2.0 | FOG |
| | 4.2586 | 3.313 | 280.05 | 25.3/1.9 | FOG+SOG |
| | 4.636 | 3.5045 | 274.08 | 5.4/0.2 | [3] |
| Propyl benzoate | 4.7323 | 3.6401 | 277.16 | 17.7/1.4 | FOG |
| | 4.6421 | 3.6624 | 278.74 | 29.0/1.4 | FOG+SOG |
| | 3.587 | 4.0173 | 322.70 | 2.8/1.3 | fitted to [3] |
| | 4.6655 | 3.653 | 281.56 | 0.9/1.0 | fitted to [4] |
| Butyl benzoate | 5.1158 | 3.6675 | 276.19 | 11.5/1.8 | FOG |
| | 5.0256 | 3.6883 | 277.63 | 12.4/1.7 | FOG+SOG |
| | 4.0960 | 3.9644 | 312.50 | 5.4/0.9 | fitted to [3] |
| | 4.9127 | 3.7073 | 283.08 | 0.6/2.3 | fitted to [4] |
| Phenyl acetate | 4.2470 | 3.4773 | 275.03 | 29.4/3.0 | FOG |
| | 4.446 | 3.4136 | 273.38 | 3.5/0.9 | fitted to [3] |

The results in Table 7.1 indicate that the SOG contribution, which in this case is the ACCOO group, in the pure parameter estimations does not improve the predictions of vapour pressures nor the liquid densities of the investigated aromatic esters. On the contrary, indications of larger deviations from the experimental data are observed when introducing the contributions from SOG as well. However, due to the small number of investigated aromatic esters and their internal similarities (all belonging to alkyl benzoates), care should be taken when drawing final conclusions regarding the application of SOG for this family of compounds.

### 7.2.2 Phytochemicals (Cineole and Limonene)

Phytochemicals are non-nutritive plant chemicals that have protective or disease preventive properties. It is well-known that a plant produces these chemicals to protect itself but recent research has demonstrated that they can even protect humans against diseases [5, 6]. Phytochemicals are naturally present in many foods, but it is expected that bioengineering will enable development of new plants with higher levels making it easier to incorporate enough phytochemicals in our food [7].

One of these phytochemicals of particular interest is limonene. It is a relatively stable terpene, which can be distilled without decomposition. It is a major constituent in several citrus oils (orange, lemon, mandarin, lime, and grapefruit). Various studies have shown that limonene has anti-cancer effects, anti-inflammatory and pain-relieving efficiency, as well as large market potential [8,9]. Another important compound is the pharmaceutically active component of eucalyptus oil called 1,8-cineole (often just referred to as 'cineole'). It is a cyclic ether where the carbon atoms linked to the ether oxygen are fully substituted endowing cineole with stability and low chemical reactivity [6]. Cineole has a future as an industrial and commercial solvent, as well as the potential to control insects and weeds in an environmentally acceptable manner, in addition to its well documented and proven existing use in pharmaceuticals [7]. Due to a substantial number of applications of these two compounds, predictions of their thermodynamic properties are desired.

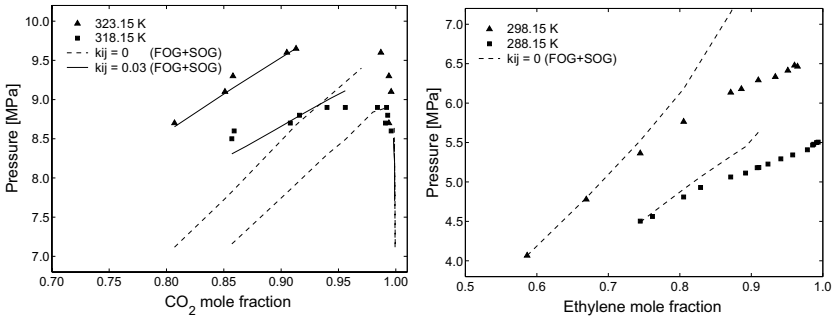


Figure 7.1: VLE of limonene–$CO_2$ at 318.15 and 323.15 K (left) and limonene–ethylene at 288.15 and 298.15 K (right). Symbols are experimental data [10, 11]. Dashed lines are GC sPC-SAFT predictions ($k_{ij} = 0$) using FOG+SOG. Solid lines (left) are correlations ($k_{ij} = 0.03$) using FOG+SOG.

Consideration of Figures 7.1 and 7.2 leads to the conclusion that sPC-SAFT without binary interaction parameters only qualitatively describes the experimental $P, x$ data for the binary systems of phytochemicals. The description of these experimental data can be improved by introduction of $k_{ij}$. This is clearly the case for the $CO_2$–limonene system

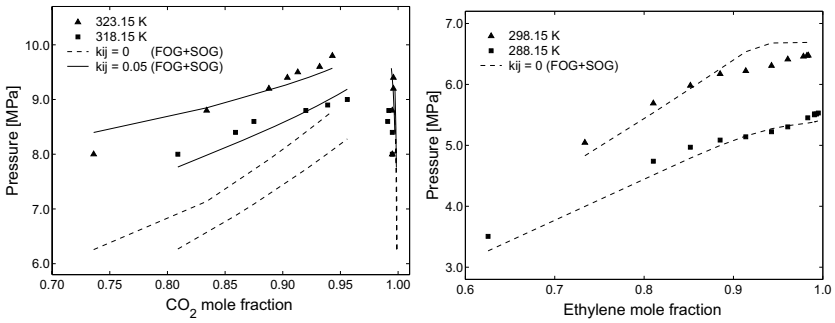


Figure 7.2: VLE of cineole–$CO_2$ at 318.15 and 323.15 K (left) and cineole–ethylene at 288.15 and 298.15 K (right). Symbols are experimental data [10, 11], dashed lines are GC sPC-SAFT predictions ($k_{ij} = 0$) using FOG+SOG, and solid lines (left) are correlations ($k_{ij} = 0.05$) using FOG+SOG.

where the optimum temperature independent $k_{ij}$ is 0.03; and for the $CO_2$–cineole system the value of $k_{ij}$ is 0.05. For the other two systems where the solvent is ethylene, the predictions of sPC-SAFT give good results. Unfortunately, due to limited experimental data for binary systems with phytochemicals, it is not possible to perform a more detailed analysis and therefore no final conclusion is given on the performance of the model.

### 7.2.3 Sulfur Containing Compounds

The content of sulfur in petroleum products has to be reduced in accordance with the environmental protection legislation. Petroleum refiners and natural gas processors face the various challenges of removing the increased sulfur content and doing it cost-effectively. This can be done either by improving desulfurization processes or by employing better thermodynamic characterization of sulfur compounds in different petroleum cuts [12]. Sulfur compounds are generally grouped into three classes: sulfides, thiols, and thiophenes.

This section aims at calculating PC-SAFT parameters for some sulfur containing compounds; investigating at the same time how well the model can predict their individual vapour pressures.

#### 7.2.3.1 Alkyl and Aryl Sulfides

The GC sPC-SAFT EoS is applied to predict vapour pressures for various alkyl and aryl sulfide compounds, which are compared to experimental data reported by Sawaya *et al.* [13]. There are no experimental PVT data available for these compounds in the DIPPR database [4]. Therefore no comparison is included.

The presented GC method is able to reproduce the experimental $P^{sat}$ of sulfides over

a wide range of temperatures. The results are graphically presented in Figure 7.3. For a purely predictive method the current accuracy is considered reasonably good and possibly sufficient for first-hand engineering calculations.

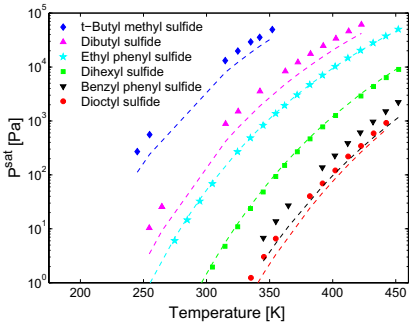


Figure 7.3: Vapor pressure of alkyl and aryl sulfides. Symbols are experimental data [13] and dashed lines are predictions with GC sPC-SAFT with sulfides parameters obtained from the proposed GC method.

#### 7.2.3.2 Thiols

If a sulfur distribution is carried out on a petroleum distillate, the majority of the sulfur-containing fractions appear at boiling points, which do not correlate with known sulfur compounds. This indicates that azeotropes are formed between sulfur compounds and hydrocarbons, which is perhaps to be expected, as the different types of hydrocarbons are known to form azeotropes among themselves [14]. When looking through the available literature, it is apparent that the information available on the occurrence and properties of these azeotropes is quite limited, which is surprising since hydrocarbons are found associated with sulfur compounds not only in petroleum products but also in coal tars and shale oils. Therefore, the study of thiols, often referred to as mercaptans, with sPC-SAFT is initiated to possibly increase knowledge of the chemical and physical properties of the sulfur compounds present in petroleum distillates.

Results obtained for some representative mixtures are shown in Table 7.2, where the overall average deviation for vapour pressure is 8.8 % of predictions and 2.4 % of correlations using a temperature-independent $k_{ij}$.

Table 7.2: Comparison of predicted and correlated results for binary VLE of different thiol-systems using GC sPC-SAFT.

| System | Temp. [K] | AAD $P$ [%] $k_{ij} = 0$ | $k_{ij}$ optimal | AAD $P$ [%] | AAD $P$ [%] $k_{ij} = 0.03$ | Ref. |
|---|---|---|---|---|---|---|
| Methanethiol+$n$-hexane | 253.15 | 17.1 | | 5.1 | 5.1 | |
| | 263.15 | 16.7 | 0.03 | 4.2 | 4.2 | [15] |
| | 273.13 | 15.4 | | 3.3 | 3.3 | |
| Methanethiol+$n$-decane | 315.15 | 10.5 | 0.03 | 1.9 | 1.9 | [15] |
| Ethanethiol+1-propylene | 253.15 | 7.1 | 0.01 | 1.7 | 12.4 | [16] |
| | 323.15 | 4.2 | | 0.9 | 20.1 | |
| Propanethiol+$n$-butane | 343.15 | 6.0 | 0.02 | 0.8 | 3.5 | [17] |
| | 383.15 | 4.2 | | 1.1 | 3.8 | |
| Butanethiol+$n$-hexane | 323.15 | 5.7 | | 3.8 | 3.6 | |
| | 353.15 | 3.3 | 0.025 | 1.5 | 1.6 | [18] |
| | 372.66 | 2.3 | | 1.3 | 1.7 | |
| Butanethiol+toluene | 323.05 | 16.6 | | 2.7 | 2.7 | |
| | 353.15 | 6.8 | 0.03 | 2.8 | 2.8 | [18] |
| | 371.53 | 7.1 | | 2.7 | 2.7 | |
| AAD [%] overall | | 8.8 | | 2.4 | 5.0 | |

Figures 7.4–7.6 show the total system pressure as a function of liquid and vapour composition to illustrate the performance of the model for this type of compounds.

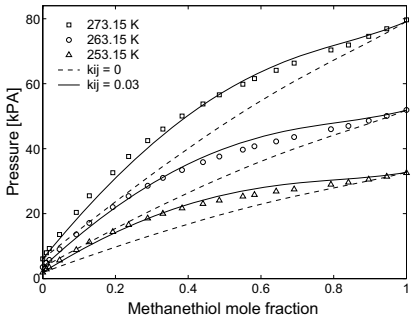


Figure 7.4: P,x-diagram of methanethiol–$n$-hexane at 253.15, 263.15, and 273.15 K. Symbols represent experimental data [15], where lines are GC sPC-SAFT modelling results.

In Figure 7.5, for the ethanethiol–1-propylene system, the 253.15 K isotherm shows positive deviations from Raoult's law, while at 323.15 K there is significant non-ideality in the liquid phase causing the total pressure to lie below Raoult's law in the propylene-rich region of the system. In both cases, GC sPC-SAFT is well capable of predicting the observed behaviour.

Results of the propanethiol–$n$-butane system at 343.15 and 383.15 K are plotted in

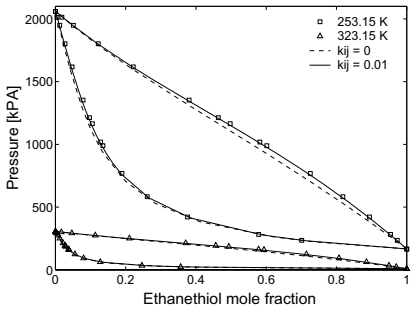


Figure 7.5: P,x,y-diagram of ethanethiol–1-propylene at 253.15 and 323.15 K. Symbols represent experimental data [16], where lines are GC sPC-SAFT modelling results.

Figure 7.6. The figure shows that a single $k_{ij} = 0.02$ correlates the results quite satisfactorily, but even so pure predictions ($k_{ij} = 0$) are able to follow the trends in the experimental data.

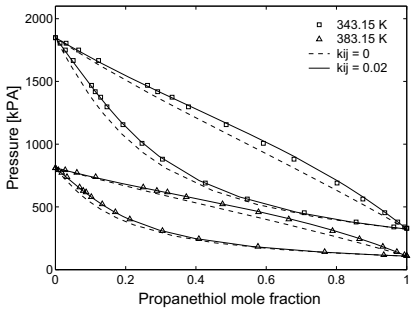


Figure 7.6: P,x,y-diagram of propanethiol–*n*-butane at 343.15 and 383.15 K. Symbols represent experimental data [17], where lines are GC sPC-SAFT modelling results.

As observed in Table 7.2, the optimum $k_{ij}$ values for the thiol systems tend to lie between 0.01 and 0.03. Additionally, Table 7.2 includes AAD for correlations using a fixed $k_{ij} = 0.03$, which performs well for all the investigated systems except for ethanethiol–1-propylene. Therefore, from a practical point of view, it can be expected that transferable binary parameters in this range allow straightforward extension of the model to other thiol-containing binary mixtures without any additional fitting.

### 7.2.4 Polynuclear Aromatic Hydrocarbons

Polynuclear aromatic hydrocarbons (PAHs) comprise a group of more than 100 different chemical compounds that result from incomplete combustion of organic materials such as coal, oil, wood, etc. They have a wide range of potential commercial applications in fields ranging from use as pharmaceuticals and cosmetic additives to use as additives in electron- and photo-resists, proton-conducting membranes for fuel cells, optical limiting materials and devices, lithium battery anodes, active elements in organic transistors, and as pigments [19–21]. Due to the presence of ring structures, they are quite good test compounds for the effect of SOG on the overall calculations.

The relative deviations obtained on vapour pressures for some investigated PAHs are given in Table 7.3.

Table 7.3: Pure component PC-SAFT parameters for some investigated PAHs and AAD % from the experimental $P^{sat}$ [4, 22].

| Compound | $m$ [–] | $\sigma$ [Å] | $\epsilon/k$ [K] | AAD $P^{sat}$ [%] | Method |
|---|---|---|---|---|---|
| Phenanthrene | 3.7431 | 4.0130 | 375.67 | 60.3 | FOG |
| | 3.7313 | 4.0283 | 379.84 | 36.5 | FOG+SOG |
| Benzo[a]pyrene | 4.4474 | 4.1485 | 432.24 | 101.7 | FOG |
| | 4.4177 | 4.1795 | 441.43 | 33.2 | FOG+SOG |
| Tetralin | 3.0256 | 4.0204 | 329.54 | 58.6 | FOG |
| | 3.0681 | 3.9996 | 330.47 | 39.3 | FOG+SOG |
| | 3.2987 | 3.8755 | 325.73 | 0.4 | fitted to [4] |
| Biphenyl | 3.7703 | 3.9069 | 333.97 | 6.5 | FOG |
| Dibenzofuran | 2.8087 | 4.2072 | 408.82 | 15.9 | FOG |
| | 3.1176 | 4.0714 | 388.66 | 11.6 | FOG+SOG |
| | 2.3829 | 4.5718 | 452.21 | 2.1 | fitted to [4] |
| Acenaphthene | 2.9906 | 4.1058 | 389.14 | 44.6 | FOG |
| | 3.2936 | 3.9901 | 374.30 | 8.3 | FOG+SOG |
| | 3.6387 | 3.8560 | 355.5 | 2.3 | fitted to [4] |

From Table 7.3, it appears that the accuracy of the predictions with the GC sPC-SAFT EoS is not always convincing. E.g., when comparing the predicted $P^{sat}$ of tetralin with the experimental data from Ruuzicka *et al.* [22], absolute deviations of 58.6 and 39.3 % are obtained with FOG and FOG+SOG contributions respectively. A comparison of the same predicted parameter sets to experimental data from the DIPPR database [4] yields absolute deviations of 39.7 and 26.2 % for FOG and FOG+SOG contributions respectively. These differences suggest some uncertainty in the available experimental data, but still the present GC approach seems to have some difficulties in capturing the nature of these complex aromatic compounds. Nonetheless, it is observed that application of SOG provides substantial improvements of the modeling results.

In the work presented by Nguyen Huynh *et al.* [23], several more PAHs are treated with their version of the GC PC-SAFT EoS, and the predictions of $P^{sat}$ and $\rho$ are somewhat

lower (generally within 3 % on both properties) than the ones from this work. However, in addition to the usual terms, a quadrupolar-quadrupolar contribution is used as well, which seems to improve the predictive capability of the approach.

Figures 7.7 and 7.8 show attempts to model VLE of binary mixtures of tetralin with biphenyl/dibenzofuran as measured by Coon *et al.* [24]. The figures reveal substantial deviations from the experimental values; especially the prediction of the bubble point curves. However, when considering the already observed deviations in the predicted $P^{sat}$ values in Table 7.3 above, the observed deviations in Figures 7.7 and 7.8 do not come unexpected.

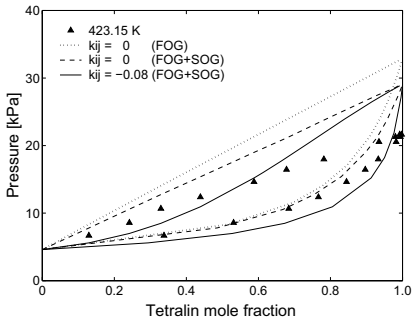


Figure 7.7: VLE of tetralin–biphenyl at 423.15 K. Symbols represent experimental data [24]. Dashed and dotted lines are predictions with GC sPC-SAFT with and without SOG, respectively.

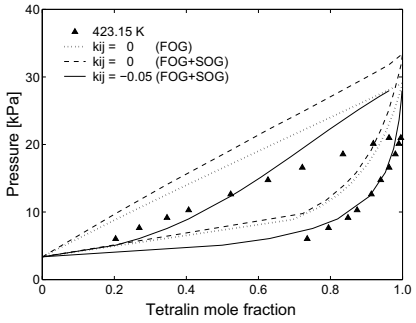


Figure 7.8: VLE of tetralin–dibenzofuran at 423.15 K. Symbols represent experimental data [24]. Dashed and dotted lines are predictions with GC sPC-SAFT with and without SOG, respectively.

Both Figures 7.7 and 7.8 show that the modeling results approach the experimental data when the tetralin mole fraction becomes low. This is most pronounced when $k_{ij} \neq 0$. It indicates that the model is able to capture the pure component properties of biphenyl and dihydrofuran, which is also consistent with the somewhat lower deviations of pure compound $P^{sat}$ for these compounds, as listed above in Table 7.3. The main difficulty in the validation of the proposed method is the lack of sufficient experimental data, especially for binary mixtures containing at least one PAH compound.

## 7.3 Biodiesel

The use of vegetable oils as fuel for diesel engines goes back to the 1900s, when Dr. Rudolph Diesel, the inventor of the engine that bears his name, used peanut oil to fuel one of his engines at the Paris Exposition. He declared that 'the diesel engine can be fed with vegetable oil and will help considerably in the development of the agriculture of the countries which use it' [25]. At that time, the vegetable oil fuels were not acceptable because they were more expensive than petroleum fuels. However, with recent increases in petroleum prices and uncertainties concerning petroleum availability, there is renewed interest in this area. The earliest known use of alkyl esters for fuel is documented in a Belgian patent granted in 1937 to G. Chavanne [26].

Biodiesel, defined as the mono-alkyl esters of vegetable oils or animal fats, is an alternative diesel fuel that is accepted in a steady growing number of countries around the world. It contains no petroleum but it can be blended at any level with petroleum diesel to create a biodiesel blend. Application of this kind of fuel contributes to the mitigation of our environmental issues such as global warming and air pollution since its feedstock of biomass is carbon neutral and has a low content of sulfur and aromatic carcinogenic compounds. It is considered a renewable resource, due to the fact that it is derived from products that can be grown and produced domestically [27].

The transesterification of an oil or fat with a monohydric alcohol; in most cases methanol due to its low price and least reactivity, and an alkaline catalyst such as potassium or sodium hydroxide, yields the corresponding mono-alkyl esters, which are defined as biodiesel. As this is a reversible reaction, 60 to 200 % excess methanol is typically added during the reaction in order to force the equilibrium in the direction of the desired products [28–30].

The final biodiesel product is dominated by methyl ester with a hydrocarbon chain of 18 carbon atoms and 1, 2, or 3 unsaturated bonds representing more than 90 % of the material. The residuals are the methyl esters with hydrocarbon chains from 12 to 22 and small amounts of un-reacted oil, glycerol, etc. [31].

Temperature-independent vapour pressures of i.e. methyl esters of fatty acids that are commonly present in biodiesel fuel are usually predicted by the Antoine equation and in some cases group contributions. These esters have the general molecular formula

$CH_3(CH_2)_nCOOCH_3$ (see Appendix D). Boiling point, $T_b$, is a key fuel property for biodiesel [32] in relation to quality control. Besides its importance for quality control, boiling point at atmospheric pressure, called *normal* boiling point, is also the basis for the prediction of the critical properties, and temperature-dependent properties such as vapour pressure, density, latent heat of vapourization, viscosity, and surface tension of biodiesel. Determination of these properties requires measurements over a wide range of temperatures, which can, in practice, be a substantial obstacle. Therefore, accurate $T_b$ of pure fatty acid esters and their biodiesel mixtures are useful for predicting fuel properties. Although the normal boiling points of some fatty acid esters have been published, those of real world biodiesel fuels are scarce. For example, most of the reported data focus on the short chain saturated fatty acid methyl esters (FAMEs) ($C_8$–$C_{14}$), while data for $C_{16}$ and $C_{18}$ are very limited and not available; especially those with carbon atoms 20 or more [32].

In 2004, Ceriani and Meirelles [33] proposed a GC method for the estimation of the vapour pressure of fatty compounds. The method seems to be accurate when used together with the UNIFAC model for estimating VLE of binary and multicomponent fatty acid ester mixtures.

Another important property that is of interest to the biodiesel industry is predicting infinite dilution activity coefficients. Biodiesel is a high boiling solvent well-suited for volatile organic compounds (VOC) absorption due to its beneficial physical properties and low market prices. In addition, the high-boiling solvent used, once spent, must be treated as hazardous waste with great expenses, while biodiesel is a readily biodegradable matter. However, this last advantage requires particular attention regarding the stability of the fuel. If exposed to a specific 'oxidation stress', i.e., high temperatures and frequent contact with atmospheric oxygen, it ages faster than normal mineral diesel. For this purpose, environmentally friendly additives, so-called antioxidants, are added during the production of biodiesel [34].

In order to use biodiesel effectively as an absorption solvent for a specific waste gas problem, it is important to determine the activity coefficients at infinite dilution of the VOCs to be separated with biodiesel. The affinity of the solvent towards a VOC [34] can be expressed using Henry's law in terms of partial pressure $P_i$ of the VOC and its mole fraction $x_i$ in the solvent phase at infinite dilution. Here, the activity coefficient of the VOC in the solvent at infinite dilution ($\gamma_1^\infty$) is determined by taking into account the vapour pressure of the VOC at the same temperature, $P_i^{sat}$:

$$\gamma_i^\infty = \frac{H}{P_i^{sat}} \quad \text{where} \quad H = \lim_{x_i \to 0} \frac{P_i}{x_i} \tag{7.1}$$

In this case, both $H$ and $\gamma_i^\infty$ allow the assessment of the mutual affinity of the compounds under consideration. The vapour pressures of biodiesels are almost zero at low temperatures. This is a desired property as it prevents secondary emissions or loss of

solvent by evapouration. Additionally, biodiesel must be suitable for use during winter at temperatures around –20 °C. Additives are typically applied to ensure this. Hence, the antioxidants, winter additives, and methanol remaining from the production, represent the volatile fraction of the biodiesel [34].

The next sections will cover:

- Prediction of vapour pressure for the most common FAMEs (i.e. methyl caprylate, methyl caprate, methyl laurate, methyl myristate, methyl palmitate, etc.) and modeling VLE of numerous systems with these esters investigated in the literature.
- Modeling of VLE for binary mixtures of carbon dioxide and fatty acid methyl esters, particularly, methyl stearate, methyl palmitate, methyl myristate, and methyl oleate at four different temperatures. Investigation of mixtures of these compounds that exhibit nearly, but not entirely, ideal VLE behaviour. The non-ideality is a negative deviation from Raoult's law.
- Existing experimental data of the infinite dilution activity coefficients for VOCs (1,2-chloroethane, benzene, and toluene) in methyl oleate are available at three temperatures, and these will be compared with the predicted values from GC sPC-SAFT and two versions of the UNIFAC model.

### 7.3.1 Vapour Pressure Predictions

Experimental vapour pressure-temperature data for numerous FAMEs are reported by Rose and Supina [35]. Table 7.4 presents the vapour pressure descriptions of saturated fatty acid methyl esters using the GC sPC-SAFT model including a comparison with experiments. The absolute deviations seem to decrease with the size of the saturated FAMEs. Figure 7.9 shows comparisons of the experimental and predicted vapour pressures specifically for methyl oleate and methyl stearate using the parameters listed in Table 7.5. The prediction of $P^{sat}$ using GC sPC-SAFT in the right graph in Figure 7.9 shows excellent correlation with both sets of experimental data [35, 36], while some deviations are observed in the left graph, when using the GC sPC-SAFT parameter sets (dashed lines). The molecular structures of methyl oleate and methyl stearate differ by a single double bond, which may suggest that the GC method has difficulties accounting for this particular structural phenomenon.

In an article by van Genderen *et al.* [37], experimental vapour pressures have been reported for a number of fatty acid methyl and ethyl esters, and these values are compared against data available from other sources. However, even in this article, the databases only go up to methyl stearate with carbon number 19. Predictions of vapour pressure is an important issue when no data for desired FAMEs are available. There are numerous correlations proposed in the literature based on various theoretical approaches, but only a few can deal with heavier fatty acid esters with carbon atom of 20 or more.

Table 7.4: Pure component parameters for investigated FAMEs calculated using the GC scheme for use with the sPC-SAFT EoS. $C_{n:m}$ indicates $n$ total number og carbon atoms and $m$ number of double bonds.

| FAMEs | | $m$ [−] | $\sigma$ [Å] | $\epsilon/k$ [K] | $T$ range [K] | AAD $P$ [%] |
|---|---|---|---|---|---|---|
| Methyl caprylate | $C_{9:0}$ | 5.0277 | 3.6592 | 241.82 | 374–419 | 46.7 |
| Methyl caprate | $C_{11:0}$ | 5.7947 | 3.7044 | 244.78 | 381–462 | 29.3 |
| Methyl laurate | $C_{13:0}$ | 6.5616 | 3.7383 | 247.04 | 430–486 | 17.1 |
| Methyl myristate | $C_{15:0}$ | 7.3286 | 3.7647 | 248.84 | 440–511 | 9.4 |
| Methyl palmitate | $C_{17:0}$ | 8.0956 | 3.7858 | 250.29 | 467–506 | 3.4 |
| Methyl stearate | $C_{19:0}$ | 8.8625 | 3.8031 | 251.49 | 477–513 | 3.8 |
| Methyl oleate | $C_{19:1}$ | 8.9962 | 3.7639 | 253.79 | 430–212 | 41.5 |

Table 7.5: Comparison of sPC-SAFT parameters for methyl oleate.

| FAMEs | $m$ [−] | $\sigma$ [Å] | $\epsilon/k$ [K] | $T$ range [K] | AAD $P$ [%] | Method |
|---|---|---|---|---|---|---|
| Methyl oleate | 9.3898 | 3.6881 | 243.32 | 430–212 | 5.59 | DIPPR fitted |
| | 8.9962 | 3.7639 | 253.79 | | 41.5 | GC |

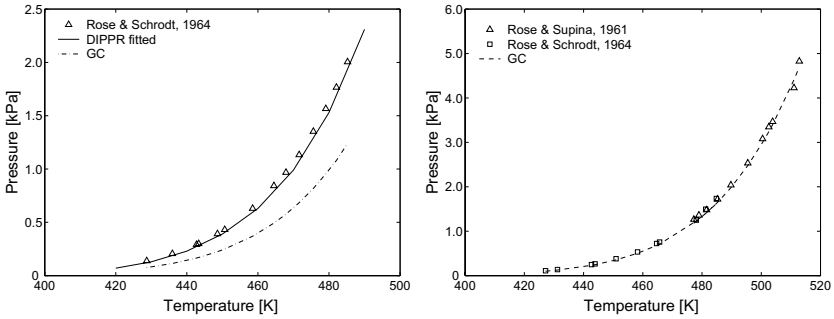


Figure 7.9: Predicting $P^{sat}$ for methyl oleate (left) and methyl stearate (right) with sPC-SAFT using parameters fitted to DIPPR and calculated from the GC scheme as shown in Tables 7.4 and 7.5. Experimental data are taken from ref. [35, 36].

### 7.3.2 Phase Equilibria

There are very few experimental data on VLE of the fatty ester systems. Rose and Supina [35] are some of the few researches who have conducted intensive experimental measurements of the VLE for various binary systems involving FAMEs under isobaric conditions. Table 7.6 shows overall results of the predictions with the GC sPC-SAFT EoS. Moreover, a comparison of experimental and predicted values at isobaric conditions

is given in Figure 7.10 in terms of $x - y$ diagrams for methyl myristate–methyl palmitate mixtures. The results are considered to be satisfactory.

Table 7.6: GC sPC-SAFT predictions ($k_{ij} = 0$) of VLE mixtures of FAMEs.

| Mixture | $T$ or $P$ [K] or [kPa] | AAD $T$ or $P$ [%] | AAD $y$ [%] | Ref. |
|---|---|---|---|---|
| Methyl oleate + methyl sterate | 470 K | 21.39 | — | [36] |
| | 480 K | 30.65 | — | |
| Methyl laurate + methyl myristate | 4.0 kPa | 14.96 | 1.94 | [35] |
| | 5.3 kPa | 14.17 | 2.42 | |
| | 6.7 kPa | 14.79 | 3.62 | |
| | 13.3 kPa | 14.92 | 2.63 | |
| Methyl caprate + methyl laurate | 4.0 kPa | 27.53 | 2.01 | [35] |
| | 5.3 kPa | 17.89 | 1.59 | |
| | 6.7 kPa | 26.36 | 3.28 | |
| | 13.3 kPa | 25.87 | 2.13 | |
| Methyl myristate + methyl palmitate | 4.0 kPa | 6.16 | 1.72 | [35] |
| | 5.3 kPa | 5.01 | 1.93 | |
| | 6.7 kPa | 5.34 | 2.53 | |
| | 13.3 kPa | 5.32 | 1.72 | |

The ability of the GC sPC-SAFT EoS to predict isothermal VLE data from four binary mixtures of $CO_2$ and FAMEs at four temperatures is further evaluated in Figures 7.11–7.14. The experimental data are reported by Inomata *et al.* [38]. Figure 7.14 also contains results for $CO_2$–methyl oleate when applying PC-SAFT parameters obtained from fitting data from DIPPR [4].

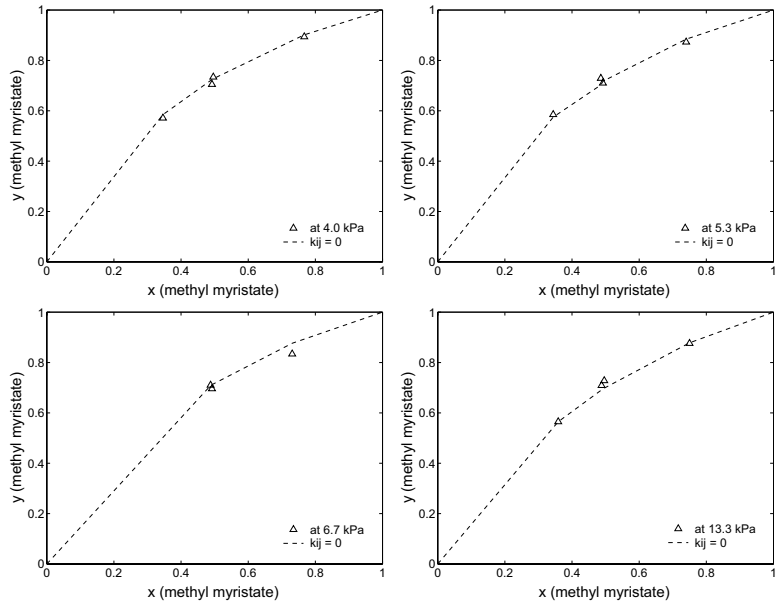


Figure 7.10: VLE of methyl myristate–methyl palmitate at pressures from 4.0 to 13.3 kPa. Symbols represent experimental data [35], and lines are predictions with GC sPC-SAFT.

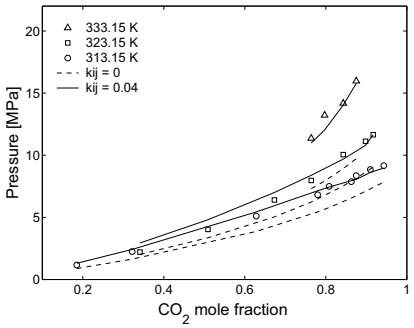


Figure 7.11: VLE of $CO_2$–methyl myristate [38]with GC sPC-SAFT.

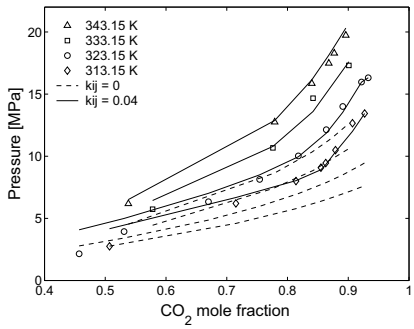


Figure 7.12: VLE of $CO_2$–methyl stearate [38] with GC sPC-SAFT.

Figures 7.11–7.14 show that the solubility of saturated methyl esters increases with the pressure and decrease with the carbon number of the esters. In most cases, satisfactory correlations of the solubility's are obtained using a temperature independent $k_{ij} = 0.04$. It

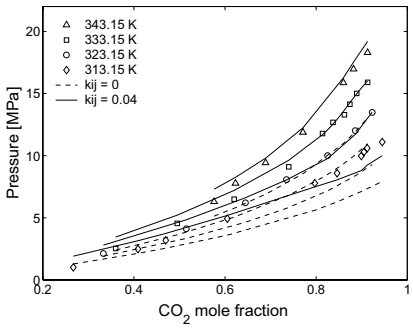


Figure 7.13: VLE of $CO_2$–methyl palmitate [38] with GC sPC-SAFT.

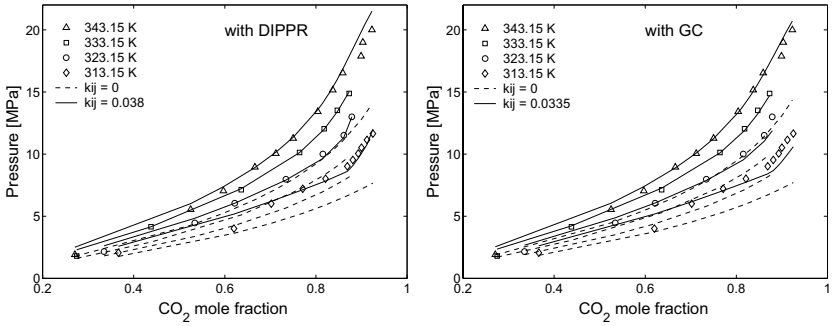


Figure 7.14: VLE of $CO_2$–methyl oleate [38] using sPC-SAFT with parameters fitted to DIPPR (left) and calculated using the GC scheme (right).

is observed that the solubility with lower mole fraction of $CO_2$ is more difficult to capture by the model. Furthermore, Figure 7.14 shows that there is little difference between the performance of parameter sets based on data from DIPPR and the GC scheme.

### 7.3.3 Evaluation of $\gamma^\infty$

Group contribution methods like UNIFAC are commonly used for the estimation of $\gamma^\infty$ for different substances. Therefore, the values of $\gamma^\infty$ of the three VOCs (1,2-dichloroethane, toluene, and benzene) in methyl oleate reported experimentally and calculated with two different UNIFAC methods, original UNIFAC and Lyngby Modified UNIFAC, by Bay *et al.* [34] are compared with predictions of GC sPC-SAFT. Tabulated values are given in Table 7.7, while a graphical illustration is provided in Figure 7.15. The results show

that the methodology used in this work performs equally well as other well-established predictive tools (for activity coefficients and vapour pressure).

Table 7.7: Comparison of experimental and calculated $\gamma_i^\infty$ values for VOCs in methyl oleate. Results for original UNIFAC and Lyngby Modified UNIFAC are reported by Bay *et al.* [34].

| Component | Temp. [K] | Exp. $\gamma_i^\infty$ | Predicted $\gamma_i^\infty$ ($k_{ij}=0$) UNIFAC | LBY-UNI | GC sPC-SAFT |
|---|---|---|---|---|---|
| 1,2-Dichloroethane | 303.15 | 0.647 | 0.740 | 1.252 | 0.707 |
| | 308.15 | 0.668 | 0.735 | 1.228 | 0.700 |
| | 313.15 | 0.699 | 0.732 | 1.203 | 0.694 |
| Benzene | 303.15 | 0.628 | 0.580 | 0.855 | 0.712 |
| | 308.15 | 0.636 | 0.579 | 0.850 | 0.708 |
| | 313.15 | 0.647 | 0.579 | 0.846 | 0.704 |
| Toluene | 303.15 | 0.651 | 0.649 | 0.838 | 0.752 |
| | 308.15 | 0.672 | 0.651 | 0.835 | 0.749 |
| | 313.15 | 0.718 | 0.652 | 0.833 | 0.746 |
| AAD [%] overall | | | 7.80 | 46.6 | 8.81 |

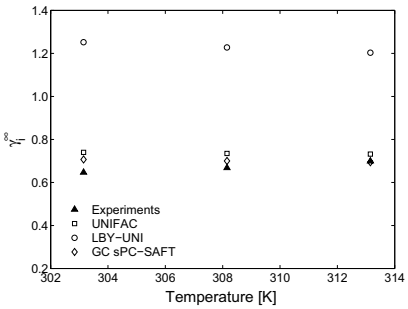


Figure 7.15: Comparison of predictivity of $\gamma_i^\infty$ as a function of temperature with various models using the system 1,2-dichloromethane in methyl oleate.

In general, the LBY-UNI yields higher values for all investigated compounds with large deviations (46.6 %) from the experimental values. With the GC sPC-SAFT model, this overall absolute deviation is reduced to 8.81 %.

## 7.4 Predicting $\gamma^{\infty}$ for Athermal Systems

In athermal systems, the enthalpy of mixing is approximately zero. This is almost the case for hydrocarbon mixtures containing short- and long-chain alkanes, and also some polymers. Although entirely athermal mixtures are very rare, it is assumed that any deviations from ideality in the liquid phase (Raoult's law) are due to size, shape, and free-volume differences between the involved compounds. It has been shown that it is generally difficult to simultaneously predict the activity coefficients of both a short-chain solute and a long-chain solvent ($\gamma_1^{\infty}$), and a long-chain solute in a short-chain solvent ($\gamma_2^{\infty}$) with the same model.

The purpose of this section is to carry out a comparison of the results obtained from existing activity coefficient models, such as Entropic-FV [39,40] and Modified UNIFAC [41] previously mentioned in Section 5.2, with results obtained from original PC-SAFT [42] and sPC-SAFT. The applied pure compound parameters in the two versions of the PC-SAFT model are obtained from both the proposed GC scheme and from fitting to vapour pressure and liquid density data from DIPPR [4].

Experimental results of mixtures of short-chain alkanes in long-chain solvents reveal negative deviations from ideality, which become more pronounced as the difference between chain lengths of the compounds increases. Negative deviations are particularly large for mixtures of hydrocarbons with cycloalkanes. It is $\gamma^{\infty}$ that describes these deviations from ideality. For higher $M_w$ systems at higher temperatures, the activity coefficient is generally independent of temperature because of low partial excess enthalpies ($h_i^E$) of these systems, as presented with Equation (7.2). However, at lower temperatures, the activity coefficients generally decrease with increasing temperatures. Therefore, it is not advisable to compare data sets at different temperatures for low $M_w$ systems. Additionally, several data sets of experimental $\gamma^{\infty}$ for alkane mixtures show a small variation with temperature indicating that these systems, including both low and high $M_w$ compounds, may not behave completely athermally.

$$\left[\frac{\partial\left(\ln\gamma_i\right)}{\partial T}\right]_{P,x} = -\frac{h_i^E}{RT^2} \tag{7.2}$$

Results of $\gamma^{\infty}$ predictions for short-chain alkanes in long-chain alkanes, and long-chain alkanes in short-chain alkanes are presented in Tables 7.8 and 7.9 respectively, and representative results are shown graphically in Figure 7.16 for $\gamma^{\infty}$ of $n$-pentane and 2,3-dimethyl butane in long chain $n$-alkanes.

The performance of the different models is evaluated using AAD % in the activity coefficient predictions. Based on the evaluation of the predictions of $\gamma_1^{\infty}$ of short-chain alkanes in long-chain alkanes, the four models perform satisfactorily with the Entropic-FV model providing the largest deviations. When $\gamma_2^{\infty}$ of long-chain alkanes in short-chain alkanes are considered, the Entropic-FV model also provides the poorest correlation with

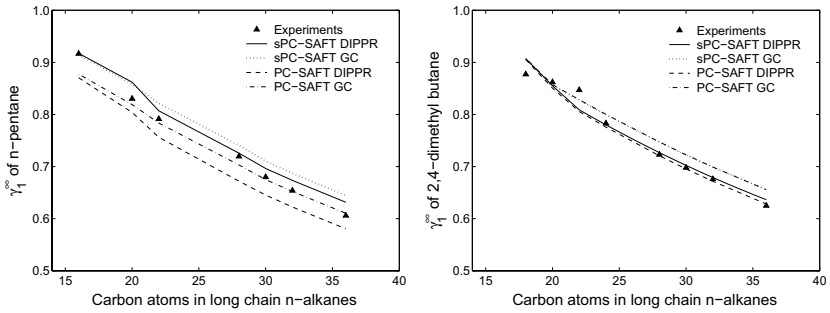


Figure 7.16: Experimental [43,44] and predicted $\gamma^{\infty}$ of $n$-pentane (left) and 2,3-dimethyl butane (right) in long chain $n$-alkanes.

the experimental data resulting in an overall deviation of 33 %. The results from the GC sPC-SAFT EoS are satisfactory and comparable to those obtained by those from Modified UNIFAC and original PC-SAFT; especially for short-chain alkanes in long-chain alkanes (Table 7.8).

The $\gamma^{\infty}$ calculations provide a convenient way of testing the performance of the model in the region where the maximum degree of non-ideality is encountered, and such evaluations are useful for solvent–polymer mixtures. Note that in the VLE calculations for solvent–polymer mixtures, the key property is usually the solvent activity, while in LLE the dominating factor is the polymer activity coefficient. In fact, the analysis of these $\gamma^{\infty}$ calculations provides indications of the suitability of the GC sPC-SAFT model for LLE calculations for polymer solutions.

Table 7.8: AAD % between experimental [43–45] and predicted (with $k_{ij} = 0$) $\gamma_1^\infty$ for short-chain alkane solutes in long-chain alkane solvents. $C_n$ indicates $n$ number of carbon atoms.

| Solute/Solvent | $T$ range [K] | PC-SAFT DIPPR[a] | PC-SAFT GC | sPC-SAFT DIPPR[a] | sPC-SAFT GC | Entropic-FV[b] | Modified UNIFAC[b] |
|---|---|---|---|---|---|---|---|
| *n*-Pentane/*n*-$C_{16,20,22,28}$ | 313–343 | 4.8 | 2.2 | 1.7 | 2.6 | 12.4 | 9.4 |
| *n*-Hexane/*n*-$C_{16,18,20,22,28}$ | 303–343 | 3.8 | 1.6 | 1.7 | 2.1 | 9.7 | 5.0 |
| *n*-Heptane/*n*-$C_{16,18,20,22,24,28,30,32,34,36}$ | 303–393 | 6.1 | 3.4 | 1.9 | 1.6 | 9.6 | 3.6 |
| *n*-Octane/*n*-$C_{18,20,22,24,28,30,32,34,36}$ | 308–393 | 6.8 | 4.2 | 2.9 | 2.0 | 9.6 | 3.0 |
| *n*-Decane/*n*-$C_{20,22,24,28,30,32,34,36}$ | 353–393 | 7.3 | 4.5 | 2.4 | 2.1 | 8.8 | 2.4 |
| Cyclohexane/*n*-$C_{16,18,20,24,28,32}$ | 298–343 | 5.8 | 5.9 | 8.5 | 7.5 | 9.1 | 3.5 |
| 2,3-Dimethylbutane/*n*-$C_{18,20,22,24,28,30,32,34,36}$ | 308–393 | 1.5 | 2.9 | 1.6 | 2.9 | 8.5 | 3.8 |
| 2,2,4-Trimethylpentane/*n*-$C_{20,22,24,28,30,32,34,36}$ | 353–393 | 2.9 | 2.3 | 3.1 | 2.2 | 11.8 | 6.8 |
| AAD [%] overall | | 4.9 | 3.4 | 3.0 | 2.9 | 9.7 | 4.9 |

[a]) For *n*-$C_{>20}$, parameters are calculated using Eq. (4.1)–(4.3) from Section 4.3. [b])Results reported by Voutsas *et al.* [46].

Table 7.9: AAD % between experimental [43, 44] and predicted (with $k_{ij} = 0$) $\gamma_2^\infty$ for long-chain alkane solutes in short-chain alkane solvents. $C_n$ indicates $n$ number of carbon atoms.

| Solute/Solvent | $T$ range [K] | PC-SAFT DIPPR[a] | PC-SAFT GC | sPC-SAFT DIPPR[a] | sPC-SAFT GC | Entropic-FV[b] | Modified UNIFAC[b] |
|---|---|---|---|---|---|---|---|
| *n*-$C_{12,16,20,22,32,36}$/*n*-hexane | 288–293 | 13.6 | 8.4 | 11.1 | 14.5 | 25.4 | 11.7 |
| *n*-$C_{16,18,20,24,32,36}$/*n*-heptane | 262–293 | 14.3 | 9.2 | 8.7 | 12.8 | 25.7 | 9.5 |
| *n*-$C_{16,22,28}$/cyclopentane | 218–274 | 46.2 | 49.9 | 86.5 | 75.8 | 48.0 | 20.1 |
| *n*-$C_{16,18,19,20,22,24,26,28,32}$/cyclohexane | 257–305 | 16.2 | 16.7 | 30.9 | 24.3 | 39.9 | 7.7 |
| *n*-$C_{16,18,20,22,28}$/2,2-dimethylbutane | 256–285 | 17.6 | 29.0 | 17.0 | 27.1 | 36.7 | 29.2 |
| *n*-$C_{16,22,28}$/2,3-dimethylbutane | 254–282 | 11.1 | 25.7 | 12.9 | 25.2 | 35.0 | 20.3 |
| *n*-$C_{16,22,28}$/2-methylpentane | 250–283 | 16.7 | 6.9 | 9.3 | 6.0 | 32.8 | 25.7 |
| *n*-$C_{16,18,20,22,28}$/3-methylpentane | 259–278 | 12.1 | 11.3 | 14.1 | 15.0 | 22.3 | 10.4 |
| AAD [%] overall | | 18.5 | 19.6 | 23.8 | 25.1 | 32.8 | 15.0 |

[a]) For *n*-$C_{>20}$, parameters are calculated using Eq. (4.1)–(4.3) from Section 4.3. [b])Results reported by Voutsas *et al.* [46].

## 7.5 Applications to Polymer Systems

With the availability of Tables 6.3 and 6.4, it is now possible to calculate the pure polymer parameters for sPC-SAFT using only the molecular structure in terms of present functional groups and the $M_w$ as necessary inputs. Detailed examples of the application of the GC method to calculate PC-SAFT parameters for PMMA and PIPMA are given in Appendix E. Using this approach, Table 7.10 presents PC-SAFT parameters for twelve commonly used polymers and the resulting average absolute deviations of experimental liquid densities from Rodgers [47]. As supplementary, Table 7.11 compares the predicted parameters from Table 7.10 with other previously published PC-SAFT parameters for polymers that have been estimated using various methods, none of which are purely predictive methods. Table 7.11 also shows absolute deviations from experimental liquid densities when all parameter sets are applied to sPC-SAFT revealing similar performance of the present GC method compared to other methods. The subsequent Table 7.12 gives an overview of the AAD % from experimental liquid densities presented in Table 7.11. It shows similar performance of the different methods including the proposed GC methodology.

Table 7.10: PC-SAFT parameters for polymers and AAD % between calculated and experimental $\rho$ of the studied polymers. These polymer parameters are calculated from the GC schemes in Tables 6.3 and 6.4. Molecular structures of the monomer units are shown in Table D.2 in Appendix D.

| Polymer | $m/M_w$ [mol/g] | $\sigma$ [Å] | $\epsilon/k$ [K] | AAD $\rho$ [%] |
|---|---|---|---|---|
| PMMA | 0.0262 | 3.6511 | 267.64 | 4.1 |
| PBMA | 0.0269 | 3.7599 | 267.21 | 1.9 |
| PIPMA | 0.0259 | 3.7543 | 267.41 | 2.1 |
| PVAc | 0.0292 | 3.3372 | 227.68 | 2.0 |
| PS | 0.0202 | 4.1482 | 367.17 | 2.9 |
| PP | 0.0255 | 4.0729 | 279.64 | 2.7 |
| PIB | 0.0210 | 4.3169 | 296.46 | 3.4 |
| PMA | 0.0292 | 3.4704 | 259.21 | 1.3 |
| BR | 0.0293 | 3.8413 | 284.70 | 1.1 |
| PBA | 0.0286 | 3.6486 | 261.43 | 2.2 |
| PEA | 0.0289 | 3.5478 | 260.15 | 1.9 |
| PB | 0.0297 | 3.7548 | 276.98 | 2.0 |
| PVC | 0.0191 | 3.8358 | 314.56 | 0.8 |
| PPA | 0.0287 | 3.6048 | 260.86 | 1.5 |
| AAD [%] overall | | | | 2.24 |

### 7.5.1 Density Predictions

As observed in Table 7.10, the GC method is able to represent the experimental densities over a wide range of temperatures and pressures with an average deviation of 2.24 %.

Table 7.11: PC-SAFT parameters for polymers obtained using the GC scheme and from other methods. Comparison of AAD % between predicted and experimental [47] $\rho$. The approach in Ref. [48] is discussed in Section 2.2.3.2, while in Ref. [49–52] corresponding VLE or LLE data are used for the regression.

| Polymer | $m/M_w$ [mol/g] | $\sigma$ [Å] | $\epsilon/k$ [K] | AAD $\rho$ [%] | $T$ range [K] | Ref. |
|---|---|---|---|---|---|---|
| PMMA | 0.0262 | 3.6511 | 267.64 | 4.1 | 305–385 | t.w. |
| | 0.027 | 3.5530 | 264.60 | 1.0 | – | [48] |
| | 0.0262 | 3.60 | 245.00 | 1.8 | – | [49] |
| PBMA | 0.0269 | 3.7598 | 267.21 | 1.9 | 390–470 | t.w. |
| | 0.0241 | 3.8840 | 264.70 | 1.0 | – | [48] |
| | 0.0268 | 3.75 | 233.80 | 3.4 | – | [49] |
| PVAc | 0.0292 | 3.3372 | 227.68 | 2.0 | 305–385 | t.w. |
| | 0.0299 | 3.4630 | 261.60 | 0.4 | – | [48] |
| | 0.0321 | 3.3970 | 204.60 | 1.9 | – | [50] |
| PS | 0.0202 | 4.1482 | 367.17 | 2.9 | 390–470 | t.w. |
| | 0.0205 | 4.1520 | 348.20 | 0.6 | – | [48] |
| | 0.0190 | 4.1071 | 267.00 | 1.2 | – | [51] |
| PP | 0.0255 | 4.0729 | 279.64 | 2.7 | 390–470 | t.w. |
| | 0.0248 | 4.1320 | 264.60 | 1.1 | – | [48] |
| | 0.0321 | 4.1 | 217.00 | 5.5 | – | [51] |
| | 0.0270 | 4.0215 | 289.33 | 1.4 | – | [52] |
| PIB | 0.0210 | 4.3169 | 296.46 | 3.4 | 390–470 | t.w. |
| | 0.0233 | 4.1170 | 267.60 | 1.4 | – | [48] |
| | 0.0235 | 4.1000 | 265.50 | 1.0 | – | [51] |
| PMA | 0.0292 | 3.4704 | 259.21 | 1.3 | 390–470 | t.w. |
| | 0.0292 | 3.5110 | 268.30 | 0.5 | – | [48] |
| | 0.0292 | 3.5 | 243.00 | 5.2 | – | [49] |
| | 0.0309 | 3.5000 | 275.00 | 3.3 | – | [50] |
| BR | 0.0293 | 3.8413 | 284.70 | 4.9 | 390–470 | t.w. |
| | 0.0245 | 4.1440 | 275.50 | 0.9 | – | [48] |
| | 0.0140 | 4.2000 | 230.00 | 7.0 | – | [50] |
| PBA | 0.0286 | 3.6486 | 261.43 | 2.2 | 390–470 | t.w. |
| | 0.0259 | 3.9500 | 224.00 | 4.5 | – | [49] |
| PEA | 0.0289 | 3.5478 | 260.15 | 1.9 | 390–470 | t.w. |
| | 0.0271 | 3.6500 | 229.00 | 3.1 | – | [49] |
| PPA | 0.0287 | 3.6048 | 260.86 | 1.5 | 390–470 | t.w. |
| | 0.0262 | 3.8000 | 225.00 | 2.4 | – | [49] |

Figure 7.17 reports predictions of densities of all the investigated polymers at the pressure of 0.1 MPa. In the particular case of poly(methyl acrylate) (PMA), the overall average deviation in liquid density predictions is only about 1 % over a wide pressure range, as shown in Figure 7.18.

For a purely predictive method the accuracy of the density predictions is considered to be satisfactory. The accuracy is similar and, in some cases, even better than the accuracy obtained when using parameters from other methods reported in the literature (references in Table 7.11).

Table 7.12: Overview of AAD % of predicted $\rho$ from Table 7.11 using GC parameters from this work (t.w.) as well as methods proposed in different literature sources.

| Ref. | PMMA | PBMA | PVAc | PS | PP | PIB | PMA | BR | PBA | PEA | PPA | $N_{DP}$ | Overall |
|---|---|---|---|---|---|---|---|---|---|---|---|---|---|
| t.w. | 4.1 | 1.9 | 2.0 | 2.9 | 2.7 | 3.4 | 1.3 | 4.9 | 2.2 | 1.9 | 1.5 | 11 | 3.3 |
| [48] | 1.0 | 1.0 | 0.4 | 0.6 | 1.1 | 1.4 | 0.5 | 0.9 | — | — | — | 8 | 0.9 |
| [49] | 1.8 | 3.4 | — | — | — | — | 5.2 | — | 4.5 | 3.1 | 2.4 | 6 | 3.4 |
| [50] | — | — | 1.9 | — | — | — | 3.2 | 7.0 | — | — | — | 3 | 4.1 |
| [51] | — | — | — | 1.2 | 5.5 | 1.0 | — | — | — | — | — | 3 | 2.6 |
| [52] | — | — | — | — | 1.4 | — | — | — | — | — | — | 1 | 1.4 |

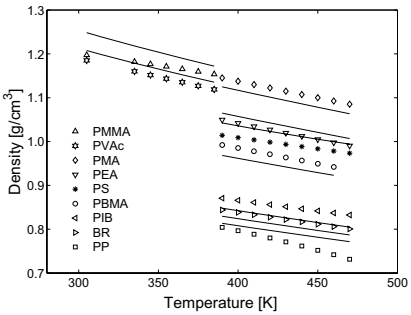


Figure 7.17: Polymer density predictions (lines) with GC sPC-SAFT as a function of temperature at $P = 0.1\,\mathrm{MPa}$. Symbols indicate experimental data [47].

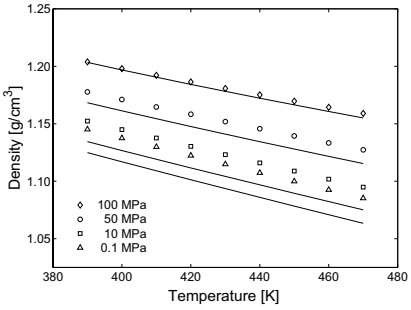


Figure 7.18: GC sPC-SAFT density predictions (lines) for PMA as a function of temperature at various pressures. Experimental data [47] are indicated with points.

In the following sections, the new polymer parameters obtained by the GC method will be evaluated for a variety of polymer–solvent systems exhibiting both VLE and LLE. Pure compound parameters for the solvents are taken from Table 4.1.

### 7.5.2 Evaluation of VLE

VLE calculations are performed for some binary polymer–solvent systems. Figure 7.19 shows VLE for the system PP with carbon tetrachloride ($CCl_4$) and methylene chloride ($CH_2Cl_2$). A single system specific binary interaction parameter is needed in order to obtain accurate correlations of these two systems.

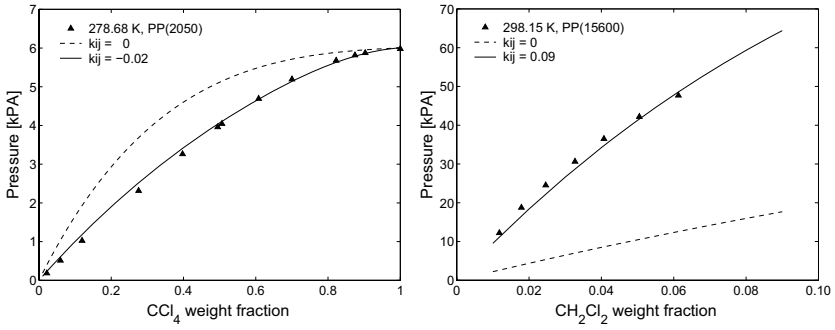


Figure 7.19: VLE of the PP–$CCl_4$ and PP–$CH_2Cl_2$ systems. Experiments [53] and GC sPC-SAFT correlations using PP parameters from Table 7.10.

As shown in Figures 7.20–7.22, promising results can also be obtained when the GC-predicted polymer parameters are used for polymer systems with PS and PMMA. In all cases, the interaction parameters have reasonably low values.

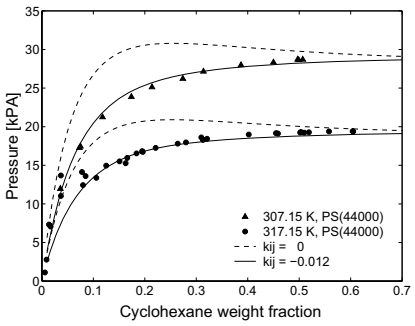


Figure 7.20: VLE of the PS–cyclohexane system. Experiments [54] and GC sPC-SAFT correlations using PS parameters from Table 7.10.

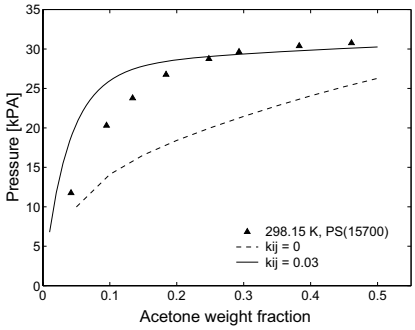


Figure 7.21: VLE of the PS–acetone system. Experiments [55] and GC sPC-SAFT correlations using PS parameters from Table 7.10.

For the PMMA–methyl ethyl ketone system in Figure 7.22 (right), pure predictions ($k_{ij} = 0$) with sPC-SAFT give excellent results with an average deviation for vapour pressure within 1 %.

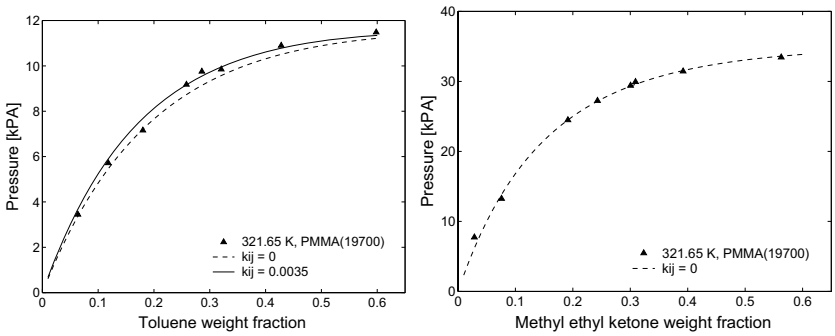


Figure 7.22: VLE of the PMMA–toluene (left) and PMMA–MEK (right) systems. Experiments [56] and GC sPC-SAFT correlations using PMMA parameters from Table 7.10.

VLE calculations for PVAc–methyl acetate at three temperatures are presented in Figure 7.23. The pure predictions ($k_{ij} = 0$) are in good agreement with the experiments, and excellent correlations are achieved using a small negative temperature-independent binary interaction parameter ($k_{ij} = -0.005$).

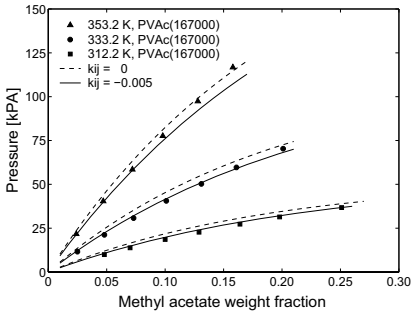


Figure 7.23: VLE of the PVAc–methyl acetate system. Experiments [57] and GC sPC-SAFT correlations using PVAc parameters from Table 7.10.

Not all studied binary polymer–solvent mixtures are presented graphically in this section. Instead, Table 7.13 summarizes the results by showing AAD % between experimental VLE data and predicted and correlated modelling results.

Table 7.13: AAD % of predicted ($k_{ij} = 0$) and correlated ($k_{ij} \neq 0$) bubble point pressures of binary mixtures with PS, PIB, and PMMA and various solvents using polymer parameters from Table 7.10.

| Solvent | PS | | | PIB | | | PMMA | | |
|---|---|---|---|---|---|---|---|---|---|
| | $k_{ij} = 0$ AAD $P$ [%] | $k_{ij}$ | AAD $P$ [%] | $k_{ij} = 0$ AAD $P$ [%] | $k_{ij}$ | AAD $P$ [%] | $k_{ij} = 0$ AAD $P$ [%] | $k_{ij}$ | AAD $P$ [%] |
| Acetone | 15.3 | –0.01485 | 8.6 | — | — | — | 4.8 | 0.00268 | 2.9 |
| Benzene | 26.4 | –0.02949 | 6.8 | 5.2 | –0.00601 | 4.1 | — | — | — |
| *n*-Butane | — | — | — | 36.3 | –0.02194 | 4.7 | — | — | — |
| Chloroform | 32.5 | –0.04048 | 13.0 | — | — | — | 39.7 | –0.04189 | 5.3 |
| Cyclohexane | 6.9 | –0.01731 | 0.7 | 5.6 | –0.00907 | 2.5 | — | — | — |
| MEK | 21.5 | –0.01872 | 7.8 | — | — | — | 5.3 | 0.00433 | 4.4 |
| Ethyl benzene | — | — | — | 13.4 | –0.00646 | 4.9 | — | — | — |
| *n*-Hexane | — | — | — | 24.1 | –0.01806 | 6.6 | — | — | — |
| *i*-Butane | — | — | — | 37.4 | –0.0212 | 1.9 | — | — | — |
| *i*-Pentane | — | — | — | 35.8 | –0.01851 | 3.6 | — | — | — |
| *n*-Nonane | 50.1 | –0.01634 | 2.5 | — | — | — | — | — | — |
| *n*-Octane | — | — | — | 0.3 | –0.0013 | 0.2 | — | — | — |
| *n*-Pentane | — | — | — | 12.2 | –0.01268 | 6.0 | — | — | — |
| Propyl acetate | 28.2 | –0.02277 | 9.8 | — | — | — | — | — | — |
| Tetrachloromethane | 46.6 | –0.03263 | 4.8 | — | — | — | — | — | — |
| Toluene | 10.0 | –0.02653 | 3.1 | 12.1 | –0.00282 | 6.5 | 3.7 | 0.00199 | 2.4 |
| AAD [%] overall | 26.4 | | 6.3 | 18.2 | | 4.1 | 13.4 | | 3.8 |

#### 7.5.2.1 Polar Systems

The proposed GC methodology is primarily targeted at solutions that do not form hydrogen bonds with other molecules, i.g. non–associating compounds where $m$, $\sigma$, and $\epsilon/k$ are the only required PC-SAFT parameters. Regardless hereof, this section presents modelling results of the phase behaviour of polar and non-polar polymers with a variety of polar solvents using sPC-SAFT with the current GC scheme both with hydrogen bonding, i.e. alcohols, and non–hydrogen bonding compounds, i.e. ketones. PC-SAFT parameters for polar solvents are taken from Reference [58], which are assigned with the two association sites, often referred to as the 2B model in the terminology of Huang and Radosz [59]. The polymer parameters are taken from Table 7.10.

As mentioned earlier, knowledge of the solubility of vapours of low $M_w$ solvents in polymers is required for the design and operation of polymer plants so that residual monomers, oligomers, and polymerization solvents can be removed from polymer products. VLE and solubility data for systems containing polar solvents are rather scarce, and often only available at infinite-dilution conditions. Experimental solubilities of many polar organic solvents in polymers at 313, 333, and 353 K reported by Wibawa *et al.* [57] are used in this work. PBMA and PVAc are polar polymers, and PIB is a non-polar polymer.

The effect of solvent self-association is considered in this work, while the effects of polarity are not considered explicitly. Therefore, it is expected that modelling polar systems using only three pure compound parameters might not be as successful as for non-polar polymer mixtures, especially for polymers that contain polar groups. This is, in fact, observed in Table 7.14 where the AAD % between experimental and calculated vapour pressures for the studied polymer–solvent mixtures with GC sPC-SAFT are shown. High deviations of the predictions with GC sPC-SAFT are corrected with a small value of the binary interaction parameter. One may argue that a three-site model could provide a better physical description of pure alcohols used in the calculations, and with that improve the obtained VLE predictions of the binary mixtures. However, the extra complexity required in using a three-site model is not justified in this case because of the complexity of the polar polymer systems.

Table 7.14: VLE results for PIB–, PBMA–, and PVAc–solvent systems with GC sPC-SAFT.

| System | $T = 313.2\,\mathrm{K}$ | | | $T = 333.2\,\mathrm{K}$ | | | $T = 353.2\,\mathrm{K}$ | | |
|---|---|---|---|---|---|---|---|---|---|
| | $k_{ij} = 0$ AAD $P$ [%] | $k_{ij}$ | AAD $P$ [%] | $k_{ij} = 0$ AAD $P$ [%] | $k_{ij}$ | AAD $P$ [%] | $k_{ij} = 0$ AAD $P$ [%] | $k_{ij}$ | AAD $P$ [%] |
| **PIB *with solvents*** | | | | | | | | | |
| 1-Propanol | 152.0 | –0.035 | 28.0 | 109.1 | –0.035 | 21.3 | 52.3 | –0.025 | 5.1 |
| 2-Propanol | 134.0 | –0.04 | 7.8 | 120.3 | –0.04 | 12.7 | 91.0 | –0.04 | 9.5 |
| 1-Butanol | 99.1 | –0.03 | 16.4 | 69.4 | –0.025 | 14.1 | 59.4 | –0.02 | 18.2 |
| 2-Butanol | 64.1 | –0.02 | 5.5 | 43.8 | –0.015 | 6.4 | 37.9 | –0.01 | 12.9 |
| 2-Methyl-1-propanol | 57.6 | –0.015 | 10.9 | 34.4 | –0.010 | 14.2 | 17.6 | –0.005 | 8.8 |
| Methyl acetate | 24.1 | 0.02 | 2.5 | 29.1 | 0.020 | 2.2 | 31.2 | 0.02 | 4.0 |
| Propyl acetate | 9.3 | 0.005 | 4.5 | 9.2 | 0.005 | 4.8 | 11.9 | 0.005 | 4.8 |
| Methyl ethyl ether | 25.2 | 0.015 | 3.2 | 23.8 | 0.015 | 2.7 | 9.5 | — | — |
| AAD [%] overall | 80.8 | | 9.9 | 54.9 | | 9.8 | 38.9 | | 9.1 |
| **PBMA *with solvents*** | | | | | | | | | |
| Ethanol | — | –0.20 | 18.1 | — | –0.2 | 15.3 | — | –0.2 | 20.2 |
| 1-Propanol | 130.0 | –0.035 | 26.7 | 141.0 | –0.035 | 32.6 | 176.0 | –0.06 | 13.7 |
| 2-Propanol | 172.0 | –0.04 | 33.8 | 144.0 | –0.04 | 30.6 | 148.0 | –0.04 | 38.7 |
| 1-Butanol | 163.0 | –0.03 | 39.2 | 129.0 | –0.03 | 32.9 | 59.4 | –0.03 | 18.2 |
| 2-Butanol | 93.3 | –0.03 | 9.7 | 90.9 | –0.03 | 13.7 | 81.1 | –0.03 | 14.7 |
| 2-Methyl-1-propanol | 98.5 | –0.025 | 24.2 | 81.8 | –0.02 | 27.8 | 77.3 | –0.025 | 16.7 |
| Methyl acetate | 21.5 | –0.01 | 3.4 | 14.2 | –0.01 | 3.2 | 11.4 | –0.01 | 9.6 |
| Propyl acetate | 17.6 | –0.008 | 3.4 | 19.3 | –0.008 | 4.3 | 17.4 | –0.008 | 5.8 |
| Methyl ethyl ether | 12.3 | –0.005 | 3.7 | 15.2 | –0.005 | 7.0 | 18.9 | –0.005 | 11.7 |
| AAD [%] overall | 85.5 | | 18.0 | 79.4 | | 18.6 | 73.7 | | 16.6 |
| **PVAc *with solvents*** | | | | | | | | | |
| 1-Propanol | 103.0 | –0.025 | 17.3 | 106.0 | –0.035 | 25.4 | 105.0 | –0.04 | 14.6 |
| 2-Propanol | 172.0 | –0.025 | 52.1 | 108.0 | –0.035 | 39.9 | 143.0 | –0.045 | 26.0 |

*Continues on next page*

| System | $T = 313.2\,\mathrm{K}$ | | | $T = 333.2\,\mathrm{K}$ | | | $T = 353.2\,\mathrm{K}$ | | |
|---|---|---|---|---|---|---|---|---|---|
| | $k_{ij} = 0$ AAD $P$ [%] | $k_{ij}$ | AAD $P$ [%] | $k_{ij} = 0$ AAD $P$ [%] | $k_{ij}$ | AAD $P$ [%] | $k_{ij} = 0$ AAD $P$ [%] | $k_{ij}$ | AAD $P$ [%] |
| 1-Butanol | 71.7 | –0.02 | 17.2 | 101.0 | –0.02 | 38.1 | 101.0 | –0.03 | 21.4 |
| 2-Butanol | 30.8 | –0.01 | 4.9 | 60.6 | –0.02 | 13.0 | 52.4 | –0.03 | 13.4 |
| 2-Methyl-1-propanol | 43.1 | –0.015 | 11.7 | 37.0 | –0.015 | 13.2 | 64.4 | –0.015 | 24.4 |
| Methyl acetate | 11.4 | –0.005 | 3.3 | 14.3 | –0.005 | 4.9 | 5.6 | –0.005 | 3.5 |
| Propyl acetate | 9.9 | — | — | 1.4 | — | — | 2.7 | — | — |
| Methyl ethyl ether | 3.1 | — | — | 5.9 | — | — | 6.0 | — | — |
| Acetone | 191.2 | –0.08 | 24.1 | 159. | –0.06 | 16.8 | 144.1 | –0.06 | 8.0 |
| Propylamine | 27.3 | –0.01 | 4.0 | — | — | — | — | — | — |
| Isopropylamine | 10.2 | –0.007 | 2.8 | — | — | — | — | — | — |
| AAD [%] overall | 61.2 | | 15.3 | 65.9 | | 21.6 | 69.4 | | 15.9 |

To examine whether any trends related to structural effects of the solvents could be observed and captured with the GC sPC-SAFT model, solubilities of solvents in polymers are shown in Figures 7.24–7.33.

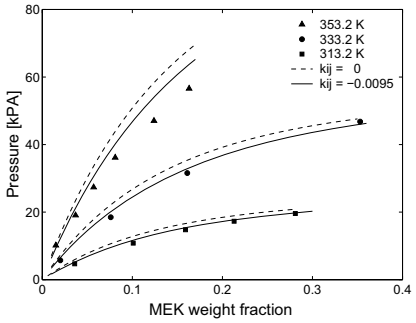


Figure 7.24: Pressure-weight fraction of PBMA–MEK. Symbols represent experimental data [57], and lines are GC sPC-SAFT modelling results.

In Figure 7.24, a representative calculation is shown for the PBMA–MEK mixture. Model predictions are in fair agreement with the experimental data, while the use of a temperature-independent $k_{ij} = -0.0095$ improves correlation of the data over the entire composition range.

For the PBMA–1-propanol system presented in Figure 7.25, pure predictions result in substantial deviations from the experimental data while good correlations are obtained with $k_{ij} = -0.035$ at 313.2 and 333.2 K. A higher value of $k_{ij} = -0.06$ is required for the correlation of the data at 353.2 K.

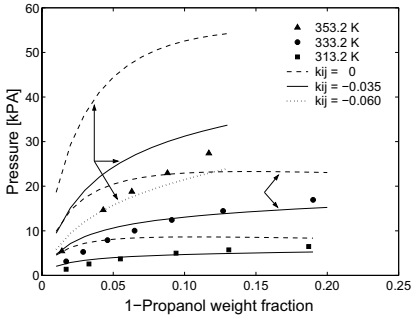


Figure 7.25: Pressure-weight fraction of PBMA–1-propanol. Symbols represent experimental data [57], where lines are GC sPC-SAFT modelling results.

Solubilities of 2-methyl-1-propanol in both PBMA and PIB are graphically presented in Figure 7.26. The $k_{ij}$ value required to accurately correlate the PBMA system (left) is higher than $k_{ij}$ for the PIB system (right), which may be attributed to the more polar nature of the PBMA system.

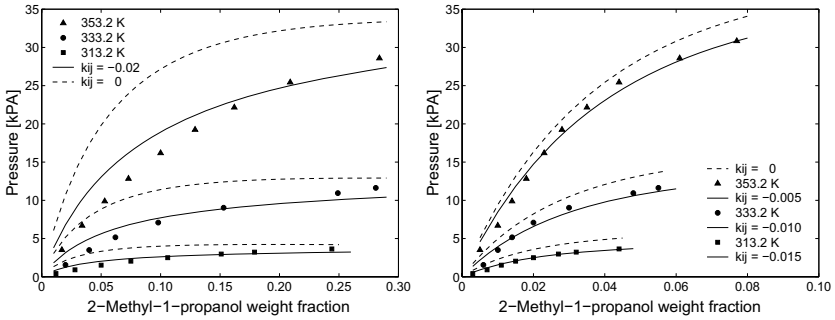


Figure 7.26: Pressure-weight fraction of PBMA–2-methyl-1-propanol (left) and PIB–2-methyl-1-propanol (right). Symbols represent experimental data [57], while lines are GC sPC-SAFT modelling results.

In Figure 7.27, very good agreement is obtained for the PIB–methyl acetate system at 313.2, 333.2, and 353.2 K using the temperature-independent $k_{ij} = 0.02$. For this particular system, the overall average deviation at 313.2 K is improved from 24.1 % for predictions to 2.5 % for correlations, as shown in Table 7.14, where the deviations for all other investigated binary PIB systems are also given.

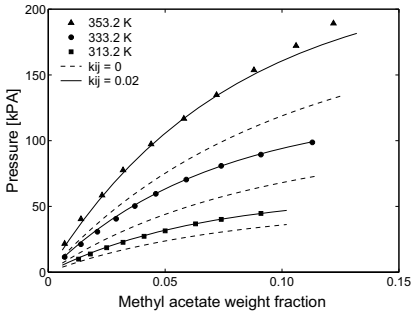


Figure 7.27: Pressure-weight fraction of PIB–methyl acetate. Symbols represent experimental data [57], while lines are GC sPC-SAFT modelling results.

The two graphs in Figure 7.28 show that the polar solvents are more soluble in polar PBMA than in non-polar PIB at the same temperature. In general, the lowest solubilities

of all investigated solvents are obtained in PIB, which is shown by the experimental data and reproduced with GC sPC-SAFT with accurate correlations.

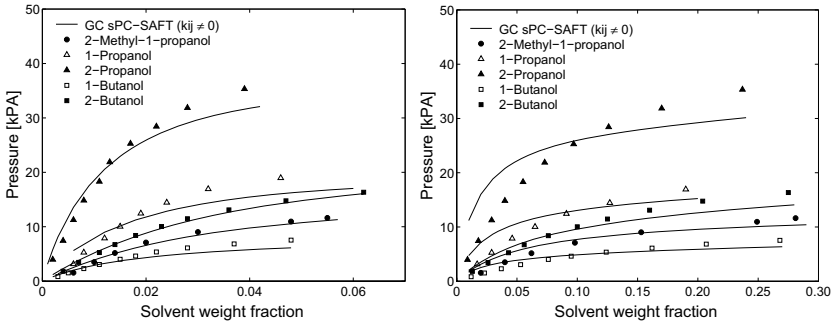


Figure 7.28: Pressure-weight fraction of various alcohols in PBMA (left) and PIB (right) at 333.2 K. Symbols represent experimental data [57], while lines are correlations with GC sPC-SAFT.

The more alcoholic nature the solvent is in polar polymer mixtures, the more problematic is the modelling with the sPC-SAFT model. This is observed in Figures 7.29 and 7.30, where both predictions and correlations of solubilities of various solvents in PIB and PBMA are presented. Even with inaccurate predictions, as shown for example in Figure 7.29, the solubility of polar solvents with hydrogen bonding, e.g. alcohols, is lower than that of polar solvents without hydrogen bonding, e.g. MEK and ketone, in investigated polymers. While for polar solvents without hydrogen bonding, the effect of solvent compounds on solubility is not significant in polar polymers such as PBMA.

The VLE phase diagram of PVAc–propanol [60] is shown in Figure 7.31 where the three different PVAc parameter sets from Table 7.11 are used including those obtained from the GC scheme. A comparison of the obtained correlations with $k_{ij} = -0.025$ is chosen for the evaluation of the PVAc parameters. The performance is not satisfactory. The absolute average deviations are 16.6, 15.9, and 15.5 % for parameters of Ref. [48], [50], and this work, respecively. Similar accuracy for correlating the phase behaviour of this system is obtained by Elliott and Natarajan [61] using a GC form of the ESD EoS discussed in Section 3.2.

Generally, results presented in Section 7.5.2.1 show that the presented GC method is applicable to polymer systems involving self-associating solvents, but requires a binary interaction parameter to improve accuracy in most of the investigated systems.

Often, comparisons of modelling results with experimental LLE data provide a more rigorous test and challenge for a model and its parameters than comparison with experimental VLE data. Some LLE results are presented in the next section.

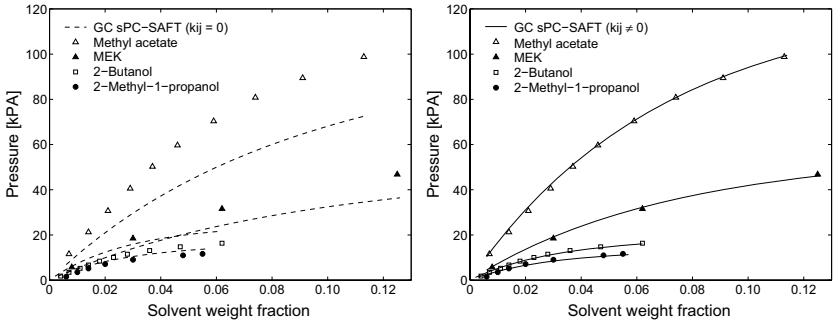


Figure 7.29: Pressure-weight fraction of various solvents in PIB at 333.2 K. Symbols represent experimental data [57], while lines are predictions (left) and correlations (right) with GC sPC-SAFT.

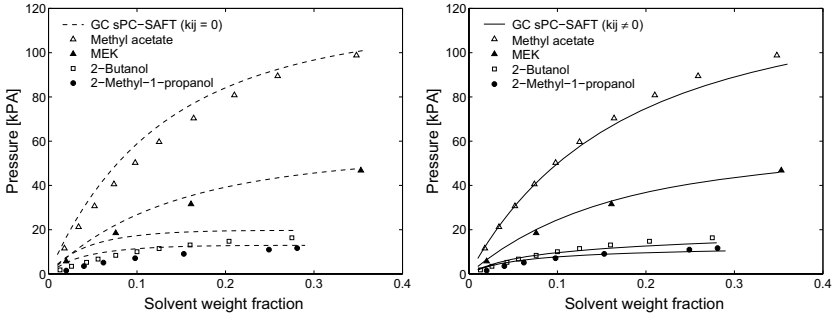


Figure 7.30: Pressure-weight fraction of various solvents in PBMA at 333.2 K. Symbols represent experimental data [57], while lines are predictions (left) and correlations (right) with GC sPC-SAFT.

### 7.5.3 Evaluation of LLE

Liquid-liquid equilibria (LLE) calculations of a few polymer–solvent systems have been performed. Mixtures with PMMA and PBMA have been considered. Figure 7.32 shows different PMMA solutions with 4-heptanone and chlorobutane, respectively. Both systems display UCST behaviour and are well correlated using small positive binary interaction parameters. However, the flatness of the curve towards increased polymer weight fractions cannot be accurately described. This is expected to be a weakness of the model rather than of the polymer parameters [62]. Very similar behaviour is observed for the PBMA–octane system in Figure 7.33 using a small negative value of $k_{ij} = -0.0038$.

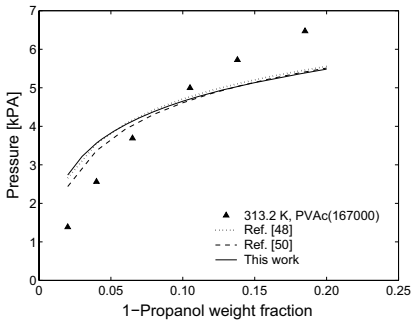


Figure 7.31: VLE of the PVAc–1-propanol system. Symbols are experimental data [60] and lines are GC sPC-SAFT correlations ($k_{ij}$=-0.025) with PVAc parameters from Table 7.11.

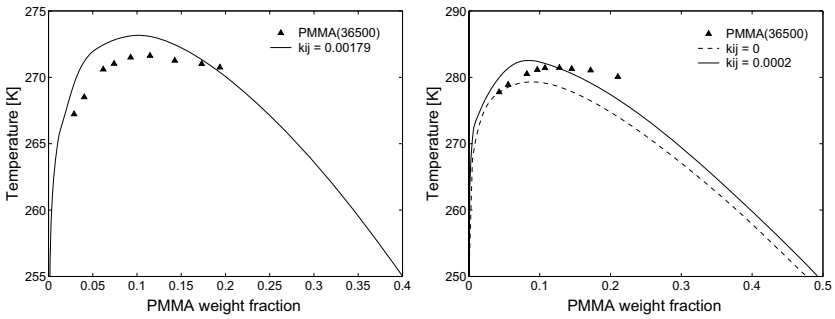


Figure 7.32: LLE of the PMMA–4-heptanone (left) and PMMA–chlorobutane (right) systems. Symbols are experimental data [63] and lines are GC sPC-SAFT correlations with PMMA parameters from Table 7.10.

### 7.5.4 PVC–Solvent Systems

Table 2.2 from Section 5.2.2 is slightly modified to include an additional set of PVC pure parameters calculated from the proposed GC scheme. Different sets of PC-SAFT parameters for PVC are summarised in Table 7.15.

With the GC estimated PVC parameters sPC-SAFT predicts the liquid density with 0.8 % deviation in the investigated temperature and pressure range. The accuracy is similar to the other aproaches which are based on experimental data. In the following, sPC-SAFT EoS using different parameter sets is applied to VLE for selected PVC–solvent systems.

First, the predictive capabilities of the approach are tested by predicting the vapour

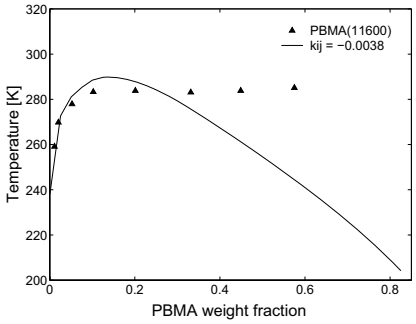


Figure 7.33: LLE of the PBMA–octane system. Symbols are experimental data [64] and lines are GC sPC-SAFT correlations with PBMA parameters from Table 7.10.

Table 7.15: Values of PC-SAFT parameters and AAD % between calculated and experimental $\rho$ of poly(vinyl chloride) (PVC) using different methods.

| Case | Data set | $m/M_w$ [mol/g] | $\sigma$ [Å] | $\epsilon/k$ [K] | $T$ range [K] | $P$ range [bar] | AAD $\rho$ [%] |
|---|---|---|---|---|---|---|---|
| 1. | Kouskoumvekaki *et al.* [48] approach | 0.0210 | 3.724 | 315.93 | 373–423 | 1–1000 | 0.5 |
| 2. | PVT + single binary VLE incl. $k_{ij}$ | 0.0121 | 4.726 | 541.56 | 373–423 | 1–1000 | 1.6 |
| 3. | PVT + single binary VLE excl. $k_{ij}$ | 0.0298 | 3.213 | 221.19 | 373–423 | 1–1000 | 1.2 |
| 4. | PVT + all binary VLE incl. $k_{ij}$ | 0.0097 | 5.030 | 495.86 | 373–423 | 1–1000 | 1.4 |
| 5. | PVT + all binary VLE excl. $k_{ij}$ | 0.0142 | 4.298 | 360.92 | 373–423 | 1–1000 | 0.8 |
| 6. | from Table 7.10 | 0.0191 | 3.8358 | 314.56 | 373–423 | 1–1000 | 0.8 |
| 7. | from [52] | 0.02136 | 3.7486 | 370.42 | 373–423 | 1–1000 | 0.2 |

pressures of different PVC systems with each set of parameters after imposing a value of $k_{ij} = 0$. The deviations are reported in Table 7.16 and are graphically presented in Figure 7.34. It is observed that parameters based on Cases 1, 5, and 6 (this work) result in the lowest overall AAD %.

Second, to evaluate the effect of a non-zero value of $k_{ij}$, optimised values of $k_{ij}$ have been determined for each binary system. Both the values of $k_{ij}$ and the resulting absolute average deviations are reported in Table 7.17. The values of $k_{ij}$ are generally low, but

Table 7.16: AAD % between experimental and predicted ($k_{ij} = 0$) bubble pressures of investigated binary PVC–solvent mixtures.

| System | AAD $P$ [%] with Case no. | | | | | | |
|---|---|---|---|---|---|---|---|
| | 1 | 2 | 3 | 4 | 5 | 6 | 7 |
| 1. Toluene | 31.9 | 123.7 | 10.6 | 88.9 | 42.8 | 27.0 | 85.1 |
| 2. Tetrachloromethane | 19.0 | 120.3 | 72.2 | 76.2 | 5.2 | 15.9 | 46.1 |
| 3. Vinyl chloride | 21.2 | 61.9 | 12.6 | 36.1 | 20.9 | 25.5 | 57.3 |
| 4. 1,4-Dioxane | 7.5 | 31.1 | 16.4 | 24.5 | 14.4 | 7.8 | 24.9 |
| 5. Tetrahydrofuran | 26.8 | 63.5 | 6.7 | 49.9 | 33.0 | 25.2 | 48.9 |
| 6. Di(1-butyl) ether | 29.6 | 150.1 | 87.1 | 114.7 | 15.9 | 27.2 | 21.8 |
| AAD [%] overall | 19.6 | 79.0 | 29.8 | 56.3 | 19.6 | 19.2 | 41.6 |

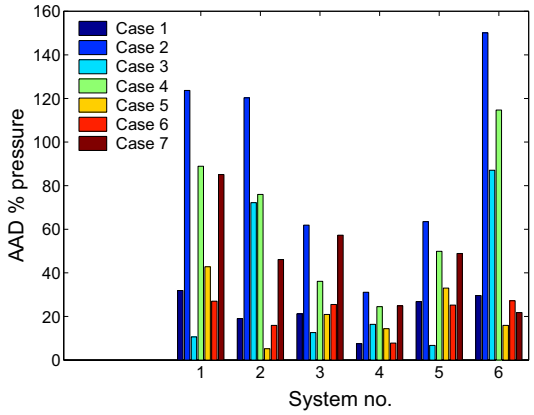


Figure 7.34: AAD % between experimental and predicted ($k_{ij} = 0$) bubble pressures of investigated binary PVC–solvent mixtures. Data, case and system no. refer to Table 7.16.

they still vary and can even be negative. Analyzing the correlated results in terms of AAD %, a significant improvement in the accuracy is obtained, this time highlighting the performance of parameters from Cases 1, 3, 6 (this work), and 7. However, the approach is no longer predictive. A more consistent approach would have been to determine a unique value of $k_{ij}$, but this has not been done because it is unlikely, in view of the variations of $k_{ij}$ in Table 7.17, that the predictions would be much improved.

The optimised $k_{ij}$ values for the investigated PVC–solvent systems listed in Table 7.17 are plotted as a function of solvents' $M_w$ and of van der Waals volume of solvents in order to test if any significant trends are obtained.

Figure 7.35 shows linear trends of the optimized $k_{ij}$ values for selected PVC–solvent

Table 7.17: Average absolute deviations (AAD %) between experimental and correlated ($k_{ij} \neq 0$) bubble point pressures of investigated binary PVC–solvent mixtures.

| System | AAD $P$ [%] with Case no. | | | | | | |
|---|---|---|---|---|---|---|---|
| | 1 | 2 | 3 | 4 | 5 | 6 | 7 |
| 1. Toluene | 6.9 | 40.6 | 4.5 | 37.2 | 13.4 | 7.7 | 8.5 |
| 2. Tetrachloromethane | 0.8 | 29.6 | 2.2 | 29.2 | 5.0 | 0.5 | 0.5 |
| 3. Vinyl chloride | 3.9 | 17.6 | 1.7 | 16.2 | 7.9 | 4.6 | 5.0 |
| 4. 1,4-Dioxane | 6.9 | 29.2 | 3.3 | 25.9 | 11.9 | 7.5 | 9.4 |
| 5. Tetrahydrofuran | 5.5 | 38.4 | 1.3 | 33.9 | 12.8 | 6.3 | 8.3 |
| 6. Di(1-butyl) ether | 4.0 | 54.2 | 2.8 | 47.9 | 11.5 | 4.7 | 6.8 |
| AAD [%] overall | 4.6 | 34.9 | 2.6 | 31.7 | 10.4 | 5.2 | 6.4 |

| Solvent | Optimized $k_{ij}$ with Case no. | | | | | | |
|---|---|---|---|---|---|---|---|
| | 1 | 2 | 3 | 4 | 5 | 6 | 7 |
| 1. Toluene | –0.01750 | –0.06702 | 0.00478 | –0.05611 | –0.02689 | 0.01571 | –0.03961 |
| 2. Tetrachloromethane | 0.00916 | 0.05729 | 0.03729 | –0.04261 | 0.00112 | 0.01290 | –0.01942 |
| 3. Vinyl chloride | –0.02219 | –0.06299 | 0.01334 | –0.04373 | –0.02571 | –0.01804 | –0.05151 |
| 4. 1,4-Dioxane | –0.00592 | –0.02990 | 0.01271 | –0.02543 | –0.01634 | –0.00634 | –0.02007 |
| 5. Tetrahydrofuran | –0.03210 | –0.08273 | –0.00806 | –0.07625 | –0.04751 | –0.03255 | –0.05066 |
| 6. Di(1-butyl) ether | 0.01166 | –0.06046 | 0.03733 | –0.05285 | –0.00693 | 0.01121 | –0.00801 |

systems listed in Table 7.17 when plotted as a function of $M_w$ and van der Waals volume of solvents. The data reveal substantial scatter; especially for the van der Waals volumes in the right graph of Figure 7.35. Hence, care should be taken to extrapolate these trend lines for use in practical applications.

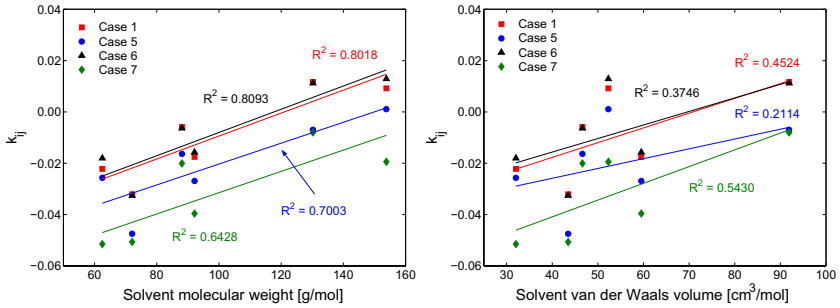


Figure 7.35: Linear trends of optimized $k_{ij}$ values for selected PVC–solvent systems. Case no. refer to the systems listed in Table 7.17.

Most of the VLE and LLE results presented for various polymer–solvent systems in Chapter 7 have already been subjected to tests with the sPC-SAFT EoS using another set

of polymer parameters estimated by Kouskoumvekaki *et al.* [48]. The results are rather similar. The overall results demonstrate that properly calculated pure predictive GC estimated polymer parameter values can result in quite accurate modelling of mixture phase equilibria. For many systems investigated, a small $k_{ij}$ value is needed before the model accurately correlates the experimental data.

## 7.6 Final Comments

Not only has it been shown that the presented GC methodology provides a good representation of the phase equilibria of heavy members of the investigated chemical families, but it also exhibits a good agreement with the experimental data of various classes of binary mixtures. Generally, the approach has proven to be a fairly reliable predictive tool for pure compounds and binary mixtures comprising the functional groups in the GC scheme of Tables 6.3 and 6.4.

With the newly developed GC scheme in hand to calculate parameters for complex compounds, the sPC-SAFT model has become a relevant and useful tool in the design and development of complex products, e.g. detergents or food ingredients, pharmaceuticals and other speciality chemicals, where predictions of various thermodynamic and phase equilibrium properties are required, but for which expected vapour pressure and/or liquid density data may not be available.

## References

[1] K. A. Connors, *Thermodynamics of Pharmaceutical Systems: An Introduction for Students of Pharmacy*. John Wiley and Sons, USA, 2002.

[2] S. L. Rose, *Fundamental Principles of Polymeric Materials*. John Wiley and Sons, USA, 1993.

[3] S. Aparicio, R. Alcalde, M. J. Dávila, B. García, and J. M. Leal, "Properties and Structure of Aromatic Ester Solvents," *J. Phys. Chem. B.*, vol. 111, pp. 4417–4431, 2007.

[4] AIChE J., *DIPPR Table of Physical and Thermodynamic Properties of Pure Compounds*. New York, USA, 1998.

[5] K. Kevin, "Phascinating Phytochemicals," *Food Processing, USA*, vol. 56, pp. 79–81, 1995.

[6] S. O. Duke, F. E. Dayan, J. G. Romagni, and A. M. Rimando, "Natural Products as Sources of Herbicides: Current Status and Future Trends," *Weed Research*, vol. 40, pp. 99–111, 2000.

[7] "Phytochemicals." `http://www.phytochemicals.info/`. General about phytochemicals, April 2008.

[8] H. Schmandke, "D-Limonene in Citrus Fruit with Anticarcinogenic Action," *Ernaehrungs-Umschau*, vol. 50, pp. 264–266, 2003.

[9] B. Arizaga, A. de Leon, N. Burgueno, A. Lopez, D. Paz, N. Martinez, D. Lorenzo, E. Dellacassa, and J. Bussi, "A Clean Process for the Production of Oxygenated Limonene Derivatives Starting from Orange Oil," *J. Chem. Tech. Biotechnol.*, vol. 82, pp. 532–538, 2007.

[10] H. A. Matos, E. Gomes De Azevedo, P. C. Simoes, M. T. Carrondo, and M. Nunes Da Ponte, "Phase Equilibria of Natural Flavours and Supercritical Solvents," *Fluid Phase Equilibria*, vol. 52, pp. 357–364, 1989.

[11] E. Gomes de Azevedo, H. A. Matos, and M. Nunes de Ponte, "Phase Equilibria of Ethene+Limonene and Ethene+Cineole from 285 K to 308 K and Pressures to 8 MPa," *Fluid Phase Equilibria*, vol. 83, pp. 193–202, 1993.

[12] J. G. Speight, *The Desulfurization of Heavy Oils and Residua*. CRC Press, USA, 1999.

[13] T. Sawaya, I. Mokbel, E. Rauzy, J. Saab, C. Berro, and J. Jose, "Experimental Vapour Pressure of Alkyl and Aryl sulfides. Prediction by a Group Contribution Method," *Fluid Phase Equilibria*, vol. 226, pp. 283–288, 2004.

[14] C. H. Twu, V. Tassone, and W. D. Sim, "Accurately Predict the VLE of Thiol–Hydrocarbon Mixtures," *Chem. Eng. Progress*, vol. 100, pp. 39–45, 2004.

[15] H. Wolff, J. Szydlowski, and L. Dill-Staffenberger, "Vapor-Liquid Equilibria of Deuteroisomeric Methanethiols and Their Mixtures with *n*-Hexane," *J. Chem. Thermodyn.*, vol. 12, pp. 641–652, 1980.

[16] N. F. Giles, H. L. Wilson, and W. V. Wilding, "Phase Equilibrium Measurements on Twelve Binary Mixtures," *J. Chem. Eng. Data*, vol. 41, pp. 1223–1238, 1996.

[17] N. F. Giles, H. L. Wilson, and W. V. Wilding, "Phase Equilibrium on Eight Binary Mixtures," *J. Chem. Eng. Data*, vol. 42, pp. 1067–1074, 1997.

[18] J. Kilner, S. E. McBain, and M. G. Roffey, "(Vapour+ Liquid) Equilibria of (Methanthiol or Ethanethiol or Propane-1-thiol or Butan-1-thiol + *n*-Hexane or *n*-Decane or Toluene or Water) for Mole Fractions X=0 to 0.2 of Thiol at Temperatures Between 323 and 373 K," *J. Chem. Thermody.*, vol. 22, pp. 203–210, 1990.

[19] S. Monarca, "Polycyclic Aromatic Hydrocarbons in Petroleum Products for Medicinal and Cosmetic Uses-Analytical Procedure," *Sci. Total Environ*, vol. 14, pp. 233–243, 1980.

[20] S. Monarca, F. Fagioli, and G. Morozzi, "Evaluation of the Potential Carcinogenicity of Paraffins for Medical and Cosmetic Uses-Dash Determination of Polycyclic Aromatic Hydrocarbons," *Sci. Total Environ*, vol. 17, pp. 83–93, 1981.

[21] R. S. Hamir, *Handbook of Chromatography: Liquid Chromatography of Polycyclic Aromatic Hydrocarbons*. CRC Press, USA, 1993.

[22] K. Ruuzicka, I. Mokbel, V. Majer, V. Ruuzicka, J. Jose, and M. Zábranský, "Description of Vapor-Liquid and Vapor-Solid Equilibria for a Group of Polycondensed Compounds of Petroleum Interest," *Fluid Phase Equilibria*, vol. 148, pp. 107–137, 1998.

[23] D. N. Huynh, M. Benamira, J.-P. Passarello, P. Tobaly, and J.-C. de Hemptinne, "Application of GC-SAFT EOS to Polycyclic Aromatic Hydrocarbons," *Fluid Phase Equilibria*, vol. 254, pp. 60–66, 2007.

[24] E. J. Coon, J. E. Auwaerter, and E. McLaughlin, "A Comparison of Solid-Liquid Equilibrium with Vapour-Liquid Equilibrium for Prediction of Activity Coefficients in Systems Containing Polynuclear Aromatics," *Fluid Phase Equilibria*, vol. 44, pp. 305–345, 1989.

[25] G. Morton, *Diesel: The Man and The Engine*. Atheneum, NY, USA, 1978.

[26] C. E. Goering, A. W. Schwab, M. J. Daugherty, E. H. Pryde, and A. J. Heakin, "Fuel Properties of Eleven Vegetable Oils," *Transactions of the ASAE*, vol. 25, pp. 1472–1477, 1982.

[27] L. G. Schumacher, J. van Gerpen, and B. Adams, "Biodiesel Fuels," *Encyclopedia of Energy*, vol. 1, pp. 151–162, 2004.

[28] A. Demirbas, "Recent Developments in Biodiesel Fuels," *Int. J. Green Energy*, vol. 4, pp. 15–26, 2007.

[29] M. A. Dubé, A. Y. Tremblay, and J. Liu, "Biodiesel Production Using a Membrane Reactor," *Bioresource Technology*, vol. 98, pp. 639–647, 2007.

[30] H. Fukuda, A. Kondo, and H. Noda, "Review: Biodiesel Fuel Production by Transesterification of Oils," *Journal of Bioscience and Bioengineering*, vol. 92, pp. 405–416, 2001.

[31] G. Knothe, "Dependence of Biodiesel Fuel Properties on the Structure of Fatty Acid Alkyl Esters," *Fuel Processing Technology*, vol. 86, pp. 1059–1070, 2005.

[32] W. Yuan, A. C. Hansen, and Q. Zhang, "Vapor Pressure and Normal Boiling Point Predictions for Pure Methyl Esters and Biodiesel Fuels," *Fluid*, vol. 84, pp. 943–950, 2005.

[33] R. Ceriani and A. J. A. Meirelles, "Predicting Vapour-Liquid Equilibria of Fatty Acids," *Fluid Phase Equlibria*, vol. 215, pp. 227–236, 2004.

[34] K. Bay, H. Wanko, and J. Ulrich, "Absorption of Volatile Organic Compounds in Biodiesel. Determination of Infinite Dilution Activity Coefficients by Headspace Gas Chromatography," *Chem. Eng. Res. Des.*, vol. 84, pp. 22–28, 2006.

[35] A. Rose and W. R. Supina, "Vapor Pressure and Vapor-Liquid Equilibrium Data for Methyl Esters and the Common Saturated Normal Fatty Acids," *Ind. Eng. Chem. Data*, vol. 6, pp. 173–179, 1961.

[36] A. Rose and V. N. Schrodt, "Vapor-Liquid Equilibria for the Methyl Oleate and Methyl Stearate Binary Mixtures," *Ind. Eng. Chem. Data*, vol. 9, pp. 12–16, 1964.

[37] A. C. G. van Genderen, J. C. van Miltenburg, G. B. Jacobus, M. J. van Bommel, P. J. van Ekeren, G. J. K. van den Berg, and H. A. J. Oonk, "Liquid-Vapour Equilibria of the Methyl Esters of Alkanoic Acids: Vapour Pressures as a Function of Temperature and Standard Thermodynamic Function Changes," *Fluid Phase Equlibria*, vol. 202, pp. 109–120, 2002.

[38] H. Inomata, T. Kondo, S. Hirohama, K. Arai, Y. Suzuki, and M. Konno, "Vapour-Liquid Equilibria for Binary Mixtures of Carbon Dioxide and Fatty Acid Methyl Esters," *Fluid Phase Equlibria*, vol. 46, pp. 41–52, 1989.

[39] H. S. Elbro, A. Fredenslund, and P. Rasmussen, "A New Simple Equation for the Prediction of Solvent Activities in Polymer Solutions," *Macromolecules*, vol. 23, pp. 4707–4713, 1990.

[40] G. M. Kontogeorgis, P. Coutsikos, D. P. Tassios, and A. Fredenslund, "Improved Models for the Prediction of activity Coefficients in Nearly Athermal Mixtures," *Fluid Phase Equilibria*, vol. 92, pp. 35–66, 1994.

[41] B. L. Larsen, P. Rasmussen, and A. Fredensund, "A Modified UNIFAC Group-Contribution Model for Prediction of Phase Equilibria and Heats of Mixing," *Ind. Eng. Chem. Res.*, vol. 26, pp. 2274–2286, 1987.

[42] J. Gross and G. Sadowski, "Perturbed-Chain SAFT: An Equation of State Based on Perturbation Theory for Chain Molecules," *Ind. Eng. Chem. Res.*, vol. 40, pp. 1244–1260, 2001.

[43] K. Kniaz, "Influence of the Size and Shape Effect on the Solubility of Hydrocarbons: The Role of the Combinatorial Entropy," *Fluid Phase Equilibria*, vol. 68, pp. 35–46, 1991.

[44] K. Kniaz, "Solubility of *n*-Docosane in *n*-Hexane and Cyclohexane," *J. Chem. Eng. Data*, vol. 36, pp. 471–482, 1991.

[45] J. F. Parcher, P. H. Weiner, C. L. Hussey, and T. N. Westlake, "Specific Retention Volumes and Limited Activity Coefficients of $C_4$–$C_8$ Alkane Solutes in $C_{22}$–$C_{36}$ *n*-Alkane Solvents," *J. Chem. Eng. Data*, vol. 20, pp. 145–151, 1975.

[46] E. C. Voutsas, N. S. Kalospiros, and D. P. Tassios, "A Combinatorial Activity Coefficient Model for Symmetric and Asymmetric Mixtures," *Fluid Phase Equilibria*, vol. 109, pp. 1–15, 1995.

[47] P. A. Rodgers, "Pressure Volume Temperature relationships for Polymeric Liquids – A Review of Equations of State and Their Characteristic Parameters for 56 Polymers," *J. Appl. Polym. Sci.*, vol. 48, pp. 1061–1980, 1993.

[48] I. A. Kouskoumvekaki, N. von Solms, T. Lindvig, M. L. Michelsen, and G. M. Kontogeorgis, "Novel Method for Estimating Pure-Component Parameters for Polymers: Application to the PC-SAFT Equation of State," *Ind. Chem. Eng. Res.*, vol. 43, pp. 2830–2838, 2004.

[49] F. Becher, M. Buback, H. Latz, G. Sadowski, and F. Tumakaka, "Cloud-Point Curves of Ethylene–(meth)acrylate Copolymers in Fluid Ethene up to High Pressures and Temperature. Experimental Study and PC-SAFT Modeling," *Fluid Phase Equilibria*, vol. 215, pp. 263–282, 2004.

[50] J. Gross, O. Spuhl, F. Tumakaka, and G. Sadowski, "Modeling Copolymer Systems Using the Perturbed-Chain SAFT Equation of State," *Ind. Eng. Chem. Res.*, vol. 42, pp. 1266–1274, 2003.

[51] J. Gross and G. Sadowski, "Modeling Polymer Systems Using the Perturbed-Chain Statistical Associating Fluid Theory Equation of State," *Ind. Eng. Chem. Res.*, vol. 41, pp. 1084–1093, 2002.

[52] P. Arce and M. Aznar, "Modeling the Phase Behavior of Commercial Biodegradable Polymers and Copolymer in Supercritical Fluids," *Fluid Phase Equilibria*, vol. 238, pp. 242–253, 2005.

[53] R. W. Kershaw and G. N. Malcolm, "Thermodynamics of Solutions of Polypropylene Oxide in Chloroform and in Carbon Tetrachloride," *Trans. Faraday Soc.*, vol. 64, pp. 323–336, 1968.

[54] W. R. Kriegbaum and D. O. Geymer, "Thermodynamics of Polymer Solutions. The Polystyrene–Cyclohexane System Near the Flory Theta Temperature," *J. Am. Chem. Soc.*, vol. 81, pp. 1859–1868, 1959.

[55] C. E. H. Bawn and M. A. Wajid, "High Polymer Solutions. Part 7: Vapor Pressure of Polystyrene Solutions with Acetone, Chloroform and Propyl Acetate," *Trans. Faraday Soc.*, vol. 52, pp. 1658–1664, 1956.

[56] P. J. T. Tait and A. M. Abushihada, "Comparative Studies on the Use of Gas Chromatographic and Vapour Pressure Techniques for the Determination of the Interaction Energy Parameter," *Polymer*, vol. 18, pp. 810–816, 1977.

[57] G. Wibawa, R. Hatano, Y. Sato, S. Takishima, and H. Masuoko, "Solubilities of 11 Polar Organic Solvents in Four Polymers Using the Piezoelectric-Quartz Sorption Method," *J. Chem. Eng. Data*, vol. 47, pp. 1022–1029, 2002.

[58] I. A. Kouskoumvekaki, N. von Solms, M. L. Michelsen, and G. M. Kontogeorgis, "Application of a Simplified Perturbed Chain SAFT Equation of State to Complex Polymer Systems Using Simplified Mixing Rules," *Fluid Phase Equilibria*, vol. 215, pp. 71–78, 2004.

[59] S. H. Huang and M. Radosz, "Equation of State for Small, Large, Polydisperse, and Associating Molecules," *Ind. Eng. Chem. Res.*, vol. 29, pp. 2284–2294, 1990.

[60] R. J. Kokes, A. R. Dipietro, and F. A. Long, "Equilibrium Sorption of Several Organic Diluents in Polyvinyl Acetate," *J. Am. Chem. Soc.*, vol. 75, pp. 6319–6325, 1953.

[61] J. R. Elliott and R. N. Natarajan, "Extension of the Elliott-Suresh-Donohue Equation of State to Polymer Solutions," *Ind. Eng. Chem. Res.*, vol. 41, pp. 1043–1050, 2002.

[62] N. von Solms, I. A. Kouskomvekaki, T. Lindvig, M. L. Michelsen, and G. M. Kontogeorgis, "A Novel Approach to Liquid-Liquid in Polymer Systems with Application to Simplified PC-SAFT," *Fluid Phase Equlibria*, vol. 222–223, pp. 87–93, 2004.

[63] B. A. Wolf and G. Blaum, "Measured and Calculated Solubility of Polymers in Mixed Solvents: Monotony and Consolvency," *J. Polym. Sci.*, vol. 13, pp. 1115–1132, 1975.

[64] A. Saraiva, M. Pleuss, O. Persson, and A. Fredenslund, *A Study of the Miscibility/Immiscibility of Low Molecular Weight Poly(n-butyl methylate)/ Single Solvent Systems by Thermo Optical Analysis by Microscopy.* Internal Report SEP9412, Department of Chemical Engineering, Technical University of Denmark, DK-2800 Kgs. Lyngby, 1994.

# Chapter 8

# Conclusion and Future Work

*"Learn from yesterday, live for today, hope for tomorrow. The important thing is not to stop questioning."* by Albert Einstein

## 8.1 Conclusions

In this thesis a predictive group contribution (GC) simplified perturbed chain-statistical associating fluid theory (sPC-SAFT) has been developed to extend the applicability of the sPC-SAFT equation of state (EoS) to treat molecules of different types. Within the GC formalism, a system (that can be both a pure component or a mixture) is treated at the level of representative functional groups, and the properties of the system are obtained by considering the contributions of each individual group. By incorporating the GC approach within a molecular and statistical mechanical theory such as SAFT, it is possible to develop a predictive thermodynamic model that can accurately describe complex chain-like systems.

A detailed review of the literature shows that a large amount of work has been devoted to the development of GC methods and that the various available GC thermodynamic models are based on fundamentally different theories. Although the GC activity coefficient models, like UNIFAC, etc., are a popular and rather convenient choice for the prediction of mixture phase behaviour, they also have serious limitations. These limitations are mainly associated with the fact that such models are based on lattice (quasi-chemical) theories, which do not provide a good representation of the structure of the fluid. As a result, they are mainly suitable for liquid phase description and have difficulties capturing e.g. pressure effects. In particular, the lower critical solution behaviour of a polymer solution is highly sensitive to pressure variations due to the fact that the volumetric expansion of the solvent that induces phase separation upon heating is partially governed by the pressure of the system. These deficiencies are overcome by using GC EoS.

In time, a number of EoS, including SAFT, have been modified in order to use the GC formalism to obtain a more predictive EoS. The existing GC approaches that are based on

the SAFT EoS have been developed at the level of the molecular parameters, which are then introduced as average values into the standard homonuclear versions of the theory. Moreover, the adjustment of binary interaction parameters ($k_{ij}$) when considering the phase equilibria of mixtures plays an important role.

In this work and in the same manner, the development of a GC approach within the sPC-SAFT formalism is presented, where a predictive GC approach by Constantinou-Gani from 1994 with an extended parameter table is implemented. This choice is made because, unlike other approaches found in the literature, this GC methodology includes two levels of contributions: both first-order groups (FOG) and second-order groups (SOG) that, to some extent, allow capture of proximity effects and distinguish among structural isomers.

Traditionally, parameters for molecular based EoS are obtained by fitting experimental vapour pressures and liquid densities. A drawback of this technique is the requirement of extensive experimental data on pure compounds to obtain reliable parameters. Additionally, a fast computational routine (e.g. a Marquardt algorithm) is required to perform the multivariable search for the parameters, as well as, in many cases, the critical region is overpredicted. It generally requires more time and effort than the average user of the EoS may be willing to invest. Therefore, the unavailability of fluid-specific parameters is still a major obstacle in the application of EoS. With that in mind, the most important future efforts in improving SAFT, and in fact any molecular based EoS, should explore the possibility and consequences of parameterizing them. As a preliminary work in this line, a way to estimate molecular based EoS parameters for a wide variety of fluids is explored.

The main achievements of the work presented in this thesis are the following:

- A detailed review of the available GC methods in order to get an overview of advantages and deficiencies of various models is given in Chapter 1.
- A brief description of the models that are used throughout this thesis are provided in Chapter 2, and a short overview of the use of the GC formalism within the SAFT formalism explaining the GC concept based on the so-called *conjugation principle* in Chapter 3.
- Pure component parameters for the PC-SAFT model ($m$, $\sigma$, and $\epsilon/k$) are obtained through a regression method for approximately 500 non-associating compounds. Investigations of trends and the physical significance of the numerous models' parameters are performed indicating an existing trend of linearity in the specific groupings of the parameters as presented in Chapter 4.
- An extensive evaluation of the sPC-SAFT description of fluid phase equilibria of several chemical families obtaining satisfactory estimations with or without $k_{ij}$. Fur-

thermore, the application of sPC-SAFT in modelling both VLE and LLE of a variety of binary polymer mixtures with either non-associating or associating solvents is successfully tested. Considering the complexity of molecules and the presence of various types of intermolecular interactions within these mixtures, satisfactory results are obtained. Typical results of VLE, LLE, activity coefficients at infinite dilution, and azeotropic data for various binary systems are shown in Chapter 5.

- Generation of the parameter table for the PC-SAFT EoS from newly estimated compound parameters in a sequential procedure that includes 45 FOG and 26 SOG is given in Chapter 6. The parameters of a new compound can then be calculated by summing up the contributions of certain defined groups of atoms, at the same time considering the number of occurrences of each group within the molecule.

- An investigation of the predictive capability of the GC sPC-SAFT EoS through comparison of the method's predictions for compounds with high $M_w$, and several selected binary mixtures of high industrial performance with experimental data, such as benzene derivatives, sulfur containing compounds, biodiesel, and various polymer–solvent mixtures and blends. The results are summarised in Chapter 7. The model is slightly more accurate in the case of mixtures modelling than in the case of pure compounds, but the quality of the predictions still remains satisfactory, especially when one keeps in mind that no direct experimental data were used in the parameter estimation.

The work presented in this thesis demonstrates the capability of sPC-SAFT to model binary systems of different chemical natures, and to use it in order to obtain a better understanding of the thermodynamics and phase equilibria of these systems. This is largely facilitated by the extensive table covering newly estimated PC-SAFT parameters for numerous pure non-associating compounds.

Due to a present need for the adjustment of $k_{ij}$ when considering the phase equilibria of mixtures, special emphasis is made on their characteristics, e.g. specific values, temperature dependency, and range of applicability (temperature, pressure, composition). As a possibility, a more predictive way to calculate $k_{ij}$ values has been investigated in Chapter 4 based on the recent work of Haslam *et al.* The methodology makes use of an additional physical parameter (ionization energy of involved compounds) and shows some promising results, which can be useful in situations where no experimental data are available.

The variety of functional groups in the presented GC schemes ensure broad applications of the GC sPC-SAFT EoS. Moreover, the quality of results obtained in this thesis is generally comparable to those of previous significant works from the literature when it has been possible to perform direct comparisons. This is considered as a strength of the proposed GC sPC-SAFT EoS.

## 8.2 Suggestions for Future Work

In the following, a number of suggestions for future work are given that may improve further applicability of the GC sPS-SAFT EoS for modelling of the phase behavior of fluids.

### 8.2.1 Extension of the Parameter Table

The applicability range and thus the engineering utility of any GC method are primarily determined by the extent of the available parameter table. Therefore, in order to enhance the utility of the GC sPC-SAFT approach, the current parameter table (now including 45 FOG and 26 SOG) should be extended with other important functional groups in a way similar to the one presented in Appendix C. This will allow the investigation of e.g. more highly branched hydrocarbons and halogenated hydrocarbons, among others. Moreover, extending the table to treat associating molecules will be another advantage, as this type of compounds are of significant importance in the chemical, biochemical, pharmaceutical, and food industries, as well as for environmental protection.

### 8.2.2 Multicomponent Modelling

The phase equilibria for binary mixtures as a function of temperature, pressure, and composition can generally be measured experimentally and modelled with various existing thermodynamic models, such as sPC-SAFT. However, measurements of multicomponent systems are very complex, time consuming, and costly. Therefore, the treatment of these multicomponent systems with sPC-SAFT is particularly appealing.

### 8.2.3 SLE Modelling

The solubility of solid solutes in common organic solvents is a key property of concern for the pharmaceutical industry because pharmaceutical product purification is often carried out through crystallisation at low temperatures. However, solubility data for new drug molecules are often scarce, and solubility experiments are costly and time consuming. Hence, the ability of the proposed GC method to be successfully applied in a predictive manner for solid-liquid equilibria (SLE) should also be investigated. Additionally, solubility of steroids in polymers is of importance in the design of controlled drug release devices.

### 8.2.4 Applications to Complex Polymer Mixtures

The study of polymer systems comprised of compounds that exhibit wide disparities in molecular size would benefit from availability of an accurate EoS. Of more significant importance to the polymeric scientific community would be:

- The study of Flory-Huggins' parameters.
- Modelling of second order properties of pure polymer and polymer mixtures, e.g. specific heats at constant pressure and volume, or the speed of sound.
- A detailed study of copolymers, not only for the prediction of phase equilibria, but also for studying the formation of aggregates. For the copolymer concept of the sPC-SAFT, pure compound parameters of the respective homopolymers composing the copolymer chain and an additional parameter to correct the dispersive interactions between unlike segment types in chains are additionally required.
- Adequate modelling of associating polymers.

It is evident from the investigations carried out in this work that existing thermodynamic methods may provide only a rough estimation of the phase behaviour of systems for which experimental data are unavailable. This is specially the case for complex mixture and polymer containing systems. When at least some experimental data are available for a given system, it may be possible to interpolate and extrapolate to other conditions, but the scarcity of experimental data for many important types of phase equilibria results in a need of additional experimental data and more reliable predictive thermodynamic models.

Information obtained from computational chemistry and modelling will probably never be a complete replacement for the data obtained from experiments, but can definitely supplement experimental work, with the result that each approach feeds off information derived by the other. Thus, any effort in directing this work in product design and discovery processes is worthwhile, because, once established, the empirical approach together with the information derived from computational modelling can be used to derive the required thermodynamic properties.

# Appendix A

# $\Omega_1^\infty$ for PVC–Solvents Systems using Different Models

Table A.1 presents comparisons of calculated values of $\Omega_1^\infty$ for PVC-solvents systems with experimental values using different thermodynamic models. The table is a supplement to Table 5.3 in Section 5.2.2.2. It is adopted from the Bachelor Thesis of the author [1].

Table A.1: Experimental and calculated $\Omega_1^\infty$ values for PVC–solvent systems using different models. Percentage values show AAD % from experiments[a]. See Section 5.2 for explanations of abbreviations.

| No. | System | Temp. [K] | Exp. $\Omega_1^\infty$ | ENTROPIC-FV $\Omega_1^\infty$ | | UNIFAC-FV $\Omega_1^\infty$ | | | UNIFAC $\Omega_1^\infty$ | | GCLF $\Omega_1^\infty$ | PC-SAFT $\Omega_1^\infty$ | |
|---|---|---|---|---|---|---|---|---|---|---|---|---|---|
| | | | | 2 coeff. | 1 coeff. | Fred'75 | 2 coeff. | 1 coeff. | 1 coeff. | 2 coeff. | | $k_{ij}=0$ | $k_{ij}$ Eq.(5.1) |
| 1 | PVC(40000)– | 383.15 | 6.197 | 4.85 | 2.45 | 3.03 | 3.43 | 4.47 | 3.72 | 3.19 | 6.15 | 3.73 | 16.5 |
| | monochlorobenzene | | | 21.7% | 60.5% | 51.1% | 44.7% | 27.9% | 40.0% | 48.2% | 0.8% | 39.8% | 165.% |
| 2 | PVC(170000)– | 393.15 | 6.05 | 5.46 | 4.21 | 4.17 | 3.92 | 4.01 | 2.35 | 2.40 | 4.54 | 19.66 | 35.8 |
| | chloroform | | | 9.8% | 30.4% | 31.1% | 35.2% | 33.7% | 61.2% | 60.3% | 25.3% | 225.% | 491.% |
| 3 | PVC(170000)– | 393.15 | 8.16 | 2.74 | 4.96 | 4.78 | 4.77 | 2.62 | 2.65 | 2.65 | 4.72 | 23.7 | 22.9 |
| | dichloromethane | | | 66.4% | 39.2% | 41.4% | 41.5% | 67.9% | 67.5% | 67.5% | 42.6% | 190.% | 181.% |
| 4 | PVC(97000)– | 398.15 | 7.56 | 5.92 | 7.51 | 7.43 | 7.54 | 6.03 | 5.11 | 4.08 | [b] | 16.11 | 12.7 |
| | nitroethane | | | 21.7% | 0.7% | 1.7% | 0.3% | 20.2% | 32.8% | 46.0% | | 113.% | 67.7% |
| 5 | PVC(34000)– | 315.15 | 9.61 | 10.24 | 18.89 | 18.32 | 18.32 | 9.98 | 13.47 | 7.33 | 5.65 | 6.79 | 6.99 |
| | 1,4-dioxane | | | 6.6% | 96.6% | 90.6% | 90.6% | 3.9% | 40.2% | 23.7% | 41.2% | 29.3% | 27.3% |
| 6 | PVC(97000)– | 398.15 | 7.33 | 5.08 | 11.26 | 15.02 | 10.21 | 4.96 | 6.25 | 3.03 | 6.05 | 18.3 | 13.9 |
| | tetrahydrofurane | | | 30.7% | 53.6% | 105.% | 39.3% | 32.3% | 14.7% | 58.7% | 17.5% | 150.% | 89.4% |
| 7 | PVC(34000)– | 315.65 | 7.44 | 9.26 | 10.94 | 16.51 | 10.69 | 7.99 | 7.0 | 5.32 | 6.55 | 8.43 | 5.77 |
| | tetrahydrofurane | | | 24.5% | 47.0% | 121.9% | 43.7% | 7.4% | 5.9% | 28.5% | 12.0% | 13.3% | 22.4% |
| 8 | PVC(97000)– | 413.15 | 6.89 | 4.55 | 11.38 | 14.66 | 10.03 | 4.49 | 6.14 | 2.75 | 6.00 | 17.9 | 13.8 |
| | tetrahydrofurane | | | 34.0% | 65.2% | 112.8% | 45.6% | 34.8% | 10.9% | 60.1% | 13.0% | 160.% | 99.6% |
| 9 | PVC(175000)– | 393.15 | 12.87 | 5.26 | 11.23 | 15.13 | 10.27 | 5.12 | 6.29 | 3.14 | 6.08 | 32.4 | 24.4 |
| | tetrahydrofurane | | | 59.1% | 12.7% | 17.6% | 20.2% | 60.2% | 51.1% | 75.6% | 52.8% | 35.2% | 89.9% |
| 10 | PVC(97000)– | 398.15 | 7.47 | 3.42 | 5.13 | 3.12 | 4.63 | 5.33 | 3.10 | 3.58 | 8.44 | 17.40 | 19.6 |
| | toluene | | | 53.6% | 31.3% | 58.2% | 38.0% | 28.7% | 58.5% | 52.1% | 13.0% | 133.% | 162.% |
| 11 | PVC(340000)– | 316.35 | 12.22 | 5.12 | 4.28 | 4.09 | 4.10 | 4.92 | 2.93 | 3.51 | 8.91 | 79.8 | 93.9 |
| | toluene | | | 58.1% | 65.0% | 66.5% | 66.5% | 59.7% | 76.0% | 71.3% | 27.1% | 553.% | 669.% |
| 12 | PVC(97000)– | 398.15 | 7.363 | 6.104 | 5.72 | 5.167 | 5.17 | 5.55 | 3.18 | 3.39 | 7.94 | 17.5 | 14.7 |
| | benzene | | | 17.1% | 22.3% | 29.8% | 29.8% | 24.6% | 56.8% | 54.0% | 7.8% | 138.% | 99.2% |
| 13 | PVC(97000)– | 398.15 | 10.82 | 9.52 | 10.32 | 10.39 | 10.39 | 9.59 | 5.71 | 5.27 | 9.12 | 27.7 | [c] |
| | acetone | | | 12.0% | 4.6% | 4.0% | 4.0% | 11.4% | 47.2% | 51.3% | 15.7% | 156.% | |
| 14 | PVC(41000)– | 393.15 | 11.81 | 9.33 | 10.19 | 10.39 | 10.39 | 9.52 | 5.72 | 5.24 | 9.01 | 11.82 | [c] |
| | acetone | | | 21.0% | 13.7% | 12.0% | 12.0% | 19.4% | 51.6% | 55.6% | 23.7% | 0.0% | |

*Continues on next page*

| No. | System | Temp. [K] | Exp. $\Omega_1^\infty$ | ENTROPIC-FV $\Omega_1^\infty$ | | UNIFAC-FV $\Omega_1^\infty$ | | | UNIFAC $\Omega_1^\infty$ | | GCLF $\Omega_1^\infty$ | PC-SAFT $\Omega_1^\infty$ | |
|---|---|---|---|---|---|---|---|---|---|---|---|---|---|
| | | | | 2 coeff. | 1 coeff. | Fred'75 | 2 coeff. | 1 coeff. | 1 coeff. | 2 coeff. | | $k_{ij}=0$ | $k_{ij}$ Eq.(5.1) |
| 15 | PVC(34000)– | 315.35 | 26.46 | 12.203 | [d] | 16.98 | [d] | [d] | [d] | [d] | 22.06 | 19.5 | 33.3 |
| | di-*n*-propyl ether | | | 53.9% | | 35.8% | | | | | 16.6% | 26.2% | 26.0% |
| 16 | PVC(97000)– | 383.15 | 34.44 | 15.11 | 14.97 | 14.76 | 14.80 | 14.93 | 9.65 | 14.97 | 22.93 | 45.2 | 195. |
| | *n*-nonane | | | 56.1% | 56.5% | 57.1% | 57.0% | 56.7% | 72.2% | 56.5% | 33.4% | 31.3% | 467.% |
| 17 | PVC(97000)– | 383.15 | 34.32 | 14.88 | 14.76 | 14.62 | 14.65 | 14.77 | 9.11 | 9.18 | 21.78 | 45.5 | 108.5 |
| | *n*-octane | | | 56.6% | 57.0% | 57.4% | 57.3% | 57.0% | 73.5% | 73.3% | 36.5% | 32.6% | 216.% |
| 18 | PVC(97000)– | 393.15 | 38.65 | 16.57 | 16.66 | 15.84 | 15.86 | 15.78 | 7.73 | 7.69 | 20.66 | 50.9 | 37.5 |
| | *n*-pentane | | | 57.1% | 56.9% | 59.0% | 59.0% | 59.2% | 80.0% | 80.0% | 46.6% | 31.7% | 2.90% |
| 19 | PVC(97000)– | 398.15 | 31.89 | 14.73 | 14.93 | 14.43 | 14.43 | 14.23 | 8.46 | 8.35 | 20.67 | 21.3 | 31.5 |
| | *n*-heptane | | | 53.8% | 53.2% | 54.8% | 54.8% | 55.4% | 73.5% | 73.8% | 35.2% | 33.2% | 1.16% |

a: AAD% is calculated from AAD $\% = \frac{1}{N_{data}} \sum \left| \Omega^{exp} - \Omega^{calc} \right| / \Omega^{exp} \times 100$.
b: $\Omega_1^\infty$ cannot be calculated by GCLF, since the group parameter table does not include $CH_2NO_2$.
c: $\Omega_1^\infty$ cannot be calculated as $M_w$ of acetone is out of range.
d: $\Omega_1^\infty$ cannot be calculated due to unavailable parameters.

## References


[1] A. Tihic, *Investigation of the Miscibility of Plasticizers in PVC.* Bachelor Thesis, Department of Chemical Engineering, Technical University of Denmark, DK-2800 Kgs. Lyngby, 2003.

# Appendix B

# The Tamouza *et al.* Approach

With reference to Section 6.4.2 in Chapter 6, this appendix presents the GC scheme with the contributions of FOG and SOG for each of the three PC-SAFT parameters, $m$, $\sigma$, and $\epsilon/k$, when using the Tamouza *et al.* [1] approach.

Tables B.1 and B.2 list the contributions of FOG and SOG that have been defined for the new GC scheme. Statistical results with this scheme and the number of compounds used in the regressions are provided in Table B.3.

Since the GC scheme for PC-SAFT parameters proposed in this appendix is not tested exhaustively, this work should merely be considered as supplementary material to the work presented in Chapter 6.

Table B.1: First-Order Group (FOG) contributions from the parameters $m$, $\sigma$, and $\epsilon/k$ using the Tamouza *et al.* [1] approach.

| First-order group (FOG) | Contribution | | | UNIFAC notation [2] | Sample group assignment (occurrences) |
|---|---|---|---|---|---|
| | $m$ [–] | $\sigma$ [Å] | $\epsilon/k$ [K] | | |
|  | 0.6444 | 3.7092 | 197.27 | "–$CH_3$" | propane (2) |
|  | 0.3843 | 3.9114 | 264.07 | "–$CH_2$" | *n*-butane (2) |
|  | 0.04383 | 4.3789 | 372.17 | "–CH<" | *i*-butene (1) |
|  | –0.4921 | 5.5162 | 595.14 | ">C<" | neopentane (1) |
|  | 1.0315 | 3.6808 | 238.51 | "$CH_2$=CH–" | propylene (1) |
|  | 0.9006 | 3.6030 | 323.81 | "–CH=CH–" | *cis*-2-butane (1) |
|  | 0.7397 | 3.7830 | 312.55 | "$CH_2$=C<" | *i*-butene (1) |
|  | 0.5136 | 3.6030 | 401.78 | "–CH=C<" | 2-methyl-2-butene (1) |
|  | 0.3772 | 3.8300 | 607.38 | ">C=C<" | 2,3-dimethyl-2-butene (1) |
|  | 1.5884 | 3.3869 | 293.65 | "$CH_2$=C=CH–" | 1,2-butadiene (1) |

*Continues on next page*

| First-order group (FOG) | Contribution | | | UNIFAC notation [2] | Sample group assignment (occurrences) |
|---|---|---|---|---|---|
| | $m$ [–] | $\sigma$ [Å] | $\epsilon/k$ [K] | | |
| 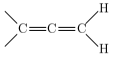 | 1.3284 | 3.4982 | 366.11 | "$CH_2$=C=C<" | 3-methyl-1,2-butadiene (1) |
| 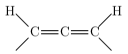 | 1.4795 | 3.2558 | 360.61 | "CH=C=CH–" | 2,3-pentadiene (1) |
| 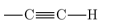 | 1.1723 | 3.114 | 254.42 | "CHEC–" | propyne (1) |
| 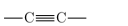 | 0.7155 | 3.6996 | 488.34 | "CEC" | 2-butyne (1) |
|  | 0.3663 | 3.7811 | 292.25 | "ACH" | benzene (6) |
|  | 0.0107 | 4.2387 | 571.41 | "AC" | napthalene (2) |
| 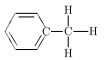 | 0.8369 | 3.7272 | 279.54 | "$ACCH_3$" | toluene (1) |
|  | 0.3898 | 4.3414 | 398.83 | "$ACCH_2$–" | *m*-ethyltoluene (1) |
|  | –0.0362 | 5.3612 | 637.74 | "ACCH<" | *sec*-butylbenzene (1) |
|  | 1.7938 | 3.4732 | 301.00 | "$CH_3CO$" | methyl ethyl ketone (1) |
| 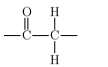 | 1.5521 | 2.8993 | 472.20 | "$CH_2CO$" | cyclopentanone (1) |

*Continues on next page*

| First-order group (FOG) | Contribution | | | UNIFAC notation [2] | Sample group assignment (occurrences) |
|---|---|---|---|---|---|
| | $m$ [–] | $\sigma$ [Å] | $\epsilon/k$ [K] | | |
|  | 1.0851 | 0.9303 | 452.64 | "CHCO" | diisopropyl ketone (1) |
|  | 1.8896 | 1.1906 | 174.66 | "CHO" | 1-butanal (1) |
|  | 2.3626 | 2.3331 | 221.19 | "$CH_3COO$" | ethyl acetate (1) |
|  | 1.9527 | 2.4164 | 249.00 | "$CH_2COO$" | methyl propionate (1) |
|  | 1.7458 | 1.7607 | 224.27 | "HCOO" | *n*-propyl formate (1) |
|  | 1.4391 | 2.2379 | 250.95 | "COO" | ethyl acetate (1) |
|  | 1.5270 | 1.9976 | 153.20 | "$CH_3O$" | methyl ethyl ether (1) |
|  | 1.2263 | 2.6560 | 214.26 | "$CH_2O$" | ethyl vinyl ether (1) |
|  (cyclic) | 1.1019 | 2.8410 | 288.22 | "$CH_2O$ (cyclic)" | 1,4-dioxane (2) |
|  | 1.5442 | 1.1906 | 174.66 | "CHO" | diisopropyl ether (1) |
| —O— (except as above) | –0.0886 | 5.9777 | 555.20 | "O (except as above)" | divinyl ether (1) |

*Continues on next page*

| First-order group (FOG) | Contribution | | | UNIFAC notation [2] | Sample group assignment (occurrences) |
|---|---|---|---|---|---|
| | $m$ [–] | $\sigma$ [Å] | $\epsilon/k$ [K] | | |
|  | 1.3920 | 3.1702 | 392.66 | "$CH_3S$" | methyl ethyl sulfide (1) |
|  | 0.9709 | 3.7494 | 452.17 | "$CH_2S$" | diethyl sulfide (1) |
|  | 0.9281 | 3.4438 | 648.84 | "CHS" | diisopropyl sulfide (1) |
|  | 0.8902 | 4.0107 | 559.02 | "I" | isopropyl iodide (1) |
|  | 0.8889 | 3.2222 | 376.51 | "Br" | 2-bromopropane (1) |
|  | 1.2097 | 3.3761 | 328.93 | "$CH_2Cl$" | *n*-butyl chloride (1) |
|  | 0.8101 | 3.7828 | 361.84 | "CHCl" | isopropyl chloride (1) |
|  | 0.7136 | 3.9058 | 454.69 | "ACCl" | *m*-dichlorobenzene (2) |
|  | 1.4581 | 2.4549 | 89.46 | "ACF" | fluorobenzene (1) |
|  | 0.6158 | 4.1168 | 185.88 | "$CF_3$" | *n*-perfluorohexane (2) |
|  | 0.9338 | 3.3674 | 164.66 | "$CF_2$" | perfluoromethylcyclohexane (5) |

*Continues on next page*

| First-order group (FOG) | Contribution | | | UNIFAC notation [2] | Sample group assignment (occurrences) |
|---|---|---|---|---|---|
| | $m$ [–] | $\sigma$ [Å] | $\epsilon/k$ [K] | | |
| 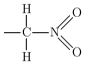 | 2.2101 | 2.7072 | 438.54 | "$CH_2NO_2$" | 1-nitropropane (1) |
| 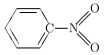 | 2.3410 | 1.6797 | 297.99 | "$ACNO_2$" | nitrobenzene (1) |

Table B.2: Second-Order Group (SOG) contributions from the parameters $m$, $\sigma$, and $\epsilon/k$ using the Tamouza *et al.* [1] approach.

| Second-order group (SOG) | Contribution | | UNIFAC notation [2] | Sample group assignment (occurrences) |
|---|---|---|---|---|
| | $m$ [–] | $\sigma$ [Å] | | |
|  | 0.0162 | 3.6462 | "$(CH_3)_2$–CH–" | *i*-butane (1) |
|  | 0.0414 | 3.9389 | "$(CH_3)_3$–C–" | neopentane (1) |
|  | –0.0463 | 4.1748 | "–CH($CH_3$)–CH($CH_3$)–" | 2,3-dimethylbutane (1) |
|  | –0.1015 | 4.4495 | "–CH($CH_3$)–C$(CH_3)_2$–" | 2,2,3-trimethylpentane (1) |
|  | –0.1833 | 4.8299 | "–C$(CH_3)_2$–C$(CH_3)_2$–" | 2,2,3,3-tetramethylpentane (1) |

*Continues on next page*

| Second-order group (SOG) | Contribution | | UNIFAC notation [2] | Sample group assignment (occurrences) |
|---|---|---|---|---|
| | $m$ [–] | $\sigma$ [Å] | | |
|  | 0.6728 | 3.8793 | ”ring of 3 carbons” | cyclopropane (1) |
|  | 0.5069 | 2.9877 | ”ring of 4 carbons” | cyclobutane (1) |
|  | 0.3095 | 3.1221 | ”ring of 5 carbons” | cyclopentane (1) |
|  | 0.0642 | 3.7952 | ”ring of 6 carbons” | cyclohexane (1) |
|  | 0.1216 | 3.5540 | ”ring of 7 carbons” | cycloheptane (1) |
| 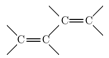 | –0.1122 | 3.8806 | ”–C=CC=C–” | 1,3-butadiene (1) |
|  | 0.0135 | 3.7139 | ”$CH_3$–C=” | *i*-butene (2) |
|  | –0.0435 | 3.9996 | ”–$CH_2$–C=” | 1-butene (1) |
|  (X = H or C) | 0.0841 | 3.4806 | ”–C{H or C}–C=” | 3-methyl-1-butene (1) |

*Continues on next page*

| Second-order group (SOG) | Contribution | | UNIFAC notation [2] | Sample group assignment (occurrences) |
|---|---|---|---|---|
| | $m$ [–] | $\sigma$ [Å] | | |
| 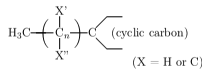 (X = H or C) | –0.1455 | 5.1113 | "string in cyclic" | ethylcyclohexane (1) |
| 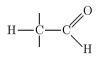 | 0.2549 | 3.0597 | ">CHCHO" | 2-methyl butyraldehyde (1) |
| 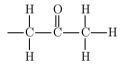 | –0.0387 | 2.7533 | "$CH_3(CO)CH_2$–" | 2-pentanone (1) |
| 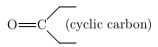 | –0.0309 | 2.7518 | "C(cyclic)==O" | cyclopentanone (1) |
| 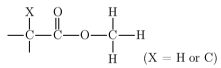 (X = H or C) | 0.0890 | 2.8948 | "$CH_3(CO)OC\{H$ or $C\}<$" | *i*-butyric acid (1) |
| 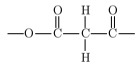 | –0.0109 | 3.6268 | "$(CO)C\{H_2\}COO$" | ethyl acetoacetate (1) |
| 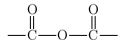 | –0.0771 | 3.7230 | "(CO)O(CO)" | propanoic anhydride (3) |
| 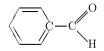 | –0.2422 | 3.5525 | "ACHO" | benzaldehyde (1) |
|  | –0.1236 | 2.9199 | "ACBr" | bromotoluene (1) |
| 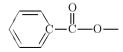 | –0.0800 | 3.1588 | "ACCOO" | benzoic acid ethyl ester (1) |

*Continues on next page*

| Second-order group (SOG) | Contribution | | UNIFAC notation [2] | Sample group assignment (occurrences) |
|---|---|---|---|---|
| | $m$ [–] | $\sigma$ [Å] | | |
|  | –0.0001 | 4.5000 | "AC($ACH_m$)$_2$AC($ACH_n$)$_2$" | benzoic acid ethyl ester (1) |
|  (cyclic structure) | 0.3635 | 3.1608 | "O(cyclic)–C(cyclic)=O" | diketene (3) |

Table B.3: Statistical results with the Tamouza *et al.* [1] approach implemented in the sPC-SAFT EoS.

| Parameter | $N_{DP}$ | Std. dev.[a] | | AAE[a] | | AAD[a] [%] | |
|---|---|---|---|---|---|---|---|
| | | FOG | FOG+SOG | FOG | FOG+SOG | FOG | FOG+SOG |
| $m$ | 399 | 0.27 | 0.26 | 0.19 | 0.17 | 5.11 | 4.54 |
| $\sigma$ | 381 | 0.08 | 0.07 | 0.06 | 0.06 | 1.68 | 1.51 |
| $\epsilon/k$ | 393 | 21.4 | — | 12.6 | — | 4.79 | — |

[a] Std. dev. $= \sqrt{\sum (X^{est} - X^{exp}) / (N_{DP} - 1)}$; AAE $= (1/N_{DP}) \sum \left| X^{est} - X^{exp} \right|$; AAD $= (1/N_{DP}) \sum \left( \left| X^{est} - X^{exp} \right| / X^{exp} \right) 100\,\%$. $N_{DP}$ is the number of experimental data points; $X^{est}$ is the estimated value of the property $X$, and $X^{exp}$ is the experimental value of the property $X$.

## References


[1] S. Tamouza, J.-P. Passarello, P. Tobaly, and J.-C. de Hemptinne, "Group Contribution Method with SAFT EoS Applied to Vapor Liquid Equilibria of Various Hydrocarbon Series," *Fluid Phase Equilibria*, vol. 222-223, pp. 67–76, 2004.

[2] A. Fredenslund, R. L. Jones, and J. M. Prauznitz, "Group-Contribution Estimation of Activity Coefficients in Nonideal Liquid Mixtures," *AIChE J.*, vol. 21, pp. 1086–1099, 1975.

# Appendix C

# Improvements of the FOG and SOG Schemes

With reference to Section 6.5 in Chapter 6, this appendix presents the results of the latest efforts to further improve the current GC methodology in terms of the FOG and SOG schemes.

Since the GC PC-SAFT parameters proposed in this appendix are not tested exhaustively, this work should merely be considered as supplementary material to the completed work presented in Chapter 6 and 7, and serve as inspiration for future work in the field.

## C.1 Extension of the GC Scheme

The GC schemes in Tables 6.3 and 6.4 (Chapter 6) are based on a regression approach that includes 399 compounds; each with PC-SAFT parameters fitted to DIPPR correlations [1] or similar. From this, FOG and SOG are extracted with separate parameter sets. The detailed approach is described in Section 6.4 and illustrated in Figure 6.1 on page 133.

The substantial number of compounds on which this approach relies is important for the achievement of an acceptable accuracy. Extending the number of compounds will eventually dilute outliers and inter-family variations of the chemical compounds provided the underlying experimental data exhibit low uncertainties. It will also likely result in appearances of new FOG and SOG embedded within the molecular structures of the additional compounds, which can then be added to the existing FOG and SOG schemes.

The first attempt to improve the existing GC scheme consists of first removing a few of the 399 compounds from the database that produce the most significant deviations and then add several new compounds. It is unknown whether the removed outliers arise from experimental uncertainties or limitations in the GC approach, but there is a trend that small compounds, like $C_{3-4}$, produce significant deviations. This emphasizes the enhanced applicability of the GC sPC-SAFT EoS for larger compounds, as it has previously been observed during the parameter testing in Chapter 6. For this reason, the new compounds

added to the database are all $C_{\geq 5}$. In total, the compound database is subjected to a net increase of 35 compounds from different families as part of the current update.

After the adjustment of the experimental compound database, all parameter sets are recalculated using the same approach as described in Section 6.4 and illustrated in Figure 6.1. As previously, pure component PC-SAFT parameters for the additional compounds are obtained by fitting vapour pressure and liquid density data extracted mainly from the DIPPR correlations [1]. This approach is hereafter denoted "Approach (I)".

### C.1.1 Recalculation of $\epsilon/k$

Experiences with the GC sPC-SAFT EoS and the impact of deviations in $m$, $\sigma$, and $\epsilon/k$ on model predictions show that the accuracy of $\epsilon/k$ is of particular importance in order to obtain accurate results. This is consistent with previous observations from the scatter plots in Figure 6.2 on page 144, which displayed a less linear relationship between GC estimated $\epsilon/k$ parameters of ∼400 different molecules with experimental reference values from DIPPR than the trends observed for $m$ and $\sigma$.

In the pursuit of higher accuracies of $\epsilon/k$, a second approach is proposed where $m\epsilon/k$ is recalculated using already fitted GC parameters of $m$ and $m\sigma^3$ from Approach (I). By fitting values of $m\epsilon/k$ to values of $P^{sat}$ and $\rho$ from DIPPR, while fixing the other two parameters $m$ and $m\sigma^3$, the resulting values of $m\epsilon/k$ will ensure an overall exact match to $P^{sat}$ and $\rho$ from DIPPR where uncertainties to the individual parameters can be attributed solely to $m$ and $\sigma$ besides, of course, the experimental uncertainties. In the following, this approach is called "Approach (II)".

The methodology behind Approach (II) is illustrated in Figure C.1.

## C.2 Updated FOG and SOG Schemes

The extended GC scheme with updated values of $m$, $\sigma$, and $\epsilon/k$ of both FOG and SOG using Approach (I) and Approach (II) are shown in Tables C.1 and C.2 respectively. Statistical results with the updated schemes are provided in Table C.3.

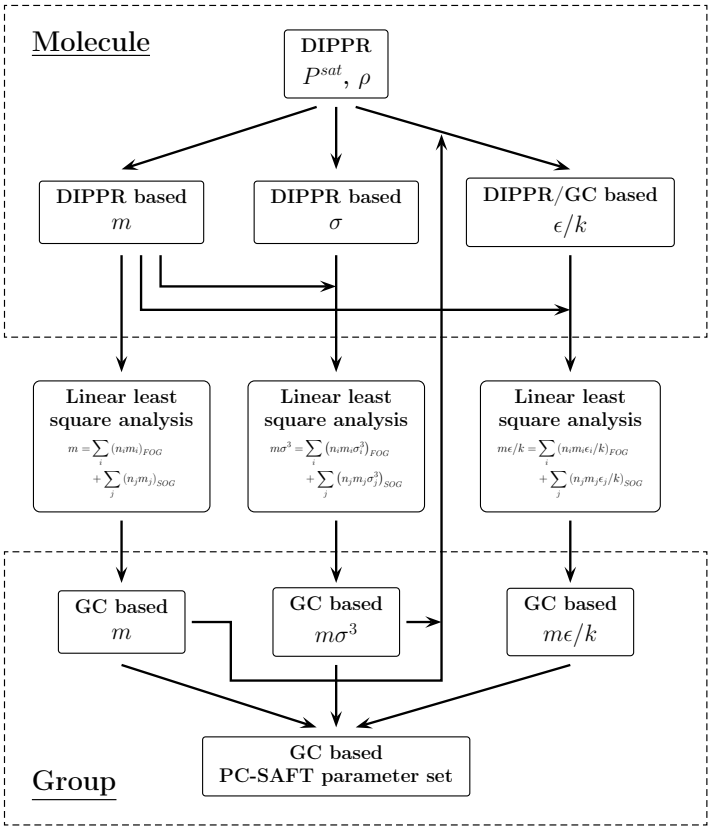


Figure C.1: Schematic illustration of the GC methodology for recalculation of $\epsilon/k$ using already calculated GC values for $m$ and $m\sigma^3$, i.e. Approach (II).

Table C.1: Updated First-Order Group (FOG) contributions from the parameters $m$, $m\sigma^3$, and $m\epsilon/k$. (I) and (II) refer to the new approaches.

| First-order group (FOG) | Contribution | | | | UNIFAC notation [2] | Sample group assignment (occurrences) |
|---|---|---|---|---|---|---|
| | $m$ [–] | $m\sigma^3$ [Å$^3$] | $m\epsilon/k$ (I) [K] | $m\epsilon/k$ (II) [K] | | |
|  | 0.6406 | 34.1710 | 126.028 | 122.837 | "–$CH_3$" | propane (2) |
|  | 0.3832 | 23.9051 | 101.539 | 101.459 | "–$CH_2$" | *n*-butane (2) |
|  | 0.0643 | 14.6544 | 72.9380 | 81.358 | "–CH<" | *i*-butene (1) |
|  | –0.4842 | 2.6700 | –2.921 | 6.489 | ">C<" | neopentane (1) |
|  | 1.0382 | 53.0549 | 241.872 | 243.144 | "$CH_2$=CH–" | propylene (1) |
|  | 0.8911 | 40.6927 | 257.496 | 258.903 | "–CH=CH–" | *cis*-2-butane (1) |
|  | 0.7435 | 41.2436 | 229.668 | 233.088 | "$CH_2$=C<" | *i*-butene (1) |
|  | 0.5259 | 29.8519 | 217.432 | 224.739 | "–CH=C<" | 2-methyl-2-butene (1) |
|  | 0.3923 | 17.0648 | 250.547 | 265.873 | ">C=C<" | 2,3-dimethyl-2-butene (1) |
| 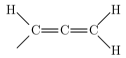 | 1.5925 | 67.6036 | 416.749 | 419.964 | "$CH_2$=C=CH–" | 1,2-butadiene (1) |

*Continues on next page*

| First-order group (FOG) | Contribution | | | | UNIFAC notation [2] | Sample group assignment (occurrences) |
|---|---|---|---|---|---|---|
| | $m$ [–] | $m\sigma^3$ [Å$^3$] | $m\epsilon/k$(I) [K] | $m\epsilon/k$(II) [K] | | |
| 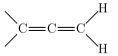 | 1.3359 | 57.7619 | 382.383 | 294.356 | "$CH_2$=C=C<" | 3-methyl-1,2-butadiene (1) |
| 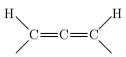 | 1.4870 | 56.3539 | 415.663 | 422.047 | "CH=C=CH–" | 2,3-pentadiene (1) |
| 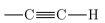 | 1.1743 | 42.6077 | 292.951 | 294.356 | "CHEC–" | propyne (1) |
| 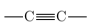 | 0.7218 | 33.4703 | 283.451 | 288.808 | "CEC" | 2-butyne (1) |
|  | 0.3831 | 20.8141 | 111.198 | 111.758 | "ACH" | benzene (6) |
|  | –0.0159 | 8.4451 | 74.339 | 73.130 | "AC" | napthalene (2) |
| 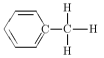 | 0.8233 | 42.6528 | 233.803 | 233.858 | "$ACCH_3$" | toluene (1) |
|  | 0.3330 | 31.5584 | 155.137 | 155.697 | "$ACCH_2$–" | *m*-ethyltoluene (1) |
|  | –0.0919 | 21.7108 | 93.672 | 97.180 | "ACCH<" | *sec*-butylbenzene (1) |
|  | 1.7917 | 61.6920 | 489.820 | 508.249 | "$CH_3CO$" | methyl ethyl ketone (1) |
|  | 1.5061 | 52.1167 | 500.118 | 484.951 | "$CH_2CO$" | cyclopentanone (1) |

*Continues on next page*

| First-order group (FOG) | Contribution | | | | UNIFAC notation [2] | Sample group assignment (occurrences) |
|---|---|---|---|---|---|---|
| | $m$ [–] | $m\sigma^3$ [Å$^3$] | $m\epsilon/k$(I) [K] | $m\epsilon/k$(II) [K] | | |
|  | 1.0797 | 14.9294 | 356.375 | 360.721 | "CHCO" | diisopropyl ketone (1) |
|  | 1.8611 | 30.7200 | 438.229 | 438.985 | "CHO" | 1-butanal (1) |
|  | 2.3621 | 66.3943 | 539.966 | 538.376 | "$CH_3COO$" | ethyl acetate (1) |
|  | 2.0670 | 55.4808 | 497.570 | 526.708 | "$CH_2COO$" | methyl propionate (1) |
|  | 1.7485 | 44.8107 | 433.891 | 436.028 | "HCOO" | $n$-propyl formate (1) |
|  | 1.4096 | 33.4971 | 351.731 | 349.814 | "COO" | ethyl acetate (1) |
|  | 2.6712 | 42.0130 | 375.570 | 470.720 | "$CH_3O$" | methyl ethyl ether (1) |
|  | 1.2287 | 33.2820 | 285.831 | 290.893 | "$CH_2O$" | ethyl vinyl ether (1) |
|  (cyclic) | 1.1030 | 33.2904 | 308.461 | 308.541 | "$CH_2O$ (cyclic)" | 1,4-dioxane (2) |
|  | 1.5372 | 16.4277 | 334.034 | 328.008 | "CHO" | diisopropyl ether (1) |
| —O— (except as above) | –0.2027 | 8.6761 | –36.757 | –39.939 | "O (except as above)" | divinyl ether (1) |

*Continues on next page*

| First-order group (FOG) | Contribution | | | | UNIFAC notation [2] | Sample group assignment (occurrences) |
|---|---|---|---|---|---|---|
| | $m$ [–] | $m\sigma^3$ [Å$^3$] | $m\epsilon/k$(I) [K] | $m\epsilon/k$(II) [K] | | |
|  | 1.3972 | 61.9364 | 433.125 | 435.259 | "$CH_3S$" | methyl ethyl sulfide (1) |
|  | 0.9968 | 50.8832 | 358.507 | 367.221 | "$CH_2S$" | diethyl sulfide (1) |
|  | 0.9227 | 39.8484 | 372.129 | 376.475 | "CHS" | diisopropyl sulfide (1) |
|  | 1.3103 | 58.7256 | 422.558 | 424.425 | "$CH_2SH$" | $n$-butyl mercaptane (1) |
| 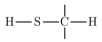 | 0.6283 | 31.3543 | 233.637 | 235.107 | "CHSH" | cyclohexyl mercaptane (1) |
|  | 2.0770 | 97.0760 | 682.647 | 688.963 | "$C_4H_3S$" | 2-methyl thiophene (1) |
| —SH | 2.9261 | 114.1668 | 825.603 | 826.252 | "SH (except as above)" | 2-mercaptobenzothiazole (1) |
|  | 2.2889 | 43.2149 | 881.839 | 889.977 | "$SO_2$" | sulfolene (1) |
| —S— (except as above) | 0.6198 | 27.0604 | 220.548 | 218.362 | "S (except as above)" | thiophene (1) |
| —I | 0.8331 | 47.0096 | 333.812 | 332.220 | "I" | isopropyl iodide (1) |
| —Br | 0.8008 | 36.6446 | 264.671 | 271.156 | "Br" | 2-bromopropane (1) |
|  | 1.2112 | 54.2026 | 370.087 | 370.328 | "$CH_2Cl$" | $n$-butyl chloride (1) |

*Continues on next page*

| First-order group (FOG) | Contribution | | | | UNIFAC notation [2] | Sample group assignment (occurrences) |
|---|---|---|---|---|---|---|
| | $m$ [–] | $m\sigma^3$ [Å$^3$] | $m\epsilon/k$(I) [K] | $m\epsilon/k$(II) [K] | | |
|  | 0.8118 | 42.8695 | 275.411 | 277.266 | "CHCl" | isopropyl chloride (1) |
|  | 0.6701 | 38.6808 | 262.512 | 261.029 | "ACCl" | $m$-dichlorobenzene (2) |
|  | 0.5608 | 26.0483 | 142.374 | 143.636 | "ACF" | fluorobenzene (1) |
|  | 1.7826 | 45.8243 | 181.806 | 173.358 | "$CF_3$" | $n$-perfluorohexane (2) |
|  | 0.3601 | 36.0467 | 114.201 | 112.940 | "$CF_2$" | perfluoromethylcyclohexane (5) |
| —F (except as above) | 0.6714 | 11.3185 | 52.786 | 56.583 | "F (except as above)" | 2-floropropane (1) |
|  | 2.2145 | 65.7995 | 706.137 | 709.369 | "$CH_2NO_2$" | 1-nitropropane (1) |
| 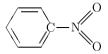 | 2.3060 | 45.6174 | 679.147 | 677.934 | "$ACNO_2$" | nitrobenzene (1) |

Table C.2: Updated Second-Order Group (SOG) contributions from the parameters $m$, $m\sigma^3$, and $m\epsilon/k$. (I) and (II) refer to the new approaches.

| Second-order group (SOG) | Contribution | | | | UNIFAC notation [2] | Sample group assignment (occurrences) |
|---|---|---|---|---|---|---|
| | $m$ [–] | $m\sigma^3$ [Å$^3$] | $m\epsilon/k$(I) [K] | $m\epsilon/k$(II) [K] | | |
| 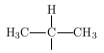 | 0.0057 | –0.0443 | –9.393 | –9.779 | "$(CH_3)_2$–CH–" | *i*-butane (1) |
| 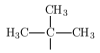 | 0.0402 | 1.6701 | –2.547 | –2.358 | "$(CH_3)_3$–C–" | neopentane (1) |
|  | –0.0688 | –3.2665 | –3.357 | –7.650 | "–CH($CH_3$)–CH($CH_3$)–" | 2,3-dimethylbutane (1) |
|  | –0.1090 | –2.7240 | –1.332 | –3.400 | "–CH($CH_3$)–C$(CH_3)_2$–" | 2,2,3-trimethylpentane (1) |
|  | –0.1740 | –7.9255 | 24.201 | 24.421 | "–C$(CH_3)_2$–C$(CH_3)_2$–" | 2,2,3,3-tetramethylpentane (1) |
|  | 0.6728 | 5.8265 | 121.088 | 113.201 | "ring of 3 carbons" | cyclopropane (1) |
|  | 0.5112 | 4.2086 | 104.566 | 103.366 | "ring of 4 carbons" | cyclobutane (1) |
|  | 0.3083 | 1.7362 | 61.561 | 48.719 | "ring of 5 carbons" | cyclopentane (1) |
|  | 0.0434 | 0.0310 | 15.247 | –59.338 | "ring of 6 carbons" | cyclohexane (1) |

*Continues on next page*

| Second-order group (SOG) | Contribution | | | | UNIFAC notation [2] | Sample group assignment (occurrences) |
|---|---|---|---|---|---|---|
| | $m$ [–] | $m\sigma^3$ [Å$^3$] | $m\epsilon/k$(I) [K] | $m\epsilon/k$(II) [K] | | |
|  | 0.1366 | –2.8849 | 77.742 | 56.390 | ”ring of 7 carbons” | cycloheptane (1) |
| 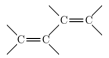 | –0.1106 | -1.9186 | –23.002 | –14.845 | ”–C=CC=C–” | 1,3-butadiene (1) |
|  | 0.0151 | 0.2645 | 5.079 | 5.411 | ”$CH_3$–C=” | *i*-butene (2) |
|  | –0.0363 | 1.1423 | –4.439 | –2.454 | ”–$CH_2$–C=” | 1-butene (1) |
|  (X = H or C) | 0.0733 | –1.8595 | –4.958 | –7.826 | ”–C{H or C}–C=” | 3-methyl-1-butene (1) |
| 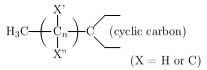 (cyclic carbon) (X = H or C) | –0.1372 | 1.6713 | 11.267 | 69.087 | ”string in cyclic” | ethylcyclohexane (1) |
|  | 0.3060 | 6.0822 | 36.490 | 29.676 | ”>CHCHO” | 2-methyl butyraldehyde (1) |
| 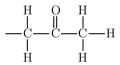 | –0.0347 | –0.7783 | –1.975 | 12.985 | ”$CH_3$(CO)$CH_2$–” | 2-pentanone (1) |
| 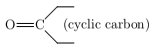 (cyclic carbon) | 0.0060 | 0.1356 | –26.275 | –19.128 | ”C(cyclic)==O” | cyclopentanone (1) |

*Continues on next page*

| Second-order group (SOG) | Contribution | | | | UNIFAC notation [2] | Sample group assignment (occurrences) |
|---|---|---|---|---|---|---|
| | $m$ [–] | $m\sigma^3$ [Å$^3$] | $m\epsilon/k$(I) [K] | $m\epsilon/k$(II) [K] | | |
|  (X = H or C) | 0.0787 | –1.8520 | –12.880 | –8.497 | "$CH_3$(CO)OC{H or C}<" | *i*-butyric acid (1) |
|  | 0.0590 | 2.8874 | 55.434 | 65.891 | "(CO)C{$H_2$}COO" | ethyl acetoacetate (1) |
|  | –0.1159 | 2.9321 | –66.568 | –77.330 | "(CO)O(CO)" | propanoic anhydride (3) |
|  | –0.2367 | –1.0993 | –11.176 | –12.973 | "ACHO" | benzaldehyde (1) |
|  | –0.0532 | 0.6848 | –22.544 | –29.335 | "ACBr" | bromotoluene (1) |
|  | –0.0645 | –0.0215 | –17.376 | –12.152 | "ACCOO" | benzoic acid ethyl ester (1) |
|  | –0.0137 | 0.9180 | 4.161 | 4.377 | "AC($ACH_m$)$_2$AC($ACH_n$)$_2$" | benzoic acid ethyl ester (1) |
|  (cyclic structure) | 0.3026 | 4.5682 | 207.807 | 218.908 | "O(cyclic)–C(cyclic)=O" | diketene (3) |
|  (cyclic structure) | 0.2089 | –3.6855 | 121.645 | 113.201 | "–S–(cyclic)" | tetrahydrothiophene (1) |

Table C.3: Statistical results with the updated GC method implemented in the sPC-SAFT EoS and comparison with the proposed GC schemes in Tables 6.3 and 6.4 (this work = t.w.).

| Parameter | $N_{DP}$ | Std. dev.[a] | | AAE[a] | | AAD[a] [%] | |
|---|---|---|---|---|---|---|---|
| | | FOG | FOG+SOG | FOG | FOG+SOG | FOG | FOG+SOG |
| $m$ | 423 | 0.28 | 0.27 | 0.19 | 0.18 | 5.20 | 4.72 |
| $m$ (t.w.) | 399 | 0.27 | 0.26 | 0.19 | 0.18 | 5.11 | 4.54 |
| $m\sigma^3$ | 422 | 6.46 | 6.30 | 3.67 | 3.42 | 1.68 | 1.55 |
| $m\sigma^3$ (t.w.) | 399 | 4.11 | 3.94 | 2.77 | 2.55 | 1.38 | 1.25 |
| $m\epsilon/k$ (I) | 423 | 40.9 | 29.5 | 24.5 | 20.4 | 2.52 | 2.10 |
| $m\epsilon/k$ (II) | 424 | 46.2 | 38.6 | 26.9 | 24.4 | 2.76 | 2.52 |
| $m\epsilon/k$ (t.w.) | 399 | 41.7 | 36.6 | 31.1 | 27.8 | 3.26 | 2.87 |

[a] Std. dev. $= \sqrt{\sum \left(X^{est} - X^{exp}\right) / \left(N_{DP} - 1\right)}$; AAE $= (1/N_{DP}) \sum \left|X^{est} - X^{exp}\right|$; AAD $= (1/N_{DP}) \sum \left(\left|X^{est} - X^{exp}\right| / X^{exp}\right) 100\,\%$. $N_{DP}$ is the number of experimental data points; $X^{est}$ is the estimated value of the property $X$, and $X^{exp}$ is the experimental value of the property $X$.

The comparison of statistical results from the updated and proposed GC schemes in Table C.3 reveals small deteriorations of the three overall statistical indicators of $m$ and $m\sigma^3$ when using the extended compound database for the linear regression. On the other hand, the statistical indicators for $m\epsilon/k$ have generally improved; especially for Approach (I). As discussed in Section C.1.1, the accuracy of $\epsilon/k$ is of particular importance to the performance of the GC sPC-SAFT EoS, and the obtained results, hence, encourage further testing of the model using the currently updated GC schemes.

Figures C.2 and C.3 show scatter plots of the updated GC estimated parameters of molecules from the extended database in terms of linear correlations and % deviations from corresponding experimental reference values from DIPPR [1]. The reader is reminded that Approaches (I) and (II) share the values of $m$ and $\sigma$ in Figure C.2, while different values of $\epsilon/k$ are obtained, as shown in Figure C.3.

The linear correlations and % deviations of $m$ and $\sigma$ are similar to those obtained for the original approach outlined in Section 6.4 (see the scatter plots in Figure 6.2 on page 144). The ranges marked by dashed lines in Figure C.2 (right) contain 89.6 and 97.6 % of the datapoints for $m$ and $m\sigma^3$ respectively, which is comparable to the corresponding values of 90.2 and 98.2 % obtained with the original approach in Figure 6.2, and consistent with the results in Tabel C.3 above.

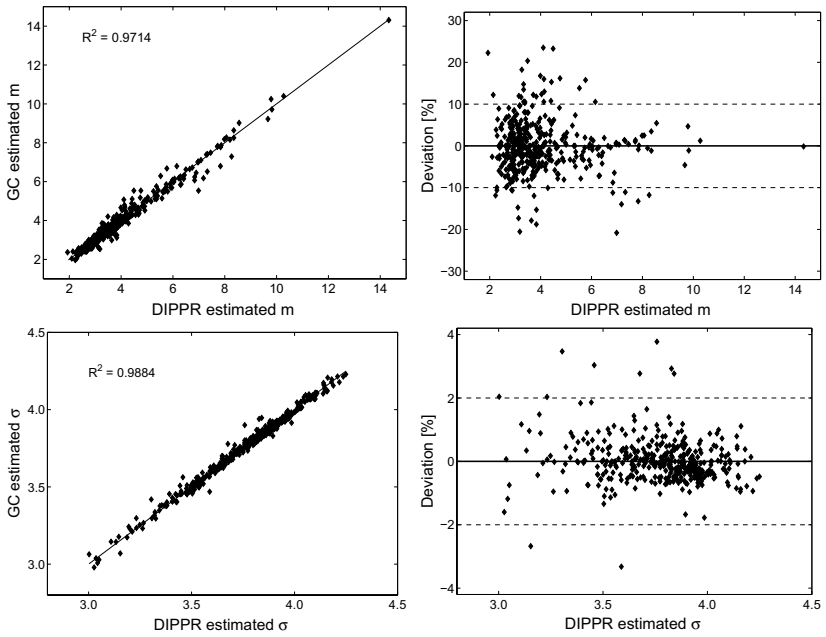


Figure C.2: Scatter plots showing linear correlations (left) and % deviations (right) of GC- vs. DIPPR-estimated parameters: $m$ (top) and $\sigma$ (bottom) using an extended compound database. Dashed lines (right) mark ranges of deviating datapoints and are used to compare different GC approaches; see text.

The revision and extension of the compound database has lead to an improvement of the linear correlation of $\epsilon/k$ and % deviation from DIPPR estimated parameters compared to the original approach in Figure 6.2. This can be seen from the values of $R^2$, which yield 0.9686 and 0.9578 for Approach (I) and (II) respectively, compared to $R^2 = 0.9152$ with the original approach. Moreover, 93.3 and 90.2 % of the datapoints applied in Approach (I) and (II) respectively, lie within the ranges of the dashed horisontal lines. Only 83.9 % of the datapoints used with the original approach revealed the same low deviation of $<5$ %.

Based on these observations, the newly proposed approaches are expected to perform somewhat better than the original approach.

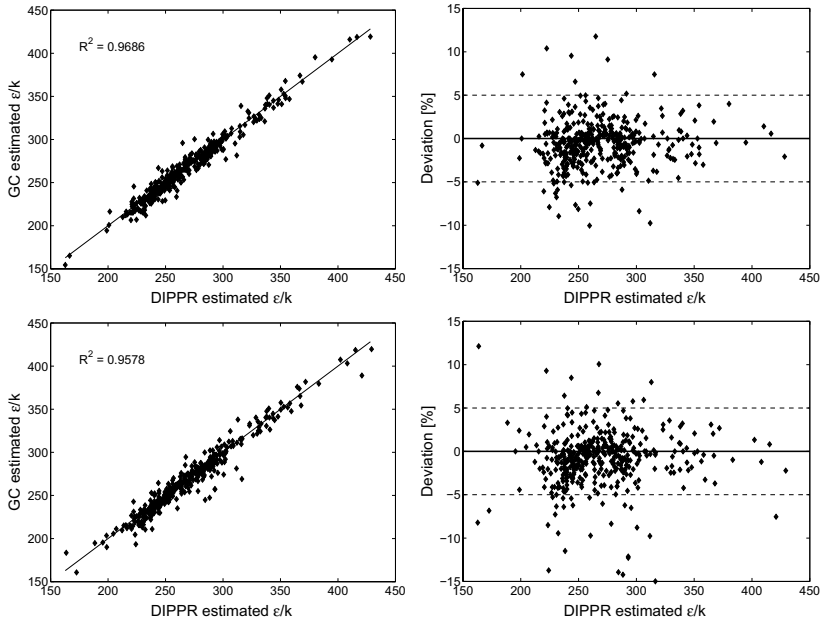


Figure C.3: Scatter plots showing linear correlations (left) and % deviations (right) of GC- vs. DIPPR-estimated PC-SAFT parameters $\epsilon/k$ using an extended compound database (Approach I, top), and an extended compound database with the updated methodology from Figure C.1 (Approach II, bottom). Dashed lines (right) mark ranges of deviating datapoints and are used to compare different GC approaches; see text.

### C.2.1 Comparisons of $\epsilon/k$ and Predicted $P^{sat}$ and $\rho$

#### C.2.1.1 $n$-Alkanes

Table C.4 shows estimated PC-SAFT parameters for various $n$-alkanes obtained from both directly fitting to data from DIPPR [1] and by using Approaches (I) and (II). Moreover, model predictions are compared in terms of AAD % to values of $P^{sat}$ and $\rho$ also drawn from DIPPR. Figure C.4 contains a graphical comparison of $\epsilon/k$ of Approaches (I) and (II), while Figure C.5 shows AAD % of $P^{sat}$ and $\rho$ for $n$-alkanes with lower carbon numbers.

Table C.4: GC estimated PC-SAFT parameters for various $n$-alkanes using Approaches (I) and (II), and the resulting AAD % of $P^{sat}$ and $\rho$ predictions when compared to values from DIPPR [1].

| $n$-Alkane | GC estimated parameters | | | $T$ range | AAD [%] | AAD [%] |
|---|---|---|---|---|---|---|
| | $m$ [–] | $\sigma$ [Å] | $\epsilon/k$ [K] | [K] | $P^{sat}$ | $\rho$ |
| *DIPPR fitted* | | | | | | |
| $n$-Pentane | 2.6896 | 3.7729 | 231.2 | 143–469 | 1.5 | 0.8 |
| $n$-Hexane | 3.0576 | 3.7983 | 236.77 | 177–503 | 0.3 | 0.7 |
| $n$-Heptane | 3.4831 | 3.8049 | 238.4 | 182–623 | 0.3 | 2.1 |
| $n$-Octane | 3.8176 | 3.8373 | 242.78 | 216–569 | 0.8 | 1.6 |
| $n$-Nonane | 4.2079 | 3.8448 | 244.51 | 219–595 | 0.9 | 0.3 |
| $n$-Decane | 4.6627 | 3.8384 | 243.87 | 243–617 | 0.2 | 1.2 |
| *Approach (I)* | | | | | | |
| $n$-Pentane | 2.4309 | 3.8623 | 229.00 | 240–380 | 107.8 | 1.2 |
| $n$-Hexane | 2.8141 | 3.8766 | 233.90 | 260–450 | 77.8 | 1.9 |
| $n$-Heptane | 3.1973 | 3.8877 | 237.62 | 280–480 | 67.0 | 1.5 |
| $n$-Octane | 3.5805 | 3.8962 | 240.55 | 290–510 | 60.0 | 1.0 |
| $n$-Nonane | 3.9638 | 3.9030 | 242.91 | 300–530 | 53.5 | 0.8 |
| $n$-Decane | 4.347 | 3.9087 | 244.85 | 310–550 | 49.0 | 0.3 |
| $n$-Undecane | 4.7302 | 3.9134 | 246.48 | 320–570 | 42.9 | 0.3 |
| $n$-Dodecane | 5.1134 | 3.9174 | 247.87 | 350–590 | 34.3 | 0.4 |
| $n$-Tridecane | 5.4967 | 3.9208 | 249.06 | 340–580 | 33.4 | 1.1 |
| $n$-Tetradecane | 5.8799 | 3.9238 | 250.09 | 350–610 | 27.8 | 0.8 |
| $n$-Pentadecane | 6.2631 | 3.9264 | 251.00 | 360–610 | 23.6 | 1.0 |
| $n$-Hexadecane | 6.6463 | 3.9287 | 251.81 | 370–630 | 18.9 | 1.0 |
| $n$-Heptadecane | 7.0296 | 3.9307 | 252.52 | 370–630 | 17.6 | 0.9 |
| $n$-Octadecane | 7.4128 | 3.9326 | 253.17 | 380–660 | 11.5 | 1.0 |
| $n$-Nonadecane | 7.796 | 3.9342 | 253.75 | 390–680 | 7.2 | 1.2 |
| $n$-Eicosane | 8.1793 | 3.9357 | 254.27 | 390–680 | 5.3 | 1.2 |
| $n$-Docosane | 8.9457 | 3.9383 | 255.19 | 410–690 | 4.0 | 1.1 |
| $n$-Tricosane | 9.3289 | 3.9395 | 255.60 | 410–690 | 4.5 | 1.9 |
| $n$-Tetracosane | 9.7122 | 3.9405 | 255.96 | 410–690 | 8.6 | 2.3 |
| *Approach (II)* | | | | | | |
| $n$-Pentane | 2.4309 | 3.8623 | 226.27 | 240–420 | 133.6 | 1.9 |
| $n$-Hexane | 2.8141 | 3.8766 | 231.52 | 260–450 | 95.3 | 2.8 |
| $n$-Heptane | 3.1973 | 3.8877 | 235.50 | 275–480 | 82.0 | 2.2 |
| $n$-Octane | 3.5805 | 3.8962 | 238.63 | 290–500 | 73.6 | 1.7 |
| $n$-Nonane | 3.9638 | 3.9030 | 241.15 | 310–520 | 66.1 | 1.3 |
| $n$-Decane | 4.347 | 3.9087 | 243.24 | 310–540 | 60.6 | 0.7 |
| $n$-Undecane | 4.7302 | 3.9134 | 244.98 | 320–570 | 53.7 | 0.5 |
| $n$-Dodecane | 5.1134 | 3.9174 | 246.46 | 350–590 | 43.7 | 0.3 |
| $n$-Tridecane | 5.4967 | 3.9208 | 247.74 | 340–580 | 43.3 | 0.7 |
| $n$-Tetradecane | 5.8799 | 3.9238 | 248.85 | 350–610 | 36.7 | 0.4 |
| $n$-Pentadecane | 6.2631 | 3.9264 | 249.82 | 360–610 | 32.0 | 0.6 |
| $n$-Hexadecane | 6.6463 | 3.9287 | 250.68 | 370–630 | 26.7 | 0.7 |
| $n$-Heptadecane | 7.0296 | 3.9307 | 251.45 | 370–630 | 25.4 | 0.6 |

*Continues on next page*

| $n$-Alkane | GC estimated parameters | | | $T$ range | AAD [%] | AAD [%] |
|---|---|---|---|---|---|---|
| | $m$ [–] | $\sigma$ [Å] | $\epsilon/k$ [K] | [K] | $P^{sat}$ | $\rho$ |
| $n$-Octadecane | 7.4128 | 3.9326 | 252.13 | 380–660 | 18.6 | 0.6 |
| $n$-Nonadecane | 7.796 | 3.9342 | 252.76 | 390–680 | 13.8 | 0.8 |
| $n$-Eicosane | 8.1793 | 3.9357 | 253.32 | 390–680 | 11.8 | 0.9 |
| $n$-Docosane | 8.9457 | 3.9383 | 254.27 | 410–690 | 2.3 | 0.9 |
| $n$-Tricosane | 9.3289 | 3.9395 | 254.73 | 410–690 | 1.4 | 1.5 |
| $n$-Tetracosane | 9.7122 | 3.9405 | 255.12 | 410–690 | 3.0 | 2.1 |

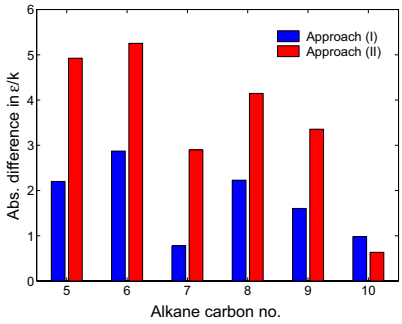


Figure C.4: Comparison of $\epsilon/k$ from Approaches (I) and (II) with DIPPR fitted values for $n$-alkanes with lower carbon numbers. Data are from Table C.4.

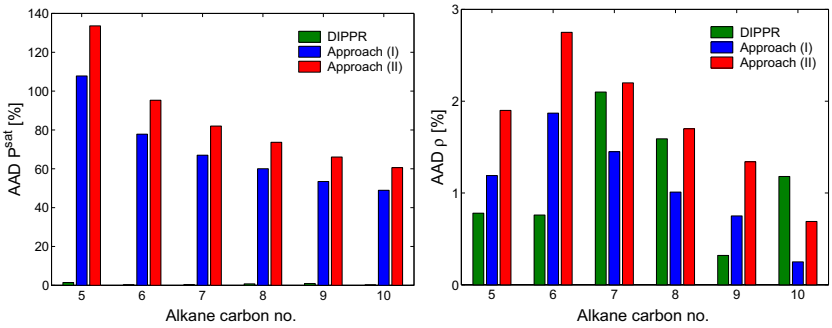


Figure C.5: AAD % of experimental [1] and calculated $P^{sat}$ and $\rho$ for $n$-alkanes with lower carbon numbers using DIPPR fitted parameters and parameters from Approaches (I) and (II). Data are from Table C.4.

The general trend is observed that deviations from DIPPR based values are reduced with increasing $n$-alkane carbon number. This trend is particularly pronounced for $P^{sat}$ predictions, as shown in Figure C.5 (left), where AAD >100 % is obtained for $n$-pentane, but falling to approximately half the value for $n$-decane. It is expected that this trend will continue with carbon numbers >10. Figure C.4 shows that $\epsilon/k$ values are more accurately determined with Approach (I) when the alkane carbon number is low. At higher numbers, similar values of $\epsilon/k$ are typically obtained with the two approaches, as can be observed in Table C.4. Predictions of $\rho$ by Approaches (I) and (II) yield similar AAD % as the DIPPR based parameters, which indicates that these values are probably accurate to the limit of the underlying experimental uncertainties.

Based on the investigated data, it is concluded that for $n$-alkane predictions, Approach (I) displays more promising performance than Approach (II).

#### C.2.1.2 1-Alkenes

Table C.5 shows estimated PC-SAFT parameters for 1-alkenes of increasing carbon number obtained from directly fitting to data from DIPPR [1] and by using Approaches (I) and (II). Model predictions are compared in terms of AAD % to values of $P^{sat}$ and $\rho$ also drawn from DIPPR. Figure C.6 compares $\epsilon/k$ from Approaches (I) and (II), while Figure C.7 shows AAD % of $P^{sat}$ and $\rho$ for the investigated 1-alkanes.

Table C.5: GC estimated PC-SAFT parameters for 1-alkenes using Approaches (I) and (II), and the resulting AAD % of $P^{sat}$ and $\rho$ predictions when compared to values from DIPPR [1].

| 1-Alkene | GC estimated parameters | | | $T$ range | AAD [%] | AAD [%] |
|---|---|---|---|---|---|---|
| | $m$ [–] | $\sigma$ [Å] | $\epsilon/k$ [K] | [K] | $P^{sat}$ | $\rho$ |
| *DIPPR fitted* | | | | | | |
| 1-Butene | 2.2864 | 3.6431 | 222. | 87–419 | 0.7 | 0.5 |
| 1-Pentene | 2.6006 | 3.7399 | 231.99 | 108–464 | 0.3 | 1.0 |
| 1-Hexene | 2.9853 | 3.7753 | 236.81 | 133–504 | 0.4 | 1.2 |
| 1-Heptene | 3.3637 | 3.7898 | 240.62 | 174–534 | 1.0 | 1.0 |
| 1-Octene | 3.7424 | 3.8133 | 243.02 | 171–567 | 0.8 | 0.8 |
| 1-Nonene | 3.99 | 3.8746 | 249.27 | 232–592 | 1.0 | 0.6 |
| 1-Decene | 4.37 | 3.8908 | 250.35 | 207–607 | 1.8 | 0.9 |
| *Approach (I)* | | | | | | |
| 1-Butene | 2.0257 | 3.8127 | 229.55 | 230–375 | 28.2 | 2.8 |
| 1-Pentene | 2.409 | 3.8379 | 235.17 | 250–410 | 26.9 | 1.9 |
| 1-Hexene | 2.7922 | 3.8560 | 239.26 | 280–450 | 27.2 | 1.6 |
| 1-Heptene | 3.1754 | 3.8696 | 242.37 | 290–480 | 25.2 | 1.7 |
| 1-Octene | 3.5587 | 3.8801 | 244.79 | 320–510 | 20.5 | 1.9 |
| 1-Nonene | 3.9419 | 3.8887 | 246.76 | 310–530 | 17.9 | 1.4 |

*Continues on next page*

| 1-Alkene | GC estimated parameters | | | $T$ range | AAD [%] | AAD [%] |
|---|---|---|---|---|---|---|
| | $m$ [–] | $\sigma$ [Å] | $\epsilon/k$ [K] | [K] | $P^{sat}$ | $\rho$ |
| 1-Decene | 4.3251 | 3.8957 | 248.37 | 330–550 | 14.7 | 0.7 |
| *Approach (II)* | | | | | | |
| 1-Butene | 2.0257 | 3.8127 | 229.54 | 230–375 | 31.2 | 2.8 |
| 1-Pentene | 2.409 | 3.8379 | 235.14 | 250–410 | 29.3 | 1.9 |
| 1-Hexene | 2.7922 | 3.8560 | 239.20 | 280–450 | 27.5 | 1.6 |
| 1-Heptene | 3.1754 | 3.8696 | 242.29 | 290–480 | 25.6 | 1.8 |
| 1-Octene | 3.5587 | 3.8801 | 244.70 | 320–510 | 21.0 | 1.9 |
| 1-Nonene | 3.9419 | 3.8887 | 246.65 | 310–530 | 20.4 | 1.5 |
| 1-Decene | 4.3251 | 3.8957 | 248.26 | 330–550 | 17.3 | 0.8 |

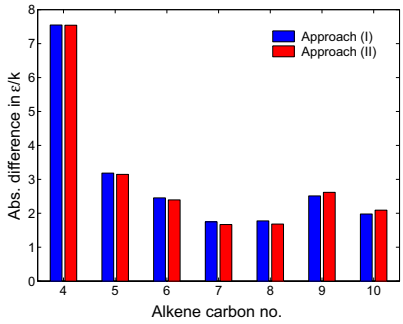


Figure C.6: Comparison of $\epsilon/k$ from Approaches (I) and (II) with DIPPR fitted values for several 1-alkenes. Data are from Table C.5.

Figures C.6 and C.7 display very similar performance of Approaches (I) and (II). There is a substantial absolute difference in $\epsilon/k$ for the smallest 1-alkene (1-butene), but, otherwise, the absolute differences are fairly constant with increasing carbon numbers in Figure C.6. For $P^{sat}$ predictions in Figure C.7 (left), the investigated 1-alkenes show the same trend of increasing accuracy of the two approaches with increasing carbon number as observed for $n$-alkanes in Section C.2.1.1. Predictions of $\rho$ by Approaches (I) and (II) yield slightly higher AAD % than the DIPPR based parameters, but are still within a satisfactory accuracy.

### C.2.1.3 1-Alkynes

Table C.6 presents estimated PC-SAFT parameters of four 1-alkynes with increasing carbon number obtained from direct fitting to data from DIPPR [1] and by using Approaches (I) and (II). Model predictions are compared in terms of AAD % to values of $P^{sat}$ and $\rho$ also drawn from DIPPR. Predicted values of $\epsilon/k$ from Approaches (I) and (II) are

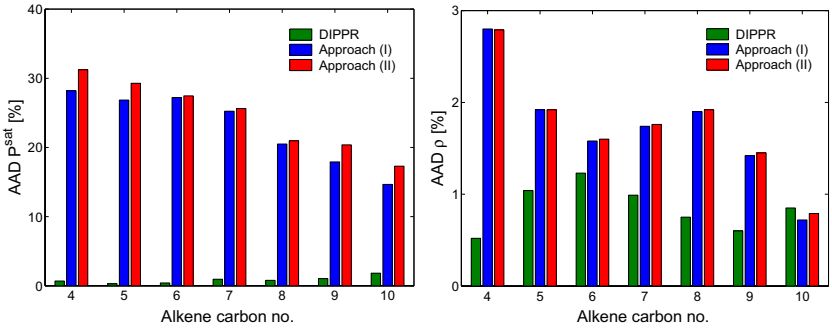


Figure C.7: AAD % of experimental [1] and calculated $P^{sat}$ and $\rho$ for 1-alkenes with increasing carbon number using DIPPR fitted parameters and parameters from Approaches (I) and (II). Data are from Table C.5.

compared in Figure C.8, while Figure C.9 presents AAD % of $P^{sat}$ and $\rho$ for the four 1-alkynes.

Table C.6: GC estimated PC-SAFT parameters for 1-alkynes using Approaches (I) and (II), and the resulting AAD % of $P^{sat}$ and $\rho$ predictions when compared to values from DIPPR [1].

| 1-Alkyne | GC estimated parameters | | | $T$ range | AAD [%] | AAD [%] |
|---|---|---|---|---|---|---|
| | $m$ [–] | $\sigma$ [Å] | $\epsilon/k$ [K] | [K] | $P^{sat}$ | $\rho$ |
| *DIPPR fitted* | | | | | | |
| 1-Pentyne | 2.8902 | 3.5105 | 228.48 | 245–430 | 0.8 | 2.8 |
| 1-Hexyne | 3.1555 | 3.5961 | 237.56 | 260–465 | 0.8 | 0.1 |
| 1-Heptyne | 3.2242 | 3.7744 | 252.76 | 280–490 | 1.6 | 0.7 |
| 1-Octyne | 3.7647 | 3.7327 | 247.34 | 290–510 | 1.1 | 0.2 |
| *Approach (I)* | | | | | | |
| 1-Pentyne | 2.5814 | 3.6409 | 240.98 | 255–430 | 10.4 | 2.8 |
| 1-Hexyne | 2.9646 | 3.6862 | 244.08 | 260–460 | 4.6 | 0.9 |
| 1-Heptyne | 3.3478 | 3.7204 | 246.47 | 280–500 | 5.4 | 0.2 |
| 1-Octyne | 3.7311 | 3.7471 | 248.37 | 300–500 | 0.8 | 0.2 |
| *Approach (II)* | | | | | | |
| 1-Pentyne | 2.5814 | 3.6409 | 240.22 | 255–430 | 13.5 | 2.6 |
| 1-Hexyne | 2.9646 | 3.6862 | 243.36 | 260–460 | 3.7 | 0.8 |
| 1-Heptyne | 3.3478 | 3.7204 | 245.84 | 280–500 | 4.1 | 0.2 |
| 1-Octyne | 3.7311 | 3.7471 | 247.78 | 300–500 | 2.0 | 0.3 |

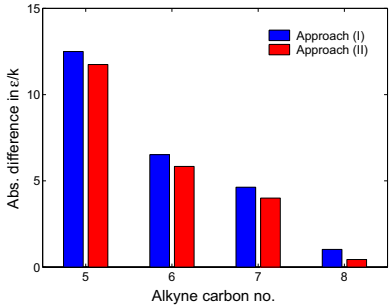


Figure C.8: Comparison of $\epsilon/k$ from Approaches (I) and (II) with DIPPR fitted values for four 1-alkynes. Data are from Table C.6.

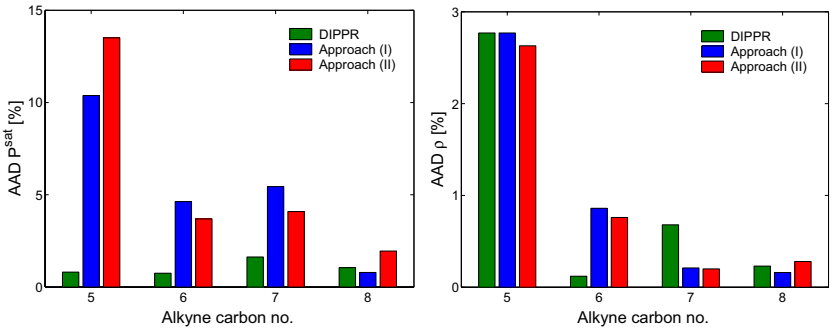


Figure C.9: AAD % of experimental [1] and calculated $P^{sat}$ and $\rho$ for four 1-alkynes with increasing carbon number using DIPPR fitted parameters and parameters from Approaches (I) and (II). Data are from Table C.6.

Predictions of $P^{sat}$ and $\rho$ of the four investigated 1-alkynes generally exhibit low deviations from experiments; especially when compared to the corresponding predictions of $n$-alkanes and 1-alkenes in Section C.2.1.1 and C.2.1.2, respectively. Like for $n$-alkanes, AAD % of $\rho$ with Approaches (I) and (II) are within the same range as predictions based on the DIPPR fitted parameters. Approach (II) yields values of $\epsilon/k$ that are slightly closer to the DIPPR-fitted values than Approach (I), which is opposite $n$-alkanes and 1-alkenes (see Figures C.4 and C.6). Again, there is a clear trend that deviations decline with increasing carbon number.

#### C.2.1.4 Acetates

Table C.7 provides estimated PC-SAFT parameters of several alkyl acetates with increasing carbon number obtained from direct fitting to data from DIPPR [1] and by using Approaches (I) and (II). Model predictions are compared in terms of AAD % to values of $P^{sat}$ and $\rho$ also drawn from DIPPR. Figure C.10 compares predicted $\epsilon/k$ from Approaches (I) and (II). Figure C.11 shows AAD % of $P^{sat}$ and $\rho$ for the investigated acetates.

Table C.7: GC estimated PC-SAFT parameters for alkyl acetates using Approaches (I) and (II), and the resulting AAD % of $P^{sat}$ and $\rho$ predictions when compared to values from DIPPR [1].

| Acetate | GC estimated parameters | | | $T$ range | AAD [%] | AAD [%] |
|---|---|---|---|---|---|---|
| | $m$ [–] | $\sigma$ [Å] | $\epsilon/k$ [K] | [K] | $P^{sat}$ | $\rho$ |
| *DIPPR fitted* | | | | | | |
| Propyl acetate | 3.7861 | 3.4227 | 235.76 | 290–543 | 1.1 | 1.2 |
| Butyl acetate | 3.9808 | 3.5427 | 242.52 | 290–510 | 2.0 | 1.3 |
| Pentyl acetate | 4.7077 | 3.4729 | 243.49 | 205–595 | 0.6 | 0.2 |
| Hexyl acetate | 4.8447 | 3.5834 | 241.42 | 195–615 | 0.8 | 0.4 |
| Heptyl acetate | 5.3796 | 3.5874 | 239.08 | 225–635 | 1.5 | 0.9 |
| Octyl acetate | 5.9596 | 3.5603 | 236.43 | 235–650 | 0.9 | 0.3 |
| Nonyl acetate | 6.8356 | 3.495 | 235.63 | 250–660 | 1.2 | 0.3 |
| Decyl acetate | 6.8956 | 3.5745 | 234.94 | 260–675 | 3.6 | 0.2 |
| *Approach (I)* | | | | | | |
| Propyl acetate | 3.7691 | 3.4018 | 230.58 | 280–495 | 33.9 | 0.2 |
| Butyl acetate | 4.1524 | 3.4619 | 233.75 | 280–500 | 20.8 | 0.6 |
| Pentyl acetate | 4.5356 | 3.5103 | 236.39 | 300–540 | 13.2 | 0.3 |
| Hexyl acetate | 4.9188 | 3.5502 | 238.61 | 310–550 | 6.5 | 0.7 |
| Heptyl acetate | 5.302 | 3.5836 | 240.52 | 320–570 | 3.8 | 1.8 |
| Octyl acetate | 5.6853 | 3.6119 | 242.16 | 326–580 | 2.4 | 1.3 |
| Nonyl acetate | 6.0685 | 3.6364 | 243.60 | 335–590 | 14.2 | 3.2 |
| Decyl acetate | 6.4517 | 3.6577 | 244.87 | 340–610 | 14.2 | 1.8 |
| *Approach (II)* | | | | | | |
| Propyl acetate | 3.7691 | 3.4018 | 229.27 | 280–495 | 42.4 | 0.6 |
| Butyl acetate | 4.1524 | 3.4619 | 232.54 | 280–500 | 27.8 | 0.4 |
| Pentyl acetate | 4.5356 | 3.5103 | 235.26 | 300–540 | 19.1 | 0.2 |
| Hexyl acetate | 4.9188 | 3.5502 | 237.56 | 310–550 | 11.8 | 0.3 |
| Heptyl acetate | 5.302 | 3.5836 | 239.53 | 320–570 | 9.5 | 1.6 |
| Octyl acetate | 5.6853 | 3.6119 | 241.22 | 326–580 | 4.2 | 1.0 |
| Nonyl acetate | 6.0685 | 3.6364 | 242.71 | 335–590 | 9.8 | 2.8 |
| Decyl acetate | 6.4517 | 3.6577 | 244.02 | 340–610 | 9.9 | 1.3 |

The acetates display a somewhat different behavior from the $n$-alkanes, 1-alkenes, and 1-alkynes. Figure C.10 shows a decreasing absolute difference of predicted $\epsilon/k$ of Approaches (I) and (II) with increasing alkyl carbon numbers going from 3 to 7, but the absolute differences begin to increase again at alkyl carbon numbers >7. Moreover,

Approach (I) yields slightly lower differences for the lower carbon numbers (3 to 6), while Approach (II) provides the smallest differences above carbon number 6. A similar behavior is observed for predicted values of $P^{sat}$ in Figure C.11 (left). Here, the lowest deviation is observed at carbon number 8 above which, Approach (I) begins to yield more accurate predictions than Approach (II). Predictions of $\rho$ are more accurate when the alkyl chain contains fewer carbon atoms. From carbon numbers >7 significant differences from DIPPR based predictions are observed with Approach (I) yielding the largest AAD.

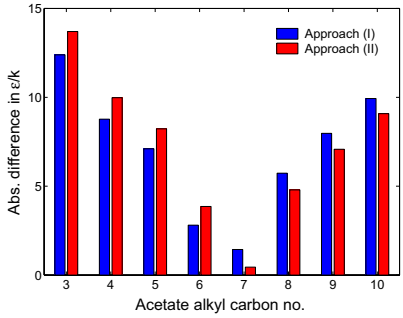


Figure C.10: Comparison of $\epsilon/k$ from Approaches (I) and (II) with DIPPR fitted values for several alkyl acetates. Data are from Table C.7.

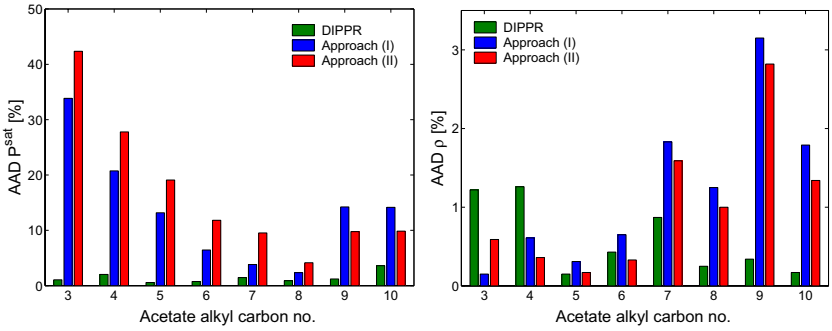


Figure C.11: AAD % of experimental [1] and calculated $P^{sat}$ and $\rho$ for several alkyl acetates of increasing alkyl carbon number using DIPPR fitted parameters and parameters from Approaches (I) and (II). Data are from Table C.7.

In general, the alkyl acetate predictions indicate that some proximity effects operates within the generic molecular structure that is most accurately captured by the GC methodology when the alkyl chain contains 6–8 carbon atoms.

#### C.2.1.5 Mercaptans

Estimated PC-SAFT parameters of some alkyl mercaptans, also known as thiols, with increasing carbon numbers are presented in Table C.8. The parameter sets are obtained from direct fitting to data from DIPPR [1] and by using Approaches (I) and (II). Model predictions are compared in terms of AAD % to values of $P^{sat}$ and $\rho$ also drawn from DIPPR. Predicted values of $\epsilon/k$ from Approaches (I) and (II) are compared in Figure C.12, while Figure C.13 provides AAD % of $P^{sat}$ and $\rho$.

Table C.8: GC estimated PC-SAFT parameters for alkyl mercaptans using Approaches (I) and (II), and the resulting AAD % of $P^{sat}$ and $\rho$ predictions when compared to values from DIPPR [1].

| Mercaptan | GC estimated parameters | | | $T$ range | AAD [%] | AAD [%] |
|---|---|---|---|---|---|---|
| | $m$ [–] | $\sigma$ [Å] | $\epsilon/k$ [K] | [K] | $P^{sat}$ | $\rho$ |
| *DIPPR fitted* | | | | | | |
| Propyl mercaptan | 2.4564 | 3.654 | 276.82 | 285–482 | 0.9 | 1.0 |
| Butyl mercaptan | 2.7253 | 3.7499 | 281.41 | 285–513 | 0.6 | 1.0 |
| Pentyl mercaptan | 3.1788 | 3.7578 | 275.26 | 300–538 | 0.9 | 0.8 |
| Hexyl mercaptan | 3.4471 | 3.8209 | 278.9 | 315–560 | 0.6 | 0.4 |
| Heptyl mercaptan | 3.8330 | 3.8372 | 276.75 | 330–580 | 0.7 | 0.9 |
| Octyl mercaptan | 4.1432 | 3.8728 | 277.22 | 335–600 | 0.6 | 0.6 |
| Nonyl mercaptan | 4.6257 | 3.8494 | 272.37 | 340–610 | 0.6 | 0.9 |
| Decyl mercaptan | 5.0016 | 3.8442 | 271.7 | 350–626 | 0.2 | 0.5 |
| *Approach (I)* | | | | | | |
| Propyl mercaptan | 2.3341 | 3.6850 | 278.53 | 285–482 | 26.8 | 1.4 |
| Butyl mercaptan | 2.7173 | 3.7273 | 276.62 | 285–513 | 22.1 | 0.8 |
| Pentyl mercaptan | 3.1005 | 3.7585 | 275.18 | 300–538 | 18.5 | 1.7 |
| Hexyl mercaptan | 3.4837 | 3.7825 | 274.06 | 315–560 | 13.8 | 0.9 |
| Heptyl mercaptan | 3.8670 | 3.8014 | 273.15 | 330–580 | 11.6 | 1.2 |
| Octyl mercaptan | 4.2502 | 3.8168 | 272.42 | 335–600 | 6.9 | 1.3 |
| Nonyl mercaptan | 4.6334 | 3.8296 | 271.80 | 340–610 | 2.9 | 1.4 |
| Decyl mercaptan | 5.0167 | 3.8403 | 271.27 | 350–626 | 0.4 | 0.2 |
| *Approach (II)* | | | | | | |
| Propyl mercaptan | 2.3341 | 3.6850 | 277.93 | 285–482 | 29.2 | 1.2 |
| Butyl mercaptan | 2.7173 | 3.7273 | 276.08 | 285–513 | 24.4 | 0.7 |
| Pentyl mercaptan | 3.1005 | 3.7585 | 274.68 | 300–538 | 20.8 | 1.6 |
| Hexyl mercaptan | 3.4837 | 3.7825 | 273.59 | 315–560 | 15.9 | 0.8 |
| Heptyl mercaptan | 3.8670 | 3.8014 | 272.70 | 330–580 | 13.7 | 1.1 |
| Octyl mercaptan | 4.2502 | 3.8168 | 271.99 | 335–600 | 4.4 | 1.4 |
| Nonyl mercaptan | 4.6334 | 3.8296 | 271.39 | 340–610 | 4.7 | 1.3 |
| Decyl mercaptan | 5.0167 | 3.8403 | 270.88 | 350–626 | 1.9 | 0.2 |

It is not possible to deduce a general trend in the behavior of the absolute differences in $\epsilon/k$ with varying carbon numbers based on Figure C.12. Approach (I) yields marginally lower differences from the DIPPR fitted values than Approach (II) though, with propyl

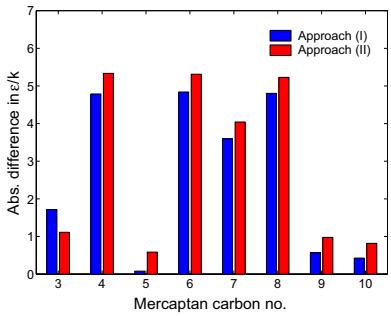


Figure C.12: Comparison of $\epsilon/k$ from Approaches (I) and (II) with DIPPR fitted values for some mercaptans. Data are from Table C.8.

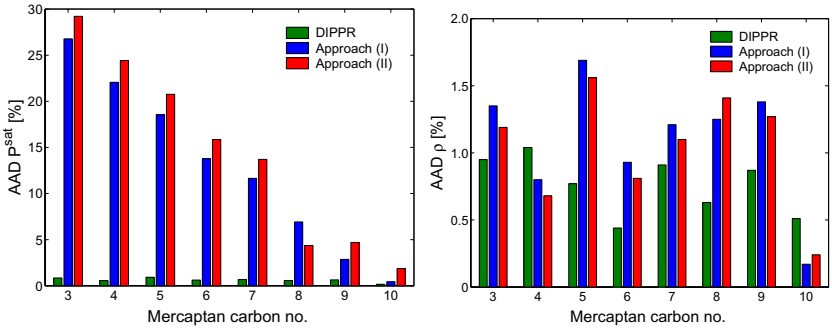


Figure C.13: AAD % of experimental [1] and calculated $P^{sat}$ and $\rho$ for some mercaptans of increasing carbon number using DIPPR fitted parameters and parameters from Approaches (I) and (II). Data are from Table C.8.

mercaptan as the only exception among the investigated mercaptans.

In contrast, a pronounced decrease in AAD of $P^{sat}$ predictions is observed in Figure C.13 with decreasing carbon number. Approach (I) generally yields the highest accuracy. Predictions of $\rho$ exhibit similar low AAD as predictions based on DIPPR fitted parameters.

Based on the current observations, it is recommended to apply Approach (I) to yield the most accurate predictions for alkyl mercaptans.

### C.2.2 Summary of Observations

Approaches (I) and (II) have resulted in improvements of the linear correlations between the GC estimated $\epsilon/k$ parameters and experimental reference values from DIPPR as well as deviations of individual datapoints.

For almost all investigated compounds, AAD of $P^{sat}$ predictions decrease with increasing carbon numbers. The same trend is observed for the absolute differences in $\epsilon/k$. Alkyl acetates are the only exception from this trend, since AAD of $P^{sat}$ and abs. differences of $\epsilon/k$ here begin to increase again with carbon numbers >7–8. Predictions of $\rho$ are typically very accurate and in range of the AAD obtained when predicting $\rho$ using parameter sets obtained from direct fitting to data from DIPPR.

Based on an overall evaluation of the performance of Approaches (I) and (II), the former is generally recommended for more accurate predictions. Since the GC scheme of Approach (I) is based on a slightly larger database of compounds, it is also expected to exhibit similar, or even better, accuracy than the GC scheme proposed in Chapter 6, even though more rigorous testing is required to confirm this.

## References

[1] AIChE J., *DIPPR Table of Physical and Thermodynamic Properties of Pure Compounds*. New York, USA, 1998.

[2] A. Fredenslund, R. L. Jones, and J. M. Prauznitz, "Group-Contribution Estimation of Activity Coefficients in Nonideal Liquid Mixtures," *AIChE J.*, vol. 21, pp. 1086–1099, 1975.

# Appendix D

# Molecular Structures of Complex Compounds

As supplementary information and help to the reader, this appendix presents molecular structures of complex compounds (Table D.1) as well as monomer unit of polymers (Table D.2) investigated in this work.

Table D.1: Molecular structures of investigated complex compounds.

| Compound | Molecular structure | Contained groups (UNIFAC notation) |
|---|---|---|
| Limonene | 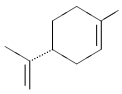 | FOG: 2×$CH_3$, 3×$CH_2$, 1×CH, 1×$CH_2$=C<, 1×–CH=C<<br>SOG: 1×ring of 6 carbons, 1×$CH_3$–C= |
| Cineole | 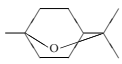 | FOG: 3×$CH_3$, 4×$CH_2$, 1×CH, 2×C, 1×O (except as above)<br>SOG: 1×ring of 6 carbons |
| Methyl benzoate | 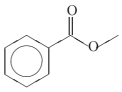 | FOG: 1×$CH_3$, 5×ACH, 1×AC, 1×COO,<br>SOG: 1×ACCOO |
| Ethyl benzoate | 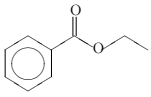 | FOG: 1×$CH_3$, 1×$CH_2$, 5×ACH, 1×AC, 1×COO<br>SOG: 1×ACCOO |
| Propyl benzoate | 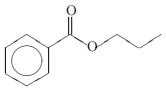 | FOG: 1×$CH_3$, 2×$CH_2$, 5×ACH, 1×AC, 1×COO<br>SOG: 1×ACCOO |

*Continues on next page*

| Compound | Molecular structure | Contained groups (UNIFAC notation) |
|---|---|---|
| Butyl benzoate | 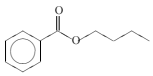 | FOG: 1×$CH_3$, 3×$CH_2$, 5×ACH, 1×AC, 1×COO<br>SOG: 1×ACCOO |
| Phenyl acetate | 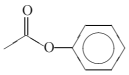 | FOG: 5×ACH, 1×AC, 1×$CH_3$COO |
| Methyl caprylate | 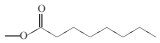 | FOG: 2×$CH_3$, 5×$CH_2$, 1×$CH_2$COO |
| Methyl caprate | 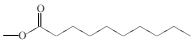 | FOG: 2×$CH_3$, 7×$CH_2$, 1×$CH_2$COO |
| Methyl laurate | 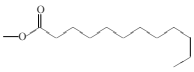 | FOG: 2×$CH_3$, 9×$CH_2$, 1×$CH_2$COO |
| Methyl myristate | 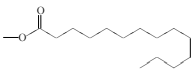 | FOG: 2×$CH_3$, 11×$CH_2$, 1×$CH_2$COO |
| Methyl palmitate | 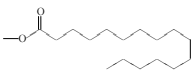 | FOG: 2×$CH_3$, 13×$CH_2$, 1×$CH_2$COO |
| Methyl stearate | 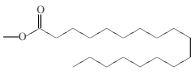 | FOG: 2×$CH_3$, 15×$CH_2$, 1×$CH_2$COO |
| Methyl oleate | 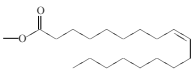 | FOG: 2×$CH_3$, 13×$CH_2$, 1×–CH=CH–, 1×$CH_2$COO<br>SOG: 1×–$CH_2$–C= |
| Dibutyl sulfide | 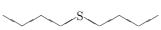 | FOG: 2×$CH_3$, 5×$CH_2$, 1×$CH_2$S |
| Di-*sec*-butyl sulfide | 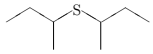 | FOG: 4×$CH_3$, 2×$CH_2$, 1×CH, 1×CHS |

*Continues on next page*

| Compound | Molecular structure | Contained groups (UNIFAC notation) |
|---|---|---|
| *tert*-butyl methyl sulfide |  | FOG: 3×$CH_3$, 1×C, 1×$CH_3S$<br>SOG: 1×$(CH_3)_3$–C– |
| Dihexyl sulfide |  | FOG: 2×$CH_3$, 9×$CH_2$, 1×$CH_2S$ |
| Dioctyl sulfide | 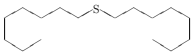 | FOG: 2×$CH_3$, 13×$CH_2$, 1×$CH_2S$ |
| Ethyl phenyl sulfide | 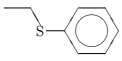 | FOG: 2×$CH_3$, 5×ACH, 1×AC, 1×$CH_2S$ |
| Benzyl phenyl sulfide | 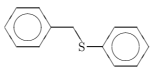 | FOG: 10×ACH, 2×AC, 1×$CH_2S$ |
| Dibenzyl sulfide | 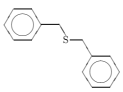 | FOG: 10×ACH, 2×AC, 1×$ACCH_2$, 1×$CH_2S$ |
| Methyl cyclopentane sulfide | 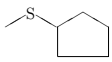 | FOG: 4×$CH_2$, 1×CH, 1×$CH_3S$,<br>SOG: 1×ring of 5 carbons |
| Methyl phenyl sulfide | 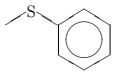 | FOG: 5×ACH, 1×AC, 1×$CH_3S$ |
| Tetralin | 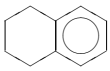 | FOG: 4×$CH_2$, 4×ACH, 2×AC<br>SOG: 1×ring of 6 carbons |
| Biphenyl | 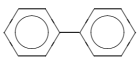 | FOG: 10×ACH, 2×AC |
| Dibenzofuran | 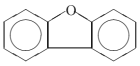 | FOG: 8×ACH, 4×AC, 1×O (except as above)<br>SOG: 1×ring of 5 carbons |

*Continues on next page*

| Compound | Molecular structure | Contained groups (UNIFAC notation) |
|---|---|---|
| Phenanthrene | 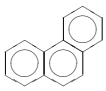 | FOG: 10×ACH, 4×AC<br>SOG: 2×AC(ACH$_m$)$_2$AC(ACH$_n$)$_2$ |
| Acenapthene |  | FOG: 2×CH$_2$, 6×ACH, 4×AC<br>SOG: 1×ring of 5 carbons<br>1×AC(ACH$_m$)$_2$AC(ACH$_n$)$_2$ |
| Benzo[a]pyrene | 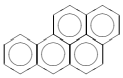 | FOG: 12×ACH, 8×AC<br>SOG: 6×AC(ACH$_m$)$_2$AC(ACH$_n$)$_2$ |

Table D.2: Molecular structures of monomer units of investigated polymers.

| Molecular structures | | | | |
|---|---|---|---|---|
| PMMA | PBMA | PIPMA | PVAc | PS |
| 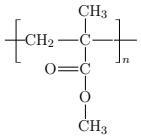 | 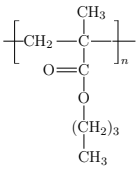 | 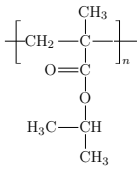 | 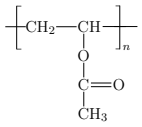 | 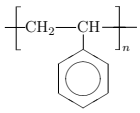 |
| PP | PIB | PMA | PBA | PEA |
| 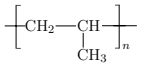 | 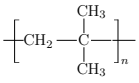 | 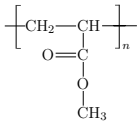 | 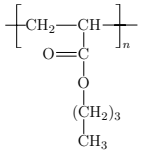 | 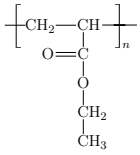 |
| PVC | PPA | PE | P-$\alpha$MS | PDMS |
| 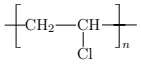 | 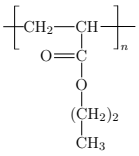 | 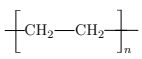 | 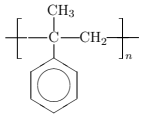 | 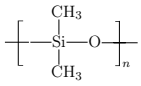 |
| BR | PB | PDMSM | | |
| 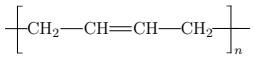 | 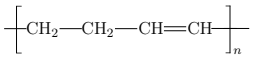 | 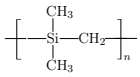 | | |

# Appendix E

# Application of the GC Method

This appendix presents typical examples of the application of the proposed GC method for calculating the PC-SAFT parameters ($m$, $\sigma$, and $\epsilon/k$) for two polymers.

## E.1 Example 1: Poly(methyl methacrylate) (PMMA)

The repeating polymer unit of PMMA is:

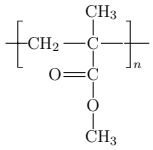

The molecular weight of the repeating unit is $100.12\,\mathrm{g/mol}$. There are only first-order groups (FOG) present. Using the values of the FOG contributions from Table 6.3, the following results are obtained:

| FOG($i$) | $n_i$ | $m_i$ | $m_i\sigma_i^3$ | $m_i\epsilon_i/k$ |
|---|---|---|---|---|
| $CH_3$ | 2 | 1.288724 | 68.3391 | 258.7732 |
| $CH_2$ | 1 | 0.384329 | 24.33981 | 102.3238 |
| C | 1 | −0.49208 | 2.325415 | −10.983 |
| COO | 1 | 1.43911 | 32.51328 | 351.1344 |
| | | $\sum n_i m_i = 2.62008$ | $\sum n_i m_i \sigma_i^3 = 127.5176$ | $\sum n_i m_i \epsilon_i/k = 701.2483$ |

From those values, the following PC-SAFT parameters are calculated:

$$\frac{m}{MW} = \frac{2.62008}{100.12} = 0.0262\,\mathrm{mol/g}$$

$$\sigma = \sqrt[3]{\frac{m\sigma^3}{m}} = \sqrt[3]{\frac{127.5176}{2.62008}} = 3.6511\,\text{Å}$$

$$\epsilon/k = \frac{m\epsilon/k}{m} = \frac{701.2483}{2.62008} = 267.64\,\mathrm{K}$$

With this parameter set calculated from the group-contribution scheme, the AAD % between sPC-SAFT calculations and the experimental liquid density is 4.1 %, in the temperature range 300–400 K and pressures up to 1000 bar.

## E.2 Example 2: Poly(isopropyl methacrylate) (PIPMA)

The repeating polymer unit of PIPMA is:

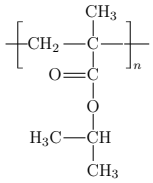

The molecular weight of the repeating unit is 128.17 g/mol. There are both FOG and SOG present. Using the values of the FOG and SOG contributions from Table 6.3 and 6.4, the following results are obtained:

| FOG($i$) | $n_i$ | $m_i$ | $m_i\sigma_i^3$ | $m_i\epsilon_i/k$ |
|---|---|---|---|---|
| $CH_3$ | 3 | 1.93309 | 102.5086 | 388.1598 |
| $CH_2$ | 1 | 0.384329 | 24.33981 | 102.3238 |
| CH | 1 | 0.043834 | 13.95391 | 68.20842 |
| C | 1 | −0.49208 | 2.325415 | −10.983 |
| COO | 1 | 1.43911 | 32.51328 | 351.1344 |
| | | $\sum n_i m_i = 3.30828$ | $\sum n_i m_i \sigma_i^3 = 175.64107$ | $\sum n_i m_i \epsilon_i/k = 898.8434$ |

| SOG($j$) | $n_j$ | $m_j$ | $m_j\sigma_j^3$ | $m_j\epsilon_j/k$ |
|---|---|---|---|---|
| $(CH_3)_2CH$ | 1 | 0.01626 | 0.28087 | −9.83615 |
| | | $\sum n_j m_j = 0.01626$ | $\sum n_j m_j \sigma_j^3 = 0.28087$ | $\sum n_j m_j \epsilon_j/k = -9.83615$ |

From those values, the following PC-SAFT parameters are calculated:

$$\frac{m}{MW} = \frac{3.30828 + 0.01626}{128.17} = 0.02594\,\mathrm{mol/g}$$

$$\sigma = \sqrt[3]{\frac{m\sigma^3}{m}} = \sqrt[3]{\frac{175.922}{3.3245}} = 3.7543\,\text{Å}$$

$$\epsilon/k = \frac{m\epsilon/k}{m} = \frac{889.0073}{3.3245} = 267.41\,\mathrm{K}$$

With this parameter set calculated from the group-contribution scheme, the AAD % between sPC-SAFT calculations and the experimental liquid density is 2.1 %, in the temperature range 300–400 K and pressures up to 1000 bar.

Department of Chemical
and Biochemical Engineering
DTU Building 229
Søltofts Plads
DK-2800 Kgs. Lyngby
www.kt.dtu.dk